

A Thesis Entitled

**“Target based synthesis of novel heterocyclic chemical
entity and their application”**

Submitted to

The

Gujarat University

For the Degree of

Doctor of Philosophy

In

Chemistry

By

Mahesh S. Vasava



Under the supervision of

Dr. Hitesh D. Patel

Professor
Department of Chemistry,
School of Sciences,
Gujarat University,
Navarangpura,
Ahmedabad-380 009
Gujarat (INDIA).

APRIL 2019

Dr. Hitesh D. Patel

Professor
Department of Chemistry
School of Sciences
Gujarat University
Ahmedabad-380009
Gujarat (INDIA)



Residence:

401, Sarjan - 1
Opp. Madhur hall, Setellite,
Ahmedabad-380015
Gujarat (INDIA)

Tel: (M) +91-9428417765

(O) 079-26300969

E-mail: drhiteshpatel1@gmail.com

Certificate

This is to certify that the work incorporated in the thesis entitled “**Target based synthesis of novel heterocyclic chemical entity and their application**” submitted by **Mr. Mahesh S. Vasava** (Registration No. **7095**, Date: **09/10/2015**) was carried out by candidate under my guidance and supervision at the Department of Chemistry, School of Sciences, Gujarat University, Ahmedabad for the degree of **Doctor of Philosophy**. To The best of my knowledge: (i) The candidate has not submitted the same research work to any other institution for any award/degree/diploma, Associateship, Fellowship or other similar titles (ii) the thesis submitted is a record of original research work done by student during the period of study under my supervision and (iii) the thesis represents independents research work on the part of student.

Date: 05/04/2019
Place: Ahmedabad

Dr. Hitesh D. Patel

Research Guide &
Professor,
Department of Chemistry,
School of Sciences,
Gujarat University,
Navarangpura,
Ahmedabad-380 009

Dr. V.K. Jain

Professor and Head,
Department of Chemistry,
School of Sciences,
Gujarat University,
Navarangpura,
Ahmedabad-380 009

Declaration

I hereby declare that the thesis entitled “**Target based synthesis of novel heterocyclic chemical entity and their application**” submitted by me for the degree of **Doctor of Philosophy** is not substantially same as the one which has already been submitted for the award of any other degree or diploma to this or any other university or examining body in India or in other country.

I further declare that the material obtained from other sources has been duly acknowledge in thesis.

I shall be solely responsible for any plagiarism or other irregularities, if noticed in the thesis.

Date: 05/04/2019

Mahesh S. Vasava

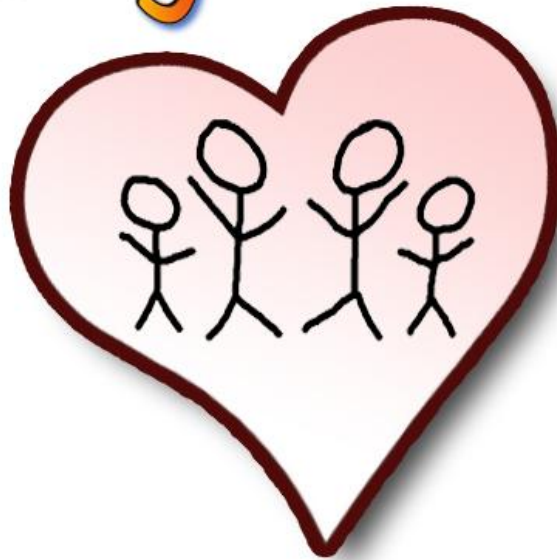
Department of Chemistry,
Gujarat University,
Ahmedabad-380009
Gujarat (INDIA)

Dedicated

To

My

Family & Friends





“THE FEAR OF GOD IS THE BEGINNING OF
WISDOM”

Praise be to *Lord Shiva*, who has given me the
Strength, Confidence and Capacity to complete the
work.

A journey is easier when you travel together. Interdependence is certainly more valuable than independence. It gives me immense pleasure that I have an opportunity to place on record of long travelled path, the contributions of several people, some of whom were with me from the beginning, some who joined me at some stage during the journey, whose rally round kindness, love and blessings have brought me to this day. I wish to thank each and every one who have been instrumental in crystallising this thesis.

A teacher is guide, philosopher and friend whom I could find in my guide **Prof. Hitesh D. Patel**, Department of Chemistry, School of Sciences, Ahmedabad, with deep sense of gratitude. I would like to express my special thanks to my guide for continues support of my Ph.D. study and research, for his patience, motivation, enthusiasm, and immense knowledge. His guidance helped me in all the time of research and writing of this thesis. Our interactions were always quite informal and friendly. I consider myself quite fortunate to have had such an understanding and caring adviser, throughout the course of my research at the Institute. I could not have imagined having a better advisor and mentor for my Ph.D. study and I could not imagine writing this thesis acknowledgement without his support.

I deeply acknowledge and my heartfelt thanks to **Prof. V.K Jain Sir**, Head of the Department, Department of Chemistry for providing me all the laboratory facilities and his moral and ethical support.

I owe a great deal of appreciation and gratitude to **Dr. N.K Shah** and **Dr. K.H. Chikhalia** Former Heads, Department of Chemistry, Gujarat University for their co-operation and encouragement at every stage of this research work.

I wish to express my sincere thanks to **Dr. Pranav Shrivastav, Dr. Dilip Vasava, Dr. M.M. Maisuriya, Dr. Harjindar Kuar, Dr. J.J. Maru, Dr. Hitesh Parekh,** and **Dr. Hitesh Prajapati** for their constant support and encouragements to keep my moral high in times of difficulties.

I, at this moment of time, cannot express in words the invaluable guidance, support and through wisdom given by my friends, lab mates, seniors, colleague **Dr. Manoj N. Bhoi, Dr. Mayuri A. Borad, Mr. Sanjay Rathwa, Dr. Kinjal D. Patel** and **Dr. Sneha G. Nair**, whose deep sharing and synergy have moved me many levels beyond my own thinking. Apart from their technical and scientific guidance, systemic style of working, unbiased nature and perpetual encouragement has kindled in me the desire to learn the art of research work.

I would like to thanks **Dr. Himanshu Pandya** (VC Gujarat University), **Dr. Rikin Patel, Chirag Patel** and **Shilpa Shetty** Department of Botany and Bioinformatics, Gujarat University, Ahmedabad, is one who has ignited my interest in Computational Chemistry and provided me the necessary resources to explore my ideas.

I would also like to mention name **Dr. Edwin Pithawala** for anti-oxidant study and his time to time prodding and sharing of scientific discussion in the subject throughout my research work. It is a great pleasure to acknowledge the generosity for the kind venture he had pursued during my study.

I would like to express my special thanks to all the non-teaching staff members of my beloved institute for helping me throughout the course of my study.

I gratefully acknowledge all the research scholars of Department of Chemistry, Gujarat University, Ahmedabad, for their valuable support during my research work.

It's my fortune to gratefully acknowledge the support of some special individuals. Words fail me to express my appreciation to all my friends, colleague, lab mates, **Dr. Rajesh Vekaria, Dhaval Patel, Jinal Gajjar, Payal, Neelam Prajapati, Touhid Shaikh, Anuj Sharma, Drashti Darji, Krupa Patel, Divya Jethwa, Prachi Acharya, Zeel Bhavsar, Dr. Mayur Vekaria, Dr.**

Ravichandra, Shuvankar Dey, Manoj Vora, Nikita Mishra, Tejash Patel, Himanshu and Sunil Patel for the time they had spent for me and making my stay at campus a memorable one. I take this opportunity to thank one and all for their help directly or indirectly.

A special love and thanks to all of my friends especially to *Dr. Sandip Gamit, Dr. Faruq Qureshi, Sweta Patel, Palak Sapra, Alpesh Ahir, Jaivin Patel*, for the unconditional support, constant source of encouragement and inspiration given to me during my work.

I also express my sincere thanks to *A.J. Bharwad Sir* (Chief Warden), *P.K. Patel* (Warden) and *A. Chavda Sir* (Assistant Warden) of Gujarat University to provide joyful and very comfortable stay during my entire Ph.D. work.

I express my sincere thanks to NFDD center, Rajkot and CIF, Central University, Gandhinagar for different spectroscopic facilities, SynZeal research solutions for mass analysis. I would like to also thank *Dr. Dhanji Rajani*, Microcare laboratory, Surat for in vitro activity, *Dr. Devendrasinh Zala*, Zoology Department, Gujarat University and *Mr. Alpesh Patel*, GenExplore laboratory, Ahmedabad for MTT cytotoxicity study. I would like mention special thanks to *Vinod Devraji*, for helping in Schrodinger software. I also extend my thanks to INFLIBNET for rendering me excellent library facilities.

I take this opportunity to sincerely acknowledge the **Rajiv Gandhi National Fellowship (NFST)**, (UGC, Canara Bank), Ministry of Tribal affairs, Government of India, New Delhi, for providing financial assistance, which buttressed me to perform my work comfortably.

Educational institutions have always been the pillar of an individual's personality, they always bring the real gem out of an individual, and luckily I am not an exception of this process. Last but not the least, I pay my reverence to this institute, Department of Chemistry, School of Science, Gujarat University, Ahmedabad. I am undeniably proud to be associated with this college and express my deepest indebted thanks to my esteemed, renowned and prestigious institution for transforming me from nothing to something.

I bow my head in prayer at the feet of my parents, & my family, whose love Inspiration & support without it was moral, spiritual or financial that gave me the Strength, determination & encouragement at each & every step that I took in my Endeavor to fulfill this task.

Lastly, and above all, I would like to thank the God Almighty; for all that he has given to me.

To those I may have Wronged,

I ask Forgiveness.

To those I may have Helped,

I wish I did More.

To those I Neglected to help,

I ask for Understanding.

To those who helped me,

I sincerely Thank you

So much...

Date: 05/04/2019

Mahesh Vasava

List of Tables

Table No.	Title	Page No.
<u>Chapter: 1 (A)</u>		
1	World Birth and Death Rates.	2
2	Anti-tuberculosis agents for the treatment of drug-susceptible and drug-resistant tuberculosis.	11
3	Existing first-line anti-tuberculosis drug candidate.	12
4	Treatment regimens for Multi drug resistance Tuberculosis.	17
<u>Chapter: 1 (B)</u>		
1	Widely used virtual screening program	36
<u>Chapter: 1 (C)</u>		
1	Frist line Anti-TB agent with Mode of action and resistance	60
2	List of Currently available FDA - approved Flouroquinolone Antibacterial Drugs for systemic Use.	66
3	Second-line Anti-TB agent with Mode of action and resistance	70
<u>Chapter: 2</u>		
1	ADME prediction of 25 lead molecules from Set 1 by using QikProp, Schrodinger.	153
2	ADME prediction of 25 lead molecules from Set 2 by using QikProp, Schrodinger.	154

3	ADME prediction of 25 lead molecules from Set 3 by using QikProp, Schrodinger.	155
4	ADME prediction of 25 lead molecules from Set 4 by using QikProp, Schrodinger.	156
5	Docking scores and binding energies of 25 lead molecules from Set 1.	160
6	Docking scores and binding energies of 25 lead molecules from Set 2.	163
7	Docking scores and binding energies of 25 lead molecules from Set 3.	166
8	Docking scores and binding energies of 25 lead molecules from Set 4.	169
9	Predicted pharmacophore result of ligand 1 from set 1 with different pharmacophore hypothesis.	174
10	Predicted pharmacophore result of ligand 1 from set 2 with different pharmacophore hypothesis	176
11	Predicted pharmacophore result of ligand 1 from set 3 with different pharmacophore hypothesis.	178
12	Predicted pharmacophore result of ligand 1 from set 4 with different pharmacophore hypothesis.	180

Chapter: 3

1	The substituent information for the synthesized compounds 4a-I, 8a-f and 9b along with the details of isolated yield and melting point.	210
2	<i>In vitro</i> anti-bacterial, anti-tuberculosis and MDR-TB screening result of synthesized compounds.	213
3	<i>In vitro</i> anti-Malarial, anti-Fungal screening result of synthesized compounds.	215

4	Predicted ADME parameters for synthesized compounds.	217
5	Docking energies of synthesized compounds against targeted receptor	219

Chapter: 4

1	The substituent details for the synthesized compounds G(1-16) , GG(1-4) along with the details of melting point and isolated yield.	258
2	<i>In vitro</i> anti-bacterial, anti-tuberculosis and MDR-TB screening result of synthesized compounds.	264
3	<i>In vitro</i> anti-Malarial, anti-Fungal screening result of synthesized compounds.	263
4	<i>In vitro</i> % DPPH scavenging activity of the compounds.	268
5	<i>In vitro</i> % NO scavenging activity of the compounds.	268
6	<i>In vitro</i> % H ₂ O ₂ scavenging activity of the compounds.	269
7	Predicted ADME parameters for synthesized compounds.	271
8	Binding energy of Compounds with target protein (kcal/mol).	273

Chapter: 5

1	Synthesis of 6-amino-1-(2,4-dinitrophenyl)-4-phenyl-1,4-dihydropyrano[2,3-c]pyrazole-5-carbonitrile derivatives (5a-5u , 7a-7b and 8a) using SnCl ₂ as catalyst by Conventional and microwave irradiation method.	314
2	<i>In vitro</i> anti-bacterial, anti-tuberculosis and MDR-TB screening result of synthesized compounds.	320

3	<i>In vitro</i> anti-Malarial, anti-Fungal screening result of synthesized compounds.	322
4	<i>In vitro</i> % viability of compound 5e , 5r , 7a and 8a by MTT assay.	324
5	Predicted ADME parameters for synthesized compounds.	326
6	Binding energy of Compounds with target protein (kcal/mol).	328

Abbreviations:

HIV:-	Human immunodeficiency virus	PTP-1B:-	Protein-tyrosine phosphatase-1-B
DNA:-	Deoxyribo Nucleic Acid	MOR:-	Mu-opioid receptor
DHFR:-	Dihydrofolate reductase	po:-	Per os (oral administration)
m-DNA:-	Mitochondrial DNA	RNA:-	Ribonucleic acid
SAR:-	Structure-activity relationship	CVB-5:-	<i>Coxsackievirus</i> B5
IC ₅₀ :-	Half maximal inhibitory concentration	RSV:-	Respiratory syncytial virus
mg/mL:-	mili gram/mili liter	BVDV:-	Bovine <i>viral</i> diarrhea <i>virus</i>
ug/mL:-	micro gram/mili liter	YFV:-	Yellow fever virus
mm:-	mili molar	Reo-1:-	Reoviridae-1
nM:-	Nano molar	HSV-1:-	Herpes simplex virus
MIC:-	minimum inhibitory concentration	VV:-	Vaccinia virus
mM:-	macro molar	VSV:-	Vesicular stomatitis Indiana virus
i.p:-	Indiana pharmacopeia	HCMV:-	Human cytomegalovirus
kg:-	kilo gram	PPIs:-	Protein pump inhibitors
v/v:-	volume/volume	CYP2D6:-	Cytochrome P450 2D6
EC ₅₀ :-	half maximal effective concentration	CQ:-	Chloroquine
CC ₅₀ :-	50% cytotoxic concentration	DCM:-	Dilated cardiomyopathy
GI ₅₀ :-	growth inhibition of 50%	FDA:-	Food and drug administration
TGI:-	total growth inhibition	VTE:-	Venous thromboembolism
LC ₅₀ :-	Lethal Concentration 50	PCC:-	Prothrombin complex concentrate
GI:-	Glycemic Index	GERD:-	Gastroesophageal reflux disease
HP α CD:-	2-hydroxypropyl- α -cyclodextrin	CADD:-	Computer aided drug design
M β CD:-	Methyl- β -cyclodextrin	CCl ₄ :-	Carbon tetrachloride
HP β CD:-	2-hydroxypropyl- β -cyclodextrin	D:-	Doublet
CDs:-	Cyclodextrins	DA:-	Docking assessment
G2:-	5,6-dichloro-2-(trifluoromethyl)-1 <i>H</i> -benzimidazole	DMF:-	N,N'-Dimethylformamide
hERG:-	Human Ether-à-go-go-Related Gene	DMSO:-	Dimethyl sulfoxide
CYP:-	Cytochrome P450	EAA:-	Ethyl acetoacetate
OPDA:-	Ortho Phenylene Diamine	EI:-	Electron ionizer
DPP-iv:-	Di-peptidyl peptidase	EtOH:-	Ethanol
		Equi.:-	Equivalent

LIST OF TABLES & ABBREVIATIONS

FBS:-	Fetal bovine serum	RBF:-	Round Bottom Flask
H:-	Hour	RT:-	Room Temperature
H ₂ O:-	Water	S:-	Singlet
HiSep:-	Mononuclear cell separation from human blood	Satu. NaHCO ₃ :-	Saturated Sodium Bicarbonate
INHR-Mtb:-	Isoniazide resistant mycobacterium tuberculosis	TB:-	Tuberculosis
J:-	Coupling constant	TEA:-	Triethyl amine
KBr:-	Pottasium bromide	THF:-	Tetrahydrofuran
M:-	multiplet	TLC:-	Thin Layered Chromatography
MAA:-	Methyl acetoacetate	TMS:-	Tetra methyl silane
MDC:-	Dichloro methane	ADME:-	Absorption, Distribution, Metabolism, and Excretion
MeOH:-	Methanol	DS:-	Docking Score
MFC:-	Minimum Fungicidal Concentration	GE:-	Glide energy
mg:-	milligram	PSA:-	Polar surface area
MHz:-	Mega Hertz	TB-	Tuberculosis,
Mmol:-	Milimole	Mtb-	Mycobacterium Tuberculosis,
mL:-	Millilitre	MDR-TB-	Multi Drug Resistant Tuberculosis,
M.P.:-	Melting Point	XDR-TB-	Extensively Drug Resistant Tuberculosis,
MS:-	Mass Spectroscopy	TDR-TB-	Totally Drug Resistant Tuberculosis,
MTT:-	3-(4,5-dimethylthiazol-2-yl)-2,5-diphenyltetrazolium bromide	INH-	Isoniazid,
NaOH:-	Sodium hydroxide	WHO-	World Health Organization,
Na ₂ CO ₃ :-	Sodium carbonate	RIF-	Rifampicin,
NaHSO ₄ :-	Sodium bisulfate	PZA-	Pyrazinamide,
Nm:-	Nanometer	EMB-	Ethambutol,
NMR:-	Nuclear Magnetic Resonance	ETH-	Ethionamide,
PARP:-	Poly(ADP-ribose) polymerases	CDC-	Centers for Disease Control and Prevention,
PHOA:-	Percentage human oral absorption	CBC-	Complex Blood Count,
Ppm:-	Parts per million	GI-	Gastrointestinal,
PSA:-	Polar surface area	LFT-	Liver Function Test,
Enyl-ACP:-	Enoyl-acyl carrier protein reductase	PO-	Per Os,
QSAR:-	Quantitative structural activity relationship	katG-	Catalase-Peroxidase,

LIST OF TABLES & ABBREVIATIONS

NADP- Nicotinamide Adenine Dinucleotide
Phosphate,

MRC- Medical Research Council,

rRNA- Ribosomal RNA,

FQs- Fluoroquinolones,

FDA- Food and Drug Administration,

MIC- Minimum Inhibitory Concentration,

CYP- Cytochrome,

GLP- Good Laboratory Practice.

List of Figures

Figure No.	Title	Page No.
<u>Chapter: 1 (A)</u>		
1	Timeline history of Tuberculosis.	8
2	Graphical representation of Tuberculosis - inhalation, diagnosis and treatment.	10
3	New Anti-TB drugs with mode of action and target.	18
<u>Chapter: 1 (B)</u>		
1	Drug discovery and development challenges in modern era.	29
2	Overall computational based drug discovery process	31
3	Reduction mechanism of InhA.	42
<u>Chapter: 1 (C)</u>		
1	Global tuberculosis drug pipeline.	78
2	Two recently approved anti-tubercular agents (Delamanid and Bedaquiline) and other agents which is currently in pipeline, developing specifically for the treatment of MDR-TB infections.	93
3	Structure of 1H-benzo[d]imidazole.	99
4	Structure of anti-tuberculosis and anti-bacterial benzimidazole derivatives.	104- 105
5	Structure of anti-malarial benzimidazole based derivatives.	111- 112

6	Reported biologically active pyran derivatives.	115
---	---	-----

Chapter: 2

1	Biding interactions of compound 1 of set 1 within the pocket of receptors.	162
2	Binding interactions of compound 1 of set 2 within the pocket of receptors.	165
3	Binding interactions of compound 1 of set 3 within the pocket of receptors.	168
4	Binding interactions of compound 1 of set 4 within the pocket of receptors	171
5	(a) Selected pharmacophore and generated pharmacophore of ligand 1 from set 1. (b) Pharmacophore hypothesis and distance between sites. (c) Generated angle between pharmacophore sites. All the distance and angle are in °A unit.	173
6	(a) Generated pharmacophore feature and selected pharmacophore feature of ligand 1 from set 2. (b) Pharmacophore hypothesis and distance between sites (c) angle between pharmacophore sites. All the distance and angle are in °A unit.	175
7	(a) Generated pharmacophore feature and selected pharmacophore feature of ligand 1 from set 3. (b) Pharmacophore hypothesis and distance between sites (c) angle between pharmacophore sites. All the distance and angle are in °A unit.	177
8	(a) Selected pharmacophore and generated pharmacophore of ligand 1 from set 3. (b) Pharmacophore hypothesis and distance between sites. (c) Generated angle between pharmacophore sites. All the distance and angle are in °A unit.	179

Chapter: 3

1	Designed strategy for the targeted molecules.	190
---	---	-----

2	(a) 2d and (b) 3d docked representation of compound 9b at the active site of protein 1QG6. (c) 2d and (d) 3d representation of compound 8a at the active site of protein 2NSD.	220
3	(a) 2d and (b) 3d representation of compound 8c at the active site of protein 4TZK. (c) 2d and (d) 3d representation of compound 8f at the active site of protein 4TZZ.	221
4	Analysis of the molecular dynamics simulations of ligand 9b and protein 1QG6. (a) 2d representation of protein-ligand interaction; (b) Detailed informative plot of interaction between ligand-receptor; (c) The root mean square deviation (RMSD) of protein-ligand backbone; (d) The protein RMSF for side chain atom; (e) A timeline representation of the interactions and contacts between ligand-protein during simulation; (f) The Ligand Root Mean Square Fluctuation (L-RMSF).	224
5	The ligand torsions plot summarizes the conformational evolution of every rotatable bond (RB) in the ligand during the MD simulation trajectory.	225

Chapter: 4

1	Structure of important drugs based on Isoniazid and benzimidazole motif.	238
2	The effect of the compounds toward (a) DPPH, (b) NO and (c) H ₂ O ₂ scavenging.	269

3	(a) 2d and (b) 3d docked representation of compound G6 at the active site of protein 1QG6. (c) 2d and (d) 3d representation of compound GG4 at the active site of protein 2NSD.	274
4	(a) 2d and (b) 3d representation of compound G7 at the active site of protein 4TZK. (c) 2d and (d) 3d representation of compound G7 at the active site of protein 4TZZ.	275
5	(a) Amino acid-ligand interaction (b) RMSF of receptor-ligand (c) RMSF of ligand (d) amino-acid residue-ligand interaction (e) Timeline representation of receptor-ligand (f) RMSD of protein-ligand over a period of 10 ns of docked complex of protein 4TZK and ligand G7.	277
6	Plot and radial representation of ligand (G7) torsion showing rotatable bond over a time period of 10 ns.	278

Chapter: 5

1	<i>In vitro</i> % viability of compound 5e , 5r , 7a and 8a by MTT assay.	325
2	(a) Interacting amino acids with compound 7b in 3d (b) 3d diagram of compound 7b with surface (c) Interacting amino acids with compound 7b in 2d (d) Hydrophobic interaction of compound 7b with protein.	330
3	Docked pose of INH without co-factor and INH with co-factor NAD. (a) 3d pose of INH without co-factor, (b) 2d pose of INH without co-factor, (c) 2d pose of INH with co-factor, (d) 3d pose of INH with co-factor ribbon view, (e) 3d pose of INH with co-factor surface view.	331

4	Binding interaction of (a) compound 7a into the active site of protein 1QG6, (b) Compound 7a into the active site of protein 2B37, (c) Compound 7a into the active site of protein 4TZK.	332
5	(a) RMSD of protein-ligand (7b) over a period of 10ns, (e) RMSF of protein-ligand (7b) over a period of 10ns, (b) RMSD ligand (7b) over a period of 10ns, (c) Protein (amino acids)-ligand (7b) contact over a period of 10ns, (d) Timeline representation of Protein (amino acids)-ligand (7b) contact over a period of 10ns.	334
6	(a) Protein (amino acids)-ligand (7b) interaction over a period of 10ns (b) Superimposition of after 10ns simulation structure on docked structure of protein-ligand.	335
7	Plot and radial representation of ligand (7b) torsion showing rotatable bonds over a period of 10ns.	336

Table of Contents

Chapter: 1 (A)

1.0 Introduction.....	1
2.0 Tuberculosis.....	3
References.....	21

Chapter: 1 (B)

1.0 Introduction.....	27
2.0 Some important tool for computational based drug discovery.....	35
3.0 Enoyl ACP reductase as an attractive target for the treatment of Tuberculosis.....	41
References.....	43

Chapter: 1 (C)

1.0 Introduction.....	47
2.0 The Past.....	48
3.0 The Present.....	67
4.0 The Future.....	77
5.0 Recent developments for MDR-TB.....	87

6.0 Benzimidazole: A milestone in the field of medicinal chemistry.....	92
7.0 Biological importance of 4<i>H</i>-Pyran.....	108
8.0 Conclusion.....	110
References.....	111
Aim and Objectives of the study.....	136

Chapter: 2

1.0 Introduction.....	139
2.0 Methods and Materials	142
3.0 Result and Discussion.....	147
4.0 Conclusion.....	178
References.....	180

Chapter: 3

1.0 Introduction.....	183
2.0 Methods and Materials.....	187
3.0 Result and Discussion.....	202
4.0 Conclusion.....	221

References.....	223
------------------------	------------

Chapter: 4

1.0 Introduction.....	227
------------------------------	------------

2.0 Methods and Materials.....	232
---------------------------------------	------------

3.0 Result and Discussion.....	247
---------------------------------------	------------

4.0 Conclusion.....	271
----------------------------	------------

References.....	273
------------------------	------------

Chapter: 5

1.0 Introduction.....	279
------------------------------	------------

2.0 Methods and Materials.....	287
---------------------------------------	------------

3.0 Result and Discussion.....	303
---------------------------------------	------------

4.0 Conclusion.....	330
----------------------------	------------

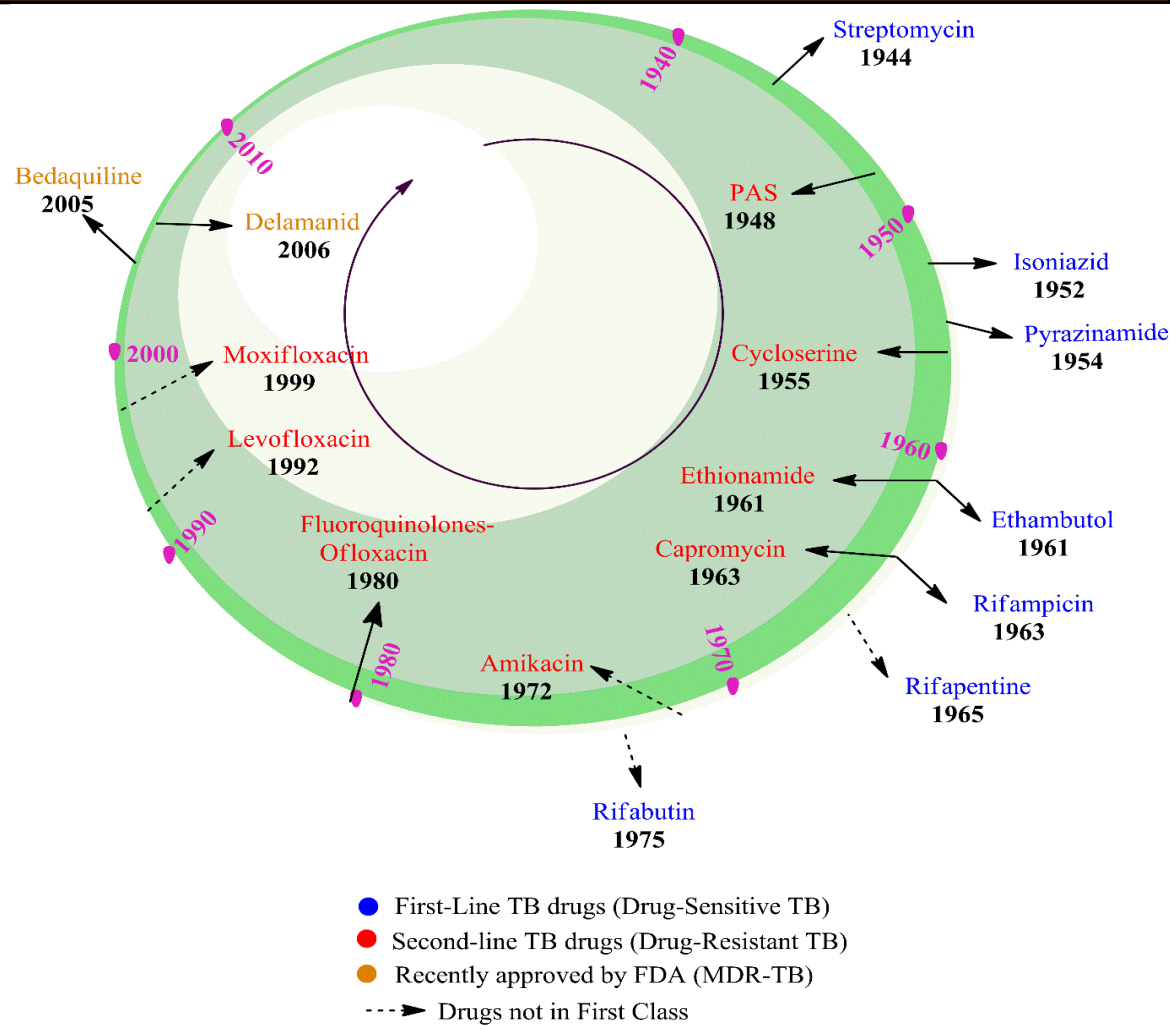
Reference.....	332
-----------------------	------------

List of Publication.....	336
---------------------------------	------------

List of Conferences/Seminars/Workshops.....	339
--	------------

Chapter: 1 (A)

Introduction



Explorative journey of existing TB drugs

Table of Contents

1.0 Introduction	1
1.1 Causes of death in recent decades	2
2.0 Tuberculosis	3
2.1 Current TB Therapy: Are We Battling TB?	8
2.3 Multi-drug resistant TB	12
2.4 Recent developments for MDR-TB	14
2.5 Extensively drug-resistant (XDR-TB) and totally drug resistant TB (TDR-TB)	18
2.6 Tuberculosis death rates	20
References	21

1.0 Introduction

There are approximately 360,000 babies born per day and 15,000 births per hour worldwide. That is more than twice the number of people who die each day. Just under half of the world's total population is comprised of children 18 and under. The average life expectancy worldwide for new babies born each year is 67 years. According to the World Health Organization, about 45 percent of all deaths of children around the world are related to malnutrition [1].

Table. 1 World birth and death rates

Birth Rate	Death Rate
19 births/1,000 population	8 deaths/1,000 population
131.4 million births per year	55.3 million people die each year
360,000 births per day	151,600 people die each day
15,000 births each hour	6,316 people die each hour
250 births each minute	105 people die each minute
Four births each second of every day	Nearly two people die each second

Sources: Population Reference Bureau & The World Fact book (Central Intelligence Agency)

As global population increases, life expectancy rises, and living standards improve, causes of death across the world are changing.

1.1 Causes of death in recent decades

At a global level we see that the majority of deaths are attributed to the category of non-communicable diseases (NCDs); these are chronic, long-term illnesses such as cardiovascular diseases (including stroke), respiratory disease, cancers, diabetes and tuberculosis. Collectively NCDs account for more than 70 percent of global deaths. Total annual number of deaths by high-level cause category. 20 million deaths due to Non-communicable diseases (NCDs) include cardiovascular disease, cancers, diabetes and respiratory disease. 50 million deaths due to injuries include road accidents, homicides and conflict, drowning, fire-related accidents, natural disasters and self-harm. The specific cause of death, which is distinguished from risk factors for death, cardiovascular diseases remains on top with approximately 17.65 million, cancers 8.93, respiratory 3.54, diabetes 3.19 million, dementia 2.38 million, lower respiratory infection 2.38 million, neonatal deaths 1.73 million, diarrheal disease 1.66 million, road accidents 1.34 million, liver disease 1.26 million, tuberculosis 1.21 million, kidney disease 1.19 million, digestive disease 1.09 million, HIV /AIDS 1.03 million, suicide 0.8 million, malaria 0.7 million and others [2].

Furthermore, India's death rate according to CIA (central intelligence agency) world fact book is about 7 per 1000. Based on this, 8.4 million people die every year in India which comes to 22,500 per day approximately. Among the numbers of deaths, over the decades a grim statistic changed little, TB kills 3 million Indians annually: one death every 2 minute [3]. In Mumbai, India, 80% of previously untreated patients were infected with *Mycobacterium tuberculosis* resistant to at least 1 drug, and 51% were infected with *Mycobacterium tuberculosis* resistant to both Isoniazid and Rifampin [4]. MDR-TB increases treatment costs by a factor of 10 - 100-fold, and TB control programs may spend

up to 30% of their budgets on the 3% of patients with TB who have with MDR-TB [5]. 300 million Indians infected by TB, which proves India is a highest TB burden country in the world, accounting for 21% global incidence [6]. Existing economical and effective four-drugs (Isoniazid, Rifampicin, Pyrazinamide and Ethambutol) were introduced before 50 years ago, and till date, no novel drug has been developed except delamanid and bedaquiline, which is used against MDR-TB [7]. Most of the arsenal composed drugs were discovered in 1950 to 1960 for first-line TB treatment. For the treatment of TB, the first compound used in 1944, was streptomycin [8]. There is an urgent need to develop newer, potent and safer anti-tubercular agents which are less prone to resistance.

2.0 Tuberculosis

The human tuberculosis are established over 6,000 years of age which is proposed from another DNA investigation of a tuberculosis genome reproduced in southern Peru, in 2014. Analysts estimate that humans initially acquired tuberculosis in Africa around 5,000 years ago [9]. It was concluded by Gutierrez and her colleagues that in East Africa an early progenitor of *Mycobacterium tuberculosis* was present as early as 3 million years ago, and it was suggested by them that, at that time it may have infected early humanoids [10]. *Mycobacterium tuberculosis*, the bacteria that cause tuberculosis (TB) was discovered by Dr. Koch on March 21, 1882. In the United States and Europe, TB killed one out of every seven people during that time. Dr. Koch's discovery was the most important step taken toward the control and elimination of this deadly disease [11]. After a century of Dr. Koch's discovery, World Health Organization (WHO) and the International Union declared the first World TB Day in 1982 [11]. The timeline history of tuberculosis is represented in **Figure 1**.

In 1997, it was estimated that one-third of the human population (approximately 1.86 billion people) are infected with *Mycobacterium tuberculosis* worldwide [12]. Tuberculosis, TB (*tubercle bacillus*), or MTB (*Mycobacterium tuberculosis*, in the past also called phthisis, phthisis pulmonitis, or consumption, is a widespread, infectious disease caused by various strains of mycobacteria, usually *Mycobacterium tuberculosis* [13]. TB is spread through inhalation of airborne *Mycobacterium tuberculosis* cells, which multiply in macrophages and within the large cystic tubercles, they form liquified tissue surrounded by infected macrophages [14]. After the inhalation of TB bacteria, it establishes with primary infection and it may cure if human have a strong immune system. But if the immune system response is weaker than bacteria will spread and the infection becomes Latent TB, which may responsible for tuberculosis disease (**Figure 2**).

The cell wall of mycobacteria plays an essential role in growing the bacteria. The cell wall of *Mycobacterium tuberculosis* is made up of two segments, upper and lower. The peptidoglycan of *Mycobacterium tuberculosis* is covalently attached to arabinogalactan which in turn is attached to mycolic acid with their long mero mycolate and short alpha chains. This is the cell wall core of *Mycobacterium tuberculosis* and is known as a mycolyarabinogalactan-peptidoglycan complex. The upper segment of the cell wall is made up of free lipids, some with longer fatty acids complementing the shorter alpha chain and vice versa. Cell wall proteins, phosphatidylinositol mannosidase, the phthiocerol containing lipids, lipomannan and lipoarabinomannan also can be found at upper segment of the cell wall [15]. Furthermore, the cell envelope of *Mycobacterium tuberculosis* also contains an additional layer beyond peptidoglycan that rich in unusual lipids, glycolipids and polysaccharides [16]. *Mycobacterium tuberculosis* is an intracellular pathogen. *Mycobacterium tuberculosis* is able to parasite human mononuclear phagocytes [17].

Mycobacterium tuberculosis will spend most of its life cycle in macrophages [18]. *Mycobacterium tuberculosis* has the ability to multiply inside the macrophage phagosome. *Mycobacterium tuberculosis* can remain dormant for a few years without the symptoms. When the immune system of the hosts is low, the dormant *Mycobacterium tuberculosis* will become active and cause the infection. There are two types of tuberculosis that are childhood-type tuberculosis and adult-type tuberculosis.

However, all age groups are at risk of TB, but it mostly affects young adults, in their productive years. In developing countries, 95% cases end in death. Tuberculosis (TB) remains one of the world's deadliest communicable diseases. TB killed around 1.5 million people (out of which 1.1 million HIV-negative and 0.4 million HIV-positive) in 2017. About 9.6 million people are estimated to be falling ill with TB worldwide in 2017 (5.4 million men, 3.2 million women, and 1.0 million children). Globally, 12% of the 9.6 million new TB cases in 2017 were HIV-positive [20]. Approximately 1000 million people were infected, over which 150 million people get sick and 36 million died of TB between 2000 and 2018 [21].

According to the worldwide survey, patients suffering from TB as well as HIV ranks the top position in leading to an increased mortality rates. The mortality rate survey done in the year 2018 for HIV indicated that 0.4 million TB death among HIV-positive people occurred out of the total of 1.2 million [21]. 15% of AIDS patients globally die of TB and approximately 12 million individuals are co-infected and roughly every year. Furthermore, the emergence of new infectious forms of TB such as multi-drug-resistant tuberculosis (MDR-TB) and extremely drug-resistant tuberculosis (XDR-TB) and its synergy with HIV has fueled its epidemic nature [11].

Over the decades a grim statistic changed little, TB kills 300000 Indians annually: one death every 2 minute [22]. In Mumbai, India, 80% of previously untreated patients were infected with *Mycobacterium tuberculosis* resistant to at least 1 drug, and 51% were infected with *Mycobacterium tuberculosis* resistant to both isoniazid and rifampin [23]. MDR-TB increases treatment costs by a factor of 10 - 100-fold, and TB control programs may spend up to 30% of their budget on the 3% of patients with TB who have with MDR-TB [24]. 300 million Indians infected by TB, which proves India is a highest TB burden country in the world, accounting for 21% global incidence [25].

MDR-TB (Multi-drug resistant) is emerging the worldwide threat [26]. MDR-TB is well-defined by the resistance to the two most potent first-line anti-TB drugs isoniazid and rifampicin, and have need of treatment with more expensive second-line drugs, which, in addition to being costly, cause more adverse events and show lower cure rates [27]. The term XDR-TB (extensively-drug resistant) introduced the first time in March 2006 and it causes via MDR-TB with additional resistance to any fluoroquinolone and one of the second-line injectable drugs (Kanamycin, Amikacin, or Capreomycin) [26][27]. Recently, cases of unclearly defined TDR-TB were reported [28]. TDR-TB (totally drug resistant, sometimes called as XDR TB or extremely drug resistant TB), is Tuberculosis bacteria which are resisting against all the first-line and second-line anti-TB drugs [29]. Human TB is linking the growing list of bacterial diseases arriving the post-antibiotic era.

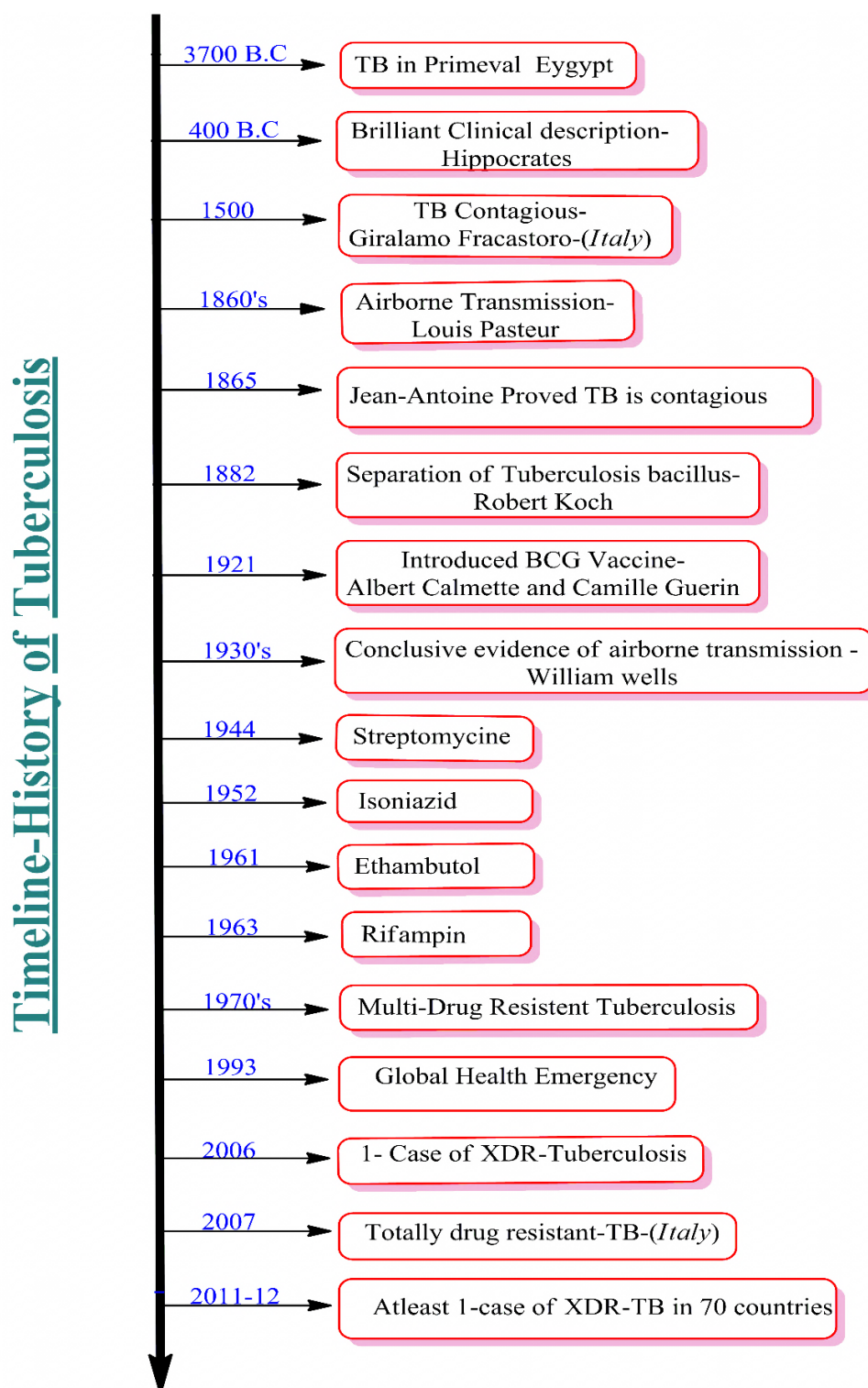


Figure 1. Timeline history of Tuberculosis

Existing economical and effective four-drugs (Isoniazid, Rifampicin, Pyrazinamide and Ethambutol) were introduced before 50 years ago, and till date, no novel drug has been

developed except delamanid and bedaquiline, which is used against MDR-TB. Most of the arsenal composed drugs were discovered in 1950 to 1960 for first-line TB treatment. For the treatment of TB, the first compound used in 1944, was Streptomycin [30]. There is an urgent need to develop newer, potent and safer anti-tubercular agents which are less prone to resistance [31].

2.1 Current TB Therapy: Are We Battling TB?

Tuberculosis (TB) treatment has become very difficult after the emergence of existing drug resistant against a bacterium named *Mycobacterium tuberculosis* which is preventable and curable. In a human body, TB bacteria can attack the spine, kidney, lungs, and brain, but lungs have more risk of attack. All TB bacteria infected peoples do not get sick. There are two TB related exist conditions, one of which is latent TB infection and other is active TB disease (**Figure 2**). In both Latent TB and Active TB case they are curable. When people have TB bacteria in the body, but they are not active and they do not get sick it's called as latent TB infection. Latent TB infection cannot spread in the human body and do not have TB symptoms. In latent TB infection, if TB bacteria become activated, it converts into TB disease and people become sick. Therefore, latent TB infected people, it is more superior to get preserved for not emerging it to TB disease. Nevertheless, if the immune system of human can't stop the evolution of TB bacteria, they are multiplying in the body and it became active TB disease. In TB disease, TB bacteria are active and make people sick. People already diagnosed with TB disease have chances of spreading it to others. The treatment duration for tuberculosis is minimum 6 to 12 months with the combination of first-line anti-TB agents. However, if the treatment is vulnerable by drug

resistance of bacteria, it further treated with the combination therapy of second line agents, fluoroquinolones, and some injectable agents (**Figure 2**).

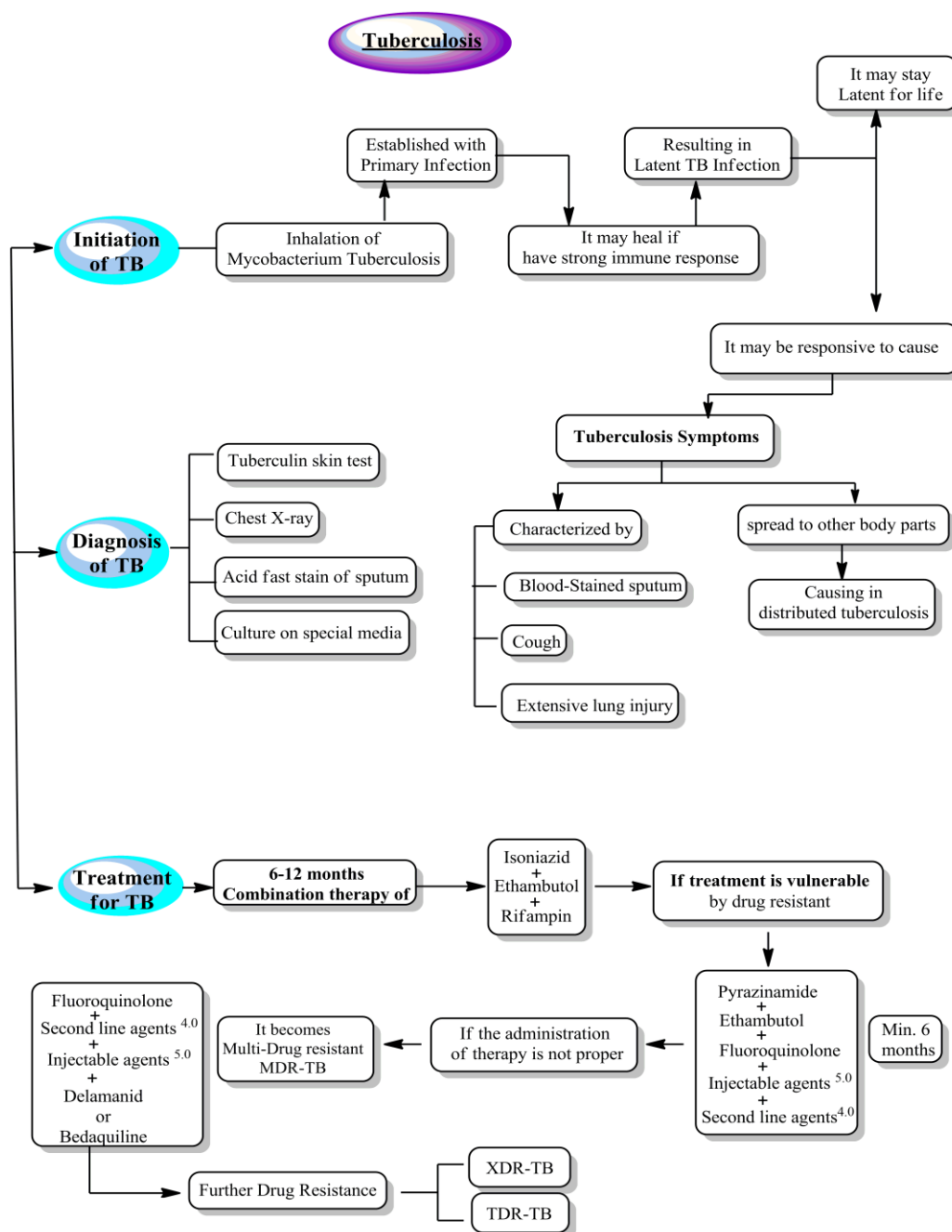


Figure 2. Graphical representation of Tuberculosis - inhalation, diagnosis and treatment

Table 2. Anti-tuberculosis agents for the treatment of drug-susceptible and drug-resistant tuberculosis

Recommended Regimens for the Treatment of Drug-susceptible pulmonary Tuberculosis				
Regimen	Initial-phase drugs	Interval/doses	Continuation-phase Drugs	Interval/doses
1	INH,RIF,PZA,EMB	7 days/week for 56 doses or 5 days/week for 40 doses	INH,RIF	7 days/week for 126 doses or 5 days/week for 90 doses or twice weekly for 36 doses or once weekly for 18 doses
2	INH,RIF,PZA,EMB	7 days/week for 14 doses, Then twice weekly for 12 doses or 5 days/week for 10 doses, then twice weekly for 12 doses	INH,RIF	Twice weekly for 26 doses or once weekly for 54 doses
3	INH,RIF,PZA,EMB	Twice weekly for 24 doses	INH,RIF	Twice weekly for 54 doses
4	INH,RIF,EMB	7 days/week for 56 doses or 5 days/week for 40 doses	INH,RIF	7 days/week for 217 doses or 5 days/week for 155 doses or twice weekly for 62 doses

Source: American Thoracic Society, CDC, and Infectious Diseases Society of America. *Treatment of tuberculosis. MMWR Recomm Rep.* 2003; 52(RR-11):1-77.

For active TB who are presumed to have a drug-susceptible disease with newly diagnosed patients, the WHO recommended the standard drug regimen by includes an initial phase of 2 months of a standard four-drug combination (INH, RIF, PZA, and EMB), followed by a continuation phase of 4 months of INH and RIF. The detail description of recommended regimens is given in **Table.2** by American Thoracic Society, CDC, and Infectious Diseases Society of America. Drugs are administered by mouth and are listed in **Table.3** with their recommended daily dose and notable adverse effects. The current

treatment for drug-susceptible TB requires four drugs used in combination for 2 months, followed by two drugs used in combination for 4 months.

Table 3. Existing first-line anti-tuberculosis drug candidate

First-line anti-tuberculosis drug candidate with side effects and monitoring				
Drugs	Dosage	Route	Opposing Effects	Observing
Isoniazid	5mg/kg/day up to 300mg/day	PO	Asymptomatic elevation of LFTs, clinical hepatitis, fatal hepatitis, peripheral neurotoxicity, central nervous system effect, lupus-like syndrome, hypersensitivity reactions, monoamine poisoning, Drug interaction	LFTs
Pyrazinamide	40- 45kg:1000mg/day 56- 75kg:1500mg/day 76- 90kg:2000mg/day	PO	Hepatotoxicity, GI symptoms, gouty polyarthralgia, asymptomatic hyperuricemia, dermatitis acute gouty arthritis, transient morbilliform rash	LFTs, serum uric acid
Ethambutol	40- 45kg:800mg/day 56- 75kg:1200mg/day 76- 90kg:1600mg/day	PO	Retrobulbar neuritis, peripheral neuritis, cutaneous reactions, fever	Vision tests
Rifampin	10mg/kg/day up to 600mg/day	PO	Hematologic toxicity, uveitis, GI reactions, polyarthralgia, hepatotoxicity, pseudojaundice, rash, flu-like syndrome, orange discoloration of bodily fluids, significant drug interactions	LFTs, CBC
Rifabutin	5mg/kg/day up to 300mg/day	PO	Cutaneous reactions, GI reactions, Flu-like syndrome, hepatotoxicity, severe immunological reactions, leukopenia, thrombocytopenia, orange discoloration of bodily fluids, significant drug interactions	LFTs, CBC
Rifapentine	10mg/kg/day up to 600mg/day	PO	Same as Rifampin	LFTs, CBC

CBC-complex blood count, GI-gastrointestinal, LFT-Liver function test, PO- per os (by mouth)

Source: American Thoracic Society, CDC, and Infectious Diseases Society of America. *Treatment of tuberculosis. MMWR Recomm. Rep.* 2003; 52(RR-11):1-77.

2.3 Multi-drug resistant TB

Drug-resistant is not a recent phenomenon. *M. tuberculosis* strains that were resistant to Streptomycin seemed soon after the introduction of the drug for the treatment of TB in 1944 [32]. Genetic resistance to an anti-TB drug is because of spontaneous chromosomal mutations at a low frequency (10^{-6} to 10^{-8}) of mycobacterial replications, amplification of genetic mutations due to human errors result in arising clinically drug resistant tuberculosis [33; 34]. The TB illness was thought of reducing. However, due to the worldwide emergence of the multidrug-resistant *Mycobacterium tuberculosis* strain it remains an alarming issue with the risk of health [35]. The WHO report of the year 2016 highlights that along with 1 million people who received treatment for rifampicin-resistant TB as well MDR-TB in 2015 and added to approximately around 4.8 million new cases of MDR-TB is seen. The year 2015 observed a success target of $\geq 75\%$ in MDR-TB patients by 43 of the 127 countries and territories that reported outcomes for the 2012 cohort, including three high MDR-TB burden countries (Estonia, Ethiopia and Myanmar).

An exceedingly high share of the global TB burden is being observed by the South-East Asia followed by India wherein one fourth of the global incident TB cases occur annually. As per WHO Global TB Report, 2015, out of the estimated global annual incidence of 9.6 million TB cases, 2.2 million were estimated to have occurred in India [36]. In 2014, India achieved complete geographical coverage for diagnostic and treatment services for multi-drug resistant TB. Yet these cases, about a third of the estimated number, cost over 40% of the annual RNTCP budget [37]. An understanding of the cause and effective response is a must to develop a drug-resistant TB. The development and factors contributing to the drug-resistant TB can be explained by two pathways (1) acquired drug

resistance and (2) primary drug resistance. These pathways are interrelated and have several contributing factors [38].

An insufficient, lacking or improper treatment that permits the selection of mutant resistant strain results in the acquired drug resistance. Subsequently, a person who has been infected with a drug-resistant TB strain is called as primary or initial drug resistance. The transmission of drug-resistant TB occurs exactly in the same way as transmission of drug-susceptible TB [39] and these acquired and primary drug resistances contribute to the development of multidrug resistance tuberculosis (MDR-TB). The bacteria that cause TB can be used to develop resistance to the antimicrobial drugs in curing the disease. A resistance to first line two most powerful anti-TB agents Isoniazid and Rifampicin is observed by Multidrug-resistant TB (MDR-TB). Patients with MDR-TB nowadays require more effective and less toxic new anti-TB agents for extended treatment [40].

Due to the mismanagement of the TB treatment and person to person transmission, multidrug resistance keeps on emerging and spreading. Most people with TB are cured via a strictly observed, six-month drug regimen that is supplied to sufferers with aid and supervision. Incompatible, or erroneous use of antimicrobial agents, or use of ineffective formulations of medicine (e.g. Use of single tablets, improper first-class drug treatments or storage conditions), and advanced stage therapy interruption can cause drug resistance, that may then be transmitted, particularly in crowded settings consisting of prisons and hospitals [41]. It is compulsory to manage combination therapy, including Rifampicin, Isoniazid, Pyrazinamide and Ethambutol for 2 months, followed by 4 months of Rifampicin and Isoniazid to treat active TB to avoid drug resistance. FDA approved multidrug resistance tuberculosis treatment regimens combination therapy is described in detail in **Table 1**. Although, drug resistance is an alarming emergence. Multi-drug resistant (MDR-TB) and

extensively drug resistant strains (XDR-TB) are on the rise and recently TDR-TB is emerging TB burden worldwide [42].

Drug resistance in TB is assumed to be mediated completely by means of chromosomal mutations, which affect both the drug target itself or bacterial enzymes that activate pro-drugs [43]. For few drugs, similar like Isoniazid and Rifampicin, a massive range of mutations were identified that confer resistance, and these mutations account for a maximum of the resistance observed amongst clinical isolates [44]. With advancement in high-throughput sequencing techniques, genotyping strategies, advanced, delicate, and huge-scale research to find out the mutations associated with resistance have been undertaken all over the world. However, potent active anti-TB agent's discovery has suffered after the over-optimism inspired by the post-genomics revolution [45]. Several reasons are responsible for the day to day development of MDR-TB [46]. However, incomplete, irregular, inadequate treatments of non-public medical physicians are the maximum common reason of getting drug resistance. In the past, patients who never received chemotherapy is an initial resistance of anti-TB drugs [47-48]. Our effort provides an outline of the current development in anti-TB drug discovery. By reviewing the currently available research and literature, we wish to outline the status of new anti-TB drug regimens. The predominant focus is on drugs that are currently in the pipeline. The purpose of this literature review is to support and simplify the future efforts in anti-TB drug discovery.

2.4 Recent developments for MDR-TB

The past few years have seen the primary approvals of new anti-tubercular medication in more than fifty years, in large part due to the coordinated efforts of government programs, nongovernmental organizations and support from pharmaceutical

corporations. As discovery and development of novel chemical entities to treat *M.TB* has increased considerably in recent years along with the technologies used to discover new agents. New technologies are developed to enhance our increased understanding of the biology of the *M.TB* life cycle and also the success and failures of previous drug development ways. Currently, as a result of a multi-stakeholder initiative, 2 new anti-TB medications were approved by the US Food and Drug Administration and by the European Medicines Agency: Bedaquiline and Delamanid. Additionally, Pretomanid, Sutezolid, SQ109 and Benzothiazinones are mentioned (Fig.1). Treatment options for MDR-TB and XDR-TB are limited and as a result, drug resistance is extended. Hence, effective, potent and less toxic drugs are extremely required. WHO recommends the use of second-line drugs which include aminoglycosides (Kanamycin, Amikacin), Capreomycin, Cycloserine, Para-aminosalicylic acid, Thioamides (Ethionamide (ETH), Prothionamide), and fluoroquinolones (Ciprofloxacin, Ofloxacin, Levofloxacin) for the treatment of MDR-TB (Table 1). In 1956, Isoniazid analogs Ethionamide and Prothionamide were discovered [49]. Some promising anti-TB drugs regimens with their inhibiting target which are shown in figure.1. There are three reasons commonly known for demanding novel tuberculosis drugs: (1) to spread out intermittent treatment more broadly and expand current therapy through shorting the length of therapy, (2) to provide for additional effective treatment of latent tuberculosis contamination (LTBI) in programs that are capable to implement this exercise, and (3) to enhance the treatment of MDR-TB.

Table. 4 Treatment regimens for Multi drug resistance Tuberculosis.

Recommended Treatment Regimens for MDR-TB					
Resistance form	INH and RIF + Strept	INH,RIF+PZA or EMB	INH,RIF,PZA, EMB	INH,RIF,PZA, EMB,FQN	INH,RIF,PZA, EMB, Injectable
Course of therapy	PZA+EMB+FQN+ Injectable agent (Min. 6 months) + Second-line agent if extensive disease	PZA or EMB + FQN + Second-line agents + Injectable agents (min. 6 months)	FQN+ 3 Second-line agents + Injectable agent for first 6-12 months	Injectable agent + Second-line agents + third-line agent	FQN + All Second-line agents consider any third-line agents if susceptible
Time period for therapy	give 18-24 months Following conversion	give 18-24 months Following conversion- consider additional agents high-dose INH	give 18-24 months Following conversion	24 months Following conversion- Consider high- dose INH, Surgery	25 months Following conversion- Consider Surgery

Modified form: - Curry International Tuberculosis centre. Drug-resistance tuberculosis: a survival guide for clinicians, 2011

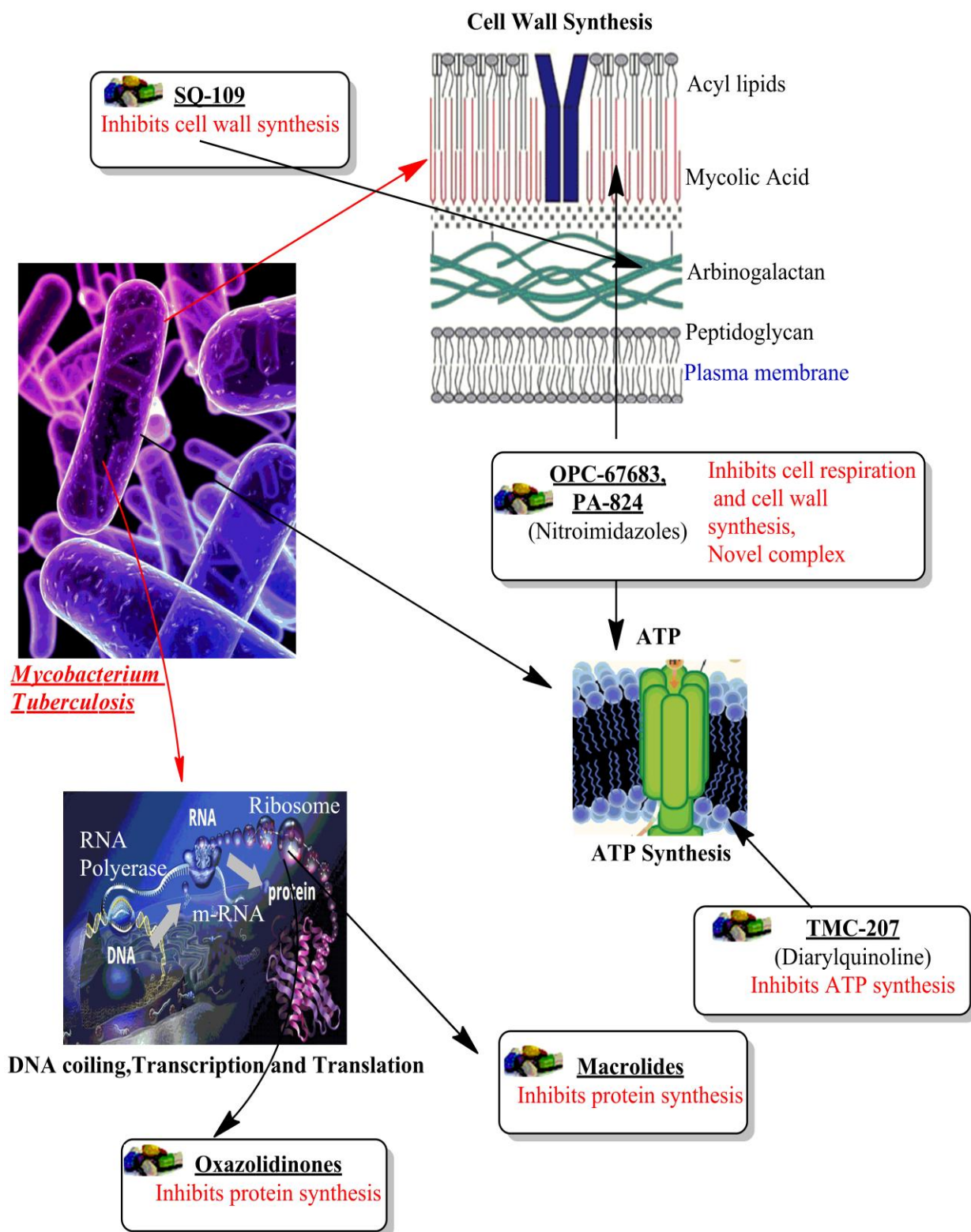


Figure. 3 New Anti-TB drugs with mode of action and target

Clinical development of tuberculosis agents is not always easy. Efficacy trials are lengthy and complex, with complexities admitted by only a few investigators. Due to the fact, only few products have been recently registered for the treatment of tuberculosis in the past four decades, present regulatory requirements are not perfectly defined or standardized, and earlier guidelines are out-of-date. A new drug should be at least as safe and effective as the standard treatment and it is typically necessary for approval by regulatory experts. This new drug will be incorporated into a multidrug regimen which will be associated with the equivalent old 6-month short-course regimen for tuberculosis.

2.5 Extensively drug-resistant (XDR-TB) and totally drug resistant TB (TDR-TB)

The term “exclusively drug resistant” (XDR) TB was first proposed by the Centre for Disease Control and Prevention (CDC) and WHO in March 2006 the definition was revised in October 2006 [50,51]. XDR-TB is a form of MDR-TB. Mismanagement of MDR-TB with erratic use of second-line drugs may develop more severe drug resistance tuberculosis known as extensively drug resistance TB. Extensively drug resistant TB is defined as the resistance to at least INH and RIF and any Fluoroquinolone and one of the three second-line injectable drugs, Kanamycin, Amikacin or Capreomycin [52-53]. XDR-TB was first described in two Italian women who died after 422 and 625 days spent in hospital, and 60 months of treatment respectively [54]. More than 400,000 cases of MDR-TB and 25,000 cases of XDR-TB cases emerge across the world every year as a result of poor management of drug sensitive as well as drug resistant TB [55]. It represents a progression from the multidrug-resistant (MDR) TB. In the presence of such resistance, treatment options are severely restricted hence the mortality rates are extremely high. XDR-TB is emerging as a global public health threat [56]. The treatment of XDR-TB is much expensive, difficult and the outcomes much severe hence the identification of risk factors

for XDR-TB are important to design effective TB control strategies [57]. The emergence of XDR-TB is mainly a manmade phenomenon being an indicator of failing TB programs. Pre-XDR-TB is another worrying international phenomenon. Pre-XDR-TB is defined as disease caused by a strain resistant to INH and RIF and either Fluoroquinolone or second-line injectable drug but not both [58]. High rates of quinolone resistance and pre-XDR-TB have been reported from California, Philippines and China [59]. The treatment of XDR-TB is costly and challenging. Ideally treatment should be done under the supervision of an expert doctor who is experienced with dealing such cases, since this treatment represents the patient's last chance of a cure [56]. In 2014 extensively drug resistant TB (XDR-TB) has been reported by 105 countries, it is estimated that 9.7% of total 480,000 people with MDR-TB have developed XDR-TB globally [21].

The last decade of previous century has witnessed the reappearance of drug-resistant TB with MDR-TB arising as a big threat to TB community along with the rising cases of XDR-TB. Recently, some parts of the world have reported the cases of extremely drug-resistant TB (XXDR-TB) and totally drug-resistant TB (TDR-TB) also called as super XDR-TB [60-61]. XXDR-TB can be defined as the isolates of *M. tuberculosis* resistant to all first-line and second-line available anti-TB drugs in addition to other drugs Rifabutin, Thiacetazone, Clofazamine, Dapsone and Clarithromycin [62]. Rifampicin-resistant TB (RR-TB) is caused by *M. tuberculosis* strains resistant to rifampicin, with or without resistance to other drugs. Both MDR-TB and XDR-TB are forms of RR-TB. The strain of *M. tuberculosis* which is resistant all first line and second line licensed anti-tubercular drugs is defined as totally drug resistant TB (TDR-TB) [62]. The clinical isolates of TDR-TB were observed in Italy for the first time in 2003 [61], next in Iran and now it has been reported from India that there were TB patients who do not respond to any of the anti-

tubercular regimens [63]. Though it is not yet prevalent, chances are bright to through a challenge of TDR-TB to researchers across the globe. It is clear that, TB is a devastating disease and cannot be eradicated completely by the current available drugs, the need of novel drugs possessing novel mechanism of action are absolutely necessary. For the discovery of novel anti-TB agents, we have in depth reviewed the literature of current treatment regimens and their limitations.

2.6 Tuberculosis death rates

At a global level there has been a one-third drop in TB deaths, falling from 1.8 million in 1990 to 1.3 million in 2017. TB deaths are relatively equally distributed across age categories over 15 years old: around 35% occur in those aged 15-49 as well as in those aged 50-69 years old and 27 percent in those aged 70+ years old. Across most countries, the death rate from TB is below 5 per 100,000. Rates in 2017 across Eastern Europe were slightly higher, between 5-10 per 100,000. Across South Asia, these reach 25-50 per 100,000, with highest rates across Sub-Saharan Africa ranging from 50 all the way up to 500 per 100,000. Rates are highest in the Central African Republic which were over 480 per 100,000 in 2017 [64].

References

1. Population Reference Bureau & The World Factbook (Central Intelligence Agency).
2. <https://ourworldindata.org/causes-of-death>.
3. Gopi PG, Subramani R, Santha T, Chandrasekaran V. Indian Journal of Medical Research. 2005; 122:243.
4. Almeida D, Rodrigues C, Udwadia ZF, Lalvani A, Gothi GD, Mehta P, Mehta A. Clinical Infectious Diseases. 2003; 36:152-154.
5. Pablos-Méndez A, Gowda DK, Frieden TR. Bulletin of the World Health Organization. 2002; 80:489-495.
6. Organization W H. Report. Global Tuberculosis Control. Epidemiology, Strategy and Financing. Geneva: WHO.2010.
7. Vasava MS, Bhoi MN, Rathwa SK, Borad MA, Nair SG, Patel HD. Indian Journal of Tuberculosis. 2017; 64(4):252-75.
8. (a) Organization W H, Global Tuberculosis Report (2013), ISBN 978924 1564656.
(b) Organization W H, Global Tuberculosis Report (2012), ISBN 978924 1564502.
9. Carl Zimmer, "Tuberculosis Is Newer Than Thought, Study Says", New York Times, 2014.
10. Gutierrez MC, Brisse S, Brosch R, Fabre M, Omaïs B, Marmiesse M, Supply P, Vincent V. PLOS Pathogens. 2005; 1:5.
11. <http://www.cdc.gov/tb/events/worldtbd/history> july-20/16: 2016.
12. Dye C, Scheele S, Dolin P, Pathania V, Ravigione MC. JAMA. 1999; 282:677-686.
13. Kumar V, Abbas AK, Fausto N, Mitchell RN. Saunders Elsevier. 2007; 516-522.
14. Bichun LA, Pedrosa MM, Trippel SJ. Springer: Connecticut, 1996.

15. Brennan PJ. Tuberculosis. 2003; 83:91-97.
16. Cole S, Brosch R, Parkhill J, Garnier T, Churcher C, Harris D, Gordon SV, Eiglmeier K, Gas S, Barry C3, Tekaia F. Nature. 1998; 393:537-544.
17. Clemens DL and Horwitz MA. Journal of Experimental Medicine. 1996; 184: 1349-1355.
18. Akif M, Chauhan R, Mande SC. Acta Crystallographica Section D: Biological Crystallography. 2004; 60:777-779.
19. Manganello R, Dubnau E, Tyagi S, Kramer FR, Smith I. Molecular Microbiology. 1999; 31:715-724.
20. Organization W H. Global tuberculosis report 2017. www.who.int/tb/publications/global_report/en/.
21. Organization W H. Tuberculosis fact sheet. Available from <http://www.who.int/gtb/publications/factsheet/index.htm>. 2018.
22. Pablos-Méndez A, Gowda DK, Frieden TR. Bulletin of the World Health Organization. 2002; 80:489-495.
23. Organization W H. Report. Global Tuberculosis Control. Epidemiology, Strategy and Financing. Geneva: WHO.2010.
24. Gandhi NR, Nunn P, Dheda K, Schaaf HS, Zignol M, Van Soolingen D, Jensen P, Bayona J. The Lancet. 2010; 375:1830-1843.
25. Caminero JA, Sotgiu G, Zumla A, Migliori GB. The Lancet Infectious Diseases. 2010; 10:621-629.
26. Udwadia ZF, Amale RA, Ajbani KK, Rodrigues C. Clinical Infectious Diseases. 2012; 54:579-581.
27. Migliori GB, Loddenkemper R, Blasi F, Raviglione MC. European Respiratory Journal. 2007; 29:423-427.

28. (a) Organization W H, Global Tuberculosis Report (2013), ISBN 978924 1564656.
(b) Organization W H, Global Tuberculosis Report (2012), ISBN 978924 1564502
29. Diacon AH, Pym A, Grobusch M, Patientia R, Rustomjee R, Page-Shipp L, Pistorius C, Krause R, Bogoshi M, Churchyard G, Venter A. The New England Journal of Medicine. 2009; 360:2397-2405.
30. Gupta A, Anupurba S. Indian Journal of Tuberculosis. 2015; 62(1): 13-22.
31. Zhang Y, Yew W. International Journal of Tuberculosis and Lung Disease. 2009; 13(11): 1320-1330.
32. Yew WW, Leung CC. Respiriology. 2008; 13(1): 21-46.
33. World Health Organization. WHO global reports 2015. Geneva: [http://www.who.int/tb/publications/global_report/gtbr2015_executive_summary.p](http://www.who.int/tb/publications/global_report/gtbr2015_executive_summary.pdf)df; 2015.
34. Central TB division. TB India annual reports.2016 RNTCP, Annual status report; 2016
35. World Health Organization. Companion handbook to the WHO guidelines for the programmatic management of drug-resistant tuberculosis; 2014.
36. <http://www.tbfacts.org/drug-resistant-tb-in-india/#sthash.IrCYIdER.dpuf>.
37. Mathys V, Wintjens R., Lefevre P, Bertout J, Singhal A, Kiass M, Kurepina N, Wang XM, Mathema B, Baulard A, et al. Antimicrobial Agents and Chemotherapy. 2009;53:2100– 2109.
38. World Health Organization. <http://www.who.int/features/qa/79/en/>.
39. Sharma SK, Mohan A. Indian Journal of Medical Research. 2004; (120): 354-376
40. Zumla A, Raviglione M, Hafner R, von Reyn CF. The New England Journal of Medicine 2013; (368): 745-755.

41. CDC. Notice to Readers: Revised Definition of Extensively Drug-Resistant Tuberculosis. *Morbidity and Mortality Weekly Report*. 2006; (55): 1176.
42. Ramaswamy S, Musser JM. *Tubercle and Lung disease*. 1998; 79(1):3-29.
43. Lew JM, Kapopoulou A, Jones LM, Cole ST. *Tuberculosis*. 2011; (91): 1-7
44. Bastian I, Rigouts L, Van Deun A, Portaels F. *Bulletin of the World Health Organization* 2000; (78): 238-51.
45. Vareldzis BP, Grosset J, de Kantor I, Crofton J, Laszlo A, Felten M, et al. *Tubercle Lung Disease*. 1994; (75): 1-7.
46. Citron KM, Girling DJ. *Oxford University Press/English Language Book Society*. 1987; 5.278-5.299.
47. Dye C, Espinal MA, Watt CJ, Mbiaga C, Williams BG. *The Journal of Infectious Diseases*. 2002; (185): 1197-202
48. Jassal MS, Nedeltchev GG, Lee JH, Choi SW, Atudorei V, Sharp ZD, et al. *PLOS ONE*. 2010; 5(8): e12451.
49. Mitrzyk BM. *Pharmacotherapy*. 2008; 28(10): 1243-1254.
50. Jain A, Dixit P, Prasad R. *Tuberculosis*. 2012; 92(5): 404-406.
51. Caminero J. *International Journal of Tuberculosis and Lung Disease*. 2006; 10(8): 829-837.
52. Dheda K, Gumbo T, Gandhi NR, Murray M, Theron G, Udwadia Z. *The Lancet Respiratory Medicine*. 2014; 2(4): 321-338.
53. Prasad R, Garg R. *Chest India*. 2007; 8: 3-4.
54. Prasad R, Srivastava DK. *Clinical Epidemiology and Global Health*. 2013; 1(3): 124-128.
55. Flor de Lima B, Tavares M. *The Clinical Respiratory Journal*. 2014; 8(1): 11-23.

56. Banerjee R, Allen J, Westenhouse J, Oh P, Elms W, Desmond E. *Clinical Infectious Diseases*. 2008; 47(4): 450-457.
57. Zhao M, Li X, Xu P, Shen X, Gui X, Wang L, et al. *PLOS ONE*. 2009; 4(2): 4370.
58. Loewenberg S. *The Lancet*. 2012; 379(9812): 205.
59. Migliori GB, Sotgiu G, Gandhi NR, Falzon D, DeRiemer K, Centis R. *European Respiratory Journal*. 2013; 42(1): 169-179.
60. Sharma SK, Mohan A. *Indian Journal of Medical Research*. 2013; 137(3): 455-493.
61. Udwardia Z, Vendoti D. *Journal of Epidemiology and Community Health*. 2013; 67(6): 471-472.
62. Mortaz E, Adcock IM, Tabarsi P, Masjedi MR, Mansouri D, Velayati AA, Casanova JL, Barnes PJ. *Journal of clinical immunology*. 2015; 35(1):1-0.
63. WHO global report. 2018;
<http://apps.who.int/iris/bitstream/handle/10665/274453/9789241565646-eng.pdf?ua=>.

Chapter: 1 (B)

Importance of computational chemistry in drug discovery

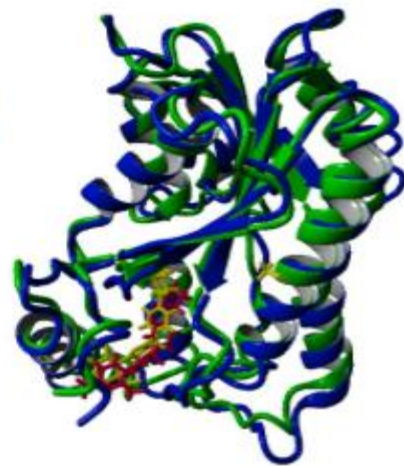
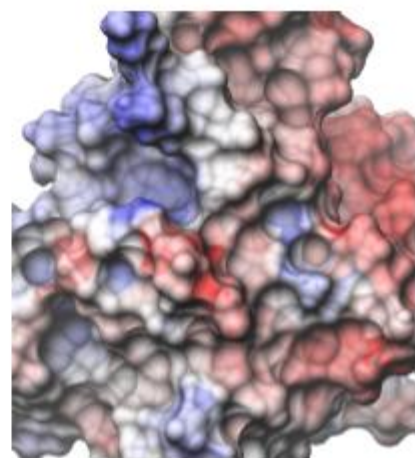
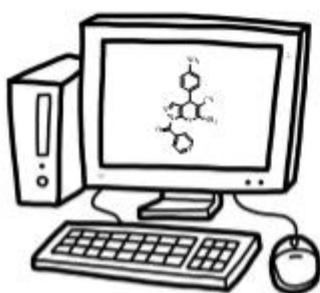


Table of Contents

1.0 Introduction	27
1.1 Role of Computer Aided Drug Design in Drug Discovery	28
1.2 Structure-based drug design	32
1.3 Ligand-based drug design	33
1.4 <i>In silico</i> virtual screening	33
2.0 Some important tool for computational based drug discovery	35
2.1 <i>de novo</i> design	35
2.2 ADME/T pharmacokinetics properties	36
2.3 Pharmacophore generation	37
2.4 Molecular docking	37
2.5 Molecular dynamics	38
2.6 QSAR study	38
2.7 DFT study	39
2.8 HOMO-LUMO study	40
3.0 Enoyl ACP reductase as an attractive target for the treatment of <i>Tuberculosis</i>	41
References	43

1.0 Introduction

The design and development of new drugs is easier when one has a full understanding of the disease development and reliable structural information about the target and its inhibitors. However, in the design of a new drug candidate, the structural information about the target molecule is normally unavailable. Proteins and enzymes are the best target because they are usually smaller and not attached to other structures and as a result it's easier to isolate and characterize them. Still, there can be problems in obtaining the structural information when enzymes and proteins are selected as drug targets. Sometimes the direct study of the target enzyme is challenging to isolate or produce in appropriate quantities. All these are the difficulties in the drug design and developments. To conquer these difficulties, computer aided molecular modelling or drug design could be an answer because this process provide few important different types of information to scientist that is important for drug designing:

- The chemical and physical characteristics and properties of a molecule,
- The three-dimensional structure of a molecule,
- Predictions of some important biological properties of a molecule,
- Visualization of complexes formed between molecules and receptors,
- Comparison of the structure with different molecules.

Developments in the computational techniques have enabled virtual screening to have a positive impact on the drug discovery process. In this thesis, efforts have been made to design various novel heterocyclic compounds by using computer aided drug design

techniques, hence, in this chapter an information about various computer aided drug designing techniques and the enzyme used in the study are discussed.

The Drug Discovery Challenge

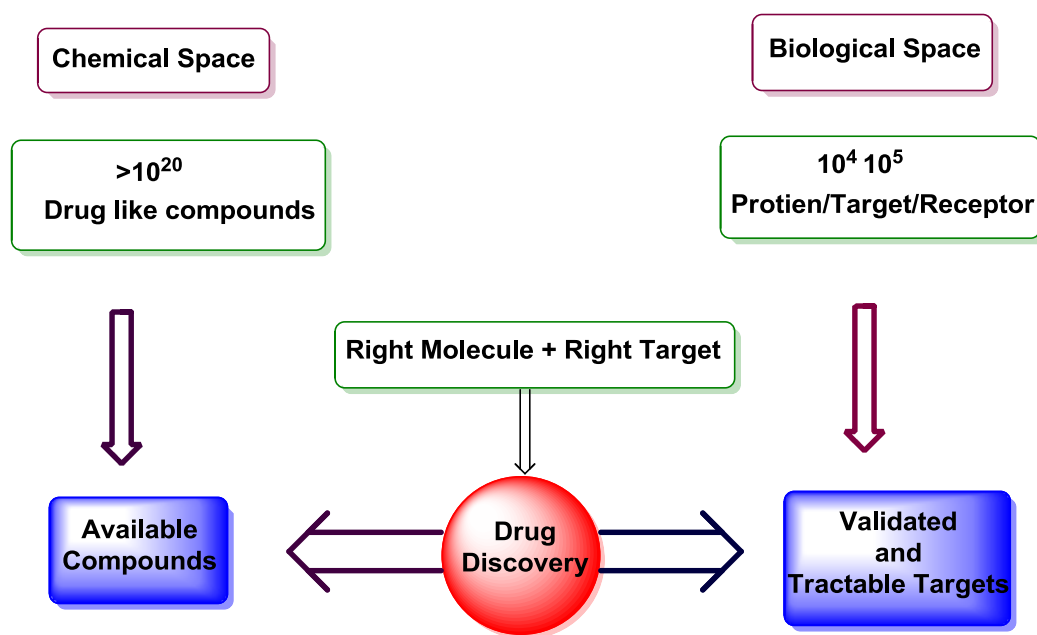


Figure. 1 Drug discovery and development challenges in modern era.

1.1 Role of Computer Aided Drug Design in Drug Discovery

The life of human is continuously threatened by diseases. Thus, medications are always in great demand for the prevention and treatment against various diseases. As a result of this, the discovery of safe drugs, techniques and methods for drug discovery and development are in great demand. The process of drug development is very expensive and time consuming process. To introduce a chemical compound in market as a new Drug requires more than 10-15 years of hard work and an enormous amount of money. Therefore, to overcome this challenge various new technologies have been developed and applied in drug research to shorten the research cycle and to reduce the expenditures. Computer-aided Drug design (CADD) is one of such evolutionary technologies in modern era [1].

Computer based drug design is a fast, powerful and reliable technique that increases the efficiency of the process of drug development and thus decreases the cost [2]. To synthesize correct drug candidates, numerous computer simulation techniques give a better information about the action of the drugs and can highlight various properties which will defiantly help to synthesize right drug. Innovative developments in computer technology reduce the number of new compounds that need to be synthesized and tested, so the process of drug discovery will be faster. This type of computational work is done on high configuration computers or workstations. Molecular modelling is in a way similar to this glamorous and thrilling profession because we all know that ‘modelling’ is the world of glamour which is attached with latest trends and fashions. Here the computer screen depicts as the ramp with beautiful graphical interface. The molecules perform a catwalk just in the same way as human models do. This catwalk is performed in order to achieve the desired conformation that is the highest stable and energetically favourable structure. The conformation of molecule which successfully clear all the stages are considered to be the best structure and selected for interaction with the targeted receptor. In other words, the selected molecule can be used for further development process.

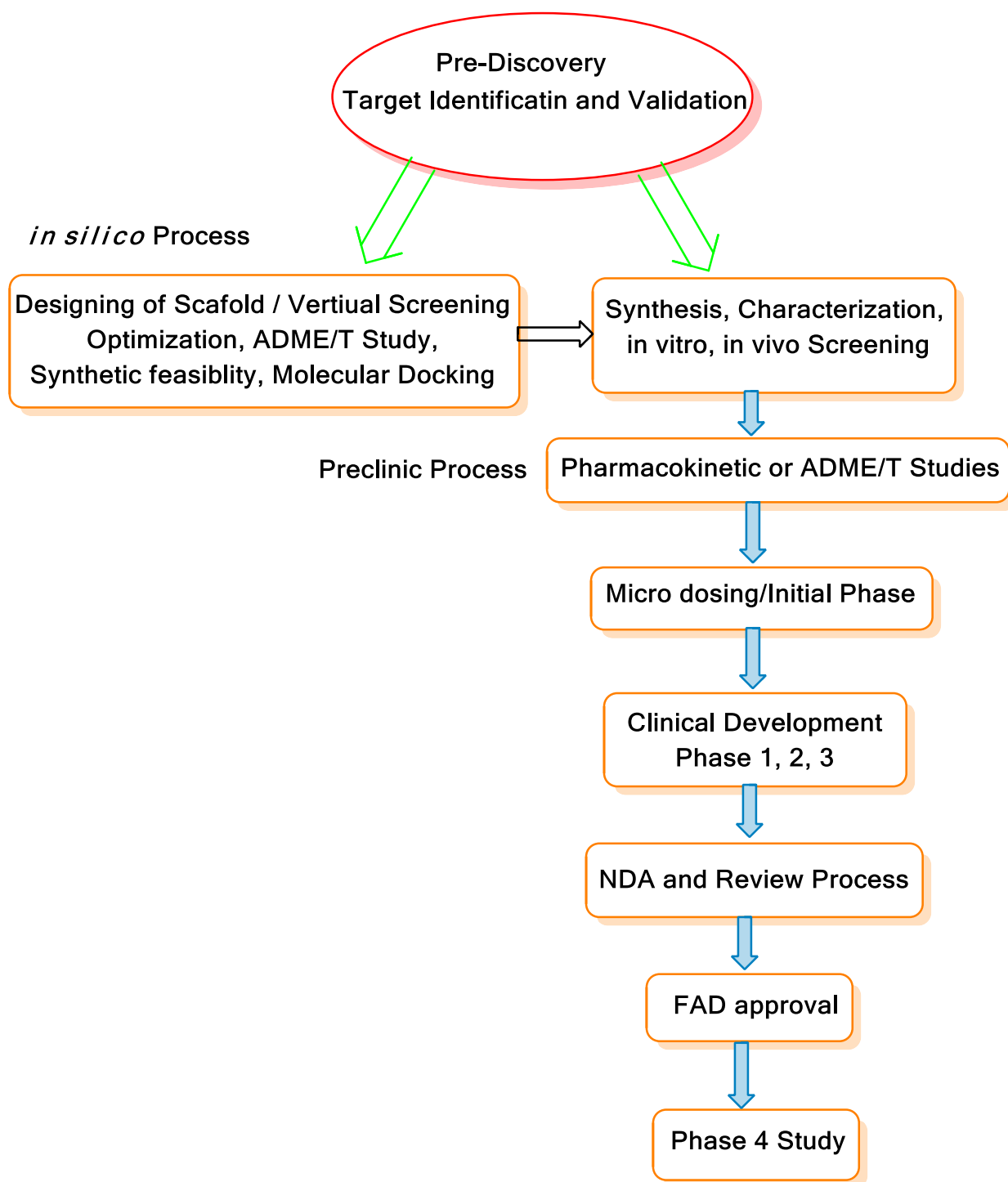


Figure. 2 Overall computational based drug discovery process

The important objectives of CADD are lead identification, lead optimization and analysis. The three-dimensional structures of drug molecules and receptors with their conformational flexibility play the important role in the drug designing process.

Molecular modelling with variety of computer-based simulation techniques, can build 3D models of molecules and calculate various molecular properties, such as energy of the conformer of the molecule with respect to the positions of atoms in molecules that highlight intra and intermolecular interactions of the system. From this above knowledge one can design a molecule with desired properties. As a result, molecular modelling helps to simulate, predict and explain the 3D structures and physiochemical properties of biomolecules, which play an important role in drug-interactions. Conformational energies are usually calculated using either quantum or molecular mechanics. CADD tools have been developed initially for lead optimization such as QSAR and then later on extended for lead discovery such as virtual screening. However, in the post genomic period, there has been a dramatic increase in information about small molecules and biomolecules. Hence, changing the strategy for the pipeline of drug discovery, CADD techniques have been applied at almost every stage of drug discovery and development [4]. CADD has expanded traditional application of lead identification and optimization in two ways [5]: (1) Upstream for target identification and validation and (2) Downstream for ADMET predictions (Preclinical study).

Producing new chemical entities for clinical use of successful drug design projects required continues efforts and a multidisciplinary team. A computational chemist can play an important role in the team and based on data can facilitate decision making on the right lead candidates for the right target enzymes [6-7]. Different techniques of computer-aided drug design are used based on the available information about the target protein and the ligands [8]. With this knowledge, either the structure-based or the ligand-based molecular design methods can be used. Structure-based drug designing uses a known set of ligands with an unknown receptor site, while ligand based drug designing approach starts with a

known receptor, such as a protein or enzyme interaction site. This both the approaches are actually very similar.

1.2 Structure-based drug design

The 3D structure of a receptor or protein offers an important information for understanding its interactions and biochemical functional properties at molecular level [9]. Moreover, the site-directed mutagenesis, pharmacophore-based strategies on the binding site can provide an important information on the interactions between the bindings of the ligands with amino acids. However, this indirect approaches cannot compete with the actual insight obtained from experimentally determined ligand-protein complexes and target-protein structures. The availability of a reliable model of the receptor/enzyme site support the structure based drug designing approach. With the great knowledge of the enzyme/receptor site, it is possible to design ligands that bind favorably at the site using molecular docking techniques. The structure-based drug design process proceeds through multiple cycles before an optimized lead candidate goes into phase I clinical trials [9]. The determination of the binding site of structure is first step using standard analysis from NMR analysis, X-ray diffraction, homology modelling or calculations including molecular mechanics or molecular orbital and molecular dynamics techniques.

The structure-based drug design process contains the following steps:

- With the use of computer algorithm, ligands from a known database are docked into the active site of receptor. These ligands are scored and ranked based on their steric and electrostatic interactions with the active site of receptor and the best ligands are tested with biological screening.
- The second step, structure determination of the complex of the target and the lead molecule which has shown micro molar inhibition in the in vitro studies, give

information of active sites on the compound that can be optimized to increase effectiveness.

- Third step comprise synthesis of the optimized compounds, which shows improvement in binding affinity and specificity for the target.

1.3 Ligand-based drug design

Ligand-based drug designing methodology is used when a series of compounds have been identified that enhance the activity of interest but the structure of the protein/enzyme is unknown. Molecular modelling of known active ligands can be used to extract indirect information about the molecular interactions at the binding site of protein in absence of the structure of the targeted protein. This techniques requires most efficiently, structurally similar compounds with high activity, with moderate activity and with a range of intermediate activities. Additionally, to identify pharmacophore site mapping the structures of the compounds used in the study, which is nothing but the template which derived from the compounds. In conclusion, the lead candidates which have been predicted to have a potent biological activity are synthesized and tested for the further development.

1.4 *In silico* virtual screening

Virtual screening is a process which includes a number of computational technique and protocols that helps chemist to decrease an enormous virtual library into a convenient size. Developed computational approaches have allowed virtual screening to have a positive effect on the drug discovery and development process. As mention above virtual screening is also based on ligand-based virtual screening and structure based virtual screening. Moreover, these techniques involves the molecular docking study which provides the binding affinity of ligand receptor, binding interactions and binding energy [10].

Virtual screening is useful when the number of available library of ligands exceeds the experimentally based screen capacity to evaluate these ligands. Virtual screening can be used to identifying a greater number of hits with screening of a random subset of compounds selected from the same library. The number of compounds that could be synthesized by using combinatorial chemistry protocols significantly increase the synthetic capability. The development of virtual screening procedures increase the potentials of molecules that do not exist physically in collection of scientist but which can be readily achieved through synthesis or purchase. The attrition rates are very high in HTS. Therefore, to filter out unpromising set of ligands at the very beginning an alternative in silico virtual High Throughput Screening (vHTS) process has become very popular nowadays. *In silico* screening or virtual screening, is a new approach increasing levels of interest in the pharmaceutical industry as a productive and low-cost effective techniques in the search for novel lead compounds [11]. Virtual screening is more favourable to the high-throughput screening of large compound libraries and can be considered as a practical substitute when the relevant binding geometries must be generated and binding affinities of ligands with the protein investigation can be predicted properly [12]. The benefits of virtual screening is based on the predicted binding interactions data, only few subset of ligands need in vitro testing which helps to reducing the time and expenditure to identify new leads for further development [13]. Numerous virtual screening programs have been developed with primarily two parts of variety where one is scoring and other is functions [14] and Optimization methods [15]. From the existing docking programs, the most widely used are Glide, GOLD [16], AutoDock [17], and DOCK [18].

Table.1 Widely used virtual screening program

METHOD	LIGAND FLEXIBILITY SAMPLING	SCORING FUNCTION
GLIDE (SCHRODINGER)	Exhaustive search	Empirical score
DOCK	Incremental build	Force field or contact score
FLEXX	Incremental build	Empirical score
SLIDE	Conformational ensemble	Empirical score
FRED (OPENEYE SOFTWARE)	Conformational ensemble	Gaussian score or empirical scores
GOLD	Genetic algorithm	Empirical score
AUTODOCK	Genetic algorithm	Force field
LIGANDFIT (ACCELRY'S)(DISCOVERY STUDIO)	Monte Carlo	Empirical score
ICM	Pseudo-Brownian sampling and local minimization	Mixed force field and empirical score
QXP	Monte Carlo	Force field

Openeye Software, <http://www.eyesopen.com>; Schrodinger, <http://www.schrodinger.com>; Accelrys, <http://www.accelrys.com>.

2.0 Some important tool for computational based drug discovery

2.1 *de novo* design

The main objective of the HTS and VS techniques is to find a lead compound by searching for hits in large compound libraries. Different pharmaceutical companies may have these compounds libraries and overlap to a certain level, thus leading to the detection of identical hits by companies that work on the same receptor or target. To overcome this problem, *de novo* designing reduce the risk of identical hit retrieval which don't have similarity directly to present compound libraries. Therefore, computational *de Novo* design may be observed as a complementary technique to HTS and VS and may provide competitive benefit [19]. *de Novo* design use to generate a novel molecular structures that

display desired biological activity and shows great binding affinity to a particular biological receptor or target. This binding interactions can be defined by either the known reference ligand (ligand-based approach) or with 3D target structure (structure-based approach) [20].

Ligand-based de novo designing is quite similar to structure-based de novo designing approaches by working individually from the 3D structure of target/receptor [21]. The requirement for ligand-based de novo design is that one or more ligands have to bind with the biological receptor/target. Ligand based designing generates primary target constraints from one or more known ligands. While, Structure-based design approach essentially works in 3D space and has to deal with the difficulty of molecular conformations. Ligand-based scoring functions identify the similarity between known reference ligands and a candidate ligand. QSAR study, pharmacophore models and chemical similarity have been used to evaluate the potential binding affinity of candidate ligands in de novo design techniques [22-23].

2.2 ADME/T pharmacokinetics properties

Lack of ADME/Tox may lead to failure of almost 40%-60% of developing drugs during the clinical trials studies. Virtual screening is should not limited to improve selectivity and binding affinity optimization only, but the pharmacokinetic properties of ligands should also be included as significant filters in virtual screening. ADME is known for adsorption, distribution, metabolism and excretion in pharmacokinetics and is an important part to test the drug likeliness of compounds [24]. The ADME is directly connected to utilizing molecular properties, such as bioavailability and membrane permeability which associated with few important molecular descriptors. These molecule descriptors include molecular weight, partition coefficient (logP) and number of hydrogen bonds acceptors and donors in a ligands [25].

2.3 Pharmacophore generation

Pharmacophore modelling is a significant tool in drug discovery and development because of significant development of pharmacophore technology. A pharmacophore can be defined as a collaborative of electrostatic and steric features that is essential to ensure optimal ligand interactions with a particular biological target and to speed up its biological response. It can also be defined as the three-dimensional arrangement of chemical features recognized by a receptor and responsible for biological activity [26]. Pharmacophore model is developed by superimposing a set of active ligands and identifying their common chemical features that helps to increase the binding interactions with the target protein. It is also beneficial if shape limitations describing the steric boundaries of the binding site which can be indirect from the dataset [27]. Such as, a region occupied by inactive molecules but not by their active analogues can be defined as sterically prohibited. A pharmacophore model can be utilized to understand the SAR of a series of compounds also use in the search for novel structures with the same pharmacophore and molecular arrangement process in 3D-QSAR. Therefore the pharmacophore model is worthwhile in lead discovery and optimization [28].

2.4 Molecular docking

Molecular docking is a key tool in structural molecular biology and computer-assisted drug development [29]. The goal of ligand-receptor/protein docking to calculate the binding interactions of a ligand with the protein of known three-dimensional structure to predict free binding energy [30]. The process of searching high-dimensional spaces successfully and using a scoring function that correctly ranks candidate dockings with the help of search algorithm. The different number of configurations created by search algorithm that also involve experimentally determined binding interactions [31]. Despite

all the potential methodologies, ligand chemistry such as tautomerism and ionization, scoring function and receptor flexibility and differentiate true binding mode still remained the challenge.

2.5 Molecular dynamics

Molecular dynamics simulations is described by force fields and which include semi empirical factors and physical equation that represent the total interactions in the ligand-protein complex system [33]. The molecular dynamics are acquired using the quantum mechanics by utilizing these parameters [33]. Then, the ligand-protein complex is solvated in a cubic box of selected solvent. This phenomena helps the selected solvents and proteins particles to collaborate between themselves with in the cubic box [34]. Eventually, energy minimization was completed by sharpest approach to evacuate the neighboring interactions [35]. The energy minimization shakes the whole outline until close contacts are reduced and the outline tends towards a most stable condition called minimized energy state. In general, the protein may carry the charge. Thus, atoms (Na^+ or Cl^-) are involved to balance the system. The system was balanced at steady temperature and weight employing NVT and NPT steps after the energy minimization. The long range electrostatic co-operations were taken care of by part network Ewald calculation along with restrains the bond distances at their equilibrium values [36]. The protocols of simulation techniques fuses different examinations to understand a protein/enzymes structure.

2.6 QSAR study

Quantitative structure-activity relationship (QSAR) and quantitative structure property relationship (QSPR) are two of the helpful methods of CADD for drug design and makes it possible to predict the activities of a given compound. Basically, untested and novel compounds having similar molecular structures as compounds used in the

development of QSAR models are similarly expected to enhance similar activities. From recent decade a number of successful QSAR models have been published which comprise a wide range of biological properties. QSAR has great prospective for modeling and designing novel compounds with potent physiochemical and biological properties by a function of structural features.

QSAR study involve few essential steps such as, designing a novel chemical or biological compounds, generation of effective descriptors, selection of reverent descriptors to include in model, development of a regression model and testing the stability and validity of the recommended model. However, the development and efficiency of QSAR study is impossible without numerous efforts in the generation and development of various molecular descriptors [37].

2.7 DFT study

DFT (Density functional theory) is a computational technique which is based on quantum mechanical modelling method used in chemistry, physics and materials science to investigate the electronic structure or ground state of many-body systems such as atoms, molecules, and the condensed phases. Quantum chemistry is important branch of chemistry whose major effort is to use the quantum mechanics in experiments of chemical systems and physical models. The information about the given system is derived by the quantum mechanical wave function. The Schrödinger equation can be solved by a simple 2-D square potential or even a hydrogen atom exactly in order to get the wave function of the system, followed by the determination of acceptable energy states of the system. However, we must include certain calculations to reduce the difficultly to soluble albeit tricky because it is difficult solve Schrodinger equation for N-Body system. DFT study is used to get the approximate solution for the Schrodinger equation of a many-body system. In the 1998,

Walter Kohn for the discovery of DFT and John Pople for the development of quantum chemical techniques represents in the Gaussian electronic structure codes got the Nobel Prize.

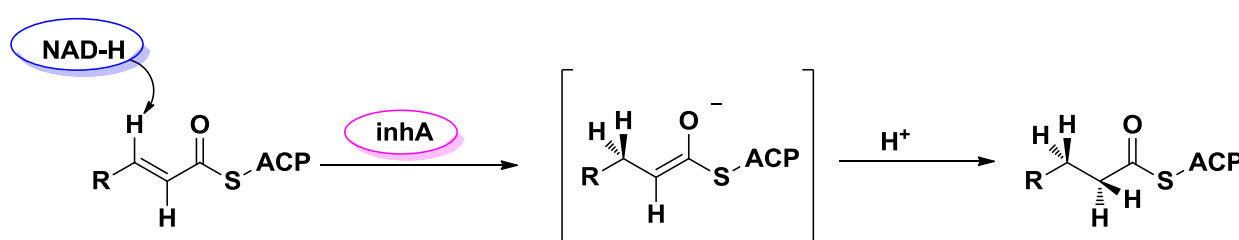
2.8 HOMO-LUMO study

The chemical stability of compound is calculated by most important Frontier Molecular Orbital (FMOs) such as highest occupied molecular orbital (HOMO) and lowest unoccupied molecular orbital (LUMO) [38]. The FMOs play a significant role in the electric and optical properties, as well as in UV-Visible spectra and quantum chemistry [39]. The HOMO study signifies the capability to donate an electron and LUMO act as an electron acceptor to accept an electron. Moreover, the chemical reactivity, optical polarizability and chemical hardness-softness of the molecule is also determine by calculating the energy gap between HOMO and LUMO [40].

3.0 Enoyl ACP reductase as an attractive target for the treatment of *Tuberculosis*

The Enoyl acyl carrier protein reductase formerly known as InhA, is most important enzyme from *Mycobacterium tuberculosis*, as it involved in the type II fatty acid biosynthesis pathway of *Mycobacterium tuberculosis*. In the past decade, beginning with the discovery of most potent first-line and most efficient anti-tubercular drug INH block the mycolic acid biosynthesis through the inhibition of InhA (2- trans-enoyl-acyl carrier protein reductase). As a result there have been several efforts to develop novel and potent InhA inhibitors as leads for development of novel TB agents. The final enzymatic step in the elongation cycle of the FAS-II pathway is catalyzed by InhA which is encoded by *Mycobacterium tuberculosis* gene *inhA* [41]. InhA is a NADH-dependent reductase that exhibits specificity for long chain enoyl thioester substrates. The reduction mechanism of this process is shown in **Figure. 3**. Furthermore, InhA enzyme inhibition leads to the inhibition of mycolic acid biosynthesis in mycobacterium, accumulation of long-chain fatty acids [43].

Figure. 3 Reduction mechanism of InhA [42].



Enoyl-[acyl-carrier-protein] reductase [NADH] FabI could be found in many known organisms, such as *Mycobacterium tuberculosis*, *Mycobacterium smegmatis*, *Escherichia coli*, *Plasmodium falciparum* and *Staphylococcus aureus* [44]. InhA molecule from *mycobacterium tuberculosis* is a homo tetramer in aqueous solution and crystal structure in

3.0 ENOYL ACP REDUCTASE AS AN ATTRACTIVE TARGET FOR THE TREATMENT OF TUBERCULOSIS

complex with NAD^+ . A fatty acyl substrate confirms that the substrate binds in a general U-shaped conformation [45]. The residues crucial for trans-enoyl reduction catalysis, Tyr 158 and Lys 165, are situated at the active site. InhA facilitates reduction by a catalytic mechanism in which a hydride is transferred to the C3 carbon of the C2-C3 double bond. The C1 carbonyl oxygen accepts a proton from the Tyr 158 hydroxyl, which forms an enolate anion [46]. The complete fatty acyl chain of the bound substrate is surrounded by hydrophobic residues where the majority of residues are located on the substrate binding loop [47]. The substrate binding loop of InhA is larger and creates a deeper substrate binding crevice, as a result the ability of InhA is recognized as a longer chain fatty acyl substrates. Residue Tyr 158 is protected in the bacterial FabIs and plant Enoyl-ACP reductases, binding with residue Tyr 158 is an important feature of the fatty acyl substrate binding common to other Enoyl-ACP reductases [48]. The decreased action of InhA leads to the death of cells due to the loss cell integrity. InhA was validated as a significant target for the development of novel anti-tubercular agents due to a crucial role of InhA in the fatty acids elongation cycle [49-50].

Furthermore, targeting mycobacterial enzymes with a small molecules and resulting disturbance of cellular homeostasis remains a most significant methodology [51-53]. There are some small molecules, which inhibit directly InhA and do not require the bio-activation by KatG and are capable to bypass mechanism of drug resistance to inhibitors, like Isoniazid and Ethambutol. Such small molecules active without bio-activation are rational approach that may further develop as a novel anti-tubercular agents. This methodology holds a potential to develop the novel InhA inhibitors which active against MDR-TB and XDR-TB strains [54].

References

1. Jorgensen, W. *Science*. 2004; 303:1813-1818.
2. Kapetanovic I. *Chemico-Biological Interactions*. 2008; 171:165-176.
3. Tang Y, Zhu W, Chen K, Jiang YL. *Drug Discovery Today: Technologies*, 2006; 3:307-313.
4. Machin P, Ford M, Livingstone D, Dearden J, Van de Waterbeemd, FL Eds.; Blackwell Publishing: Oxford, UK., 2003, pp. 1-4.
5. Ford M, Livingstone D, Dearden J, Van de Waterbeemd, FL Eds. Blackwell Publishing: Oxford, UK. 2003; 1-4.
6. Ooms F. *Current Medicinal Chemistry*, 2000; 7:141-158.
7. Bordoli L, Kiefer F, Arnold K, Benkert P, Battey J, Schwede T. *Nature Protocols*. 2009; 4:1-13.
8. Paul D. *Drug Discovery Today*. 2002; 7:1047-1055.
9. Rarey M, Kramer B, Lengauer T, Klebe G. *Journal of Molecular Biology*. 1996; 261(3): 470-489.
10. Morris, GM, Goodsell DS, Halliday R, Huey R, Hart WE, Belew RK, Arthur J. *Journal of Computational Chemistry*. 1998; 19:1639-1644.
11. Kuntz ID, Blaney JM, Oatley SJ, Langridge R, Ferrin TE. *Journal of Molecular Biology*. 1982; 161:269-288.
12. Friesner RA, Banks JL, Murphy RB, Halgren TA, Klicic JJ, Mainz DT, Repasky MP, Knoll EH, Shelley M, Perry JK, Shaw DE, Francis P, Shenkin PS. *Journal of Medicinal Chemistry*. 2004; 47:1739-1749.
13. Flex X, Shen J, Xu X, Cheng F, Liu H, Luo X, Shen J, Chen K, Zhao W, Shen X, Jiang H. *Current Medicinal Chemistry*. 2003; 10:2327-2342.

REFERENCES

14. Anderson AC, Wright DL. *Current Computer-Aided Drug Design*. 2005; 1:103-127.
15. Kuntz ID. *Science*. 1992; 257:1078-1082.
16. Hartenfeller M, Schneider G. De novo drug design. In *Chemoinformatics and computational chemical biology 2010*; pp. 299-323. Humana Press, Totowa, NJ.
17. Fechner U, Schneider G. *Journal of Chemical Information and Modeling*. 2006; 46:699-707.
18. Stahura F, Bajotath. *Current Pharmaceutical Design*. 2005; 11:1189-1202.
19. Willett P. *Journal of Chemical Information and Modeling*. 1998; 983-996.
20. Schuller A, Suhartono M, Uli F, Yusuf T, Sven B, Ute S, Michael W, Gobel G. *Journal of Computer-Aided Molecular Design*. 2008; 2:59-68.
21. Li AP. *Drug Discovery Today*. 2001; 6(7):357-366.
22. Lipinski CA, Lombardo F, Dominy BW, Feeney PJ. *Advanced Drug Delivery Reviews*. 1997; 23(1-3):3-25.
23. Wermuth G, Ganellin E, Lindberg P, Mitscher L. *Pure and Applied Chemistry*. 1998; 70:1129-1143.
24. Van Drie, J. *Current Pharmaceutical Design*. 2003; 9:1649-1664.
25. Patel Y, Gillet V, Bravi G, Leach A. *Journal of Computer-Aided Molecular Design*. 2002; 16:653-681.
26. Kokh DB, Rebecca CW, Wenzel W. *WIREs Computational Molecular Science*. 2011; 1(2):298-314.
27. Ruppert J, Welch W, Jain AN. *Protein Science*. 1997; 6(3):524-33.
28. Taylor RD, Jewsbury PJ, Essex JW. *Journal of Computer-Aided Molecular Design*. 2002; 16(3):151-66.

29. Lindahl E, Hess B, van der Spoel D. *Journal of Molecular Modeling*. 2001; 7:306–317.
30. Cickovski T, Chatterjee S, Wenger J, Sweet CR, Izaguirre JA. *Journal of Computational Chemistry*. 2010; 31:1345-56.
31. Petrov D, Margreitter C, Grandits M, Oostenbrink C, Zagrovic BA. *PLOS Computational Biology*. 2013; 9:e1003154.
32. Figueroa M, Martínez-Oyanedel J, Matamala AR, Dagnino-Leone J, Mella C, Fritz R. *Journal of Protein Science*. 2012; 21(12):1921-8.
33. Darden T, Perera L, Li L, Pedersen L. *Structure*. 1999; 7(3):55-60.
34. Todeschini R, Consonni V. Wiley-VCH, Weinheim, 2009.
35. Gunasekaran S, Balaji RA, Kumaresan S, Anand G, Srinivasan S. *Canadian Journal of Analytical Sciences and Spectroscopy*. 2008; 53:149–162.
36. Fleming I. Wiley, London, 1976.
37. Kosar B, Albayrak C. *Spectrochimica Acta. Part A, Molecular and Biomolecular Spectroscopy*. 2011; 78:160–167.
38. Banerjee A, Dubnau E, Quemard A, Balasubramanian V, Um KS, Wilson T, Collins D, de Lisle G, Jacobs WR. *Science*. 1994; 263:227-230.
39. Dessen A, Quemard A, Blanchard JS, Jacobs WR, Sacchettini JC. *Science*. 1995; 267(5204):1638-41.
40. Kamphorst JJ, Nofal M, Commisso C, Hackett SR, Lu W, Grabocka E, Vander Heiden MG, Miller G, Drebin JA, Bar-Sagi D, Thompson CB. *Analytical Chemistry*. 2010; 82(8):3212-21.
41. Takayama K, Wang L, David HL. *Antimicrobial Agents and Chemotherapy*. 1972; 2(1): 29-35.

REFERENCES

42. Winder F.G. and Collins P.B., Whelan D. *Journal of General Microbiology*. 1971, 66:379-380.
43. Vilchèze C, Morbidoni HR, Weisbrod TR, Iwamoto H, Kuo M, Sacchettini JC, Jacobs WR. *Journal of bacteriology*. 2000; 182(14):4059-67.
44. Wang F, Nguyen M, Qin FX, Tong Q. *Aging cell*. 2007; 6(4):505-14.
45. Massengo-Tiassé RP, Cronan JE. *Cellular and Molecular Life Sciences*. 2009; 66:1507-17.
46. Rozwarski DA, Vilcheze C, Sugantino M, et al. *Journal of Biological Chemistry*. 1999; 274:15582-9.
47. Parikh S, Moynihan DP, Xiao G, Tonge PJ. *Biochemistry*. 1999; 38:13623-34
48. Lu XY, Huang K, You QD. *Expert Opinion on Therapeutic Patents*. 2011; 21:1007-22.
49. Tonge PJ, Kisker C, Slayden RA. *Current Topics in Medicinal Chemistry*. 2007; 7:489-98,
50. Maresca A, Vullo D, Scozzafava A, et al. *Journal of Enzyme Inhibition and Medicinal Chemistry*. 2013; 28:392-6
51. Maresca A, Scozzafava A, Vullo D, Supuran CT. *Journal of Enzyme Inhibition and Medicinal Chemistry*. 2013; 28:384-7
52. Maresca A, Carta F, Vullo D, Supuran CT. *Journal of Enzyme Inhibition and Medicinal Chemistry*. 2013;28:407-11
53. Pan P, Tonge PJ. *Current Topics in Medicinal Chemistry*. 2012; 12:672-93
54. Espinal MA. *Tuberculosis*. 2003; 83(1-3):44-51.

Chapter: 1 (C)

Review of literature

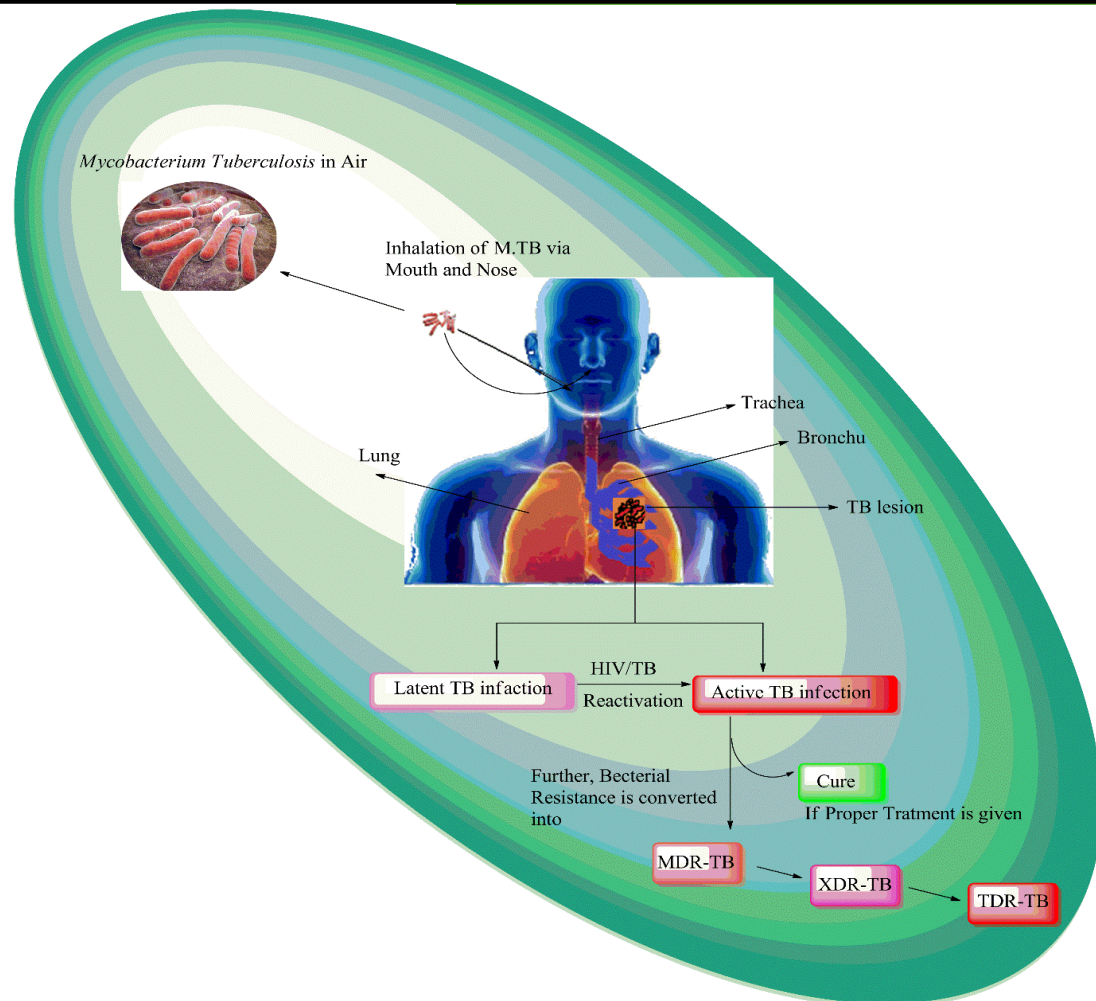


Table of Contents

1.0 Introduction	47
2.0 The Past	48
2.1 Existing first line anti-TB agents.	48
2.1.1 Rifampicin	48
2.1.2 Isoniazid.....	50
2.1.3 Pyrazinamide	52
2.1.4 Ethambutol.....	54
2.2 Existing Second line anti-TB agents.	57
2.2.1 Streptomycin.....	57
2.2.2 Ethionamide.....	59
2.2.3 Fluoroquinolone.....	61
2.2.4 Para-aminosalicylic acid.....	62
2.3 Existing Injectable anti-TB agents	62
2.3.1 Capreomycin and Viomycin.....	62
2.3.2 Kanamycin.....	64
2.3.3 Amikacin	67

3.1 Recently approved by FDA.....	67
3.1.1 OPC-67683	67
3.1.2 TMC-207	69
3.2 Currently evaluated for their anti-TB activity.....	70
3.2.1 Gatifloxacin and Moxifloxacin.....	70
3.2.2 Linezolid.....	71
4.0 The Future.....	72
4.1 Under various phases of clinical & preclinical development.....	72
4.1.1 PA-824.....	72
4.1.2 SQ109	74
4.1.3 PNO-100480.....	75
4.1.4 AZD5847	77
4.1.5 LL3858	78
4.2.1 SQ609	79
4.2.2 BTZ043.....	79
4.2.3 DC159a.....	81
4.2.4 CPZEN-45	81

4.2.5 Q-203	83
4.3.1 DNB-1	84
4.3.2 TBA-354.....	84
5.0 Recent developments for MDR-TB.....	86
5.1 Nitroimidazoles	86
5.2 Dihydroquinoline	88
5.3 Macrolides	89
5.4 Oxazolidinones.....	90
5.5 Ethylenediamine.....	91
6.0 Benzimidazole: A milestone in the field of medicinal chemistry.....	92
6.1 Anti-Tuberculosis and Anti-bacterial activities of benzimidazole.....	94
6.2 Anti-malarial activities of benzimidazole	102
7.0 Biological importance of 4H-Pyran.....	108
8.0 Conclusion.....	110
References.....	111
□ Aim and Objectives of the present work.....	136

Summary:

The emergence of multi-drug resistant tuberculosis (MDR-TB) outbreaks during the 1990s and additionally in recent times the vast deadly strains of extensively drug-resistant tuberculosis (XDR-TB) and totally drug resistance tuberculosis (TDR-TB) is hampering efforts to control and manage tuberculosis (TB). As a result, novel methodologies for the treatment of multidrug-resistant and extensive drug-resistant tuberculosis (TB) are severely desired. A number of new potential anti-tuberculosis drug candidates with novel modes of action have been entered in clinical trials in recent years. These agents are most likely to be effective against resistant strains. The treatment landscape is beginning to shift, with the recent approvals by FDA to the new TB drugs Bedaquiline and Delamanid. Also, the pipeline of potential new treatments have been fulfilled with several compounds in clinical trials or preclinical development with promising activities against sensitive and resistant *Mycobacterium tuberculosis* bacteria. An additional new chemical entity is also under development. Moreover, in the last 2-3 decades, the broad research in the application of benzimidazole and 4*H*-Pyran derivatives made it important for mankind and many scientists have found that this compounds have diverse role in the field of medicinal chemistry. Moreover, the benzimidazole and 4*H*-pyran derivatives exhibit numerous pharmacological activities. In this review of literature, the already existing drugs of TB with their treatment, anti-tuberculosis drug pipeline, various derivatives of benzimidazole and 4*H*-pyran with diverse pharmacological activities has been summarized. This findings may lead to scientists whose are working in the field of medicinal chemistry for the development of benzimidazole based drug candidates in the future.

1.0 Introduction

The already existing first-line and second-line anti-tuberculosis drugs are enormously used which were discovered way back in the 1950s. Due to meagre success attempt rate obtained in the development of novel anti-tuberculosis drugs in the recent past, a lot of problems like Drug-Resistant (DR-TB), Multi-Drug Resistant (MDR-TB), Extensively Drug Resistant (XDR-TB), and recently emerging threat Totally Drug Resistant (TDR-TB) are prevailing. So, to cure these problems there occurs an urgent need for the development of new anti-TB drugs which can be used for reducing problems as seen before. Due to limited resources, diagnosis of MDR-TB often takes place only after treatment failure. This approach leads to an increase in morbidity and mortality, as well as the development of further drug resistance that is difficult or impossible to treat. The FDA recently released draft guidance for the co-development of two unmarketed drug candidates, signalling their willingness to consider registration of new drug combinations prior to individual drug registration.

The past decade has seen the progress of few compounds into the clinical development pipeline, including new compounds specifically developed for tuberculosis. Furthermore, the challenges arise from vicious interactions between the human immunodeficiency virus (HIV) and TB in the discovery of the anti-tubercular drug [1]. For the treatment of TB, the main factors for the development of novel anti-TB drugs, better drugs, and regimens are causes of lengthy duration and complex nature of existing TB therapy and the resulting emergence of MDR-TB and XDR-TB, and the compatibility of key anti-tuberculosis drugs with antiretroviral therapy.

Tuberculosis emerging worldwide threat day by day with developing resistance against existing anti-TB drugs. So, stop this TB burden worldwide, there is an urgent need

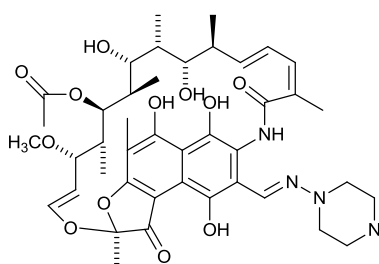
2.0 THE PAST

to discover novel anti-TB drug candidates which have a novel mechanism of action against TB bacteria and it should help to shorten the current TB treatment. The potentiality of the tuberculosis drugs, drugs in pipeline, mode of action and their limitations, mutations of bacteria and biologically important heterocycles will be discussed in this chapter.

2.0 The Past

2.1 Existing first line anti-TB agents.

2.1.1 Rifampicin



Rifampicin-1972 (1)

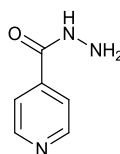
In 1957, the Lepetit Pharmaceuticals research lab in Italy was brought a soil sample for analysis from a pine forest on the French Riviera. There, a research group supervised by Piero Sensi and Maria Teresa Timbal discovered a new bacterium. This newly discovered bacterium appeared of interest since it was producing a new class of molecules with antibiotic activity. They decided to call these compounds "Rifamycins" and the reason behind the name of this newly discovered compound because of the French crime story Rififi it is about a jewel heist and rival gangs which is particularly fond by Sensi, Timbal, and the researchers [2]. In 1959, after two years of attempts to find more stable semisynthetic products, and this newly produces molecule have a high efficacy and good tolerability and was named as "rifampicin". Rifampicin (1) was first sold in 1971 [3]. In 1972, as an anti-tubercular drug Rifampicin was first introduced and it was an extremely effective against *Mycobacterium tuberculosis*. Rifampicin targets by binding with the mycobacterial DNA-dependent RNA polymerase and thereby attack the organism and kill by interfering in the transcription process [4].

Rifampicin along with Isoniazid forms the backbone of first line and short course chemotherapy by reason of its high bactericidal action. Because of the widespread application and results in the selection of mutants resistant to other components of short course chemotherapy is increasing Resistance to Rifampicin. Hence, resistance to Rifampicin can be considered as a surrogate marker for Multiple Drug Resistant Tuberculosis (MDR-TB) [5]. Spontaneous mutation, which occurs at a rate of 10^{-8} in *Mycobacterium tuberculosis* is the root for Resistance to Rifampicin [6]. RNA polymerase has a composed of four different subunits α , β , β' and σ , encoded by proA, rpoB, rpoC and rpoD, respectively, is highly conserved among bacterial species complex oligomer. Characterization of the rpoB genetic factor in E.coli confirmed that mutations within the rpoB locus conversed conformational changes resulting in defective binding of the drug and consequently resistance [7].

Consequently, the rpoB locus of *Mycobacterium tuberculosis* was characterized and mutations conferring the resistant trait were identified in an 81-bp RIF Resistance Determining Region (RRDR) of the rpoB RNA component equivalent to codons 507-533 [8][9]. The most commonly associated mutations with Rifampicin resistance in the majority of studies is mutations in codons 516, 526 and 531 [6][10]. Alternatively, mono-resistance to rifampicin is quite rare and nearly all rifampicin resistant strains are also resistant to other drugs, exclusively to Isoniazid. This is the object why Rifampicin resistance is considered as a surrogate marker for MDR-TB [11]. Recently, the genome sequencing studies have discovered the achievement of compensatory mutations in rpoA and rpoC, encoding α and β' subunits of RNA polymerase, with mutations in rpoB, in Rifampicin resistant strains [12].

2.1.2 Isoniazid

In 1952, INH (**2**) has been the keystone in tuberculosis chemotherapy for almost half a century since its discovery as an effective anti-tuberculosis drug [13]. INH is a prodrug, and its anti-tuberculosis function requires *in vivo* activation by katG, an enzyme with the dual activities of catalase and peroxidase. In the early 1990s, when the primary mycobacterial catalase-peroxidase gene (katG) was cloned and sequenced until the association of this enzyme with isoniazid activation was not demonstrated [14]. Resistance to INH is related with a variability of mutations disturbing one or more genes such as those encoding catalase-peroxidase (katG) [15], the enoyl-acyl carrier protein reductase involved in mycolic acid biosynthesis (InhA) [16].



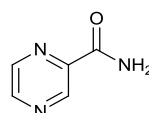
Isoniazid-1952 (**2**)

Currently, two intracellular targets for isoniazid the fatty-acid enoyl-acyl carrier protein reductase (*InhA*), and a complex of an acyl carrier protein (*AcpM*) and a β -ketoacyl-ACP synthase (*KasA*) investigated by Vilchèze et al and Slayden R.A. *et al.* [17][18]. Low-level resistance to isoniazid was exhibited via the clinical isolation of these enzymes, which are involved in the synthesis of mycolic acids, and mutations have been found in the promoter regions, or less commonly in the genes that encode these proteins (*inhA*, *acpM*, and *kasA*).

Mutations in *katG* (codon 135) or *InhA* were also found in cases of Isoniazid resistance, the role of *kasA* mutations in isoniazid resistance is currently unclear, because

similar mutations were also found in isoniazid-susceptible isolates [19]. Mutations in *dfrA* could possibly play a role in resistance to isoniazid, which is one recent interesting finding showed that the 4R isomer of the isoniazid NADP adduct origins inhibition of the dihydrofolate reductase (*DfrA*) in *Mycobacterium tuberculosis* [20]. Furthermore, 16 other proteins identified by an analysis of the proteome of isoniazid targets in *Mycobacterium tuberculosis*, in addition to *InhA* and *DfrA*, that were bound by these adducts with high affinity, which could signal other not yet clearly defined actions of isoniazid on the bacteria [21]. Several studies have found single nucleotide polymorphisms in other genes in isoniazid-resistant clinical isolates of *Mycobacterium tuberculosis*, including *kasA* and the oxy *RahpC* and fur *AKatG* intergenic regions [21][22][23]. A recent study has also found that a silent mutation in *mabA* conferred Isoniazid resistance through up regulation of *InhA* in *Mycobacterium tuberculosis* [24].

2.1.3 Pyrazinamide



Pyrazinamide-1954 (3)

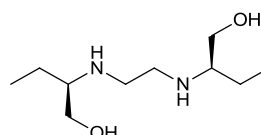
In 1936, a nicotinamide analog, Pyrazinamide (PZA) (**3**), it was first chemically synthesized [25]. In 1945, was found that a nicotinamide have tuberculostatic activity in Guinea-pigs and mice, and later, in 1947 there followed the investigation of various related drugs. Yeager *et al.* were found that an analogue of nicotinamide-Pyrazinamide to be more active in mice, and the first clinical trials of it were reported in 1952 [26]. The nicotinamide had certain activity against mycobacteria in animal models and based on an unexpected observation of this Pyrazinamide was discovered as a potent anti-TB drug [27]. TB

treatment period is 9 to 12 months and Pyrazinamide is a perilous frontline TB drug that shows an antique role in shortening it to 6 months [27][28]. The population of *Mycobacterium tuberculosis* persistence that are not killed by other drugs, it's killed by Pyrazinamide, because PZA has a powerful sterilizing activity [29]. The mechanism of action of Pyrazinamide (PZA) is well known, in *Mycobacterium tuberculosis* pyrazinoic acid (POA), the active moiety of PZA, has been shown to prevent several functions at acidic pH [30][31]. The main cause for this is often that PZA is extraordinarily absolutely different from common antibiotics, that are primarily active against growing bacterium and don't have any or very little activity against non-growing persisters. Nevertheless, PZA is precisely the alternative to common antibiotics as a result of it's no or very little activity against growing *tubercle bacilli* and is primarily active against non-growing persisters [32][33].

The Pyrazinamide (*PZase*)/ nicotinamidase, which is encoded by the *pncA* gene in *Mycobacterium tuberculosis* and as a result PZA is converted to the active form in pyrazinoic acid (POA) [34]. The conversion to pyrazinoic acid from PZA is also kind of like the nitrilase superfamily, The generates of a tetrahedral intermediate that collapses with the loss of ammonia and subsequent hydrolysis of the thioester bond by water due to the nucleophilic attack by the active site of cysteine [35][36] In 1967, McDermott's group found that the PZA resistance in *Mycobacterium tuberculosis* is related to loss of nicotinamidase and *PZase* [38][39]. The major mechanism of PZA resistance is due to mutations in the *pncA* gene encoding *PZase*/nicotinamidase [40][41]. Although the extremely different and scattered distribution of *pncA* mutations, there is some degree of clustering at three regions of *PncA*: 3–17, 61–85, and 132–142 [42]. Recently, how very diverse mutations can contribute to PZA resistance was solved by the crystal structure of

Mycobacterium tuberculosis PncA [42]. Additionally, it was shown that some PZA-resistant clinical isolates such as DHM444 without *pncA* mutations [43] and *Mycobacterium canettii* had mutations in the drug target *RpsA* [44][45]. A current study, has challenged the earlier model by suggesting that pyrazinoic acid prevents trans translation, a route of ribosome spacing in *Mycobacterium tuberculosis*. The study was accomplished in pyrazinamide resistant strains deficient mutations in *pncA* however, that had mutations in *rpsA* recognizing the ribosomal protein 1 (*RpsA*) because the planned target. pyrazinoic acid was confirmed to be bound to *RpsA* and Overexpression of *RpsA* conferred increased resistance to pyrazinamide [46]. PZA is a significant frontline drug which is a fight against TB. However, the growing emergence and epidemics of MDR, XDR-TB and TDR-TB call for the crucial development of new drugs which have the ability to kill the bacteria [47]. Developing new medicine that has an activity for persister TB bacterium is crucial for more shortening this TB medical aid.

2.1.4 Ethambutol



Ethambutol-1960 (4)

The new anti-tuberculosis agent, Ethambutol (EMB) (**4**) was discovered by the Lederle Company in 1961 [48], which was additionally shown to be active in tuberculosis-infected guinea pigs [49]. The newly discovered compound N,N-diisopropylethylenediamin by group of lederel laboratories, was highly active against members of the genus mycobacterium, particularly against *Mycobacterium tuberculosis* both *in vitro* and *in vivo* experimentally infected mice which is found during a screening program designed to rest selected compounds for potential anti-microbial activity [50],

their observation were both exciting and intriguing, since the chemical structure of this compound was completely unknown to any other known anti-tuberculosis drug. The lederle group started an autonomous program to define a structural characteristic of the diamine (organic compound) needed for its action on mycobacterium and to search out related compounds processing higher activity and lesser animal toxicity.

Wilkinson *et al.* (1961, 1962) [51][52] was first described synthesis of Ethambutol in two reports and the first study of the anti-tuberculosis activity of Ethambutol in experimental animals was first reported by Thomas *et al.* (1961) [49] and Wilkinson *et al.* (1962) [52]. The drug is usually in salt form, di-hydrochloride salt, water soluble and a white crystalline material that is heat stable. Ethambutol dihydro chloride inhibited *M. Tuberculosis* or *M. Smegmatis in-vitro* at a concentration of 1-2 mg/ml and was highly effective in the treatment of mice infected with *Mycobacterium tuberculosis* which is showed by Wilkinson *et al.* (1962) [52]. EMB has an established place as a first line anti-tuberculosis agent since more than 50 years to till date, it has a value for the protection that it offers companion drugs against the development and consequences of drug resistance. EMB shows potent activity against resistant strains of Isoniazid- and Streptomycin and organisms of the genus *Mycobacterium tuberculosis*. Thomas *et al.* was reported that EMB was inactive with other bacteria, fungi and viruses in both activity, *in vitro* and *in vivo* in tests [49][50].

Takayama and Kilburn [53] showed a method that controlled the growth of trehalose mono- and dimycolates within the medium, the transfer of arabinogalactan into the semipermeable membrane (cell wall) of *Mycobacterium smegmatis*, which is inhibited by EMB. In addition, it had been shown to inhibit the transfer of [D-14C] glucose into the D-arabinose residue of arabinogalactan [54]. Although the proof implicating

arabinosyltransferases as the target of EMB, only in recent times has insight into the molecular genetics of arabinan biosynthesis been achieved [55]. A two-gene locus (*embAB*) in *Mycobacterium avium* that encodes arabinosyltransferases mediating polymerization of arabinose into arabinogalactan is identified by Belanger *et al.* Further, newly, three genes encoding a putative EMB target in *M. smegmatis* were cloned, sequenced, and characterized by molecular genetic strategies. These genes are organized as an operon, and because two of the three genes are homologous to *embAB* in *M. avium*, they were designated *embC*, *embA*, and *embB* [56]. Telenti *et al.* have now demonstrated that natural resistance to EMB results from an accumulation of genetic events determining overexpression of the *embABC* proteins and structural mutations at codon 306 in *embB* [56]. The target(s) of EMB might presumably be arabinosyltransferases, which are included in the biosynthesis of AG and LAM and that have numerous degrees of sensitivity to EMB [57]. EMB in order inhibits arabinan biosynthesis in both AG and lipoarabinomannan (LAM) [56]. The resistance of EMB was due to overproduction of the natural EMB target and not to an EMB resistance determinant. Lately, the *embCAB* gene cluster from *Mycobacterium tuberculosis* and *M. smegmatis* was identified by Telenti *et al.* [56], and showed that EMB resistance could result from overproduction of the *emb* protein(s), structural mutation of the *EmbB* protein, or both. On the other hand, the involvement of each gene from the *embCAB* operon to EMB resistance was not determined.

Table 1. Frist line Anti-TB agent with Mode of action and resistance

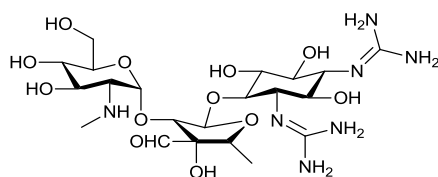
Drugs	Target	Mode of Action	Mutation
Rifampicin	<i>rpoB</i> (β-subunit of RNA polymerase)	Inhibits bacterial DNA-dependent RNA synthesis by inhibiting bacterial DNA dependent RNA-polymerase	81-Base pair Codons- 516,526 and 531 [31][28] (Ser531Leu, His526Tyr, and Asp516Val)
Isoniazid	<i>katG</i> (catalase/oxidase)		Codon 315 in <i>katG</i>
	<i>inhA</i> (enoyl reductase)	Block mycolic acid biosynthesis	(Ser315Thr) [40]
	<i>ahpC</i> (alkyl hydroperoxide reductase)		Codon- 138 and 328
Pyrazinamide	<i>pncA</i>	Inhibiting the enzyme	Mutations at amino acid residues 3–17, 61–85 and 132–142[42]
	<i>PZase</i>	fatty acid synthesis	
Ethambutol	<i>embB</i> (arabinosyl transferase)	Blocking the formation of mycobacterium cell wall	Overproduction of <i>embCAB</i> gene cluster[56] (<i>embB</i> codon 306)

2.2 Existing Second line anti-TB agents.

2.2.1 Streptomycin

A huge antimicrobial spectrum was showcased by aminoglycosides-aminocyclitol antibiotics (hereafter named amino glycosides) which are nothing but water soluble, cationic molecule. Incorporation of the six-membered aminocyclitol ring has been depicted in the vast array of structural diverse compounds, moniker amino glycosides. Due to the poor oral adsorption, amino glycosides are administered intravenously or by injection in the treatment of bacterial infections caused by both gram-positive and gram-negative organisms [58]. No matter a few troubles of toxicity and bacterial resistance, these antibiotics still continue to be a seriously vital factor of our modern antimicrobial arsenal.

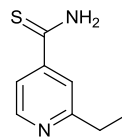
Streptomycin (**5**) turned out to be first isolated, through Albert Schatz, a graduate student, in the laboratory of Selman Abraham Waksman at Rutgers university in a studies undertaking funded via Merck and Co. [56][59][60] by Selman Waksman (for which he become awarded the Nobel Prize in physiology and medicine in 1952) on October 19, 1943 this presaged the identification and characterization of a clinically beneficial aminoglycosides over the 50 years. This led to the discovery of aminoglycoside antibiotics, Streptomycin in 1944 by Schatz et al, 1944[61]. The significance of those preliminary findings become at once obvious and its use in the therapy of tuberculosis became stated to within one year of the development of Streptomycin [62], and it stays as a key component of present anti-mycobacterial treatment [63]. The primary randomized trial of Streptomycin towards pulmonary tuberculosis was carried in 1946-1947 by means of the MRC Tuberculosis Research Unit beneath the chairmanship of Sir Geoffrey Marshall (1887-1982). The trial became each double-blind and placebo-controlled. It has been accepted widely in the primary randomized therapeutic trial [64].



Streptomycin-1943 (5)

Translational errors and slowdown of translocation occurs due to the disturbance in several steps of protein synthesis by Streptomycin [65][66][67]. Foot printing and mutation studies shows that Streptomycin is a protein synthesis inhibitor which binds firmly to single site on 16S *rRNA* [68][69][70]. Foot printing research confirmed that Streptomycin protects specific residues of 16S *rRNA* inside the 30S subunit [71] and may be connected to unique portions of 16S *rRNA* [72]. Moreover, a mutation in *Euglena* chloroplast 16S *rRNA* led to Streptomycin resistance [73] and mutations in distinct regions of *Escherichia coli* 16S *rRNA* changed the ribosomal response to Streptomycin [74][75][76][77][78][79]. Streptomycin also interacts with ribosomal proteins in the 30S subunit [80][81] and mutations in S4, S5 and S12 ribosomal proteins are shown to influence its binding [82]. Speculation in this mechanism indicates that the binding of the molecule to the 30S subunit interferes with 50S subunit association with the *mRNA* strand. This consequences in an unstable ribosomal-*mRNA* complex, leads to a frameshift mutation and defective protein synthesis; leading to cellular death [83]. Humans have ribosomes which are structurally different from the ones in bacteria, so the drug does no longer have this effect in human cells. At low concentrations, but, Streptomycin best inhibits the increase of the bacteria with the aid of inducing prokaryotic ribosomes to misinterpret *mRNA* [84]. Streptomycin can bind to *E.coli* 16S *rRNA* in the absence of ribosomal proteins and might guard bases in the interpreting centre from dimethyl sulfate (DMS) attack [85].

2.2.2 Ethionamide



Ethionamide-1960 (6)

After its discovery in 1956, Ethionamide (**6**) was used to cure tuberculosis and MDR-TB. Ethionamide generally used in treatment of drug resistant TB falls in the class of antibiotic drug with thioamide groups. The treatment of MDR and XDR-TB Ethionamide is used as a part of regimens commonly concerning five drug treatments and it has been endorsed to use in aggregate with the fluoroquinolones [86]. In 2009 Wyeth pharmaceuticals become bought Ethionamide by means of Pfizer (is an American global pharmaceutical business enterprise established in NY metropolis) and it's bought underneath the brand call Trecator or Trecator SC with the aid of Wyeth prescription drugs [87]. Due to the structural similarity of ETH and PTH (Prothionamide) to INH and it is clear that all of these drugs inhibit mycolic acid biosynthesis [88][89].

The bacterial cellular wall has been an effective target for many drugs [90]. Many anti-tuberculosis agents are acknowledged to inhibit cell wall biosynthesis. INH, which is one of the maximum efficient and the most extensively used anti-tuberculosis drugs, has been the difficulty of intensive research at some stage in the beyond decade [91][92][93]. Both *Mycobacterium tuberculosis* and *Mycobacterium Bovis* BCG are extremely liable to INH (minimum inhibitory concentrations (MIC), 0.02-0.2 mg/ml). ETH, a structural analogue of INH, is a useful second line anti-tuberculosis drug. The 2 drugs have nearly same results in that each strongly inhibit the synthesis of mycolic acids [94][95]. The cloning and characterization of the gene *Rv3855*, which we now coin *ethR*, that confers

resistance to ETH, however now not to INH when it is overexpressed in either *Mycobacterium smegmatis*, *M.Bovis* BCG or *Mycobacterium tuberculosis* on a multicopy vector. Moreover, a transposon mutant of *ethR* results in ETH allergic reaction in *M.Bovis* BCG. further, genetic and biochemical proof suggests that *ethR* encodes a transcriptional regulator that isn't directly implicated in mycolic acid biosynthesis however performs a critical function within the law of a second open reading frame (ORF), which is responsible for the activation of ETH. Evaluation of the locus surrounding *ethR* discovered the presence of an adjacent gene now termed *ethA*, which encodes a putative monooxygenase, the expected activator of ETH. Overexpression of *ethA* brought about hypersensitive reaction to ETH in mycobacteria. Therefore, the data supplied are like minded with the belief that *ethR* represses *ethA*, which encodes the equal protein of *katG* implicated inside the activation of ETH [96]. It changed into proven that a single amino acid mutation of *inhA*, S94A, was enough to confer resistance to each ETH and INH in *Mycobacterium tuberculosis* [97].

2.2.3 Fluoroquinolone

For the effective second line medication of MDR-TB, fluoroquinolones use have currently increased. The synthetic derivatives of the parent nalidixic acid results in Ciprofloxacin and Ofloxacin which are nothing but obtained as by product of the antimalarial chloroquine [98]. Two critical enzymes for bacterial viability, topoisomerase II (DNA *gyrase*) and topoisomerase IV are inhibited by fluoroquinolones serves as the basis of mechanism of action. These proteins are encoded with the aid of the genes *gyrA*, *gyrB*, *parC*, and *parE*, respectively [99]. Primary mechanism of development of fluoroquinolone resistance in *Mycobacterium tuberculosis* is through chromosomal mutations in the quinolone resistance-figure out region of *gyrA* or *gyrB*. The most common mutations

located are at position 90 and 94 of *gyrA* however mutations at position 74, 88 and 91 have additionally been stated [100][101]. At present, 8-methoxy fluoroquinolones derivatives Gatifloxacin, Moxifloxacin and DC-159a, have showed extreme activities against MDR-TB bacteria and may be able to reduce the duration of currently available TB treatment. Thus, a new anti-TB agents from quinolones are needed to develop the treatment of tuberculosis with combination regimens.

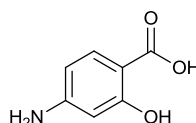
Table. 2 List of Currently available FDA- approved Flouroquinolone Antibacterial Drugs for systemic Use.

Brand Name	Avelox	Cipro	Cipro extende d- release*	Factive	Levaqui n	Moxiflo xacin Injectio n	Ofloxa cin*
Active Ingred ient	Moxiflox acin ⁺	Ciproflox acin ⁺	Ciproflo xacin extended -release ⁺	Gemiflox acin ⁺	Levoflox acin ⁺	Moxiflo xacin	Ofloxa cin ⁺

+ available as generic (Source-
<http://www.fda.gov/Drugs/DrugSafety/ucm500143.htm>)

* available only as generic

2.2.4 Para-aminosalicylic acid



Para-Aminosalicylic acid-1948 (7)

In combination with isoniazid and streptomycin, para-aminosalicylic acid or PAS (7) was initially used for the treatment of anti-tuberculosis, however now it is considered as a second line drug for the MDRTB treatment regimen. Till date its mode of action is not completely known. PAS has to compete with the dihydropteroate synthase, which is

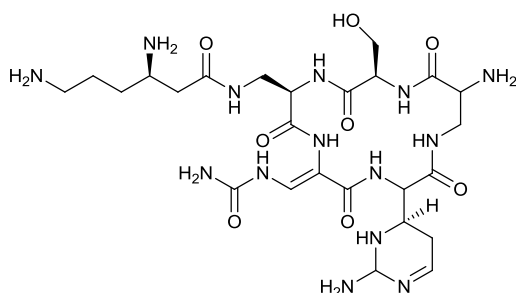
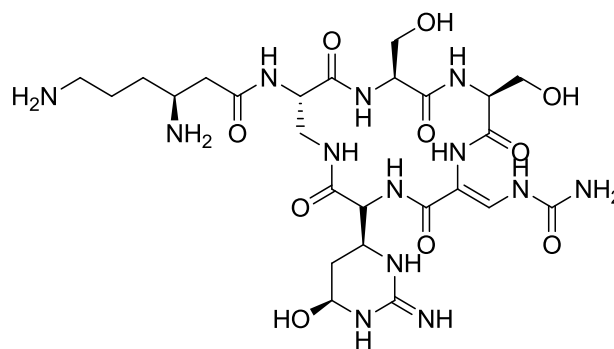
interfering in the process of folate synthesis as it is the analog of para amino benzoic acid. A study utilizing transposon mutagenesis recognized mutations as a part of the *thyA* gene connected with imperviousness to PAS that were likewise present in clinical isolates resistant to PAS [102]. In a board of 85 clinical MDR-TB detaches, transformations in folC were distinguished in five isolates resistant to PAS. In any case, only under 40% of PAS safe strains had transformations in *thyA* showing that still different components of resistance to the medication may exist [103].

2.3 Existing Injectable anti-TB agents

2.3.1 Capreomycin and Viomycin

Capreomycin (8) is an important class of antibiotics which have a good mechanism of actions against multidrug-resistant tuberculosis (MDR-TB), was discovered from *Streptomyces Capreolus* in 1960 and it belongs to the tuberactinomycins [104][105]. Capreolus a subspecies of *Saccharothrix* metabolism is produce the Capreomycin, a macro-cyclic peptide antibiotic [105]. Capreomycin seems to inhibit the translation of mycobacteria, and with the help of mycobacterial ribosomes, it can inhibit phenylalanine synthesis in an *in vitro* translation assay. Furthermore, Capreomycin does not interfere with *mRNA* binding to the ribosome which is signifying by Comparable inhibition was understood whether or not ribosomes were preincubated with *mRNA* [106].

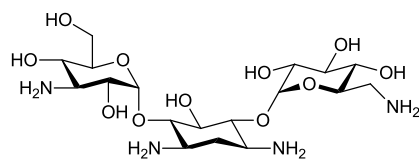
Capreomycin and Viomycin (9) are cyclic peptide antibiotics and the structurally similar scaffold which are primarily active against mycobacteria. Both drugs show potent activity against *Mycobacterium tuberculosis* by inhibition of bacterial growth via blocking protein synthesis on the ribosome [107]. Additionally, both drugs targeted bacterial protein synthesis by binding to the well-maintained intersubunit bridge B2a, made by interaction among helix 69 (H69) of the 23S *rRNA* and helix 44 (h44) of the 16S *rRNA* [108].

**Capreomycin-1963 (8)****Viomycin (9)**

After the miscarriage treatment with first-line drugs, Capreomycin is used clinically against TB bacteria [109]. Capreomycin-resistant clinical isolates are normally resistant against various anti-tuberculosis agents which include kanamycin. Cross-resistance among kanamycin and Capreomycin became previously observed in a variable fraction of kanamycin-resistant in *Mycobacterium tuberculosis* strains [110] even though the molecular mechanism of this resistance was no longer known.

Inhibition of translocation at some point of peptide elongation is the principle mechanism of drug action facilitating the activity of antibacterial drugs [111-112] the loss of 2-O-methylation of C1920 (*rRNA* nucleotides are numbered according to those for *Escherichia coli* throughout) in H69 and that of C1409 in h44 by *TlyA* reduces susceptibility to Capreomycin [113-114]. *Thermus thermophiles TlyA* modifies most effective C1920 in H69 of 23S *rRNA*, but not C1409 in h44 of 16S *rRNA*. Inactivation of *TlyA* in *T. thermophiles* does not show effect on its sensitivity to Capreomycin [115]. Maus et al. Reported that the mutations in the 3' part of the 16S *rRNA* gene (*rrs*), particularly at positions 1401, 1402, and 1484, it's responsible for Capreomycin resistance [116]

2.3.2 Kanamycin



Kanamycin-1957 (10)

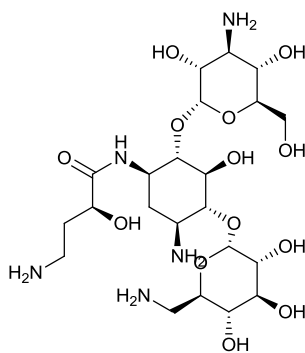
Umezawa *et al.* have first reported kanamycin (**10**) a group of aminoglycoside antibiotics in 1957 by isolation of *Streptomyces kanamyceticus* at the National Institute of Health of Tokyo, Japan. Kanamycin was first introduced as a clinical drug in 1958. Umezawa *et al.* were elucidate that the mechanism of inactivation of kanamycin due to a kanamycin- resistance organism in 1967, 10 years after the discovery of kanamycin [117][118]. Furthermore, within a year after the discovery of Kanamycin, Kanamycin A has been commercially produced as the most common form of a drug, these antibiotics gained practically instant acceptance due to their wide range of activity, specifically against severe staphylococcal and mycobacterial infections [119]. Kanamycins interact with the 30S subunit of the prokaryotic ribosome, inducing vast quantities of mistranslation and indirectly inhibiting translocation at some stage in protein synthesis, resulting in death [120].

Table.3 Second-line Anti-TB agent with Mode of action and resistance

Drugs	Target	Mode of Action	Mutation
Streptomycin	<i>rpsL</i> (S12 ribosomal protein)	binds to the 16S rRNA, interferes with translation proofreading, and thereby inhibits protein synthesis	mutation in codon 43 and 88 from lysine to arginine in <i>rpsL</i>
	<i>rrs</i> (16S rRNA)		
	<i>gidB</i> (7-methylguanosine methyltransferase)		
Capreomycin	<i>rrs</i>	inhibit protein synthesis by binding to the 70S ribosomal unit	Mutations in the 16S rRNA gene
	(16S rRNA)		
	<i>tylA</i> (rRNA methyltransferase)		
Ethionamide	<i>inhA</i> (enoyl reductase)	Inhibit the mycolic acid biosynthesis	C-15T mutation in the regulatory region S94A and I194T
p-aminosalicylic acid	<i>thyA</i> (thymidylate synthase A)	Inhibit the folic acid synthesis	mutation in <i>thyA</i> Thr202Ala
Fluoroquinolones	<i>gyrA/gyrB</i> (DNA gyrase)	Inhibiting the activity of both the DNA gyrase and the topoisomerase IV enzymes.	Mutations in quinolone resistance-determining region (QRDR) in <i>gyrA</i>
Kanamycin	<i>rrs</i> (16S rRNA) <i>eis</i> (aminoglycoside acetyltransferase)	Inhibit the protein synthesis by binding to the four nucleotides of 16S rRNA and a single amino acid of protein S12	Mutations in the codon 1401, 1402 and 1484 in the <i>rrs</i> (16S rRNA)
Amikacin	<i>rrs</i> (16S rRNA)	Inhibit the protein synthesis by binding to the 30S ribosomal subunit	Same as kanamycin

2.3.3 Amikacin

Amikacin (**11**) a nephrotoxic, ototoxic and semi-synthetic aminoglycoside antibiotic, is a derivative of kanamycin A. Amikacin disrupts bacterial protein synthesis by binding to the 30S ribosome of inclined organisms, is similar to other aminoglycosides. Binding interferes with *mRNA* binding and *tRNA* acceptor websites main to the manufacturing of non-functional or toxic peptides [121]. The bactericidal effect of amikacin may confer the mechanism of action of is not completely known.



Amikacin-1976 (11)

The mechanism of action of aminoglycosides by binding to the bacterial 30S ribosomal subunit, causing misreading of *t-RNA*, leaving the bacterium not able to synthesize proteins important to its increase. Aminoglycosides are beneficial in infections regarding aerobic, Gram-negative micro-organism, which includes *pseudomonas*, *acinetobacter*, and *enterobacter*. Further, a few mycobacteria, consisting of the micro-organism that causes tuberculosis, are susceptible to aminoglycosides. Aminoglycosides can also use against Gram-positive bacteria which is responsible for bacterial infections, however, different types of antibiotics are more potent and less destructive to the host. Especially in endocarditis, the aminoglycosides had been used along with penicillin-related antibiotics in streptococcal infections for their synergistic consequences, in the past. Aminoglycosides are mostly ineffective against the anaerobic micro-organism, viruses and

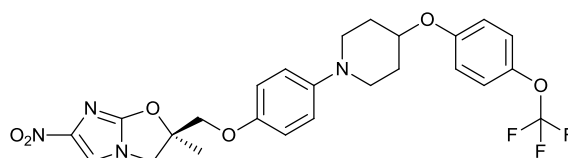
fungi's. The aminoglycosides primarily act by binding to the aminoacyl site of 16S ribosomal RNA in the 30S ribosomal subunit, leading to a misreading of the genetic code and inhibition of translocation. The preliminary steps required for peptide synthesis are uninterrupted, such as binding of *mRNA* and the affiliation of the 50S ribosomal subunit, however, elongation fails to arise due to disruption of the mechanisms for making sure translational accuracy. The ensuing antimicrobial activity is usually bactericidal against susceptible aerobic gram-negative bacilli [122].

3.0 The Present

3.1 Recently approved by FDA

3.1.1 OPC-67683

The new nitro-dihydroimidazooxazole Delamanid (Delytba™, known as OPC-67683) (**12**), in adults having resistant forms of pulmonary TB is used extensively, which has further significantly broadened the inventory of the treatment options. [123].



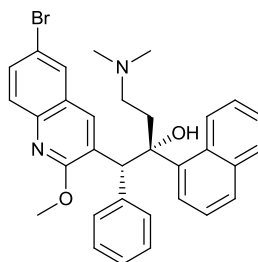
OPC-67683(Delamanid)-2006 (**12**)

Despite the inclusion of the drug in the international guidance for the treatment of MDR-TB since April 2014 [124] an easy access to countries with the greatest need till continues to be challenging. A score of less than ten patents outside the normal clinical setting could access the drug by the end of December 2014 [125]. Otsuka (the drug's developer) announced in a recent "Fight-Back Initiative" held by WHO Global Laboratory Initiative Partners Forum in Geneva that a nitro-dihydro-imidazooxazole derivative Delamanid (OPC-67683) is a mycolic acid biosynthesis inhibitor which is devoid of

mutagenicity with exceptionally high potent activity against TB including MDR-TB. This is supported by its low minimum inhibitory concentration (MIC) (range: 0.006–0.024 $\mu\text{g/ml}$) *in vitro* and highly effective therapeutic activity at low doses *in vivo* [124][126].

The primary metabolites produced by the orally dosed nitro-dihydro-imidazooxazole derivative Delamanid kill tuberculous mycobacteria by inhibiting the bacteria to create a building block that is important for their cell walls, which in turn leads to the blockage of the synthesis of mycolic acids [123]. Nitroimidazoles drugs release nitric acid on metabolization which in turn lead to destroying TB bacteria [124][127]. Patients co-infected with TB/HIV could be effectively treated due to the long half-life of OPC-67683, the lack of metabolization by CYP enzymes and its efficacy in immunocompromised mice. At relatively lower concentration methoxy-mycolic and keto-mycolic acid synthesis (like INH) are inhibited due to the uniqueness in the structure of the cell wall of mycobacteria [124]. A synergistic interaction occurs when OPC-67683 combines with RIF or EMB *in vitro* with devoid of any antagonistic interaction with the first-line drugs RIF, INH, EMB and SM [124]. When a combination of OPC-67683 with RIF and PZA is taken for two months which is further continued for 2 months by taking a combination of RIF leads to an elimination of all lung bacterial load within 3 months and complete elimination occurs in mouse models after 4 months [124]. A reductive activation by *Mycobacterium tuberculosis* is required by Delamanid to exert its activity. A mutation was found in the *Rv3547* gene in experimentally generated delamanid resistant mycobacteria, indicating its role in the commencement of the drug [124].

3.1.2 TMC-207



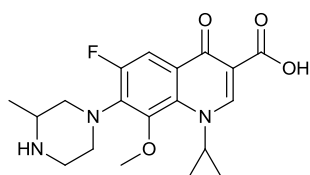
TMC-207(Bedaquiline)-2005 (13)

TMC207 (**13**) is counted on to be the most potent of molecules through subsequent in-vivo testing of activity against *Mycobacterium tuberculosis* [124]. An excellent activity against susceptible drugs like MDR and XDR *Mycobacterium tuberculosis* strains with no cross-resistance to current first-line drugs is exhibited by TMC207 MDR [128]. A greater potency is shown by TMC207 against mutated drug-resistant strains than susceptible isolates which indicates a unique mechanism of action. Despite the appearance of TMC207-resistant *Mycobacterium tuberculosis* strains, full susceptibility occurs to other anti-TB drugs such as RIF, INH, SM and EMB. On co-administration of TMC207 with RIF decrease its levels significantly as TMC207 is readily metabolized by CYP3A4 and this leads in developing incompatible with antiretrovirals [129]. Very few similarities are there between mycobacterial and human protein encoded by *atpE* gene which codes only C subunit of ATP synthase, inhibition of mycobacterium membrane-bound ATP synthase by TMC207 is of greater potential [130]. Negative cultures in mouse models after two months is observed when TMC207 is combined with first-line drugs RIF, INH and PZA. While a combination of TMC207 and PZA for only two months leads in complete eradication of lung *Mycobacterium tuberculosis* proving it to be a synergistic effect. A successful complete eradication of lung and spleen infection within two months in drug sensitive mouse model occurs by using TMC207 with MDR-TB regimen (Amikacin, Ethionamide,

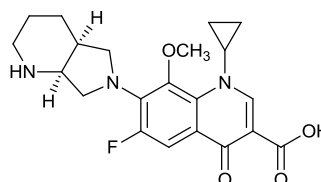
Moxifloxacin and PZA) [131]. The results obtained by the phase II clinical trials led to an increased approval in using Bedaquiline in treating MDR-TB which is available under the trade name Sirturo. However, due to unexplained deaths and QT interval prolongation a “black box” warning is also accompanied with the medicine. Recent reviews and evaluation of this new drug have been published [132][133]. A completely new target of action for an anti-mycobacterial drug was observed as Bedaquiline inhibits ATP synthase of *Mycobacterium tuberculosis*. This mode of action was revealed by analyzing *Mycobacterium tuberculosis* and *M. smegmatis* mutants defiant to bedaquiline. The only mutation observed by sequencing the genome of the mutants which is further compared to susceptible strains is observed in the *atpE* gene, which encodes the c part of the F₀ subunit of the ATP synthase [134]. A63P and I66M found in bedaquiline resistant mutants are the most prevalent mutation in the *atpE* gene. I66 due to modification by introduction, reduces the proper binding of bedaquiline to its target molecule [128][135]. It was observed in a study to assess the mechanism of resistance to bedaquiline in *Mycobacterium tuberculosis* that only 15 out of 53 resistant mutants had mutations in *atpE*. While other 38 strains lacked mutations in *atpE* or even in the F₀ or F₁ operons, which indicates that other mechanisms of resistance are still possible [136].

3.2 Currently evaluated for their anti-TB activity

3.2.1 Gatifloxacin and Moxifloxacin



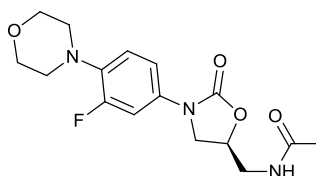
Gatifloxacin-1992 (13)



Moxifloxacin-1999 (14)

For an effective treatment of the respiratory tract infections, fluoroquinolones- Gatifloxacin (**13**) and Moxifloxacin were marketed in 1999. Both these fluoroquinolones molecules are at present in phase III clinical trials for the cure of TB [137]. A 8-methoxyquinolone, Moxifloxacin (**14**) manufactured by Bayer, Newbury, UK has been proved an important fluoroquinolone to have a wide range of activity against bacterial pathogens, including community-acquired pneumonia, and has a good safety record [138][139]. In clinical trials conducted for the execution of the respiratory infections use of this agent is readily made. The treatment of patients intolerant of first-line anti-TB agents is done by making use of Moxifloxacin which is recommended by the American Thoracic Society, Centers for Diseases Control and Prevention, and the Infectious Diseases Society of America [140]. In addition to this for the treatment of MDR-TB, Moxifloxacin of Quinolines base forms the central drug.

3.2.2 Linezolid



Linezolid-1998 (15)

For drug-resistant, gram-positive bacterial infections Linezolid (**15**) (Zyvox, Pfizer) belonging to new class of anti-microbial agents, oxazolidinones was accepted in 2000 [141]. *In vitro* activity of *Mycobacterium tuberculosis* with MIC₉₀ from 0.5 to 2.0 mg/l is depicted by linezolid [142][143]. In 2003 linezolid interaction with humans having MDR-TB was reported [144]. Protein synthesis inhibitor, linezolid interacts only with domain V of the 23S *rRNA* portion of the 50S ribosomal subunit of bacteria [145][146]. The use of linezolid in prolonged anti-TB regimens is suppressed due to its toxicity. An approximate

of 40-90% of patients suffer adverse events while 6% and 68% discontinue the use of linezolid due to the neuropathy (including optic neuritis) and myelosuppression according to the published reports [147].

4.0 The Future

4.1 Under various phases of clinical & preclinical development.

New and novel compound discovery is still challenging. Despite a lot of work been done on whole-genome sequencing of *Mycobacterium tuberculosis* genome-derived targeted approaches areas are yet to be explored to understand their complete potential [148]. A simple shifting from single-enzyme target to a phenotypic screening of whole bacterial cell leads to an impetus in the screening efficacy of the novel targets [149]. Furthermore, many novel anti-TB drug candidate with novel mechanism of actions, are in the preclinical-hit-to-lead optimization phase and also in pre-clinical developments, the pipe-line for the early clinical development phase is very small (**Fig.3**). Two exciting new drugs (Bedaquiline and Delamanid) are currently approved by FDA and two existing drug with combination dose moved beyond Phase-III study and have shown promising results in clinical trials in the past year.

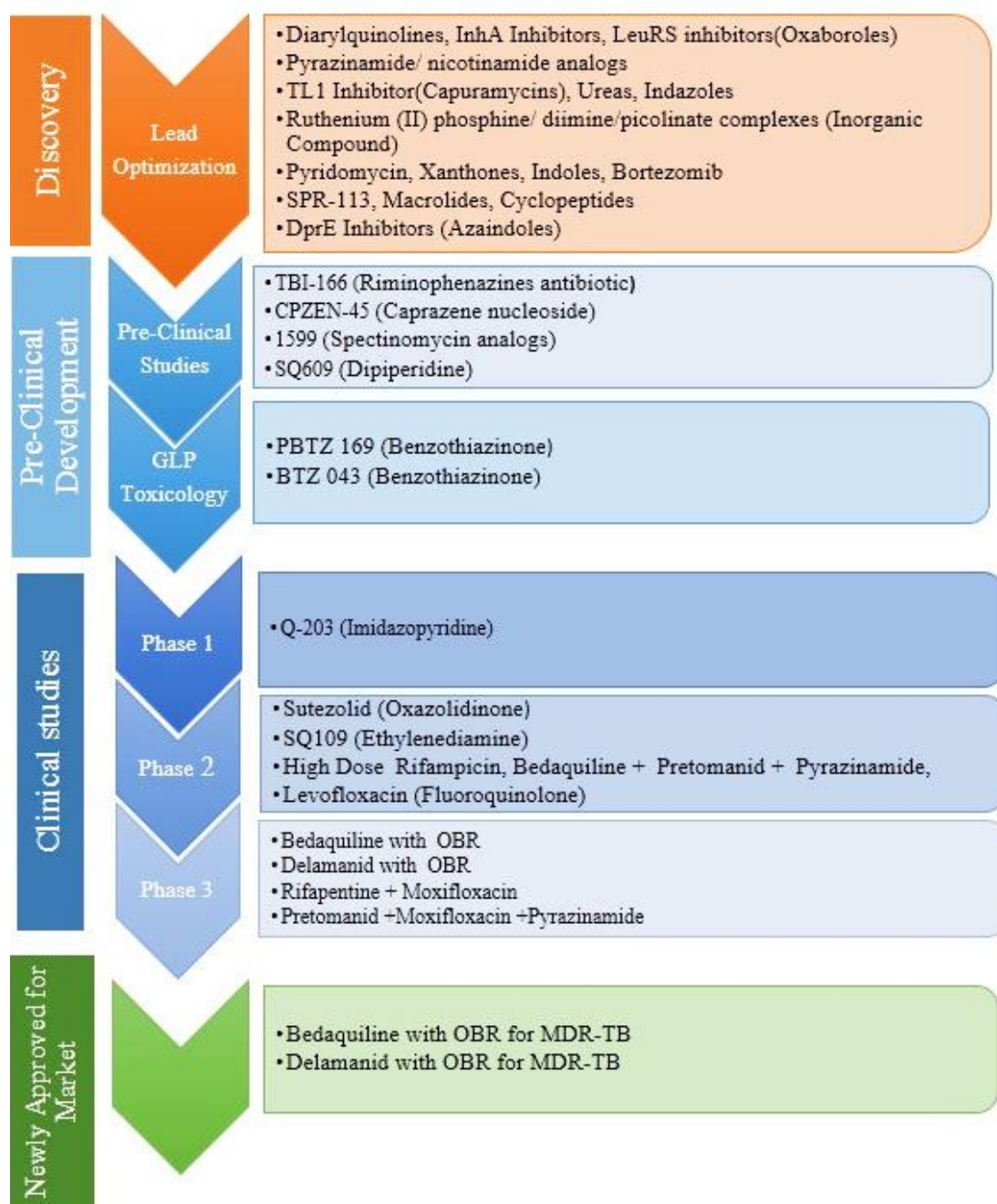
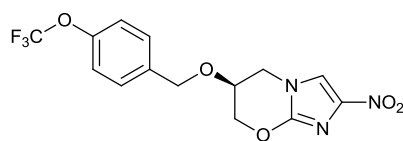


Figure.1 Global tuberculosis drug pipeline (GLP- Good Laboratory Practice)

(Source: Working Group for New TB Drugs (www.newtbdrugs.org/pipeline))

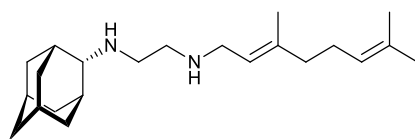
4.1.1 PA-824



Pretomanid(PA-824) (16)

PA824 (**16**) is a bicyclic subsidiary of nitroimidazole that demonstrated particular activity against *Mycobacterium tuberculosis*. PA824 should be initiated by a nitroreductase to apply its action and it hinders the amalgamation of protein and cell wall lipids [150][151]. The mechanism of resistance to PA824 has been appeared to be most ordinarily connected with the loss of a particular glucose6phosphate dehydrogenase (FGD1) or the Dezaflavin cofactor F420. As of late, a nitroimidazooxazine specific protein creating minor basic changes in the medication has additionally been identified [152].

4.1.2 SQ109



SQ-109 (17)

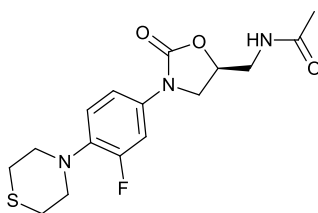
SQ109 (**17**) was develop by a collaboration of Sequella and NIH in the library of 63,000 diamine scaffold which is undergo broad studies in rats, dogs, and monkeys. More than 15 years was spent on research to develop SQ109 and applied its scientific expertise in tuberculosis (TB) [153]. The SQ109 scaffold is a synthetic analogue of ethambutol that has appeared *in vitro* and *in vivo* activates against drug susceptible and drug resistant *Mycobacterium tuberculosis* [154]. Combinations of SQ109 with standard anti-TB drugs demonstrate both better efficacy and shorter time to achieve the same

reduction in *Mycobacterium tuberculosis* as standard therapy with Ethambutol which is validated by numerous in vivo studies in the chronic mouse model of TB [155].

SQ109 works by interfering with mycolic acid assembly in the core of bacterial cell wall which results in trehalose monomycolate (a precursor of the trehalose dimycolate) accumulation. Transcriptional studies have demonstrated that like other cell wall inhibitors, for example, Isoniazid and Ethambutol, SQ109 impels the interpretation of the *iniBAC* operon required for efflux pump functioning [155]. Moreover, by creating spontaneously produced safe mutants to SQ109 analogs and performing entire genome sequencing, transformations in the *mmpL3* quality were distinguished, recommending *mmpL3* as the target of SQ109 and signalling *mmpL3* as a transporter of trehalose mono mycolate [156].

4.1.3 PNO-100480

The oxazolidinones (Sutezolid) (**18**) discovered by E.I. Du Pont Nemours & Company in the 1980s, and later developed at Pharmacia and Upjohn (now part of Pfizer), has promising activity against drug-susceptible and drug-resistant TB. This ultimately led to linezolid, **1**, and an analogue, Eperezolid [157]. A morpholinyl analog of linezolid Sutezolid (PNU-100480 [U-480]) in the hollow-fiber, mouse, and whole-blood models exhibited advanced efficacy against *Mycobacterium tuberculosis* [158][159]. Morpholinyl Oxazolidinone, Sutezolid (PNU-100480, PF-02341272) and AZD5847 (also known as AZD2563) have completed phase I clinical trials. Pfizer and AstraZeneca are functioning on these two identified anti-tubercular compounds [160].



Sutezolid(PNO-100480) (18)

The oxazolidinones contain another class of protein combination inhibitors that block interpretation through a novel component by keeping the arrangement of the initial complex. The anti-tuberculosis movement of PNU-100480 (PNU) was initially reported in 1996 [161]. When both drugs were administered at 100 mg/kg of body weight, it was observed that with subsequent experiments with a murine model indicated that PNU proved to be more active than LZD, but clinical relevance of LZD was not established and no clear difference was observed when their activities were compared for lower doses [162].

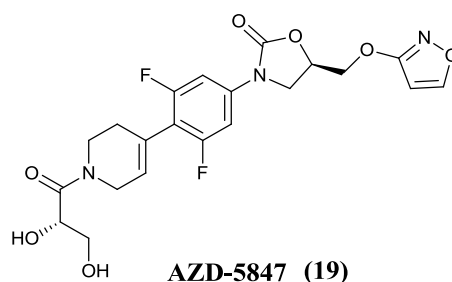
Cynamon and associates initially reported the counter TB action of PNU in a murine model after intravenous contamination of outbred CD-1 mice, the start of treatment at somewhere around 1 and 7 days after disease, and treatment for 4 weeks [163]. Sutezolid (PNU100480) is a morpholinyl analogue of linezolid with preparatory proof for prevalent adequacy against *Mycobacterium tuberculosis*. In the mouse model, Sutezolid abbreviates standard treatment by 1 month, though linezolid does not [164] in the entire blood society display, the maximal bactericidal action of Sutezolid (-0.42 log/day) is more than twice that of linezolid (-0.16 log/day, $P < 0.001$) [161]. Time-subordinate killing has been accounted for in entire blood and empty strands [165].

Bactericidal movement against intracellular mycobacteria is primarily because of the guardian (PNU100480), while a sulfoxide metabolite (PNU101603) Contributes altogether to action against extracellular mycobacteria. Phase 1 studies reveals no irregular hematologic or biochemical discoveries, nor did cases of peripheral or ophthalmic

neuropathy, in healthy volunteers who were direct Sutezolid 600 mg twice every day for 28 days [166]. Demonstrating a safety profile better than correspondingly dosed linezolid. This is the principal investigation of Sutezolid in patients with aspiratory tuberculosis. The principle discoveries were that measurements of 600 mg BID and 1200 mg QD given for 14 days were for the most safe, all around endured, and brought about promptly perceivable bactericidal movement in both sputum and blood. Its effect in sputum was managed all through the full time of treatment. These discoveries support further improvement of Sutezolid as a part of a new tuberculosis regimen [167]. Sutezolid got an Orphan Drug assignment in both U.S. and E.U. is at present in clinical improvement for the treatment of adult pumonary TB brought about by drug sensitive or drug-safe strains of *Mycobacterium tuberculosis* (IND #104806). Sutezolid was safe and very much tolerated at dosages up to 1200 mg per day for up to 14 days, or 600 mg twice every day for up to 28 days [165].

4.1.4 AZD5847

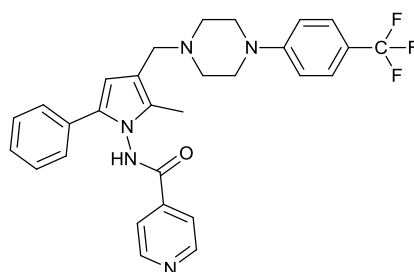
AZD5847 (19) [(5R)-3-(4-{1-[(2S)-2,3-dihydroxypropanoyl]-1,2,3,6-tetrahydropyridin-4-yl}-3,5 difluorophenyl-5-[(isoxazol-3-yloxy)methyl]-1,3-oxazolan-2-one)] belongs to the oxazolidinone drug class and has a molecular formula of $C_{21}H_{21}F_2N_3O_7$ and a relative molecular mass of 465.4 Da [166]. The agent has 2 chiral centers with no evidence of isomerization. AZD5847 has no measurable pKa over the physiological pH range, and its melting point is 153°C.



AZD2563 a novel class of Oxazolidinone was discovered by AstraZeneca and it initially intended for Gram-positive bacteria's [167]. The medication was originally named AZD2563 and considered as a pro-drug (AZD2563 disodium phosphate [DSP] for intravenous imbueement) in stage 1 clinical trial; have reprofiled AZD2563 for its hostile to TB action. In these studies, AZD2563 and AZD2563 DSP have been renamed AZD5847 and AZD5847 DSP, individually, and information on its *in vitro* antimicrobial action against a board of medication defenceless and medication safe clinical disconnects of *Mycobacterium tuberculosis*, its bactericidal movement against *Mycobacterium tuberculosis H37Rv* in broth or in human macrophages, and portrayal of resistant mutants were distributed recently [168].

4.1.5 LL3858

Extremely restricted data on the advancement of pyrroles as anti-mycobacterial agents is right now accessible. Pyrroles derivatives were observed to be dynamic

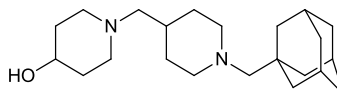


LL-3858 (20)

against standard and drug-sensitive *Mycobacterium tuberculosis* strains *in vitro* [169] that demonstrated higher bactericidal action than Isoniazid when administered as mono-therapy to infected mice. In mouse models, a 12 weeks treatment with LL-3858 (20) or more isoniazid and rifampicin, or LL-3858 or more isoniazid-rifampicin-pyrazinamide, disinfected the lungs of all contaminated mice. Tests directed in mice and dogs demonstrated that the compound is all around retained, with levels in serum over the MIC

and preferable half-life and C_{max} over those appeared by isoniazid. No data is accessible concerning the atomic components that intervene LL-3858's bactericidal action [170].

4.2.1 SQ609



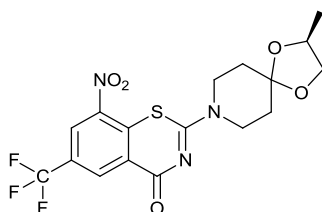
SQ-609 (21)

SQ609 (**21**) was discovered by Sequella and it is a new Diamine scaffold and currently, SQ609 is under IND-directed preclinical studies and evaluation in clinical trials. It has a different mechanism of action from existing TB drugs and potent and specific activity against both drug-sensitive and drug-resistant forms of *Mycobacterium tuberculosis*, low toxicity, activity in *in-vivo* models of *Mycobacterium tuberculosis* infection, and a favorable safety and pharmacology profile [171]. A number of new dipiperidine analogues were designed and they demonstrated activity against *Mycobacterium tuberculosis* after the clinical development of SQ109 [172]. A concentration of 4 mg/mL of SQ609 was able to restrain 90% of bacterial growth in *Mycobacterium tuberculosis* infected macrophages *in vitro* with no toxic effect. While *in-vivo* evaluation of SQ609 was done in *Mycobacterium tuberculosis* H₃₇Rv infected mice. SQ609 at 10 mg/kg for 2 weeks was used once daily for the treatment of C3H/He mice intravenously infected. SQ609 was appeared to avoid the weight reduction of the animals and could prolong therapeutic 2 weeks after the end of the treatment [172]. SQ609 is at present being assessed in preclinical studies.

4.2.2 BTZ043

BTZ043(**22**) is discovered by Medical Centre of the University of Munich (LMU), Hans-Knöll-Institut (HKI) and German Center for Infection Research (DZIF) and it is

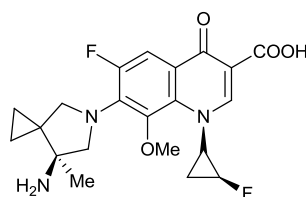
currently in a preclinical development [173]. BTZ043 was described as 1, 3-benzothiazin-4-one or benzothiazinone (BTZ), is a new class of TB drug candidate with novel and high antimycobacterial activity [174].



BTZ043 (22)

Furthermore, the lead compound, (S)-2-(2-methyl-1,4-dioxaspiro[4.5]decan-8-yl)-8-nitro-6-(trifluoromethyl)-4H-benzo[e][1,3]thiazin-4-one (BTZ043) was demonstrate that have *in-vitro*, *ex-vivo* and *in-vivo* activity against *Mycobacterium tuberculosis* and also found to be active against drug susceptible and MDR clinical isolates of *Mycobacterium tuberculosis* [175]. The mechanism of action of BTZ043 was initially spotted at the cell wall biogenesis level by transcriptome analysis. Moreover, the target of the drug was identified at the level of the gene *rv3790* via genetic analysis, using *in vitro* generated mutants, which together with *rv3791* encode proteins that catalyze the epimerization of decaprenylphosphoryl ribose (DPR) to decaprenylphosphoryl arabinose (DPA), a precursor for arabinan synthesis needed for the bacterial cell wall [173]. *DprE1* and *DprE2* were proposed as names for these two key enzymes [172]. More recent, studies have characterized more precisely the mechanism of action of BTZ043 by showing that the drug is activated in the bacteria through reduction of an essential nitro group to a nitroso derivative, which can react with a cysteine residue in *DprE1* [176].

4.2.3 DC159a



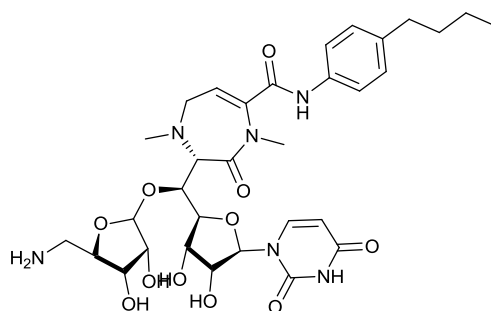
DC-159a (23)

DC-159a (**23**) is a new class of compound for the treatment of MDR-DB which is derived from a new generation of fluoroquinolones. DC-159a illustrate potent activity against various respiratory pathogens, as well as *GyrA* activity, which shows very significant roles in DNA replication, same as other quinolone derivatives. But the mechanism of action of DC-159a is still under investigation [177][178]. Some other anti-TB fluoroquinolones get resist against quinolone resistant multidrug-resistant tuberculosis strains (QR-MDR-TB) and they become inactive, but DC-159a showed good *in-vitro* and *in-vivo* activities against MDR-TB. However, DC-159a-resistant mutants shown patterns of mutations in *GyrA* diverse than the ones observed in quinolones-resistant strains [179]. As a result, it has been suggested that DC-159a may possibly be a replacement of new drug candidate for the cases of QR-MDR-TB treatment. DC-159a showed MIC₉₀ of 0.06 mg/mL against drug-susceptible strains (n ¼ 21) and 0.5 mg/mL against QR-MDR strains (n ¼ 11) [180]. In *Mycobacterium tuberculosis* H₃₇Rv infected mice, during the initial phase of treatment (2 months), the activity of DC-159a alone (25 mg/kg) was superior to Moxifloxacin at 25 mg/kg and equivalent to Moxifloxacin at 50 mg/kg [181]. Additional preclinical studies are currently in progress.

4.2.4 CPZEN-45

CPZEN-45 (**24**) was derived from the Caprazamycins, which are natural products isolated from *Streptomyces* sp. MK730-62F2. Caprazene (CPZEN), a core structure of the

Caprazamycins, proved to be a good precursor of anti-TB antibiotics. CPZEN-45 was the most promising new tuberculosis drug candidate based on the study of structure activity relationships on a range of CPZEN derivatives showed excellent activity against *Mycobacterium tuberculosis* [182]. Due to the poor absorption from the gastrointestinal (GI) tract of the compound, it shows a solubility of around 10 mg/ml in water and has low oral bioavailability. CPZEN- 45 shows excellent activity against MTB strains *in vitro* and as a result, it appears to be a promising candidate for the treatment of TB. The minimum inhibitory concentration (MIC) of CPZEN- 45 is 1.56g/ml for *Mycobacterium tuberculosis* (*H37Rv*) and 6.25g/ml for MDR-TB [183].



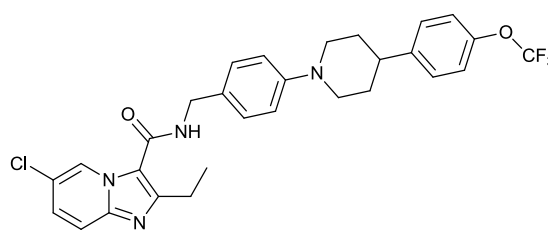
CPZEN-45,(Caprazene-45) (24)

CPZEN-45 can be a very good candidate for the treatment of MDR-TB and XDR-TB because it has in no way been utilized in treatment; therefore, no bacterial strain resistance to this compound is estimated. No matter its appealing capabilities, development of an oral formulation for CPZEN-45 won't be possible because of its meager solubility and potentially low bioavailability. The parenteral preparation of this compound may be possible, however, the everyday injections for TB treatment are undesirable and would reduce the enthusiasm for its use by patients and clinicians. Consequently, unconventional drug transport strategies have to be explored for this new drug. The efficacy of TB treatment with this new TB drug candidate can hypothetically increase due to a preparation of

CPZEN-45 as a powder for inhalation. Hence, the overall goal is to illustrate that when administered to the lungs as a respirable powder that CPZEN-45 is powerful in reducing TB infection. For the purpose of identification of the major objective of CPZEN-45, the effect of Caprazamycin and CPZEN-45 on the incorporation of radio labelled precursors into cellular macromolecules was estimated in *B. subtilis* 168. Furthermore, CPZEN-45 inhibited glycerol incorporation dominantly in *B. subtilis* [184][185].

4.2.5 Q-203

Q203 (**25**) is a new class of TB drug candidate which is derived from imidazopyrimidines [186], it blocks the respiratory cytochrome bc1 complex which is very important to preserve the proton gradient and ATP synthesis and as a result the growth of *Mycobacterium tuberculosis* is prevented.



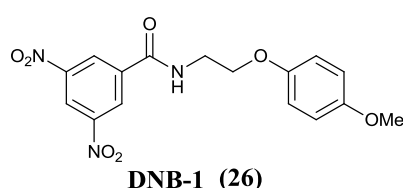
Q-203 (25)

Despite the fact that the drug has a comparable target as Bedaquiline, it inhibits ATP synthesis more potently in both aerobic and hypoxic environments. Furthermore, Q203 is shown potent activity against multidrug-resistant (MDR-TB) and extensively drug resistant (XDR-TB) bacteria of *Mycobacterium tuberculosis* from humanoid, and data from

mice models show a 100–1000-fold reduction of colony-forming units and a blocking of granuloma formation [187].

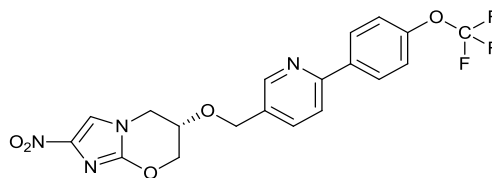
4.3.1 DNB-1

Dinitrobenzamide analogs as DNB1 (**26**), these derivatives were also shown to inhibit decaprenylphospho-arabinose synthesis by targeting decaprenylphosphoribose 20 epimerase *DprE1* and are currently under development.



4.3.2 TBA-354

The researchers at the Auckland Cancer Society Research Centre (ACSRC) and Maurice Wilkins Centre for Molecular Bio discovery was designed new in the compound, TBA-354 (**27**) in collaboration with the University of Illinois at Chicago and the TB Alliance group. Preclinical studies showed that TBA-354 has been more potent than another compound in its class, however, PA-824 was already shown ability in clinical trials. Approximately after 50 years, this is the first novel class of drugs to be developed for TB and it is newly designed to work against the persistent form of the TB [188]. According to TB Alliance, TBA is currently under phase-1 clinical trial. This research program arose from a rather speculative offer to the GATB (Global Alliance for Tuberculosis Drug Development) from the ACSRC (Auckland Cancer Society Research Centre) to help with their PA-824 second generation development program due to their specialty in the chemistry of nitroimidazole.

**TBA-354 (27)**

Since the introduction of metronidazole, the nitroimidazoles were extensively used to treat anaerobic bacterial and protozoal infections [189]. Under specific environmental situation or selectively bio-reduced by an enzyme specific to the target pathogen the compounds of this group are safe. Various nitroimidazole derivatives have shown potent activity against members of the *Mycobacterium tuberculosis* bacteria [190]. More than one thousand nitroimidazole analogs have been pursued by the Global Alliance for the development of TB drugs [191][192][193]. Due to this procedure TBA-354 identified as a latent next-generation nitroimidazole with highly powerful activity compared to PA-824 with *in vitro* activity against *Mycobacterium tuberculosis*, PA-824 has a potentially superior pharmacokinetic profile as compared to this nitroimidazole. Which is currently being administered twice daily as a result of the greater metabolic stability than Delamanid when administered at 100 mg/kg/day in acute and chronic murine infection models of TB [194].

In mid-2005, the first clinical trial of pretomanid (PA-824) was carried out by GATB and the success to develop a new second generation tuberculosis candidate by ACSRC and also takes over the entire second generation Med Chem program in 2006. Independent research article to understand the mechanism of Pretomanid was published by ACSRC and the US national institute of Allergy Infectious Diseases in 2008. In 2009, SN-31354 currently known as TBA-354 preferred as second generation tuberculosis drug and lately in Oct 2011, International committee was allowed to proceed to IND filing of TBA-354. TBA-354 was first publicly disclosed in the 52nd Inter-science Conference on

5.0 RECENT DEVELOPMENTS FOR MDR-TB

Antimicrobial Agents & Chemotherapy (ICAAC) in San Francisco, Sept 2012. After the public disclosure of TBA-354, US FDA approved the IND to proceed to clinical trials and the first clinical trials of TBA-354 was begin lately in 2014 [193].

March 11, 2016, tb alliance announced the withdrawal of tuberculosis drug candidate tba-354 due to side effects in the initial cohort during the mad (multiple ascending dose) studies, which is designed to test the pharmacokinetics and tolerability of ascending doses of tba-354 in healthy volunteers. As a result, the tb alliance together with its scientific advisors made the decision to stop the clinical trial and the clinical development program of tba-354 due to observed side effects and pharmacokinetic data of tba-354 generated in this cohort [194].

5.0 Recent developments for MDR-TB

5.1 Nitroimidazoles

The prospective to reduce TB treatment in animal models and clinical trials have been demonstrated by numerous novel agents in clinical development. The nitroimidazooxazine Pretomanid (PA-824)(**28**), was the first of the clinically-useful compounds initially discovered by the small company Pathogenesis and further developed to clinical trial by GATB [196]. PA-824 showed significant *in-vitro* and *in-vivo* activity against both non-replicating and replicating cultures of *M.TB* [197]. A nitroimidazole PA-824 (Pretomanid) is the only novel compound which is currently in the (advanced) phase II clinical trials for the treatment for TB. From the available clinical data for PA-824 it suggests that the outcome of trials may determine the future directions of drug development for anti-tubercular nitroimidazoles. A significant contribution to future TB treatment can be expected from this class of drugs [198].

Several nitroimidazole subclasses have demonstrated activity against members of the *M. TB* [199]. Compounds of this class are selectively bio-reduced by an enzyme specific to the target pathogen or under specific environmental conditions. A combination of PA-824 (Pretomanid), Pyrazinamide and Fluoroquinolone Moxifloxacin were found effective in a Phase II-advanced early bactericidal activity (EBA) trial (where a new drug replaces a standard drug in a combination for 14 days) [16-17]. Furthermore, the nitroimidazooxazole Delamanid (**27**), has been recently approved from the USFDA for use in TB treatment which is a related compound of this class was developed by Otsuka Pharmaceutical [200].

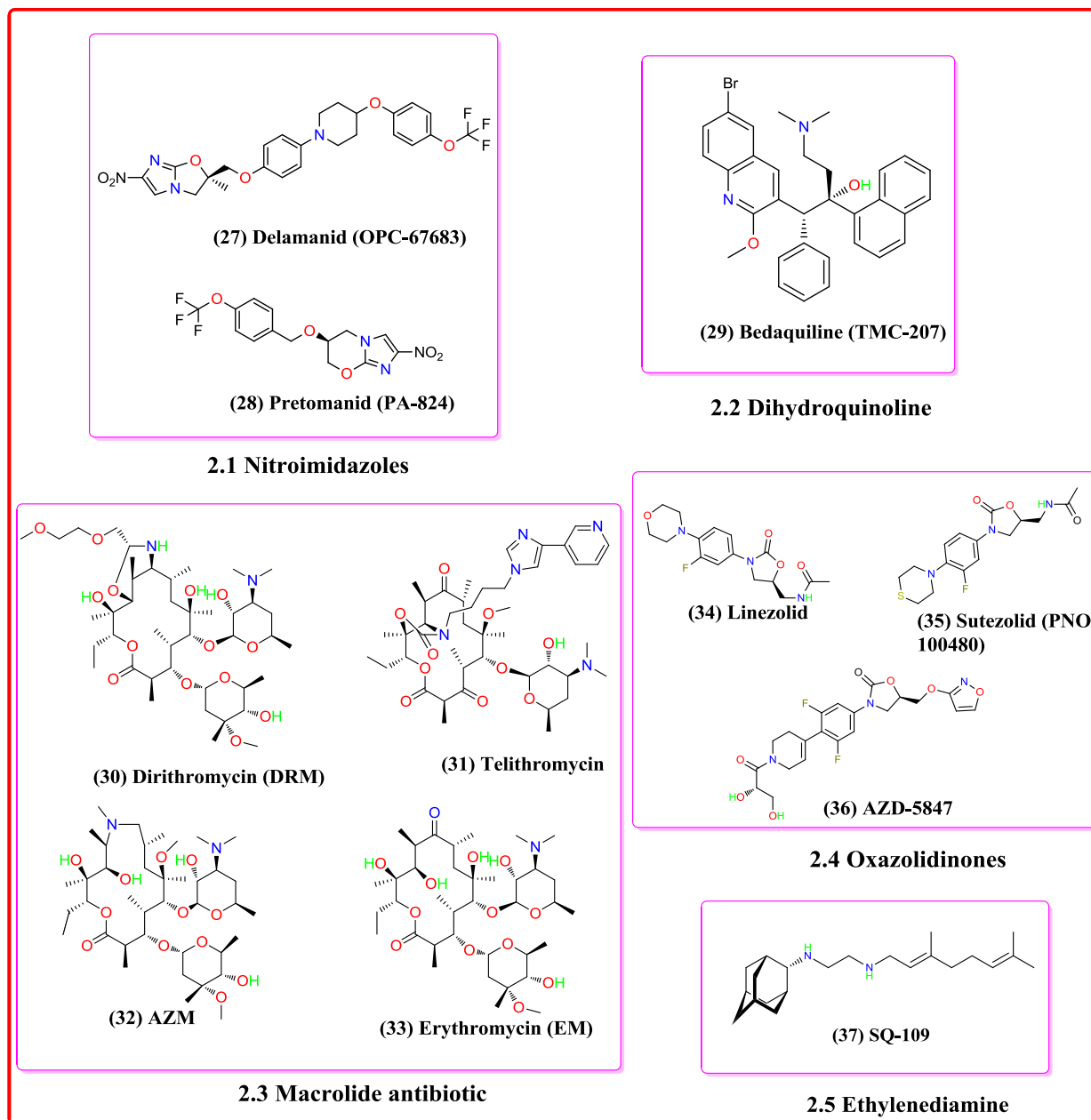


Figure. 2 Two recently approved antitubercular agents (Delamanid and Bedaquiline) and other agents which is currently in pipeline, developing specifically for the treatment of MDR-TB infections.

5.2 Dihydroquinoline

Bedaquiline (**29**) is a diarylquinoline with a novel mechanism of action, it inhibits mycobacterial ATP synthase, which is disrupted by the energy metabolism of mycobacteria

[201]. Janssen Pharmaceuticals (Titusville, NJ, USA) had developed Bedaquiline with a

heterocyclic nucleus with a quinolinic in center and alcohol and amine as side chains. This structure is responsible for the antimycobacterial activity of this new anti-TB drug [202-203]. Bedaquiline is one of the recently introduced drugs for the treatment of MDR-TB; it is also under clinical evaluation for the treatment of drug-susceptible TB [204]. A cationic amphiphilic drug, Bedaquiline is mainly metabolized by N-demethylation catalyzed by the cytochrome P450 (CYP) 3A4 enzyme. The subsequent metabolite M2, is three to six-fold less active *in-vitro* in comparison to Bedaquiline. An *in-vitro* study suggested that M2 may cause cytotoxicity and phospholipidosis at lower concentrations than the parent drug [204].

Bedaquiline usage greatly increased in the treatment of MDR-TB after the provisional guideline provided by the WHO, it then gained momentum in the USA (2012) and Europe (2014) after the FDA approval [205]. Bedaquiline can be used in the treatment of XDR-TB, which does not include the resistance of Isoniazid and Rifampicin against *M.TB*. Both drug-resistant and drug-susceptible cases with the same regimen are thought to be treated with Bedaquiline [206]. Additionally, these new regimens will allow easier administration of HIV co-infected people in the absence of any negative interactions between Rifamycins and Antiretrovirals [207].

5.3 Macrolides

A cladinose and desosamine deoxy sugars attached to a 14, 15 or 16 membered massive macrocyclic lactone ring is present in the macrolides that belongs to the polyketide family of natural products. Presently, macrolides are used to fight respiratory tract infections. It demonstrated pharmacological features and potential antibacterial drug activity which is now experiencing a reemergence globally as it shows potent activity against multi drug- resistance tuberculosis [208]. Macrolides are usually suggested for the treatment of various bacterial infections. By inhibiting protein synthesis in pathogenic

bacteria antibacterial activity is exerted in macrolides. Macrolides are currently in lead-optimization stage in drug discovery and it is being developed by Sanofi, TB alliance [209]. Due to acceptable pharmacological and toxicological profiles of the current antibiotic drugs of macrolide family, Dirithromycin (**30**), Telithromycin (**31**), AZM (**32**) and Erythromycin (**33**) are optimized nowadays for potent activity against *M.TB* they are currently in the pipeline for the treatment of MDR-TB [210].

Novel macrolides represent a major therapeutic advance for MAC (*Mycobacterium avium* complex) lung disease; they are gradually appreciated for their immunomodulatory and anti-inflammatory outcome [211-212]. The macrolides inhibit the bacterial protein biosynthesis by inhibiting the peptidyl transferase from adding the increasing peptide linked to *t-RNA* to the next amino acid as well as preventing ribosomal translation [123]. However, various aspects of macrolide action and resistance remain ambiguous. Mechanisms of macrolide resistance seem to depend on interfaces between the ribosome-bound macrolide molecule and the promising peptide, the inducible appearance of methyl transfers and peptide-mediated resistance. According to the WHO strategies, the efficiency of macrolides against *M.TB* is negligible [214].

5.4 Oxazolidinones

Oxazolidinones offer a novel and effective drug candidates against tuberculosis that exert their function by inhibiting protein synthesis. Two Oxazolidinones Linezolid (**34**) and Sutezolid (**35**) may be a significant option for the treatment of MDR and XDR-TB, which may shorten the duration of the current TB treatment. Various side effects are observed due to the prolonged usage of linezolid as the current treatment duration accounts for 18-24 months [215]. The Oxazolidinones antibiotic inhibits the protein synthesis by binding the 23S ribosomal *RNA* (*rRNA*) portion of the bacterial 50S ribosomal subunit [216].

Linezolid is sold with the trade name Zyvox by Pfizer (in the United States, United Kingdom, Australia, and several other countries) and it was approved in 2000 for the treatment of gram-positive bacterial infections and drug-resistant [217]. Linezolid exhibits *in-vitro* bacteriostatic activity with a minimum inhibitory concentration of less than 1 µg/ml against *Mycobacterium tuberculosis*, including multidrug-resistant (MDR) and extensively drug-resistant (XDR) strains [218]. However, severe side effects such as anaemia, thrombocytopenia, and peripheral neuropathy may be caused when long-term administration of Linezolid is taken by patients [219]. Recently, with superior efficiency in numerous experimental TB models and the potential for a greater safety profile that has been reported by Sutezolid, a Thiomorpholine analogue of Linezolid [220]. Sutezolid and linezolid were both developed by Pfizer (an American global pharmaceutical Company). Presently, Sutezolid has been transferred to Sequella (a biopharmaceutical company, USA). Furthermore, novel Oxazolidinones AZD5847 (AZD) (**36**) [221], Radezolid [222] and Tedizolid [223] which are in the clinical development, are being optimized for the treatment of infections caused by Gram-positive bacteria.

5.5 Ethylenediamine

SQ109 (**37**) (N-geranyl-N'-(2-adamantyl) ethane-1, 2-diamine) belongs to an ethylene diamine family of anti-tubercular drug which is presently in phase II clinical trials for adult pulmonary TB. SQ109 inhibits static or slow developing bacteria as a result it demonstrated strong thermal stability. In fact, pre-treatment of cultures with a bacteriostatic concentration of Chloramphenicol (Cm) synergized the effects of typically bacteriostatic concentrations of SQ109 to the level of bacterial killing [224]. SQ109, a new anti-tubercular drug is safe and well-tolerated in humans, and has the capacity to achieve intracellular bactericidal concentrations that kill *M. tuberculosis* [225]. SQ109 had both the

6.0 BENZIMIDAZOLE: A MILESTONE IN THE FIELD OF MEDICINAL CHEMISTRY

best antibacterial activity and the most promising toxicity. SQ109 was selected as the lead TB drug candidate from the library and underwent an extensive *in-vitro* and *in-vivo* pharmacological and toxicological studies [226]. Recent years have shown a rise in interest in the application of modern drug-discovery techniques to the field of TB, leading to an unprecedented number of new TB drug candidates in clinical trials and saw the application of many preconceptions of modern drug development to anti-infective and anti-tubercular drugs [227]. SQ109 does not fit the mould of traditional pharmaceuticals, and its development has been slowed that its basic structure does not fit the norms of other non-antibiotic drug classes.

6.0 Benzimidazole: A milestone in the field of medicinal chemistry

In the 1800s, the history of heterocyclic chemistry was begun with the development of organic chemistry. Currently, about 65% of organic chemistry literature is based on heterocyclic chemistry [228]. Heterocyclic compounds are essential for life and extensively distributed in nature; they play a significant role in the metabolism of all living cells. Among them, Nitrogen based heterocyclic compounds play important role for mankind. Also, many synthetic nitrogen heterocycles are highly relevant to pharmacology and medicine. Particularly, benzimidazole has an immense importance not only biologically but also industrially among all the nitrogen based heterocyclic compounds [229]. Moreover, benzimidazole (figure 1) has been an intriguing field of study since decade. It is a standout amongst the most encouraging moieties that is available in numerous clinically valuable drug candidate [230]. Hobrecker revealed the first benzimidazole synthesis of 2,5 and 2,6-dimethylbenzimidazole in 1872, and he never supposed that benzimidazole compound would turn out to be such a pre-prominent structure [231]. In 1950s, more interest in the field of benzimidazole based chemistry was produced, when 5,6-dimethyl-

6.O BENZIMIDAZOLE: A MILESTONE IN THE FIELD OF MEDICINAL CHEMISTRY

1-(α -D-ribofuranosyl) benzimidazole was found as a basic unit of the structure of vitamin B12 [232]. Benzimidazole moiety has been fused into pharmaceutical operators to DNA inhibitors and enzymatic inhibitors [6]. Benzimidazole and their derivatives have a wide range of applications in the medicinal chemistry. Over the past 25 years, a huge number of reviews that discuss the synthesis of combinatorial libraries directed toward solving drug discovery problems have been published [233]. Moreover, substituted benzimidazole based derivatives have discovered various medicinal applications, for example, in antibacterial, antimicrobial and antiprotozoal impacts [234], anti-allergic action [235], HIV inhibitors, antiviral impact [236], antihypertensive specialists [237], cardio tonic action [238], antiulcer action [239], anti-proliferative action [240], anti-inflammatory effect [241], anti-analgesic and antispasmodic action [242], anti-oxidant action [243], antiprotozoal movement [244], anti-asthmatic and anti-diabetic activity [245], diuretic action [246], androgen receptor [247], anticonvulsant agents [248], bovine DHFR, m-DNA binding properties [249], antitumor [250] and anticoagulant [251-252].

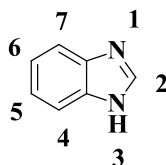


Figure 3. Structure of 1H-benzo[d]imidazole

Moreover, the electron-rich nitrogen heterocycles could not just promptly receive or give protons, but also leads to the formation of diverse weak interactions. These exceptional auxiliary highlights of benzimidazole rings with required electron-rich trademark is gainful for benzimidazole derivatives to punctually bind with a wide variety of biological targets, Thus benzimidazole moiety showing extensive pharmacological activities [253]. The work highlighted in this article identifies with the clinically valuable

6.1 ANTI-TUBERCULOSIS AND ANTI-BACTERIAL ACTIVITIES OF BENZIMIDAZOLE

benzimidazole based drug candidate with their development. In addition to this the mechanism of action, SAR points have been displayed to assist medicinal chemistry and biology to planning an important novel drugs covering benzimidazole moiety's for the treatment of various disorders. It is predicted that this review will be useful for the new development of more active and intense medications for future medicinal research.

The benzimidazole based derivatives are great multipurpose application and it have involved in several clinically utilized medications with high restorative control and market approval. Therefore, the related research and medication discovery in the benzimidazole class of compounds are speedily generating and have proficient incredible advance towards medicinal chemistry. There has been several articles distributed describing characteristics found in drug-like molecules in the benzimidazole based compounds. Here, we have described the detailed biological result of benzimidazole derivatives which have synthesized by many researcher.

6.1 Anti-Tuberculosis and Anti-bacterial activities of benzimidazole

Tuberculosis Infection (MTB) was observed as early as 5000 years ago with evidence, which is a primeval enemy of the human. Tuberculosis infection is caused by *Mycobacterium tuberculosis* pathogen; it is a vital cause of morbidity and mortality in poor low-income countries as well as in developing countries because of non-availability of reliable laboratory facilities. The available treatment for drug-resistant tuberculosis (TB) is lengthy, difficult, and associated with serious harmful side effects and poor outcomes. The current cure against tuberculosis has substantial restrictions, in terms of their efficiency, side-effect outline, and complication of handling [254]. Microbial Infectious disease a critical threat worldwide due to longer treatment than any other from life or microbes have resisted prophylaxis. The problems of multidrug resistance microorganism have reached an alarming level in many countries around the world in recent eras. Infections cause by

6.1 ANTI-TUBERCULOSIS AND ANTI-BACTERIAL ACTIVITIES OF BENZIMIDAZOLE

Mycobacterium tuberculosis bacteria pose a serious challenge to the medicinal community and the requirement for an effective therapy has led to search for novel anti-microbial drug candidate. Despite this knowledge, various researcher have reported that benzimidazole and its derivatives are biologically active and find application in the treatment of tuberculosis.

Malleshappa Noolvi *et al.* have synthesized a series of 1-methyl-N-[(substituted-phenylmethylidene)-1H-benzimidazol-2-amines **38 - 44, 45 - 51**) (figure 17) via cycloaddition of o-phenylenediamine with cyanogen bromide in the presence of aqueous base followed by N-methylation with methyl iodide in the presence of anhydrous potassium carbonate in dry acetonitrile. Synthesized compounds was screened for their *in vitro* antimicrobial activity against Gram +ve bacteria (*Staphylococcus aureus*, *Bacillus pumillus*) and Gram -ve bacteria (*Pseudomonas aeruginosa*, *Escherichia coli*) by measuring the zone of inhibition at concentration 100 lg/mL (mm), minimum inhibitory concentration (lg/mL) and % inhibition, respectively. Compounds **38** (12.4, 10.2, 11.9 and 10.8 mm), **40** (12.9, 11.3, 11.8 and 10.8 mm), 242 (13.2, 11.2, 13.6, 11.4 mm), 243 (13.6, 12.4, 13.4 and 11.7 mm) and **48** (13.2, 11.5, 12.8, 11.3 mm) against *Staphylococcus aureus*, *Bacillus pumillus*, *Escherichia coli* and *Pseudomonas aeruginosa* displayed good antimicrobial activities as compared to the standard drug Ampicillin (13.8, 11.8, 13.2 and 12.4 mm). Among all the synthesized Compounds, compounds **44, 45, 46** and **51** shown 25 lg/mL MIC against *Staphylococcus aureus* and compounds **46** and **51** also shown 25 lg/mL MIC against *Bacillus pumillus* as compared to the standard drug Ampicillin (6.5, 12.5, 22, 25l µg/mL) against *Staphylococcus aureus*, *Bacillus pumillus*, *Escherichia coli* and *Pseudomonas aeruginosa*, respectively. Furthermore, compound **46** shown maximum %

inhibition (52.78%) as compared to the standard Ampicillin 55.26% against *Escherichia coli* [255].

Ansari *et al.* have reported the synthesis of 2-substituted-1-[(5-substituted alkyl/aryl)-1,3,4-oxadiazol-2-yl] methyl]-1H-benzimidazole (figure 17) by nucleophilic substitution of 2-substituted-1H-benzimidazole and further evaluated for their antibacterial activity. From the result of antibacterial activity it was found that the screened compounds are more active against the Gram +ve bacteria. The synthesized compound **52** and compound **53** showed significant antibacterial activity (MIC 2 µg/mL) against *Staphylococcus aureus*. Among all the synthesized compounds, analogue **52, 53, 54, 55, 56** and **57** were found to be more significant. However, in the case of *Escherichia coli*, *Pseudomonas aeruginosa* and *Salmonella typhi* none of the compounds shows inhibitory effect or less active. From the above observations, the effectiveness of compounds were increased due to 2-methyl benzimidazole derivatives having para-substituted benzene ring on oxadiazole [256].

Soni B *et al.* synthesized a novel series of 5-[2-(1,3-benzothiazol-2-yl-amino) ethyl]-4-(arylideneamino)-3-mercapto-(4H)-1,2,4-triazoles **60 - 66** (figure 17) and evaluated for their antimicrobial activity to identify potential compounds. The minimum inhibitory concentration for Ciprofloxacin is approximately 10 µg/ml against all microbes used. Compounds **61, 66** and **65** are the most effective compounds against *Bacillus subtilis* and *Escherichia coli*, with a MIC of 100 µg/ml, respectively. While, Compound **60** showed the lowest antibacterial activity against all bacterial species with a MIC of 500 µg/ml. The antimicrobial result of substituted benzothiazoles against *Streptomyces griseus* proved that compounds **61, 65** and **66** were the most effective with a MIC of 100 µg/ml. It can be stated from results of antibacterial activity that compounds with a 4-hydroxy, 4-dimethylamino and 3,4-dimethoxy group on the aromatic ring displayed good antibacterial activity among

6.1 ANTI-TUBERCULOSIS AND ANTI-BACTERIAL ACTIVITIES OF BENZIMIDAZOLE

all the synthesized compounds. The compounds **61**, **65** and **66** exhibited somewhat less activity whereas compounds **60**, **62**, **63** and **64** exhibited poor activity as compared to the standard drug Ciprofloxacin. Their discussion is evident that compounds **61**, **65** and **66** appear as the most effective antibacterial benzothiazoles with a MIC of 100 µg/ml thus they could be promising candidates for novel anti-bacterial agents [257].

Zhang HZ *et al.* have synthesized a series of benzimidazole-incorporated sulphonamide analogue (figure 17) and evaluated for their *in vitro* antibacterial activity. Compound **67** exhibited moderate to good activity against the tested bacteria (MIC = 32 - 128 µg/mL) in comparison with clinical drugs. Remarkably, among all the synthesized analogues, compound **68** with 4-fluorobenzyl group shows the great activities against the tested Gram +ve bacteria with MIC values of 4 - 64 µg/mL. Furthermore, its anti-*Staphylococcus aureus* (MIC = 4 µg/mL) activity was 2-fold more potent as compared to the standard drug Chloromycin and Norfloxacin, and for *Bacillus subtilis* strains, it also showed two times more active than Chloromycin (MIC = 16 µg/mL). The compound **69** displayed significant bioactivities against Gram -ve bacteria with MIC values ranging from 4 to 32 µg/mL. Compound **69** exhibited eight times greater activity (MIC = 4 µg/mL) than Chloromycin against *Salmonella typhi* B.

6.1 ANTI-TUBERCULOSIS AND ANTI-BACTERIAL ACTIVITIES OF BENZIMIDAZOLE

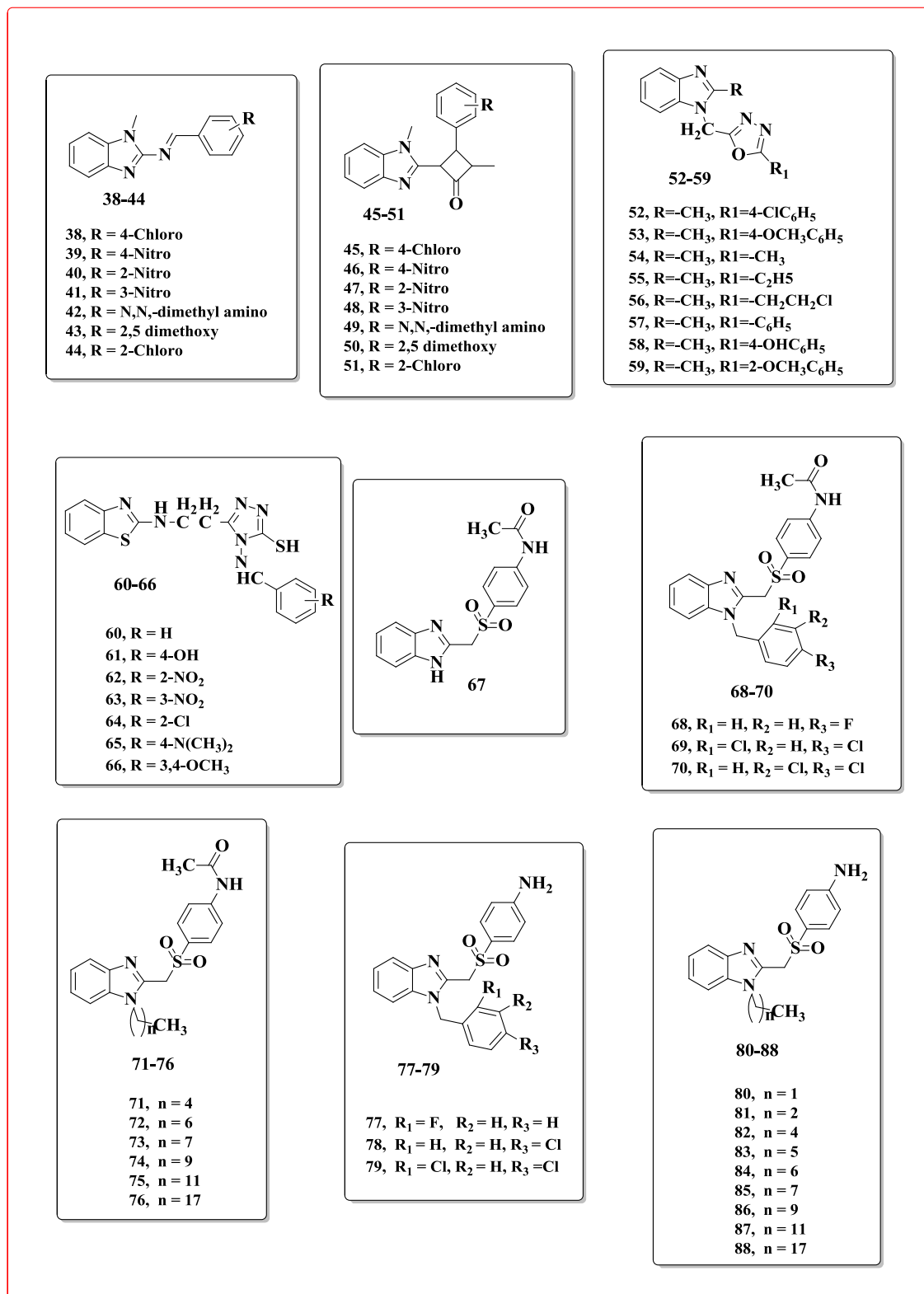


Figure. 4 Structure of anti-tuberculosis and anti-bacterial benzimidazole derivatives

6.1 ANTI-TUBERCULOSIS AND ANTI-BACTERIAL ACTIVITIES OF BENZIMIDAZOLE

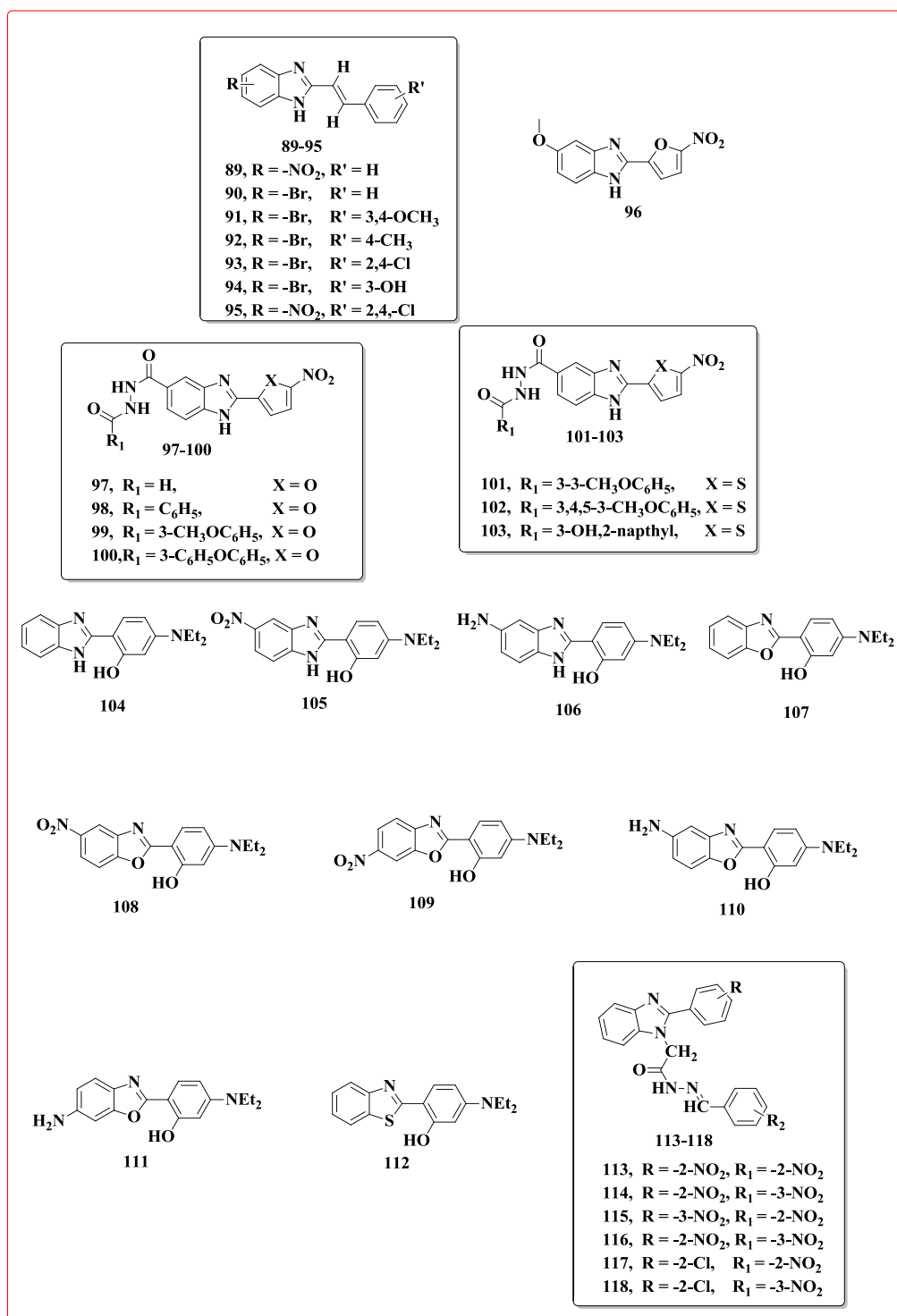


Figure. 4 Structure of anti-tuberculosis and anti-bacterial benzimidazole derivatives (Count.)

However, the substitution of 4-fluorobenzyl group in compound **68** by 3,4-dichlorobenzyl group which gave derivative **70** was not favorable for the antibacterial activities. Compound **71** shows potent anti- *Pseudomonas aeruginosa* activity with MIC value of 4 µg/mL which was 4-fold more potent than Chloromycin. Compound **72** displayed significant activity against the tested *Staphylococcus aureus* strains (MIC = 8 µg/mL). Moreover, when the alkyl substitution in compounds **73 - 76** shows relatively weaker inhibitory activity. While analogues **77** and compound **78** was 32-fold or 16-fold more effective than standard drug against *Bacillus subtilis* or *Micrococcus luteus* strains (MIC = 8 and 8 µg/mL, respectively). Analogue **79** revealed equivalent bioactivity against *Staphylococcus aureus* as compared to standard drug Chloromycin and Norfloxacin with MIC value of 8 µg/mL. However, compounds **80 - 88**, led to weak antibacterial activities [258].

Shingalapur *et al.* have reported a series of novel 5-(nitro/bromo)-styryl-2-benzimidazoles (figure 17-18) via simple, mild and efficient synthetic procedure by condensation of 5-(nitro/bromo)-o-phenylenediamine with trans-cinnamic acids in ethylene glycol and further evaluated for their antibacterial activity. The anti-bacterial activity of all the synthesized analogues against *Staphylococcus aureus* and *Enterococcus faecalis* as Gram +ve, *Klebsiella pneumoniae* and *Escherichia coli* as Gram -ve bacteria showed potent activity as compared to standard drug ciprofloxacin. Result of anti-bacterial activity apparent that among the synthesized compounds **89, 90, 91, 92, 93, 94** presented MIC value of 16-1 µg/ml. Compound **94** exhibited exceptional activity with an MIC of 1 µg/ml and 4 µg/ml against Gram +ve and Gram -ve, respectively. Compound **90** and **91** displayed MIC of 2 µg/ml against Gram +ve and 8 µg/ml against *Klebsiella pneumoniae*. Moreover, the data of the anti-tubercular activity reveals that the compounds **90, 91, 92** and

6.1 ANTI-TUBERCULOSIS AND ANTI-BACTERIAL ACTIVITIES OF BENZIMIDAZOLE

93 revealed potent activity against *Mycobacterium tuberculosis* strain, while compound **95** presented moderate activity [259].

Camacho *et al.* have reported a series of N'-substituted-2-(5-nitrofuran or 5-nitrothiophen-2-yl)-3H-benzo[d]imidazole-5-carbohydrazide derivatives (figure 18) and selected analogues were screened for their anti-tubercular activity against sensitive *Mycobacterium tuberculosis* H37Rv and multidrug-resistant tuberculosis strains. Compounds **96, 97, 98, 99, 100** and **101, 102** and **103** were tested *in vitro* for their anti-mycobacterial activity against sensitive *Mycobacterium tuberculosis* H₃₇Rv strain and a multidrug-resistant (MDR) clinical isolate. From the data it revealed that compounds **98** showed a moderated anti-mycobacterial activity, with a MIC value of 12.5 µg/mL against sensitive *Mycobacterium tuberculosis* H37Rv strain and 6.25 µg/mL against the multidrug-resistant clinical isolates and the result was compared with standard drugs Isoniazid and Rifampin MIC 0.063 and 32 µg/mL [260].

Padalkar *et al.* have reported a series of 2-(1H-benzimidazol-2-yl)-5-(diethylamino)phenol, 2-(1,3-benzoxazol-2-yl)-5-(diethylamino)phenol and 2-(1,3-benzothiazol-2-yl)-5-(diethylamino)phenol (figure 18) using p-N,N-diethyl amino salicylaldehyde with different substituted o-phenylenediamine or o-aminophenol or o-aminothiophenol. All the synthesized analogues **104-111** were evaluated for their *in vitro* antibacterial activity against *Escherichia coli* and *Staphylococcus aureus* strains by using serial dilution method. The anti-bacterial data specify that, synthesized analogues presented variable inhibitory effects on the growth of *Escherichia coli* and *Staphylococcus aureus* (bacterial strain), the compounds **104 - 111** showed potent antibacterial activity while compounds **112** showed 50% less effective against *Escherichia coli*. Moreover, compounds **104 - 106** presented tremendous antibacterial activities against *Staphylococcus aureus* and

6.1 ANTI-TUBERCULOSIS AND ANTI-BACTERIAL ACTIVITIES OF BENZIMIDAZOLE

compounds **104 - 112** displayed moderate inhibitory activity. Furthermore, the structure-activity relationship of the novel benzimidazole, benzoxazole and benzothiazole analogues **104 - 106** against the bacterial strain, the results revealed that new compounds contain benzimidazoles **104, 105** and **106** that displayed a potent antibacterial profile against tested bacterial strain as compared to 2-substituted benzoxazole and benzothiazole **107 - 112** derivatives. The electron donating and electron withdrawing groups in target molecules **104 - 112** less effective against tested bacterial strains [261]. Additionally, Soni B have synthesized a novel series of N'-(substituted benzyldene)-2-[2-(substituted phenyl)-1H-benzimidazol-1-yl] acetohydrazides **113 - 118** (figure 18) and further evaluated for their *in vitro* antimicrobial activity. The result from Antibacterial screening revealed that all the synthesized compounds exhibited potency against bacterial strain. The compounds were effective with zone of inhibition of 07 - 24 mm in diameter while standard drug Ciprofloxacin presented a zone of inhibition of 26 and 25 mm in diameter against *Staphylococcus aureus* and *Escherichia coli* at 4 ppm concentration respectively. The compound **117** shows minimum activity with substitution of 2-Cl and 2-NO₂ group on aromatic rings. All the analogues were found to be more active against *Staphylococcus aureus* than *Escherichia coli* except compounds **113, 117** and **118**. Analogues **114** and **115** were found to be potent against both the bacterial strains. Compounds **113** and **118** displayed moderate activity whereas compounds **114** were less active against *Staphylococcus aureus*. They have found from the data that compound **116** emerged as the most active antibacterial benzimidazoles [262].

6.2 Anti-malarial activities of benzimidazole

Malaria is caused by Plasmodium parasites, inflict tremendous mortality and morbidity worldwide. However, the details of how these parasites interact with their host remain largely unknown. This is particularly true, when the parasite infects and then resides

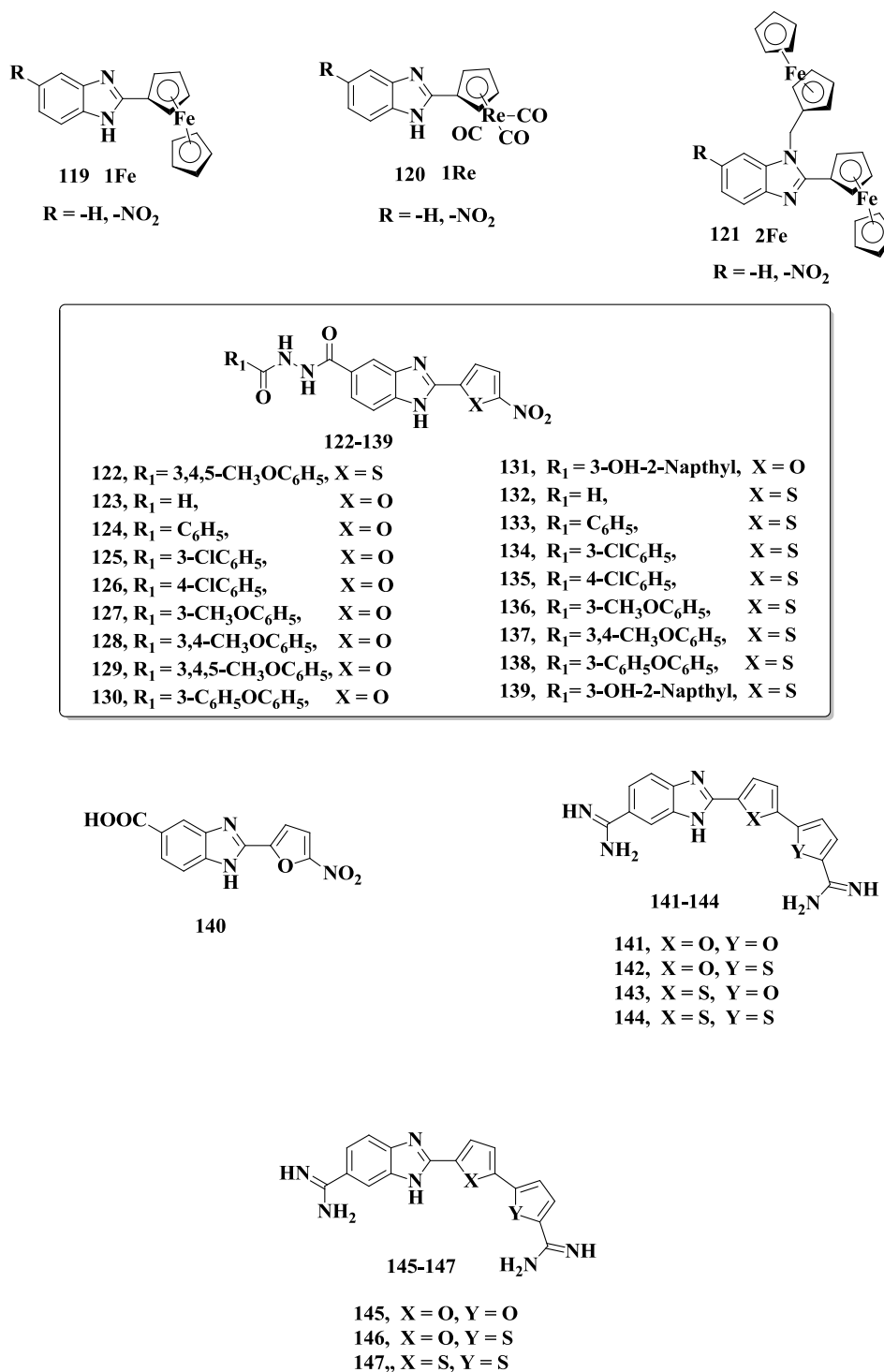
6.1 ANTI-TUBERCULOSIS AND ANTI-BACTERIAL ACTIVITIES OF BENZIMIDAZOLE

within a single hepatocyte in the liver during the first several days of mammalian infection. Whereas clinically asymptomatic, the development of liver stage (LS) development is mandatory for malaria life cycle evolution and also houses hypnozoite forms, which are the source of relapsing malaria [263, 264, 265]. Malaria caused 350-500 million clinical incidents yearly as a result over one million deaths occurs, most of effect shown in children under 5 years old in sub Saharan Africa. In recent times, clinical failure to dihydroartemisinin-piperaquine combination remedy was reported [266]. This knowledge suggesting that the problem is increasing and thus there is urgent need of new drugs development. Despite this challenge, researches which will identify new benzimidazole based chemical compounds with antimalarial profiles is described below.

Toro *et al.* have reported the synthesis of a series of ferrocenyl and cyrhetrenyl benzimidazoles derivatives (figure 19) and evaluated for their ability to inhibit malarial parasites growth using the CQ-susceptible 3D7 clone and CQ-resistant W2 clone of *Plasmodium falciparum*. From the data, they observed an improved activity for the cyrhetrenyl compound 1-Re-(H, NO₂) (IC₅₀ = 10.4 - 26.5 μ M) than its ferrocenyl analogue **119** (IC₅₀ = 23.9 - 48.0 μ M) in both strains. This occurrence can be related with the electron withdrawing properties and good lipophilicity of the cyrhetrenyl moiety present in **120** compared to the analogous ferrocenyl derivatives. Compounds with organometallic functional group (1-M; M = Re, Fe) and having the nitro group at the 5-position, into the benzimidazole moiety (1-M-NO₂) are more effective than the unsubstituted analogues (1-M-H). Compounds **121** shows better potency to inhibit the *Plasmodium falciparum* strain *in vitro* resistant to Chloroquine. In the case of compounds (1-M), there is no difference in antimalarial activity rendering to the liability of the *Plasmodium falciparum* strain to Chloroquine [267]. In addition, Camacho *et al.* have reported a series of N'-substituted-2-

(5-nitrofuran or 5-nitrothiophen-2-yl)-3H-benzo[d]imidazole-5-carbohydrazide derivatives (figure 19) and evaluated the antimalarial activity of compounds against rodent *Plasmodium berghei*. The data indicate that the 5-nitrofuranyl moiety shows potent antimalarial activity, except compound **122** having 5-nitrothiophene-2-yl showed favourable activity. Analogues **123 - 131** and **122, 132 - 139** were tested in infected mice with *Plasmodium berghei* ANKA, a Chloroquine susceptible strain of murine malaria. Dose of compounds were given to mice for four consecutive days (days 1 - 4 post-infection) and the parasitemia was determined at day fourth post-infection; the survival days were monitored and compared with control mice receiving a saline solution (untreated mice). Control mice died within 8.2 ± 0.37 days post-infection, analogues 1140, 128 and 139 improved the survival time for 17 ± 1.26 , 12.2 ± 1.65 and 18.8 ± 2.05 days, respectively, while Chloroquine protracted the survival time of the infected mice to 30 days. Compounds 140, 128 and 139 were able to inhibit the growth of malaria (4.02 ± 0.45 , 4.8 ± 2.22 and $1.8 \pm 0.49\%$), respectively but did not reduce the infection as compared to standard drug Chloroquine 1.3 ± 0.3 [268-270].

6.1 ANTI-TUBERCULOSIS AND ANTI-BACTERIAL ACTIVITIES OF BENZIMIDAZOLE

**Figure 5.** Structure of anti-malarial benzimidazole based derivatives

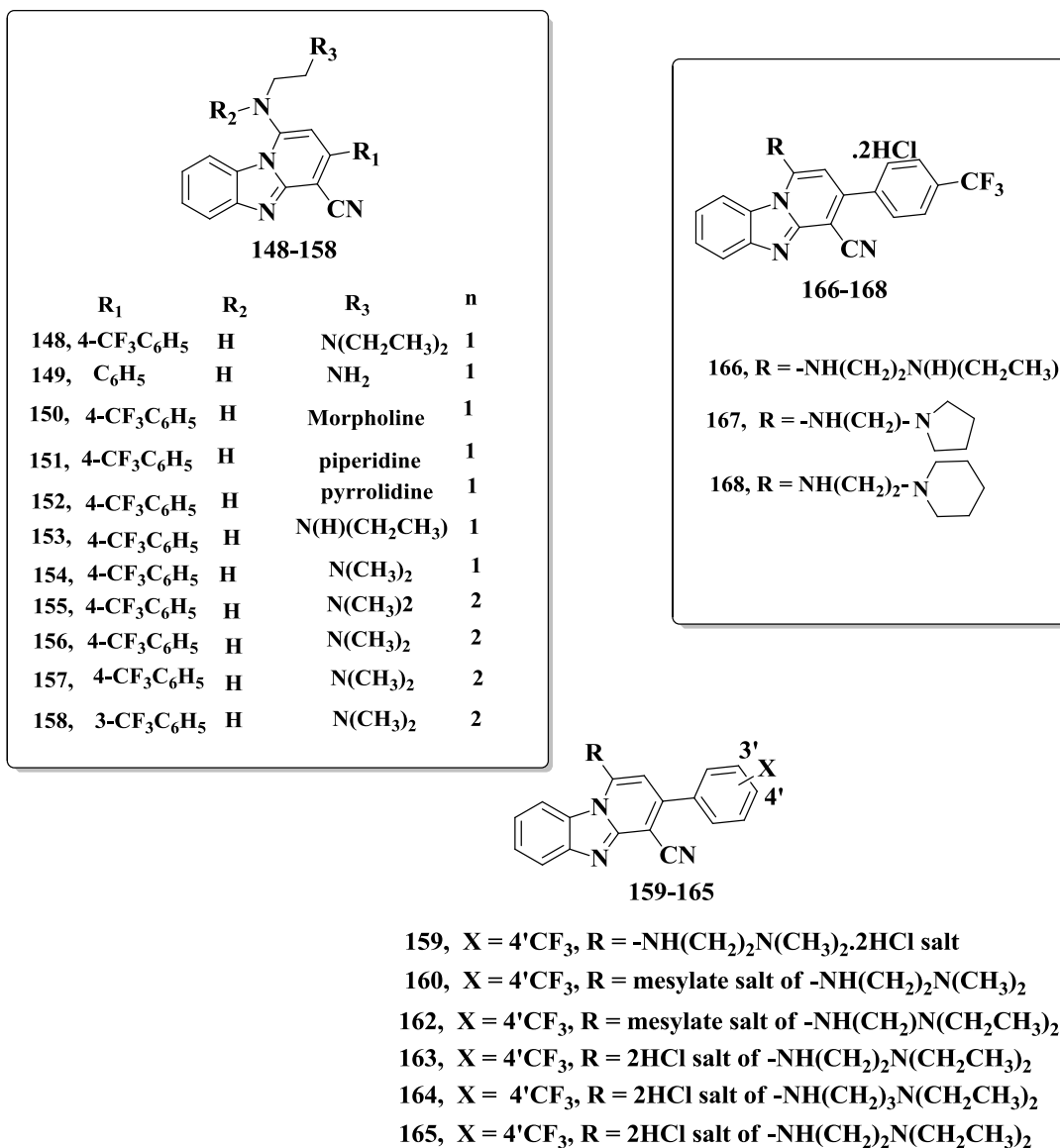


Figure 5. Structure of anti-malarial benzimidazole based derivatives (*count.*)

Farahat and co-worker have synthesized a novel series of indole and benzimidazole bichalcophene diamidine derivatives (**Figure 5**) and further screened for their antimicrobial activity against the tropical parasites and malaria. Newly synthesized indole bichalcophene analogues **141 - 144** re-tremendously active against trypanosomes (IC₅₀ values from 2 to 15 nM) and malaria (IC₅₀ from 2.9 to 7.3 nM). These indole analogues exhibited

6.1 ANTI-TUBERCULOSIS AND ANTI-BACTERIAL ACTIVITIES OF BENZIMIDAZOLE

exceptional selectivity against both parasites, with selectivity indices from 1046 to 5800 against *T. b. r.* and from 1000 to 2588 against *Plasmodium falciparum* the antitrypanosomal activity of the benzimidazole diamidines **145 - 147** (IC₅₀ values from 25 to 102 nM) was moderate as compared to the indole analogues **141 - 144**. The analogue **145** was less active (IC₅₀ of 91.9 nM) compared with its indole counterpart **141** (IC₅₀ of 2.9 nM) against malarial parasites [269]. Moreover, Ndakala *et al.* have synthesized A novel class of pyrido[1,2-a]benzimidazoles (**Figure 5**) and evaluated for their anti-malarial activity against the multidrug-resistant *Plasmodium falciparum* K1 strain. Many of the compounds showed antimalarial activity comparable to the standard drug Chloroquine (IC₅₀ = 0.17–0.20 μM), where compound **148** shows potent activity (IC₅₀ = 0.047 μM, ~ 3.5 times more potent than Chloroquine) and **149** the moderately active (IC₅₀ = 4.48 μM, ~ 22 times less potent than Chloroquine and ~ 95 times less potent than **148**). The replacement of a CF₃ group into Phenyl or mono substituents aryl groups at R1 in place of showed better activity of up to 10-fold in all cases, and activity was further improved when the R1 aryl group was substituted (CF₃, Cl, or F) at the 40 position. There is no significant effect on the *in vitro* anti-plasmodial activity while doing variation in the alkyl chain length and variation found only by one methylene unit. The morpholino derivative **150** presented moderate activity than other cycloalkylamino derivatives **151** and **152**. Compounds **148** and **153** revealed poor active variant across a wide range of drug sensitive and drug resistant strains of *Plasmodium falciparum*. Furthermore, compounds **154, 148, 155, 156, 157** and **158** with the most potent activity and selectivity from the *in vitro* screen were chosen for preliminary *in vivo* evaluation against *Plasmodium berghei* infected mice. The corresponding hydrochloride salts **159 - 165**, as well as two mesylate salts **160** and **162**, were used for the *in vivo* studies. At a repeat dose of 50 (mg/kg) per day ip for 4 days four of these **160, 163,**

162 and **164** showed significant efficacy. Subsequently they were also found to be active following oral (po) administration with 100 (mg/kg) per day (4 Days), giving > 90% inhibition of *Plasmodium berghei* parasitemia and a significant increase in the mean survival time (MSD) of the mice. The lack of *in vivo* activity with the hydrochloride salt of **154** compared to the mesylate salt **160** when given ip may be due to a poorer solubility or dissolution rate adversely affecting distribution. In single dose studies in the *Plasmodium berghei* mouse model, the hydro chloride salts of **163**, **166**, **167**, **168** analogues exhibited potent activity at 25 mg/kg and it remains same at a higher dose of 50 mg/kg, presumably due to saturation of systemic exposure. While compound **168** was weak at 50 mg/kg due to a problem with formulation arising from poor solubility. In any case the rate of reduction in parasitemia after treatment with the pyrido benzimidazoles was significantly slower than the standard drug Chloroquine [270].

7.0 Biological importance of 4H-Pyran

Owing to the vast research on anti-tubercular activity, many synthesized heterocyclic compounds have efficiently displayed anti-tubercular activity. Various studies have indicated 4H-pyran derivatives display a potent activity against mycobacterium [271-273] as well as anticancer,[274] cytotoxic,[275] anti-inflammatory,[276] anti-HIV,[277-278] antimalarial,[279] antihyperglycemic, and antidyslipidemic,[280] antineurodegenerative disorders like Alzheimer's, Parkinson disease, Huntington's disease,[281] and many more [281-288] Furthermore, substituted 4H-pyran derivatives have encouraged increasing roles in synthetic methodologies to promising compounds in the field of medicinal,[283] pigment industries,[284] agrochemical and cosmetics.[285] Figure 1 represents some of the bioactive pyran-annulated heterocyclic compounds which are good antibacterial agents. At present, a series of synthetic 2-amino-3-cyno-4H-pyrans have been evaluated to possess potent antifungal, anti-bacterial [286-291] and anti-

7.0 BIOLOGICAL IMPORTANCE OF 4H-PYRAN

rheumatic [292] properties. Furthermore, 4*H*-pyrans and pyran-annulated heterocyclic scaffolds have drawn considerable interest in medicinal chemistry from the last several years. Keeping this knowledge, synthetic chemists develop useful synthetic routes to these heterocycles. A lot of synthetic methodologies are already reported.

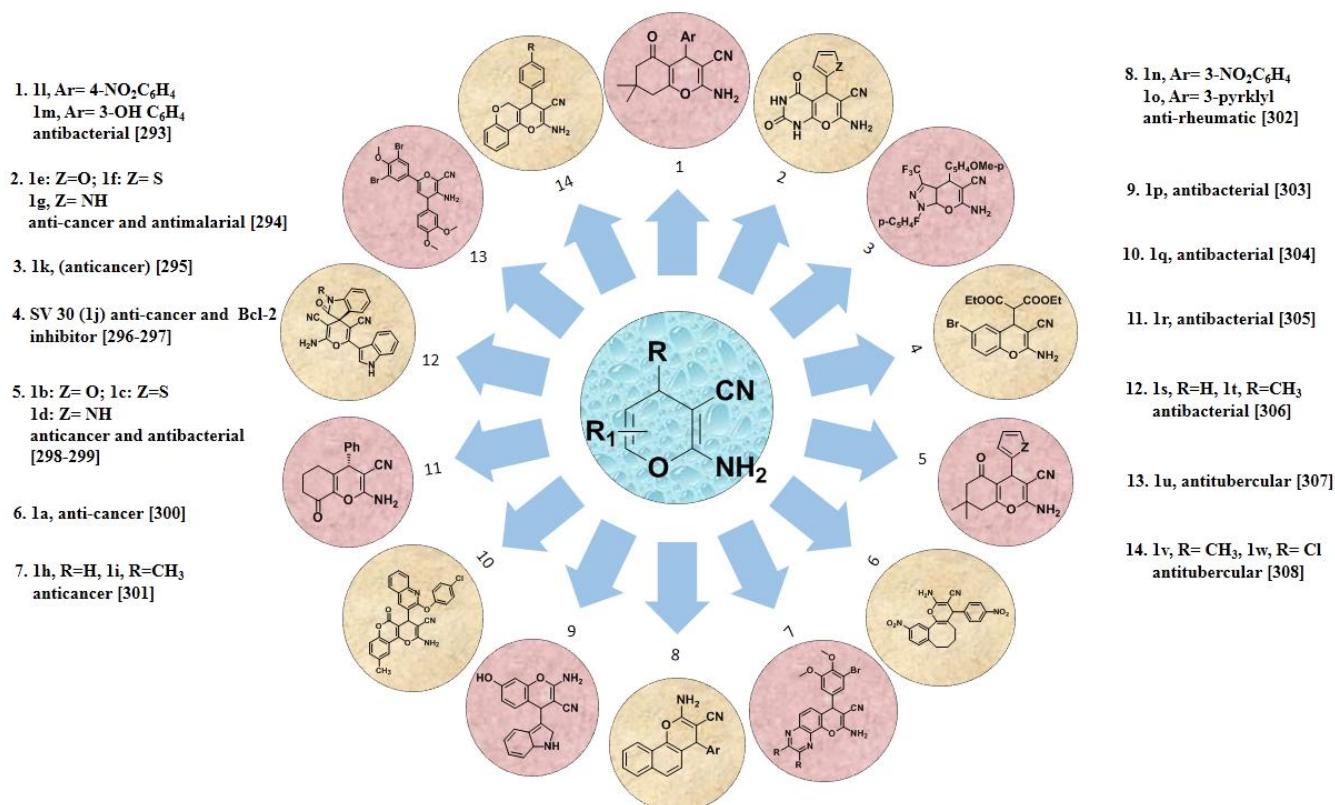


Figure 6. Reported biologically active pyran derivatives

8.0 Conclusion

It can be concluded that already existing first-line and second-line anti-tuberculosis drugs are enormously used which were discovered way back in the 1950s. Due to meagre success attempt rate obtained in the development of novel anti-tuberculosis drugs in the recent past, a lot of problems like Drug-Resistant (DR-TB), Multi-Drug Resistant (MDR-TB), Extensively Drug Resistant (XDR-TB), and recently emerging threat Totally Drug Resistant (TDR-TB) are prevailing. So, to cure these problems there occurs an urgent need for the development of new anti-TB drugs which can be used for reducing problems as seen before. Taking it to consideration about problems faced by TB, Delamanid (OPC-67683) and Bedaquiline (TMC-207) have been recently approved by FDA for their potent activity against MDR-TB and effective usage against TB treatment. Also, it was seen that there is certain novel anti-TB drug candidate in the pipeline, which is quite effective for TB of looking at the present scenario of problems faced by patients. Furthermore, we have discussed medicinally interesting benzimidazole and 4*H*-pyran based derivatives bearing different substitution on the benzene ring system as well as five membered hetero ring system. Moreover, a number of clinically used drugs having benzimidazole moiety also discussed. Many researcher found that few benzimidazole derivatives have poses tremendous biological activity against different pathogen which may lead for the new drug development novel mode of action. However, some of the compounds have several side effects in the case of toxicity. This drawback may decrease when the scientist will engage themselves in the development of active form of drugs with this moiety with help of recently developed interesting field in medicinal chemistry, computational chemistry. We hope that our findings in this study would be useful for the future development of potential drug candidate derived from benzimidazole and 4*H*-pyran.

References

1. Nunn P, Williams B, Floyd K, Dye C, Elzinga G. *Nature Reviews Immunology*. 2005; 5(10):819-826.
2. Schatz A, Waksman SA. *Experimental Biology and Medicine*. 1944; 57; 244-248.
3. When I Use a Word .I Mean It". *Brit. J. Med.* 1999; 319:972 (9 October)
4. Timothy M. D. Wallingford, Oxfordshire: CABI. 2011; 219.
5. Calvori C, Frontali L, Leoni L, Tecce G. *Nature*. 1965; 207:417-418.
6. Mani C, Selvakumar N, Narayanan S. and Narayanan PR. *Journal of Clinical Microbiology*. 2001; 39:2987-2990.
7. Rattan A, Kalia A, Ahmad N. *Emerging infectious diseases*. 1998; 4:195.
8. Sachan AS, Gupta RK, Katoch VM, Mishra K, Jakhmola P. *Indian Journal of Tuberculosis*. 2002; 39:209-211.
9. Somoskovi A, Parsons LM, Salfinger M. *Respiratory Research*. 2001;2:164-168.
10. Caws M, Duy PM, Tho DQ, Lan NT, Hoa DV, Farrar J. *Journal of Clinical Microbiology*. 2006; 44:2333–2337.
11. Traore H, Fissette K, Bastian I, Devleeschouwer M, Portaels F. *The International Journal of Tuberculosis and Lung Disease*. 2000; 4:481–484.
12. Comas I, Borrell S, Roetzer A, Rose G, Malla B, KatoMaeda M, Galagan J, Niemann S, Gagneux S. *Nature Genetics*. 2011;44:106–110.
13. Bernstein J, Lott WA, Steinberg BA, Yale HL. *The American Review of Respiratory Disease*. 1952; 65:357-364.
14. Zhang Y, Heym B, Allen B, Young D, Cole S. *Nature*. 1992; 358:591-593.
15. Banerjee A, Dubnau E, Quemard A, Balasubramanian V, Um KS, Wilson T, Collins D, De Lisle G, Jacobs Jr WR. *Science*. 1994; 263:227-9.

16. Vilchèze C, Morbidoni HR, Weisbrod TR, Iwamoto H, Kuo M, Sacchettini JC, Jacobs WR. *Journal of Bacteriology*. 2000; 182:4059-4067.
17. Slayden RA, Lee RE, Barry CE. *Molecular Microbiology*. 2000; 38:514–525
18. Lee AS, Lim IH, Tang LL, Telenti A, Wong SY. *Antimicrobial Agents and Chemotherapy*. 1999; 43:2087–2089.
19. Piatek AS, Telenti A, Murray MR, El-Hajj H, Jacobs WR, Kramer FR, Alland D. *Antimicrobial Agents and Chemotherapy*. 2000; 44:103-110.
20. Argyrou A, Vetting MW, Aladegbami B, Blanchard JS. *Nature Structural & Molecular Biology*. 2006; 13:408–413.
21. Argyrou A, Jin L, SiconilfiBaez L, Angeletti RH, Blanchard JS. *Biochemistry*. 2006;45:13947–13953.
22. Hazbón MH, Brimacombe M, Bobadilla del Valle M, Cavatore M, Guerrero MI, VarmaBasil M, BillmanJacobe H, Lavender C, Fyfe J, García-García L, León CI. *Antimicrobial Agents and Chemotherapy*. 2006;50:2640–2649.
23. Cardoso RF, Cardoso MA, Leite CQ, Sato DN, Mamizuka EM, Hirata RD, de Mello FF, Hirata MH. *Memórias do Instituto Oswaldo Cruz*. 2007; 102:59–61.
24. Ando H, Kitao T, MiyoshiAkiyama T, Kato S, Mori T, Kirikae T. *Molecular Microbiology*. 2011; 79:1615–1628.
25. Ando H, MiyoshiAkiyama T, Watanabe S, Kirikae T. *Molecular Microbiology*. 2014; 91:538–547.
26. Dalmer O, Walter E, Firma E. *Patentiert im Deutschen Reiche vom*. 1934; 8:1936.
27. Yeager RL, Munroe WG, Dessau FI. *The American Review of Respiratory Disease* 1952; 65:523-546.
28. Fox W, Ellard GA, Mitchison DA. *The International Journal of Tuberculosis and Lung Disease*. 1999; 3:S231-279.

29. Somner AR, British Thoracic Association. *British Journal of Diseases of the Chest*. 1981; 75:141-153.
30. Mitchison DA. *Tubercle*. 1985; 66:219-225.
31. Boshoff HI, Mizrahi V, Barry CE. *Journal of Bacteriology*. 2002; 184:2167-2172.
32. Zhang Y, Wade MM, Scorpio A, Zhang H, Sun Z. *Journal of Antimicrobial Chemotherapy*. 2003; 52:790-795.
33. Zhang Y, Permar S, Sun Z. *Journal of Medical Microbiology*. 2002; 51:42-49.
34. Hu Y, Coates AR, Mitchison DA. *The International Journal of Tuberculosis and Lung Disease*. 2006; 10:317-322.
35. Scorpio A, Zhang Y. *Nature Medicine*. 1996; 2:662-667.
36. Fyfe PK, Rao VA, Zemla A, Cameron S, Hunter WN. *Angewandte Chemie International Edition*. 2009; 48:9176–9179.
37. Seiner DR, Hegde SS, Blanchard JS. *Biochemistry* 2010; 49: 9613–9619.
38. Konno K, Feldmann FM, McDermott W. *The American Review of Respiratory Disease*. 1967; 95:461-469.
39. Scorpio A, Zhang Y. *Nature Medicine*. 1996; 2:662-667.
40. Scorpio A, Lindholm-Levy P, Heifets L, Gilman R, Siddiqi S, Cynamon M, Zhang Y. *Antimicrobial Agents and Chemotherapy*. 1997; 41: 540–543.
41. Petrella S, Gelus-Ziental N, Maudry A, Laurans C, Boudjelloul R, Sougakoff W. *PLOS ONE*. 2011; 6:15785.
42. Shi W, Zhang X, Jiang X, Yuan H, Lee JS, Barry CE, Wang H, Zhang W, Zhang Y. *Science*. 2011; 333:1630-1632.
43. Feuerriegel S, Koser CU, Richter E, Niemann S. *Journal of Antimicrobial Chemotherapy*. 2013; 68:1439–1440.

44. Organization W H. Anti-Tuberculosis Drug Resistance in the World, Report No. 4.
http://www.who.int/tb/publications/2008/drs_report4_26feb08.pdf. World Health Organization, Geneva, Switzerland. 2008.
45. Thomas JP, Baughn CO, Wilkinson RG, Shepherd RG. The American Review of Respiratory Disease. 1961; 83:891-893.
46. Karlson AG. The American Review of Respiratory Disease. 1961; 84:905-906.
47. Wilkinson RG, Shepherd RG, Thomas JP, Baughn C. Journal of the American Chemical Society. 1961; 83:2212-2213.
48. Wilkinson RG, Cantrall MB, Shepherd RG. Journal of Medicinal Chemistry. 1962; 5:835-845.
49. Takayama K, Kilburn JO. Antimicrobial Agents and Chemotherapy. 1989; 33:1493-1499.
50. Silve G, Valero-Guillen P, Quemard A, Dupont MA, Daffe MA, Laneelle G. Antimicrobial Agents and Chemotherapy. 1993; 37:1536-1538.
51. Belanger AE, Besra GS, Ford ME, Mikusová K, Belisle JT, Brennan PJ, Inamine JM. Proceedings of the National Academy of Sciences. 1996; 93:11919-11924.
52. Telenti A, Philipp WJ, Sreevatsan S, Bernasconi C, Stockbauer KE, Wieles B, Musser JM, Jacobs WR.. Nature Medicine. 1997; 3:567-570.
53. Deng L, Mikusova K, Robuck KG, Scherman M, Brennan PJ, McNeil M. R. Antimicrobial Agents and Chemotherapy. 1995; 39:694-701.
54. Edson RS, Terrell CL. Mayo Clinic Proceedings. 1991; 66:1158-1164.
55. Comroe Jr JH. The American Review of Respiratory Disease. 1978; 117:957-968.
56. Kingston W. Streptomycin, Schatz v. Journal of the History of Medicine and Allied Sciences. 2004; 59:441-462.

57. Schatz A, Bugle E, Waksman SA. *Experimental Biology and Medicine*. 1944; 55:66-69.
58. Hinshaw H, Feldman WH. *Proceedings of Staff Meetings of the Mayo Clinic* 1945; 20:313-318.
59. Musser JM. *Clinical Microbiology Reviews*. 1995; 8:496-514.
60. Waksman SA, Lechevalier HA. *Science*. 1949; 305-307.
61. Metcalfe NH. *Journal of Medical Biography*. 2011; 19:10-14.
62. Bilgin N, Claesens F, Pahverk H, Ehrenberg M. *Journal of Molecular Biology*. 1992; 224:1011–1027.
63. Karimi R, Ehrenberg M. *The EMBO Journal* 1996;15: 1149–1154.
64. Powers T, Noller HF. *Journal of Molecular Biology*. 1994; 235:156–172.
65. Chang F, Flaks JG. *Antimicrobial Agents and Chemotherapy*. 1972; 2:294–307.
66. Grisé-Miron L, Brakier-Gingras L. *European Journal of Biochemistry*. 1982; 123:643–646.
67. Lando D, Cousin MA, Ojasoo T, Raymond JP. *European Journal of Biochemistry*. 1976; 66:597–606.
68. Moazed D, Noller HF. *Nature*. 1986; 327:389–394.
69. Gravel M, Melancon P, Brakier-Gingras L. *Biochemistry* 1987; 26:6227–6232.
70. Montandon PE, Nicolas P, Schümann P, Stutz E. *Nucleic Acids Research*. 1985; 13:4299-4310.
71. Frattali AL, Flynn MK, De Stasio EA. *Biochimica et Biophysica Acta (BBA) - Gene Structure and Expression*. 1990; 1050:27-33.
72. Leclerc D, Melançon P, Brakier-Gingras L. *Biochimie* 1991; 73:1431–1438.

73. Lodmell JS, Gutell RR, Dahlberg AE. Proceedings of the National Academy of Sciences of the USA. 1995; 92:10555–10559.
74. Pinard R, Payant C, Melançon P, Brakier-Gingras L. The FASEB Journal. 1993; 7:173-176.
75. Powers T, Noller HF. The EMBO Journal 1991; 10:2203-2214.
76. Santer M, Santer U, Nurse K, Bakin A, Cunningham P, Zain M, *et al.* Biochemistry. 1993; 32:5539–5547.
77. Melancon P, Boileau G, Brakier-Gingras L. Cross-linking of Streptomycin to the 30S subunit of *Escherichia coli* with phenyldiglyoxal. Biochemistry 1984; 23:6697–6703.
78. Abad JP, Amils R. Journal of Molecular Biology. 1994; 235:1251-1260.
79. Hill W E. American Society for Microbiology; 1990.
80. Raymon, Lionel P. Miami, FL: Kaplan, Inc. 2011; 181.
81. Voet D, Voet JG. John Wiley & Sons. 2004; 1341.
82. Spickler C, Brunelle MN, Brakier-Gingras L. Journal of Molecular Biology. 1997; 273:586-599
83. Ethionamide. Global Tuberculosis Community Advisory Board. 2016.
84. Trecator SC tablet by Wyeth
<http://www.fda.gov/downloads/Safety/MedWatch/SafetyInformation/SafetyAlertsf orHuman Medical products/UCM164879.pdf>. 2016.
85. Winder FG, Collins PB, Whelan D. Journal of general microbiology. 1971; 66:379–380.
86. Winder F. Academic Press, London. 1982; 1:353-438
87. Heym B, Saint-Joanis B, Cole ST. International Journal of Tuberculosis and Lung Disease. 1999; 79:267-271.

88. Barry CE, Slayden RA, Mdluli K. Drug Resistance Updates. 1998; 1:128-134.
89. Loewen PC, Klotz MG, Hassett DJ. ASM News. 2000; 66:76-82.
90. Quémard AN, Lanéelle GI, Lacave CH. Antimicrobial Agents and Chemotherapy. 1992; 36:1316-1321.
91. Baulard AR, Betts JC, Engohang-Ndong J, Quan S, McAdam RA, Brennan PJ, Loch C, Besra GS. Journal of Biological Chemistry. 2000; 275:28326-28331.
92. Vilchèze C, Wang F, Arai M, Hazbón MH, Colangeli R, Kremer L, Weisbrod TR, Alland D, Sacchetti JC, Jacobs WR. Nature Medicine. 2006; 12:1027-1029.
93. Goss WA, Deitz WH, Cook TM. Journal of Bacteriology. 1965; 89:1068-1074.
94. Fàbrega A, Madurga S, Giralt E, Vila J. Microbial Biotechnology. 2009; 2:40–61.
95. Cheng AF, Yew WW, Chan EW, Chin ML, Hui MM, Chan RC. Antimicrobial Agents and Chemotherapy. 2004; 48:596–601.
96. Sun Z, Zhang J, Zhang X, Wang S, Zhang Y, Li C. The International Journal of Antimicrobial Agents. 2008; 31:115–121.
97. Rengarajan J, Sasseti CM, Naroditskaya V, Sloutsky A, Bloom BR, Rubin EJ. Molecular Microbiology. 2004; 53:275–282.
98. Tomlinson C. "TB Online - Capreomycin". 2016; [accessed on 18.08.16]
99. Farmer P, Kim JY. The BMJ. 1998; 317:671.
100. Sutton WB, Gordee RS, Wick WE, Stanfield L. Annals of the New York Academy of Sciences. 1966; 135:947-959.
101. Trnka L, Smith DW. Karger Publishers. 1970; 369-379.
102. Gale EF, Cundliffe E, Reynolds PE, Richmond MH, Waring MJ. London: Wiley. 1972.

103. Blumberg H, Burman WJ, Chaisson RE, Daley CL, Etkind SC, Friedman LN, Fujiwara P, Grzemska M, Hopewell PC, Iseman MD, Jasmer RM. *American Journal of Respiratory and Critical Care Medicine*. 2003; 167:603.
104. McClatchy JK, Kanes W, Davidson PT, Moulding TS. *Tubercle*. 1977; 58:29-34.
105. Stanley RE, Blaha G, Grodzicki RL, Strickler MD, Steitz TA. *Nature Structural & Molecular Biology*. 2010; 17:289-293.
106. Modolfl J, Vázquez D. *European Journal of Biochemistry* 1977; 81:491-497.
107. Peske F, Savelsbergh A, Katunin VI, Rodnina MV, Wintermeyer W. *Journal of Molecular Biology*. 2004; 343:1183-1194.
108. Johansen SK, Maus CE, Plikaytis BB, Douthwaite S. *Molecular Cell*. 2006; 23:173-182.
109. Maus CE, Plikaytis BB, Shinnick TM. *Antimicrobial Agents and Chemotherapy*. 2005; 49:571-577.
110. Maus CE, Plikaytis BB, Shinnick TM. *Antimicrobial Agents and Chemotherapy*. 2005; 49:3192-3197.
111. Monshupanee T, Gregory ST, Douthwaite S, Chungjatupornchai W, Dahlberg AE. *Journal of Bacteriology*. 2008; 190:7754-7761.
112. Umezawa H, Ueda M, Maeda K, Yagishita K, Kondo S, Okami Y, Utahara R, Osato Y, Nitta K, Takeuchi T. *The Journal of Antibiotics*. 1957; 10:181.
113. Umezawa H. *Annals of the New York Academy of Sciences*. 1958; 76; 20-26.
114. Garland J. Kanamycin (editorial). *N Engl J Med*. 1958; 259:352-353.
115. Wong CH, Hendrix M, Priestley ES, Greenberg WA. *Chemistry & Biology*. 1998; 5:397-406.

116. Amikacin Pharmacodynamics and Mechanism of Action.
https://medipub.blogspot.in/2011/04/amikacin-pharmacodynamics-and-mechanism_24.html.2016.
117. Udwadia ZF. Thorax. 2012; 67:286-288.
118. Matsumoto M, Hashizume H, Tomishige T, Kawasaki M, Tsubouchi H, Sasaki H, Shimokawa Y, Komatsu M. PLOS Medicine. 2006; 3:466.
119. WHO. Geneva 2014:
http://apps.who.int/iris/bitstream/10665/137334/1/WHO_HTM_TB_2014.23_eng.pdf?ua=1.2016.
120. Organization W H. The Selection and Use of Essential Medicine Report: 20–24 April. Geneva. 2015.
http://www.who.int/medicines/publications/essentialmedicines/Executive-Summary_EML-2015_7-May-15.pdf.2016; [accessed on 14.07.16]
121. Matsumoto M. 2003; Otsuka Study No. 019064.
122. Andries K, Verhasselt P, Guillemont J, Göhlmann HW, Neefs JM, Winkler H, Van Gestel J, Timmerman P, Zhu M, Lee E, Williams P. Science. 2005; 307:223-227.
123. Ralph AP, Anstey NM, Kelly P. Clinical Infectious Diseases. 2009; 49:574-83.
124. Huitric E, Verhasselt P, Andries K, Hoffner SE. Clinical Infectious Diseases. 2007; 51:4202-4204.
125. Koul A, Dendouga N, Vergauwen K, Molenberghs B, Vranckx L, Willebrords R, Ristic Z, Lill H, Dorange I, Guillemont J, Bald D. Nature Chemical Biology. 2007; 3:323-324.
126. Lounis N, Veziris N, Chauffour A, Truffot-Pernot C, Andries K, Jarlier V. Antimicrobial Agents and Chemotherapy. 2006; 50:3543-547.

127. Chahine EB, Karaoui LR, Mansour H. *Annals of Pharmacotherapy*. 2014; 48:107-115.
128. Palomino JC, Martin A. *Future Microbiology*. 2013; 8:1071-1080.
129. Petrella S, Cambau E, Chauffour A, Andries K, Jarlier V, Sougakoff W. *Antimicrobial Agents and Chemotherapy*. 2006; 50:2853-2856.
130. Segala E, Sougakoff W, Nevejans C A, Jarlier V, Petrella S. *Antimicrobial Agents and Chemotherapy*. 2012;56:2326–2634.
131. Huitric E, Verhasselt P, Koul A, Andries K, Hoffner S, Andersson D.I. *Antimicrobial Agents and Chemotherapy*. 2010;54:1022–1028.
132. Gaudillière B, Berna P, *Annual Reports in Medicinal Chemistry*. Manoj C. Desai, In: editor. 2000; 35: 340-343.
133. Woodcock JM, Andrews JM, Boswell FJ, Brenwald NP, Wise R. *Antimicrobial Agents and Chemotherapy*. 1997; 41:101-106.
134. Blumberg HM, Burman WJ, Chaisson RE, Daley CL, Etkind SC, Friedman LN, Fujiwara P, Grzemska M, Hopewell PC, Iseman MD, Jasmer RM, Koppaka V, Menzies RI, O'Brien RJ, Reves RR, Reichman LB, Simone PM, Starke JR, Vernon AA. *American Journal of Respiratory and Critical Care Medicine*. 2003; 167:603–662
135. Grossman RF, Hsueh PR, Gillespie SH, Blasi F. *International Journal of Infectious Diseases* 2014; 18:14-21.
136. Leach KL, Brickner SJ, Noe MC, Miller PF. *Annals of the New York Academy of Sciences*. 2011; 1222:49-54.
137. Brickner SJ, Hutchinson DK, Barbachyn MR, Manninen PR, Ulanowicz DA, Garmon SA, Grega KC, Hendges SK, Toops DS, Ford CW, Zurenko GE. *Journal of Medicinal Chemistry*. 1996; 39:673-679.

138. Zurenko GE, Yagi BH, Schaadt RD, Allison JW, Kilburn JO, Glickman SE, *et al.* Antimicrobial Agents and Chemotherapy. 1996; 40:839-845.
139. Hadjiangelis NP, Leibert E, Harkin TJ. American Journal of Respiratory and Critical Care Medicine. 2003; 167:868.
140. Shinabarger D. Expert Opinion on Investigational Drugs. 1999; 8:1195-1202.
141. Ippolito JA, Kanyo ZF, Wang D, Franceschi FJ, Moore PB, Steitz TA, Duffy EM. Journal of Medicinal Chemistry. 2008; 51:3353-3356.
142. Sotgiu G, Pontali E, Migliori GB. European Respiratory Journal. 2015; 45:25-29.
143. Lechartier B, Rybniker J, Zumla A, Cole S. EMBO Molecular Medicine. 2014.
144. Koul A, Arnoult E, Lounis N, Guillemont J, Andries K.. Nature. 2011; 469:483-490.
145. Stover CK, Warrener P, VanDevanter DR, Sherman DR, Arain TM, Langhorne MH, Anderson SW, Towell JA, Yuan Y, McMurray DN, Kreiswirth BN, Barry CE, Baker WR. Nature. 2000; 405:962-966.
146. Choi KP, Bair TB, Bae YM, Daniels L. Journal of Bacteriology. 2001; 183:7058-7066.
147. Manjunatha UH, Boshoff H, Dowd CS, Zhang L, Albert TJ, Norton JE, Daniels L, Dick T, Pang SS, Barry CE. Proceedings of the National Academy of Sciences of the USA. 2006; 103:431-436.
148. Protopopova M, Hanrahan C, Nikonenko B, Samala R, Chen P, Gearhart J, Einck L, Nacy CA. Journal of Antimicrobial Chemotherapy. 2005; 56:968-974.
149. Boshoff HI, Myers TG, Copp BR, McNeil MR, Wilson MA, Barry CE. Journal of Biological Chemistry. 2004; 279:40174-40184.

150. Tahlan K, Wilson R, Kastrinsky DB, Arora K, Nair V, Fischer E, Barnes SW, Walker JR, Alland D, Barry CE, Boshoff HI. *Antimicrobial Agents and Chemotherapy*. 2012; 56:1797-809.
151. Gregory WA, inventor; EI Dupont De Nemours, assignee. United States Patent US 4,461,773. 1984.
152. Louie A, Eichas K, Files K, Swift M, Bahniuk N. 51st ICAAC - American Society for Microbiology, Washington, DC. 2011.
153. Williams KN, Brickner SJ, Stover CK, Zhu T, Ogden A, Tasneen R, Tyagi S, Grosset JH, Nuermberger EL. *American Journal of Respiratory and Critical Care Medicine*. 2009; 180:371–376.
154. Villemagne B, Crauste C, Flipo M, Baulard AR, Déprez B, Willand N. *European Journal of Medicinal Chemistry*. 2012 May 31; 51:1-6.
155. Williams KN, Stover CK, Zhu T, Tasneen R, Tyagi S, Grosset JH, Nuermberger E. *Antimicrobial Agents and Chemotherapy*. 2009; 53:1314-19.
156. Cynamon MH, Klemens SP, Sharpe CA, Chase S. *Antimicrobial Agents and Chemotherapy*. 1999; 43:1189-1191.
157. Wallis RS, Jakubiec W, Kumar V, Bedarida G, Silvia A, Paige D, Zhu T, Mitton-Fry M, Ladutko L, Campbell S, Miller PF. *Antimicrobial Agents and Chemotherapy*. 2011; 55:567-574.
158. Louie A, Eichas K, Files K, Swift M, Bahniuk N. 51st ICAAC - American Society for Microbiology, Washington, DC. Abstract A1–1737. 2011.
159. Wallis RS, Dawson R, Friedrich SO, Venter A, Paige D, Zhu T, Silvia A, Gobey J, Ellery C, Zhang Y, Eisenach K. *PLOS ONE*. 2014; 9:94462.
160. Nikonenko BV, Protopopova M, Samala R, Einck L, Nacy CA. *Antimicrobial Agents and Chemotherapy*. 2007; 51:1563-1565.

161. Czock D, Keller F. *Journal of Pharmacokinetics and Pharmacodynamics*. 2007; 34:727-751.
162. Gravestock MB, Acton DG, Betts MJ, Dennis M, Hatter G, McGregor A, Swain ML, Wilson RG, Woods L, Wookey A. *Bioorganic & Medicinal Chemistry Letters*. 2003; 13:4179–4186.
163. Ragno R, Marshall GR, Di Santo R, Costi R, Massa S, Rompei R, Artico M. *Bioorganic & Medicinal Chemistry*. 2000; 8:1423-1432.
164. Abstract n.63 submitted to the American Chemical Society Meeting, Anaheim CA, March 28-April 01 2004.
165. <http://www.newtbdrugs.org/project.php?id=145> :2016; [accessed on 01.08.16]
166. Bogatcheva E, Hanrahan C, Nikonenko B, De Los Santos G, Reddy V, Chen P, Barbosa F, Einck L, Nacy C, Protopopova M. *Bioorganic & Medicinal Chemistry Letters*. 2011; 21:5353-5357.
167. Makarov V, Manina G, Mikusova K, Möllmann U, Ryabova O, Saint-Joanis B, Dhar N, Pasca MR, Buroni S, Lucarelli AP, Milano A. *Science*. 2009; 324:801-804.
168. <http://www.newtbdrugs.org/project.php?id=202802> 2016.
169. Pasca MR, Degiacomi G, Ribeiro AL, Zara F, De Mori P, Heym B, Mirrione M, Brerra R, Pagani L, Pucillo L, Troupioti P. *Antimicrobial Agents and Chemotherapy*. 2010; 54:1616-1618.
170. Mikusová K, Huang H, Yagi T, Holsters M, Vereecke D, D’Haeze W, Scherman MS, Brennan PJ, McNeil MR, Crick DC. *Journal of Bacteriology*. 2005; 187:8020-8025.
171. Trefzer C, RengifoGonzalez M, Hinner MJ, Schneider P, Makarov V, Cole ST, Johnsson K. *Journal of the American Chemical Society*. 2010;132:13663-13665.

172. Okumura R, Hirata T, Onodera Y, Hoshino K, Otani T, Yamamoto T. *Journal of Antimicrobial Chemotherapy*. 2008; 62:98-104.
173. Onodera Y, Hirata T, Hoshino K, Otani T. 47th ICAAC - American Society for Microbiology, Washington, DC. Abstract. F1-2126. 2007.
174. Sekiguchi JI, Disratthakit A, Maeda S, Doi N. *Antimicrobial Agents and Chemotherapy* 2011; 55:3958-3960.
175. Disratthakit A, Doi N. *Antimicrobial Agents and Chemotherapy*. 2010; 54:2684-2686.
176. Ahmad Z, Minkowski A, Peloquin CA, Williams KN, Mdluli KE, Grosset JH, Nuermberger EL. *Antimicrobial Agents and Chemotherapy*. 2011; 55:1781-1783.
177. Takahashi Y, Igarashi M, Miyake T, Soutome H, Ishikawa K, Komatsuki Y, Koyama Y, Nakagawa N, Hattori S, Inoue K, Doi N. *The Journal of Antibiotics*. 2013; 66:171-178.
178. Working Group on New TB Drugs CPZEN-45, Stop TB Partnership, 2009.
179. Hashizume H, Sawa R, Harada S, Igarashi M, Adachi H, Nishimura Y, Nomoto A. *Antimicrobial Agents and Chemotherapy*. 2011; 55:3821-3828.
180. Sawa R, Takahashi Y, Hashizume H, Sasaki K, Ishizaki Y, Umekita M, Hatano M, Abe H, Watanabe T, Kinoshita N, Homma Y. *Chemistry: A European Journal*. 2012; 18:15772-15781.
181. Pethe K, Bifani P, Jang J, Kang S, Park S, Ahn S, Jiricek J, Jung J, Jeon HK, Cechetto J, Christophe T. *Nature Medicine*. 2013; 19:1157-1160.
182. <https://www.fmhs.auckland.ac.nz/en/faculty/about/news-and-events/news/2012/09/21/promising-new-zealand.html>
183. Moffett M, McGill MI. *The BMJ*. 1960; 2:910.
184. Mukherjee T, Boshoff H. *Future Medicinal Chemistry*. 2011; 3:1427-1454.

185. Anderson RF, Shinde SS, Maroz A, Boyd M, Palmer BD, Denny WA. *Organic and Biomolecular Chemistry*. 2008; 6:1973-1980.
186. Kmentova I, Sutherland HS, Palmer BD, Blaser A, Franzblau SG, Wan B, Wang Y, Ma Z, Denny WA, Thompson AM. *Journal of Medicinal Chemistry*. 2010; 53:8421-8439.
187. Palmer BD, Thompson AM, Sutherland HS, Blaser A, Kmentova I, Franzblau SG, Wan B, Wang Y, Ma Z, Denny WA. *Journal of Medicinal Chemistry*. 2009; 53:282-294.
188. NCT01424670 - ClinicalTrials.gov
<https://clinicaltrials.gov/ct2/show/NCT01424670> 2016.
189. Denny WA. *Chemistry in New Zealand*. 2015; 1:18-22.
190. WGND TBA-354 Profile - Working Group on New TB Drugs
<http://www.newtbdrugs.org/project.php?id=48> 2016.
191. Dye C, Espinal MA, Watt CJ, Mbiaga C, Williams BG. *The Journal of Infectious Diseases*. 2002; (185): 1197-202.
192. Diacon AH, Dawson R, du Bois J, Narunsky K, Venter A, Donald PR, van Niekerk C, Erond N, Ginsberg AM, Becker P, Spigelman MK. *Antimicrobial Agents and Chemotherapy*. 2012; (56): 3027-3031.
193. Mukherjee T, Boshoff H. *Future Medicinal Chemistry*. 2011; (3): 1427-1454.
194. Stover CK, Warrener P, VanDevanter DR, Sherman DR, Arain TM, Langhorne MH, Anderson SW, Towell JA, Yuan Y, McMurray DN, Kreiswirth BN. *Nature*. 2000; 405(6789): 962-966.

195. Diacon AH, Dawson R, von Groote-Bidlingmaier F, Symons G, Venter A, Donald PR, van Niekerk C, Everitt D, Winter H, Becker P, Mendel CM. *The Lancet*. 2012; 380(9846):986-993.
196. Ryan NJ, Lo JH. *Drugs*. 2014; 74(9): 1041-1045.
197. Andries K, Verhasselt P, Guillemont J, *et al.* *Science*. 2005; (307): 223-227
198. Koul A, Dendouga N, Vergauwen K, Molenberghs B, Vranckx L, Willebrords R, Ristic Z, Lill H, Dorange I, Guillemont J, Bald D. *Nature Chemical Biology*. 2007; 3(6): 323.
199. European Medicines Agency. CHMP Assessment Report: SIRTURO. http://www.ema.europa.eu/docs/en_GB/document_library/Summary_of_opinion_initial_authorisation/human/002614/WC500158728.pdf.
200. Andries K, Verhasselt P, Guillemont J, Göhlmann HW, Neefs JM, Winkler H, Van Gestel J, Timmerman P, Zhu M, Lee E, Williams P. *Science*. 2005; 307(5707): 223-227.
201. Pym AS, Diacon AH, Tang SJ, Conradie F, Danilovits M, Chuchottaworn C, Vasilyeva I, Andries K, Bakare N, De Marez T, Haxaire-Theeuwes M. *European Respiratory Journal*. 2015; 724.
202. International Union against Tuberculosis and Lung Disease. Current Trials: STREAM clinical trial to test first all-oral MDR-TB treatment regimen. www.theunion.org/what-we-do/research/clinical-trials.
203. Nunn AJ, Rusen ID, Van Deun A, *et al.* *Trials* 2014; (15): 353.
204. <http://www.outsourcing-pharma.com/Preclinical-Research/Macrolide-drug-class-extended-to-treat-TB>.
205. <http://www.newtbdrugs.org/pipeline/discovery>.

206. Zhu ZJ, Krasnykh O, Pan D, Petukhova V, Yu G, Liu Y, Liu H, Hong S, Wang Y, Wan B, Liang W. *Tuberculosis*. 2008; 88: S49-63.
207. Griffith DE, Aksamit T, Brown-Elliott BA, Catanzaro A, Daley C, Gordin F, Holland SM, Horsburgh R, Huitt G, Iademarco MF, Iseman M. *American Journal of Respiratory and Critical Care Medicine*. 2007; 175(4): 367-416.
208. Mogayzel Jr PJ, Naureckas ET, Robinson KA, Mueller G, Hadjiliadis D, Hoag JB, Lubsch L, Hazle L, Sabadosa K, Marshall B. *American Journal of Respiratory and Critical Care Medicine*. 2013; 187(7): 680-689.
209. Glassford I, Teijaro CN, Daher SS, Weil A, Small MC, Redhu SK, Colussi DJ, Jacobson MA, Childers WE, Buttaro B, Nicholson AW. *Journal of the American Chemical Society*. 2016; 138(9): 3136-3144.
210. World Health Organization. Guidelines for the programmatic management of drug-resistant tuberculosis. 2011 update. Geneva, World Health Organization, 2011.
211. Vinh DC, Rubinstein E. *Journal of Infection*. 2009; 59: S59 - 74.
212. Ippolito JA, Kanyo ZF, Wang D, *et al.* *Journal of Medicinal Chemistry*. 2008; (51): 3353-3356.
213. Leach KL, Brickner SJ, Noe MC, Miller PF. *Annals of the New York Academy of Sciences*. 2011; (1222): 49-54.
214. Ashtekar DR, Costa-Periera R, Shrinivasan T, Iyyer R, Vishvanathan N, Rittel W. *Diagnostic Microbiology and Infectious Disease*. 1991; (14): 465-471.
215. Migliori GB, Eker B, Richardson MD, Sotgiu G, Zellweger JP, Skrahina A, Ortmann J, Girardi E, Hoffmann H, Besozzi G, Bevilacqua N. *European Respiratory Journal*. 2009; 34(2): 387-93.

216. Shaw KJ, Barbachyn MR. *Annals of the New York Academy of Sciences*. 2011; 1241(1):48-70.
217. Balasubramanian V, Solapure S, Iyer H, Ghosh A, Sharma S, Kaur P, Deepthi R, Subbulakshmi V, Ramya V, Ramachandran V, Balganes M. *Antimicrobial Agents and Chemotherapy*. 2014; 58(1): 495-502.
218. Prokocimer P, Bien P, Surber J, Mehra P, DeAnda C, Bulitta JB, Corey GR. *Antimicrobial Agents and Chemotherapy*. 2011; (5):583-592.
219. Schaadt R, Sweeney D, Shinabarger D, Zurenko G. *Antimicrobial Agents and Chemotherapy*. 2009; (53):3236-3239.
220. Morris O. Makobongo, Leo Einck, Richard M. Peek, Jr, D. *PLOS ONE*. 2013; 8(7): 68917.
221. Horwith G, Einck L, Protopopova M, Nacy C. 45th IDSA; Annual: Meeting, San Diego, CA, USA: Rockville, MD: Sequella, Inc. 2007.
222. Protopopova M, Hanrahan C, Nikonenko B, Samala R, Chen P, Gearhart J, Einck L, Nacy CA. *Journal of Antimicrobial Chemotherapy*. 2005; 56(5):968-974.
223. Nikonenko BV, Samala R, Einck L, Nacy CA. *Antimicrobial Agents and Chemotherapy*. 2004; 48(12): 4550-4555.
224. Gupta, R.R.; Kumar, M.; Gupta, V. Springer Science & Business Media. 2013.
225. Mohammad, A. *International Journal of Bioorganic Chemistry*. 2017, 2, 146-152.
226. Chen, Z.Z.; Li, S.Q.; Liao, W.L.; Xie, Z.G.; Wang, M.S.; Cao, Y.; Zhang, J.; Xu, Z.G.. *Tetrahedron*, 2015; 71(44):8424-8427.
227. Wright, J.B. *Chemical Reviews*. 1951; 48(3):397-541.
228. Arrang, J.M.; Garbarg, M.; Lancelot, J.C.; Lecomte, J.M.; Pollard, H.; Robba, M.; Schunack, W.; Schwartz, J.C. *Investigative Radiology*. 1988; 23: S130-S132

229. Sugumaran, M.; Kumar, M.Y. *International Journal of Pharmaceutical Sciences and Drug Research*. 2012, 4(1):80-83.
230. Horton, D.A.; Bourne, G.T.; Smythe, M.L. *Chemical Reviews*. 2003; 103(3): 893-930.
231. Rathee, P.S.; Dhankar, R.; Bhardwaj, S.; Gupta, M.; Kumar, R. *Journal of Applied Pharmaceutical Science*. 2011; 1(10):14.
232. Nakano, H.; Inoue, T.; Kawasaki, N.; Miyataka, H.; Matsumoto, H.; Taguchi, T.; Inagaki, N.; Nagai, H.; Satoh, T. *Chemical and Pharmaceutical Bulletin*. 1999; 47(11):1573-1578.
233. Fonseca, T.; Gigante, B.; Gilchrist, T.L. *Tetrahedron*. 2001; 57(9):1793-1799.
234. Serafin, B.; Borkowska, G.; Głowczyk, J.; Kowalska, I.; Rump, S. *Polish Journal of Pharmacology and Pharmacy*. 1989; 41(1):89-96.
235. Bethke, T.; Brunkhorst, D.; der Leyen, H.V.; Meyer, W.; Nigbur, R.; Scholz, H. *Naunyn-Schmiedeberg's Archives of Pharmacology*. 1988; 337(5):576-582.
236. Khan, F.R.; Asnani, A.J. *Journal of Pharmaceutical and Biomedical Analysis*. 2011; 2(2):695-700.
237. Al-Douh, M.H.; Sahib, H.B.; Osman, H.; Hamid, S.A.; Salhimi, S.M. *Asian Pacific Journal of Cancer Prevention*. 2012; 13(8):4075-4079.
238. Lazer, E.S.; Matteo, M.R.; Possanza, G.J. *Journal of Medicinal Chemistry*. 1987; 30(4):726-729.
239. Aydin, S.; Beis, R.; Can, Ö.D. *Die Pharmazie*. 2003; 58(6):405-408.
240. Ates-Alagoz, Z.; Kuş, C.; Coban, T. *Journal of Enzyme Inhibition and Medicinal Chemistry*. 2005; 20(4):325-31.

241. Kazimierczuk, Z.; Upcroft, J.A.; Upcroft, P.; Górski, A.; Starosciak, B.; Laudy, A. *Acta Biochimica Polonica*. 2002; 49(1):185-195.
242. Ramanathan, V.; Vaidya, S.D.; Kumar, B.V. Bhise, U.N.; Bhirud, S.B.; Mashelkar, U.C. *European Journal of Medicinal Chemistry*. 2008; 43(5):986-995.
243. Pashinskiĭ, V.G.; Romanova, T.V.; Mukhina, N.A.; Shkrabova, L.V.; Tetenchuk, K.P. *Farmakologiya i Toksikologiya*. 1978; 41(2):196-199.
244. Ng, R.A.; Guan, J.; Alford, Jr V.C.; Lanter, J.C.; Allan, G.F.; Sbriscia, T.; Linton, O.; Lundeen, S.G.; Sui, Z. Synthesis and SAR of potent and selective androgen receptor antagonists: 5, 6-Dichloro-benzimidazole derivatives. *Bioorganic & Medicinal Chemistry Letters*. 2007; 17(3):784-788.
245. Oya, U.; Ayla, B.; Cenk, A.; Berna, T.M.; Zafer, G. *Journal of Pharmaceutical Sciences*. 2004; 29:185-194.
246. Thakurdesai, P.A.; Wadodkar, S.G.; Chopade, C.T. *PharmacologyOnline*. 2007; 1:314-329.
247. Galal, S.A.; Hegab, K.H.; Kassab, A.S.; Rodriguez, M.L.; Kerwin, S.M.; Abdel-Mo'men, A.; El Diwani, H.I. *European Journal of Medicinal Chemistry*. 2009; 44(4):1500-1508.
248. Mederski, W.W., Dorsch, D.; Anzali, S.; Gleitz, J.; Cezanne, B.; Tsaklakidis, C. *Bioorganic & Medicinal Chemistry Letters*. 2004; 14(14):3763-3769.
249. Rathod, C.P.; Rajurkar, R.M.; Thonte, S.S. *Indo American Journal of Pharmaceutical Research*. 2013; 2323-2329.
250. Vasava, M. S.; Bhoi, M. N.; Rathwa, S. K.; Borad, M. A.; Nair, S. G.; Patel, H. D. *Indian Journal of Tuberculosis*. 2017; 64(4):252-275.
251. Noolvi, M.; Agrawal, S.; Patel, H.; Badiger, A.; Gaba, M.; Zambre, A. *The Arabian Journal of Chemistry*. 2014; 7(2):219-226.

252. Ansari, K.; Lal, C. *European Journal of Medicinal Chemistry*. 2009; 44(10): 4028-4033.
253. Soni, B.; Ranawat, M. S.; Sharma, R.; Bhandari, A.; Sharma, S. *European Journal of Medicinal Chemistry*. 2010; 45(7):2938-2942.
254. Zhang, H.-Z.; He, S.-C.; Peng, Y.-J.; Zhang, H.-J.; Gopala, L.; Tangadanchu, V. K. R.; Gan, L.-L.; Zhou, C.-H.. *European Journal of Medicinal Chemistry*. 2017; 136:165-183.
255. Shingalapur, R. V.; Hosamani, K. M.; Keri, R. S. *European Journal of Medicinal Chemistry*. 2009; 44(10):4244-4248.
256. Camacho, J.; Barazarte, A.; Gamboa, N.; Rodrigues, J.; Rojas, R.; Vaisberg, A.; Gilman, R.; Charris, J. *Bioorganic & Medicinal Chemistry*. 2011; 19(6):2023-2029.
257. Padalkar, V. S.; Borse, B. N.; Gupta, V. D.; Phatangare, K. R.; Patil, V. S.; Umape, P. G.; Sekar, N. *The Arabian Journal of Chemistry*. 2016; 9: S1125-S1130.
258. Soni, B.; Ranawat, M. S.; Bhandari, A.; Verma, R.; Sharma, R.; Prajapat, R. P. *Journal of Pharmacy Research*. 2012; 5(7):3523-3526.
259. White, N. J. *Malaria Journal*. 2011; 10(1):297.
260. Mikolajczak, S. A.; Vaughan, A. M.; Kangwanransan, N.; Roobsoong, W.; Fishbaugher, M.; Yimamnuaychok, N.; Rezakhani, N.; Lakshmanan, V.; Singh, N.; Kaushansky, A. *Cell Host & Microbe*. 2015; 17(4):526-535.
261. Krotoski, W.; Collins, W.; Bray, R.; Garnham, P.; Cogswell, F.; Gwadz, R.; Killick-Kendrick, R.; Wolf, R.; Sinden, R.; Koontz, L. *The American Journal of Tropical Medicine and Hygiene*. 1982; 31(6):1291-1293.
262. Amaratunga, C.; Lim, P.; Suon, S.; Sreng, S.; Mao, S.; Sopha, C.; Sam, B.; Dek, D.; Try, V.; Amato, R. *The Lancet Infectious Diseases*. 2016; 16(3):357-365.

263. Toro, P.; Klahn, A. H.; Pradines, B.; Lahoz, F.; Pascual, A.; Biot, C.; Arancibia, R. *Inorganic Chemistry Communications*. 2013; 35:126-129.
264. Farahat, A. A.; Ismail, M. A.; Kumar, A.; Wenzler, T.; Brun, R.; Paul, A.; Wilson, W. D.; Boykin, D. W. *European Journal of Medicinal Chemistry*. 2018; 143:1590-1596.
265. Ndakala, A. J.; Gessner, R. K.; Gitari, P. W.; October, N.; White, K. L.; Hudson, A.; Fakorede, F.; Shackleford, D. M.; Kaiser, M.; Yeates, C. *Journal of Medicinal Chemistry*. 2011; 54(13):4581-4589.
266. L.R. Morgan, B.S. Jursic, C.L. Hooper, D.M. Neumann, K. Thangaraj, B. *Bioorganic & Medicinal Chemistry Letters*. 2002; 12:3407-3411.
267. A.M. EL-Agrody, M.H. EL-Hakim, M.A. EL-Latif, A.H. Fakery, E.S. El-Sayed, K.A. EL-Ghareab. *ACTA PHARMACEUTICA*. 2000; 50:111-120.
268. AH Bedair, HA Emam, NA El-Hady, KA Ahmed, AM El-Agrody. *Il Farmaco* 56 (2001) 965-73.
269. J.Y. Wu, W.F. Fong, J.X. Zhang, C.H. Leung, H.L. Kwong, M.S. Yang, D. Li, H.Y. Cheung. *European Journal of Pharmacology*. 2003; 473:9-17.
270. T. Raj, R.K. Bhatia, M. Sharma, A.K. Saxena, M.P. *European Journal of Medicinal Chemistry*. 2010; 45:790-4.
271. D.O. Moon, K.C. Kim, C.Y. Jin, M.H. Han, C. Park, K.J. Lee, Y.M. Park, Y.H. Choi, G.Y. Kim. *International Immunopharmacology*. 2007; 7:222-9.
272. L. Hanna. *BETA: bulletin of experimental treatments for AIDS: a publication of the San Francisco AIDS Foundation* 12 (1999) e8.
273. M Rueping, E Sugiono, E Merino. *Chemistry – A European Journal*. 2008; 14:6329-6332.

274. E. Perez-Sacau, A. Estevez-Braun, A.G. Ravelo, D. Gutierrez Yapu, A. Gimenez Turba. *Chemistry & Biodiversity*. 2005; 2:264-274.
275. A. Kumar, R.A. Maurya, S. Sharma, P. Ahmad, A.B. Singh, G. Bhatia, A.K. Srivastava. *Bioorganic & Medicinal Chemistry Letters*. 2009; 19:6447-6451.
276. W.O. Foye. Padova, Italy. 1991; e416.
277. A.L. Lazzeri, E. Lapi. *Bollettino Chimico Farmaceutico*. 1960; 99:e583.
278. Y. L. Zhang, B. Z. Chen, K. Q. Zheng, M. L. Xu, X. H. Lei, X. B. Yaoxue. *Chemical abstracts*. 1982; 96:e135383.
279. A. Shaabani, R. Ghadari, A. Sarvary, A.H. Rezayan. *Journal of Organic Chemistry*. 2009; 74:4372-4374.
280. G.P. Ellis. John Wiley & Sons. 2009; 11-139
281. E.A. Hafez, M.H. Elnagdi, A.G. Elagamey, F.M. EL-Taweel. *Heterocycles*. 1987; 26:903-907.
282. D. Kumar, V.B. Reddy, S. Sharad, U. Dube, S. Kapur. *European Journal of Medicinal Chemistry*. 2009; 44:3805-3809.
283. A.H. Bedair, H.A. Emam, N.A. El-Hady, K.A. Ahmed, A.M. El-Agrody. *Il Farmaco*. 2001; 56:965-973.
284. M.M. Khafagy, A.H. El-Wahab, F.A. Eid, A.M. El-Agrody. *Il Farmaco*. 2002; 57:715-722.
285. F.A. Eid, A.H. ABD EL-Wahab, E.H. Ali, A. Gameel, M.M. Khafagy. *Acta Pharmaceutica* 2004; 54:13-26.
286. F.M. Abdelrazek, P. Metz, E.K. Farrag. *Archiv der Pharmazie*. 2004; 337:482-485.
287. P.K. Paliwal, S.R. Jetti, S. Jain. *Medicinal Chemistry Research*. 2013; 22:2984-2990.

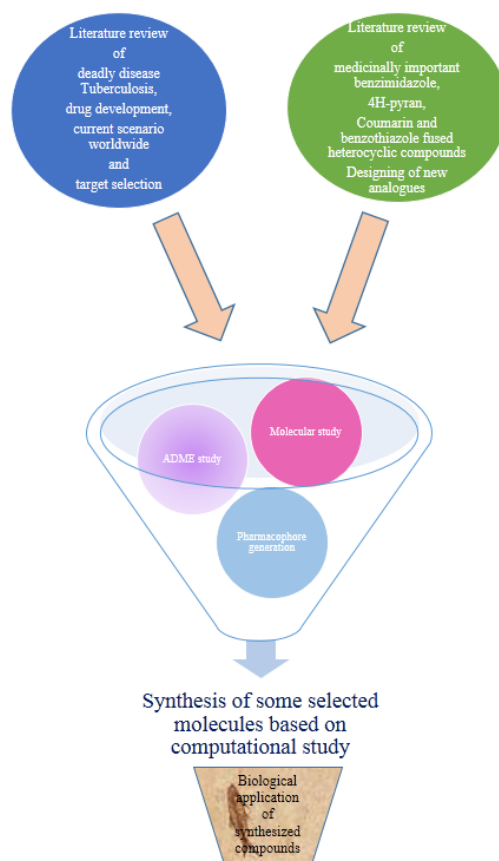
- 288.A. Sharma, B. Pallavi, R. P. Singh, P. N. Jha, P. Shukla. *Heterocycles*. 2015; 91:1615-1627.
- 289.M.N. Erichsen, T.H. Huynh, B. Abrahamsen, J.F. Bastlund, C. Bundgaard, O. Monrad, A. Bekker-Jensen, C.W. Nielsen, K. Frydenvang, A.A. Jensen, L. Bunch. *Journal of Medicinal Chemistry*. 2010; 53:7180-7191.
- 290.W. Kemnitzer, J. Drewe, S. Jiang, H. Zhang, C. Crogan-Grundy, D. Labreque, M. Bubenick, G. Attardo, R. Denis, S. Lamothe, H. Gourdeau. *Journal of Medicinal Chemistry*. 2008; 51:417-423.
- 291.M. Mahmoodi, A. Aliabadi, S. Emami, M. Safavi, S. Rajabalian, M.A. Mohagheghi, A. Khoshzaban, A. Samzadeh-Kermani, N. Lamei, A. Shafiee, A. Foroumadi. *Archiv der Pharmazie*. 2010; 343:411-416.
- 292.F.M. Abdelrazek, P. Metz, E.K. Farrag. *Archiv der Pharmazie*. 2004; 337:482-485.
- 293.P.K. Paliwal, S.R. Jetti, S. Jain. *Medicinal Chemistry Research*. 2013; 22:2984-2990.
- 294.C.W. Smith, J.M. Bailey, M.E. Billingham, S. Chandrasekhar, C.P. Dell, A.K. Harvey, C.A. Hicks, A.E. Kingston, G.N. Wishart. *Bioorganic & Medicinal Chemistry Letters*. 1995; 5:2783-2788.
- 295.M. Kidwai, S. Saxena, M.K. Khan, S.S. Thukral. *Bioorganic & Medicinal Chemistry Letters*. 2005; 15:4295-4298.
- 296.D.C. Mungra, M.P. Patel, D.P. Rajani, R.G. Patel. *European Journal of Medicinal Chemistry*. 2011; 46:4192-4200.
- 297.G. Zhang, Y. Zhang, J. Yan, R. Chen, S. Wang, Y. Ma, R. Wang. *Journal of Organic Chemistry*. 2012; 77:878-888.
- 298.A. Nandakumar, P. Thirumurugan, P.T. Perumal, P. Vembu, M.N. Ponnuswamy, P. Ramesh. *Bioorganic & Medicinal Chemistry Letters*. 2010; 20:4252-4258.

- 299.D.H. Vyas, S.D. Tala, J.D. Akbari, M.F. Dhaduk, K.A. Joshi, H.S. Joshi. Indian Journal of Chemistry. 2009; 42:833-839.
- 300.A.E. Hammam, A.F. Fahmy, A.G. Amr, A.M. Mohamed. Indian Journal of Chemistry. 2003; 42:1985-1993.
- 301.X. Fan, D. Feng, Y. Qu, X. Zhang, J. Wang, P.M. Loiseau, G. Andrei, R. Snoeck, E. De Clercq. Bioorganic & Medicinal Chemistry Letters. 2010; 20:809-813.
- 302.I.V. Magedov, M. Manpadi, M.A. Ogasawara, A.S. Dhawan, S. Rogelj, S. Van Slambrouck, W.F. Steelant, N.M. Evdokimov, P.Y. Uglinskii, E.M. Elias, E.J. Knee. Indian Journal of Chemistry. 2008; 51:2561-2570.
- 303.M. Kidwai, A. Jain, V. Nemaysh, R. Kumar, P.M. Luthra. Medicinal Chemistry Research. 2013; 22:2717-2723.
- 304.P.T. Mistry, N.R. Kamdar, D.D. Haveliwala, S.K. Patel. Journal of Heterocyclic Chemistry. 2012; 49:349-357.

➤ **Aim and Objectives of the present work**

The main aim and objective of this work is to identify target for the deadly disease Tuberculosis, design novel analogues based on selected biologically active moieties, in silico study, synthesis of virtually screened compounds, and their biological application, which help to new researcher who work in the field of drug discovery.

The computational chemistry is emerging day by day tremendous in developed countries. Computational chemistry is simply the application of chemical, mathematical and computing skills to the solution of interesting chemical problems. It also helps chemists make predictions before running the actual experiments so that they can be better prepared for making observations. The Schroedinger equation (explained in another section) is the basis for most of the computational chemistry scientist's use. Additionally, this technique reduced the cost of chemicals for the synthesis, decrease the use of hazardous chemicals with this it will be directly beneficial to the human health, time of the drug discovery also reduce by prediction of compounds in first step which identify the best compounds for the target. This inspired us to synthesize and to recognize the most active heterocyclic compounds with biological activities based on in silico study. Here, we aim to synthesize some selected compounds which were evaluate various biological activity and found as potent.

Plan of the Research work:

PLAN OF THE RESEARCH WORK:

Chapter: 2

Computation-based virtual screening for designing benzimidazole and 4H-Pyran based novel anti-tuberculosis agent by targeting Enoyl-ACP reductase

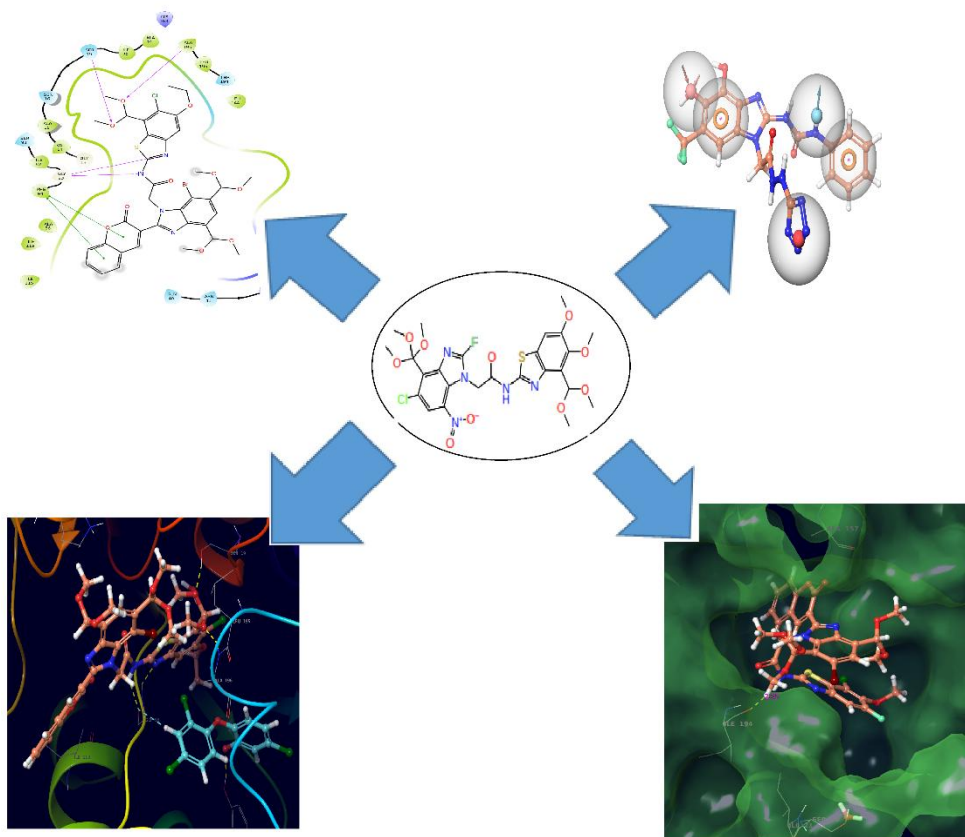


Table of Contents

1.0 Introduction	139
2.0 Materials and Methods	142
2.1 Materials.....	142
2.2 Docking methodology	142
2.3 Ligand Preparation	142
2.4 Glide	143
2.5 Target and ligand selection	143
2.6 Target and ligand preparation	144
2.7 Protein preparation and Receptor grid generation.....	144
2.8 ADME study	145
2.9 Docking Study.....	145
2.10 Pharmacophore hypothesis generation.....	146
3.0 Result and Discussion	147
3.1 ADME study	147
3.2 Docking Study.....	153
3.3 Pharmacophore hypothesis development	168
4.0 Conclusion	178
References	180

Summary:

The Enoyl acyl carrier protein reductase (InhA) from *Mycobacterium Tuberculosis*, is one of the most important enzymes involved in the type II fatty acid biosynthesis pathway to synthesize mycolic acid of *Mycobacterium tuberculosis*. Therefore, inhibitors of InhA are useful analogues for the treatment of Tuberculosis due to this reason InhA selected as target for the study. In this present study, we have described ADME, docking study combined with pharmacophore study as a rotational strategy to identification of novel leads or hits. Firstly, we have designed ligand and separated in four different set of library for the easy understanding. The basic ligands were selected based on medicinal important of the compounds and literature survey. The library of ligand more than 50,000 compounds in each set have been developed using Enumeration module in maestro. These compounds were subjected for ADME pharmacokinetics study for the primary elimination of compounds. The compounds which have good ADME properties have further subjected to virtual screening using Glide at the active site of Enoyl-ACP reductase using four different PDB (PDB ID: 2B37, 1QG6, 4TZK, 4TZZ). Furthermore, the pharmacophore hypothesis of highest glide scoring ligands were generated with the help of PHASE module. The result form this study highlights that the few compounds could be promising future inhibitors for chemotherapeutic prevention of Tuberculosis. The ADME study suggest that the few compounds have better pharmacokinetics properties than 95% drug molecules. The molecular docking study also showed that the compounds have good binding affinity with highest binding score which is better than native ligands of the targeted protein. The pharmacophore development study support our prediction regarding minimum features required for the molecules to behave as Enoyl-ACP reductase

inhibitors. The generated hits from the present study can be synthesized and will be tested in vivo as future significant anti-tuberculosis agents.

1.0 Introduction

Tuberculosis is one of the most serious infectious disease in the world. In the last few decades, Emergence of Drug resistant tuberculosis has threatened all the improvements that have been made in TB control at the worldwide. According to the 2018 World Health Organization report, released in October 2017, there were 1.4 million new TB cases in 2016 and 1.8 million deaths which include 0.4 million were co-infected with HIV [1]. Existing treatment for tuberculosis decrease drug compliance and carries significant side-effects which leads to the emergence of multi-drug resistant (MDR) TB at globally. Hence, there is an urgent need for exploring other new therapeutic agents that carry better compliance, shorten the treatment and is equally effective against TB. Despite this challenge, it is necessary to understand that there are numerous candidate molecules which show potent anti-mycobacterial activity. The molecular studies of these compounds can pave milestones evaluating their potency which can be further explored using *in-vitro* and *in-vivo* studies [2].

In this direction, a variety of new heterocyclic molecules are being synthesized to check the probable effectiveness of the molecules to fight against TB. Researcher found that INH derivatives, or derivatives of other families of active compounds such as benzimidazole show potent activity against TB [3]. Benzimidazole enhance the good anti-tubercular activity comparable with INH and that would retain their activity against a panel of INH resistant strains [3-4-5]. Due to a priceless significance of benzimidazole as a lead compound, making it a promising starting point for the discovery of new anti-TB drugs [6-7]. Additionally, different studies have indicated 4*H*-pyran derivatives display a potent activity against mycobacterium. Furthermore, substituted 4*H*-pyran derivatives have encouraged increasing roles in synthetic methodologies to promising compounds in the

field of medicinal [8]. Keeping this information in mind, we have also included this moiety to designed novel 4*H*-pyran analogues and series of compounds have been designed to study the varies properties via computational study.

However, in the past it is not easy to discover new drugs in a short time which act like existing drug. The process of drug discovery may take 10 to 20 years, which include synthesis of a number of chemical entity which check through several pharmacological and pharmacokinetic studies. Nowadays, computational methods played an important role in the drug discovery process during the last 10 years. Docking study is a part of rational drug design and used in the prediction of the binding of ligands or drug candidates with receptor, as well as in the prediction of the activity and affinity of the molecules [9]. In recent decades, the pharmaceutical industry has preferred more traditional targets advances in ligand- and receptor-based computational methods to improve ligand-binding affinity at a substrate-competitive site. This structure-based approach is thought to significantly reduce the time and cost of hit-to-lead and lead-to-drug development by reducing the number of compounds that need to be synthesized [10-11].

The antibiotics isoniazid, rifampicin, Pyrazinamide and Ethambutol is the milestone agent against TB, have been used for decades as frontline drugs to treat tuberculosis infections. However, an existing treatment strategies is not acceptable due to the rise of multi-drug resistant (MDR) and extensively drug resistant (XDR) TB bacteria and it poses a serious threat in the world [12]. Both Isoniazid and pyrazinamide inhibits the mycolic acid biosynthesis, rifampicin inhibits DNA dependent RNA polymerase and Ethambutol inhibits arbinosyltransferase in the cell wall of bacteria. There are numerous potential anti-tuberculosis drug targets which of them, an evidence proven that the Enoyl reductase (InhA) in the type II fatty acid biosynthesis pathway is a target for

INH [13-14]. EmbC is a target for the front line antibiotic EMB, the enzyme responsible for arabinan chain elongation in LAM synthesis [15]. Pyrazinamide is highly active against the persisting tubercle bacilli at an acidic pH due to this activity it plays a key role in shortening the duration of anti-tuberculosis treatment [16]. The prodrug PZA is metabolized into its active form, pyrazinoic acid (POA) by the amidase activity each target of the *Mycobacterium Tuberculosis* nicotinamidase/pyrazinamidase [17]. Moreover, the common mechanism for all antibacterially active rifamycins include Rifampicin, the inhibition of DNA-dependent RNA polymerase, leading to an elimination of RNA synthesis and cell death by targeting protein in bacteria [18].

With regards to the above mentioned molecular targets of drugs we have carryout the docking study of designed compounds with using the frontline standard drug as reference ligand to find out the binding affinity as well as potential mode of action through their interactions. The possibility of inhibition activity shown by PDB bound with existing first line inhibitors leads us to design the novel derivatives as probable anti-tuberculosis moieties by selecting the target for small group of designed inhibitors. The objective of present work was to design novel anti-TB derivatives by generating key interaction site, ADMET properties, receptor-based pharmacophore to generate its analogues leading to better inhibitors for deadly disease Tuberculosis.

2.0 Materials and Methods

2.1 Materials

For computation of designed compounds, Chem3DUltra 12.0, Marvin suite and Schrodinger software (Schrodinger, LLC, New York, NY, 2018) was used.

2.2 Docking methodology

Molecular docking is a structure-based drug design approach that has become an integral part of drug discovery imparting knowledge on thermodynamic interactions, binding affinities and binding modes of the enzyme-inhibitor complex. In the other words, molecular docking refers to the complex process of using the information accommodate in the three-dimensional structure of a macromolecular target and of correlated ligand-target complexes to design novel drugs for significant human diseases.

2.3 Ligand Preparation

The 3D structures of the main moiety (ligands) were sketched with ChemDraw and Marvin *suite* and saved as *SDF* file. The main moiety was subjected to develop a library of four different series in enumeration module in Schrodinger software. Developed library of compounds contain more 20,000 compounds in each series. Subsequently ligand were optimized using the *LigPrep* module in Maestro, which performs addition of missed hydrogens, correction of chirality's and ionization states, adjusting realistic bond lengths and angles by generating different possible structural conformation of ligands and it creates a library of 32 conformation for each ligand set. The OPLS-2005 force-field were used to assign the partial atomic charges. Finally, each of these structures was subjected to energy minimization until their average RMSD reached 0.001Å and the resulting structures were then used for carrying out docking study.

2.4 Glide

The *Glide* (Grid-Based Ligand Docking with Energetics) program of Schrödinger molecular modeling suite to gauge the binding affinity of the. Glide performs the exhaustive search of enzyme-inhibitor interactions and identification of possible binding site of the bio-macromolecular targets. Receptor-grid files were generated after preparing the correct forms of proteins and ligands using receptor-grid generation program (maestro by Schrödinger). For grid generation potential of non-polar parts of receptor was softened by scaling van der Waals radii of ligand atoms by 1.00 Å with partial charge cut-off of 0.25. It is having all types of option of speed vs accuracy. It is having three mode of docking, high-throughput virtual screening (HTVS), standard precision (SP), and extra precision (XP) mode. The XP mode is used for exhaustive sampling and advanced scoring, resulting in even higher enhancement.

2.5 Target and ligand selection

The ligand selection was based on the potent activity of benzimidazole moiety against bacteria of TB. Many researcher found that benzimidazole have tendency to kill the tuberculosis bacteria [3-4-5]. On the basis of this knowledge, we have designed number of benzimidazole derivatives and sketched in Marvin suite. The receptor were selected based on the target of existing first-line anti-tuberculosis agents. There are four different anti-tuberculosis drugs in first-line and each drugs have different target in TB bacteria. We have differentiate receptor for each drug target based on the ligand which already available in the form crystal structure of protein. The 3D structures of *Mycobacterium Tuberculosis* Enoyl Reductase (Inha) were retrieved with PDB ID: 2B37, 1QG6, 4TZK and 4TZK with resolution 2.6 Å, 1.9 Å, 1.62 Å and 2.0 Å respectively from RCSB protein data bank. The downloaded protein 2B37 having 5-octyl-2-phenoxyphenol as an inhibitor for each chain

and NAD co-factor for all the proteins. Protein 1QG6 having NAD and TCL as an inhibitor. Protein 4TZK having one chain (A), complexes with 1-cyclohexyl-n-(3,5-dichlorophenyl)-5-oxopyrrolidine-3-carboxamide Whereas, protein 4TZT has an n-(3-chloro-2-methylphenyl)-1-cyclohexyl- 5-oxopyrrolidine-3-carboxamide as inhibitor.

2.6 Target and ligand preparation

Each sets of ligands were optimized using LigPrep module in Schrodinger software by generating different possible structural confirmation of ligands set and it creates library of more than 20,000 ligand set. The ligands were first screened for ADME study using QuikPro than subjected for docking study. The target protein was prepared by deleting surrounding water molecules, bond cofactor, inhibitors together with the addition of side chain atoms followed by energy minimization and optimization protein.

2.7 Protein preparation and Receptor grid generation

The protein complex was refined for docking, using the *Protein Preparation Wizard* in *Glide* which involved assigning the correct bond orders, addition of missing hydrogens corresponding to pH 7.0 (considering the ionization states for the acidic as well as basic amino acid residues), removal of the crystallographically observed water and assigning the correct charge and protonation state of the protein structure. Finally, the Optimized Potentials for Liquid Simulations-2005 (OPLS-2005) force field were used for the energy minimization of protein until the average RMSD of the non-hydrogen atoms reached 0.3Å in order to relieve the steric mismatch between the residues due to the addition of hydrogen atoms. The receptor grid file was generated using prepared protein as an input file, the grid file was used as input file for docking study.

2.8 ADME study

Most of the new drug candidates rejects in clinical studies because of poor ADMET properties. Therefore, good ADMET property is an important aspect of drug discovery to avoid elimination of compounds in clinical studies. So in this direction, we have performed the predicted absorption, distribution, metabolism, excretion (ADME) properties of all the compounds using discovery studio 2.0. ADME properties include aqueous solubility, blood–brain barrier (BBB), plasma protein binding (PPB), absorption, hepatotoxicity, and cytochrome P450 CYP2D 6_Probability enzyme inhibition study.

2.9 Docking Study

Molecular docking study was performed by using *Ligdock* in glide, maestro (Schrödinger suite) to find out the binding affinity of the designed compounds towards selected protein to expand the knowledge of their activity against *Mycobacterium Tuberculosis*. The XP mode was used for allowing flexible torsions in ligands for performing docking studies, highly robust and very accurate. The parameter selected for the docking run was default and a model energy function named Glide score (Gscore) is used which combines force field and empirical terms for selecting the best docking pose, generated as output. The output files were visualized and analyzed using the Pose Viewer function in *Maestro* to lining the active site of the enzyme by the key thermodynamic elements of interaction with the residues. The validation of docking protocol and the parameters set for calculation were done by re-docking the native ligands into the active site of proteins.

$$\text{Gscore} = a * \text{vdW} + b * \text{Coul} + \text{Lipo} + \text{Hbond} + \text{Metal} + \text{BuryP} + \text{RotB} + \text{Site}$$

Where, vdW is van der Wall energy; Coul is Coulomb energy; Lipo is lipophilic interaction; Hbond signifies hydrogen-bonding; Metal is metal-binding term; BuryP is forgotten polar groups; RotB represents freezing rotatable bonds; Site is polar interactions at the active site; and a, b is the coefficients of vdW and Coul.

2.10 Pharmacophore hypothesis generation

Pharmacophore is the hybrid approach of ligand and structure-based technique which uses docking energy score for finding the biologically active part of ligands against the enzyme. We have generated a ligand-based pharmacophore by superposing existing drug as reference active molecules and extracting common chemical features that are significant for their biological activity. The pharmacophore hypothesis were generated by docking post-processing module of script option was selected and input file given in .xpdes format. Pharmacophore was generated by using all the default chemical features (hydrogen bond acceptor (A), hydro-gen bond donor (D), aromatic ring (R), hydrophobe (H), positive ionizable (P) and negative ionizable (N)) [19]. Common pharmacophore hypothesis were considered, which indicated five common site to selected molecule. Moreover, the best common pharmacophore hypothesis was selected based on the survival score, until at least one hypothesis was found and scored successfully. The common pharmacophore hypothesis were scored using default parameters for vector, site, selectivity, volume, energy terms and number of matches. The pharmacophore hypothesis was generated using *PHASE* module in maestro (Schrodinger software) and all the parameters were set as default.

3.0 Result and Discussion

3.1 ADME study

The absorption, distribution, metabolism and excretion study were predicted primarily for four different library of compounds. Predicted result of descriptor along with their range are given in table 1-2-3 and 4 for each set. Following principal descriptors are included in study. Molecular weight (MW), Percent human oral absorption in GI, Brain/Blood QPlogBB, HERG K⁺ channel blockage: log IC₅₀ (QPlog HERG), apparent Caco-2 permeability in nm/sec (QPPCaco), log K_{hsa} serum protein binding (QPlogK_{hsa}), van der waals polar surface area (PSA) and aqueous solubility (QPlogS) were calculated.

Table 1. ADME prediction of 25 lead molecules from Set 1 by using QikProp, Schrodinger.

Compound	MW (130- 725)	Percent human oral absorption (>80% – high & <25% – poor)	QPlog BB (-3.0 – 1.5)	QPlog HERG (below -5)	QPPCaco (<25 poor, >500 great)	QPlog K _{hsa} (-1.5 – 1.5)	PSA (70 – 200 Å)	QPlog S (-6.5 – 5)
1	476.54	41.778	-2.431	-4.041	118.434	-0.348	168.927	-3.514
2	476.54	41.778	-2.431	-4.041	118.434	-0.348	168.927	-3.514
3	476.54	41.778	-2.431	-4.041	118.434	-0.348	168.927	-3.514
4	476.54	41.778	-2.431	-4.041	118.434	-0.348	168.927	-3.514
5	530.548	38.251	-3.591	-4.317	62.456	-0.768	224.524	-4.074
6	531.456	45.839	-3.205	-4.99	35.259	-0.364	201.929	-5.055
7	531.456	45.839	-3.205	-4.99	35.259	-0.364	201.929	-5.055
8	530.511	31.286	-2.33	-4.174	68.434	-0.288	168.927	-4.078
9	530.511	31.286	-2.33	-4.174	68.434	-0.288	168.927	-4.078
10	521.538	51.035	-3.759	-4.878	33.259	-0.441	218.404	-4.365
11	499.414	26.255	-2.926	-4.428	45.137	-0.721	195.708	-4.52

3.0 RESULT AND DISCUSSION

12	499.414	26.255	-2.926	-4.428	45.137	-0.721	195.708	-4.52
13	520.51	32.501	-4.087	-4.748	102.001	-1.02	244.215	-3.284
14	519.565	37.863	-3.268	-4.684	56.148	-0.212	201.929	-4.63
15	519.565	37.863	-3.268	-4.684	56.148	-0.212	201.929	-4.63
16	488.468	57.662	-4.296	-5.088	31.209	-0.649	229.044	-5.113
17	584.483	34.018	-2.152	-4.156	119.469	-0.232	167.542	-4.472
18	542.403	29.072	-2.17	-4.388	215.769	-0.451	168.927	-4.371
19	542.403	29.072	-2.17	-4.388	215.769	-0.451	168.927	-4.371
20	479.457	61.011	-3.869	-4.68	211.701	-0.95	229.285	-2.978
21	518.62	33.209	-2.491	-4.344	318.737	-0.045	168.927	-4.622
22	518.62	33.209	-2.491	-4.344	318.737	-0.045	168.927	-4.622
23	490.404	26.864	-2.734	-4.439	77.761	-0.729	189.138	-3.467
24	447.415	58.301	-3.774	-4.53	111.673	-0.981	217.622	-3.575
25	492.376	34.927	-3.223	-4.455	342.984	-0.933	211.539	-3.047

Table 2. ADME prediction of ADME prediction of 25 lead molecules from Set 2 by using QikProp, Schrodinger.

Compound	MW (130- 725)	Percent human oral absorption (>80% – high & <25% – poor)	QPlog BB (-3.0 – 1.5)	QPlog HERG (below -5)	QPPCaco (<25 poor, >500 great)	QPlog Khsa (-1.5 –1.5)	PSA (70 – 200 Å)	QPlog S (-6.5 – 5)
1	655.72	29.921	-3.742	-5.513	221.327	0.602	217.582	-8.556
2	729.798	66.514	-1.415	-4.93	219.391	0.179	135.114	-6.968
3	771.648	82.118	-0.693	-5.311	584.372	0.601	107.29	-8.672
4	737.75	61.973	-1.518	-4.886	114.698	0.305	149.901	-7.261
5	660.137	72.213	-1.088	-5.025	160.674	0.948	119.938	-8.772
6	719.56	52.137	-1.468	-5.231	175.896	0.923	152.175	-9.013
7	669.747	29.159	-3.449	-5.448	32.415	0.718	218.422	-8.785
8	749.586	55.051	-1.996	-5.363	138.609	0.609	161.244	-8.663
9	723.633	46.448	-2.58	-5.434	99.212	1.015	191.821	-9.65

10	727.197	83.933	-0.574	-5.307	722.345	0.579	107.156	-8.566
11	660.737	35.937	-2.919	-5.218	85.342	0.748	199.273	-8.541
12	659.599	37.321	-2.743	-5.432	76.988	0.692	190.957	-8.473
13	719.759	68.218	-1.424	-4.768	143.417	0.668	147.049	-7.731
14	712.143	54.944	-1.646	-5.618	92.395	0.947	136.49	-9.622
15	670.692	35.089	-4.486	-5.46	80.275	0.549	255.106	-8.409
16	693.697	64.083	-1.485	-5.05	102.061	0.663	146.245	-8.173
17	704.788	73.147	-0.551	-4.582	924.108	0.674	113.108	-7.495
18	744.769	51.667	-2.008	-4.826	47.709	0.122	169.885	-6.805
19	749.786	67.656	-1.427	-4.844	194.392	0.341	154.072	-7.278
20	680.127	25.711	-3.335	-5.366	61.655	0.778	227.896	-8.951
21	699.773	28.972	-3.186	-5.283	53.843	0.29	224.848	-7.787
22	675.708	21.353	-3.688	-5.331	111.218	0.695	234.936	-8.656
23	674.764	40.573	-3.021	-5.499	86.471	0.891	199.658	-9.126
24	671.635	36.367	-2.902	-5.362	96.388	0.66	198.567	-8.404
25	709.727	35.874	-3.162	-5.459	97.252	0.392	187.863	-7.865

Table 3. ADME prediction of ADME prediction of 25 lead molecules from Set 3 by using QikProp, Schrodinger.

Compound	MW (130- 725)	Percent human oral absorption (>80% – high & <25% – poor)	QPlog BB (-3.0 – 1.5)	QPlog HERG (below -5)	QPPCaco (<25 poor, >500 great)	QPlog Khsa (-1.5 – 1.5)	PSA (70 – 200 Å)	QPlog S (- 6.5 –5)
1	471.484	100	-1.012	-6.524	521.376	0.572	97.957	-6.752
2	471.484	100	-1.012	-6.524	521.376	0.572	97.957	-6.752
3	483.375	100	-0.502	-5.689	613.731	0.286	97.752	-5.852
4	483.375	100	-0.502	-5.689	613.731	0.286	97.752	-5.852
5	497.479	100	-1.625	-7.896	277.013	0.721	124.237	-8.128
6	497.479	100	-1.625	-7.896	277.013	0.721	124.237	-8.128

3.0 RESULT AND DISCUSSION

7	482.464	100	-0.6	-4.291	547.847	0.564	108.337	-6.211
8	482.464	100	-0.6	-4.291	547.847	0.564	108.337	-6.211
9	482.464	100	-0.6	-4.291	547.847	0.564	108.337	-6.211
10	482.464	100	-0.6	-4.291	547.847	0.564	108.337	-6.211
11	482.464	100	-0.714	-4.159	414.53	0.555	108.328	-6.152
12	482.464	100	-0.714	-4.159	414.53	0.555	108.328	-6.152
13	482.464	100	-0.714	-4.159	414.53	0.555	108.328	-6.152
14	482.464	100	-0.714	-4.159	414.53	0.555	108.328	-6.152
15	482.464	100	-0.648	-4.271	522.509	0.557	108.382	-6.108
16	482.464	100	-0.648	-4.271	522.509	0.557	108.382	-6.108
17	482.464	100	-0.648	-4.271	522.509	0.557	108.382	-6.108
18	482.464	100	-0.648	-4.271	522.509	0.557	108.382	-6.108
19	482.464	100	-0.749	-4.128	407.131	0.544	108.348	-6.042
20	482.464	100	-0.749	-4.128	407.131	0.544	108.348	-6.042
21	482.464	100	-0.749	-4.128	407.131	0.544	108.348	-6.042
22	482.464	100	-0.749	-4.128	407.131	0.544	108.348	-6.042
23	496.491	100	-0.85	-4.072	230.913	0.832	110.805	-5.645
24	496.491	100	-0.85	-4.072	230.913	0.832	110.805	-5.645
25	471.484	100	-0.85	-4.072	230.913	0.832	110.805	-5.645

Table 4. ADME prediction of ADME prediction of 25 lead molecules from Set 4 by using QikProp, Schrodinger.

Compound	MW (130-725)	Percent human oral absorption (>80% – high & <25% – poor)	QPlog BB (-3.0 – 1.5)	QPlog HERG (below -5)	QPPCaco (<25 poor, >500 great)	QPlog Kh _{sa} (-1.5 – 1.5)	PSA (70 – 200 Å)	QPlog S (-6.5 – 5)
1	539.922	80.265	-0.859	-5.691	885.881	0.373	128.918	-6.49
2	674.36	80.453	-0.275	-6.117	3286.834	0.163	103.345	-7.104
3	585.458	80.568	-0.32	-5.973	3272.554	0.239	97.89	-6.783
4	586.994	80.309	-0.478	-5.403	2052.94	-0.472	100.633	-4.754
5	562.729	80.256	-0.974	-5.447	262.377	0.274	118.242	-6.466

6	668.946	80.592	-0.935	-6.145	1226.374	-0.26	130.649	-7.271
7	536.986	80.67	-0.375	-5.834	3281.308	0.436	96.944	-6.73
8	611.201	80.366	-0.859	-5.436	285.289	0.041	118.174	-6.296
9	677.926	80.397	-0.458	-5.25	2242.489	0.466	103.382	-6.568
10	668.946	80.272	-0.856	-5.791	1330.355	-0.309	128.398	-6.556
11	576.023	80.403	-1.081	-6.26	1124.337	-0.015	123.646	-7.534
12	608.04	80.338	-0.886	-5.935	1454.948	-0.336	126.882	-6.61
13	717.95	80.447	-0.727	-6.211	831.948	0.226	125.031	-6.56
14	614.456	80.223	-1.022	-5.622	834.026	0.178	130.523	-6.207
15	556.376	80.326	-0.881	-5.755	757.33	0.441	126.607	-6.801
16	506.243	80.579	-0.806	-5.403	256.898	0.308	115.958	-6.617
17	688.478	80.662	-1.343	-5.788	665.654	0.384	152.421	-6.885
18	583.03	80.322	-0.555	-6.155	2652.861	0.349	108.197	-7.305
19	672.909	80.611	-1.033	-5.532	687.551	0.304	122.471	-7.567
20	673.364	80.348	-0.784	-5.988	1082.842	-0.199	120.827	-7.311
21	556.376	80.327	-0.963	-5.868	693.715	0.502	127.726	-7.224
22	614.456	80.343	-1.167	-5.986	746.597	0.257	134.332	-6.969
23	632.845	80.376	-0.883	-6.008	819.35	0.232	131.223	-7.018
24	738.425	80.623	-0.591	-5.592	782.421	1.244	119.966	-8.369
25	624.495	80.264	-0.897	-6.047	1284.463	-0.309	119.71	-7.003

We have designed more than 50,000 derivatives for each set with the help of enumeration module in maestro using 40 different inbuilt fragments. Here, we have selected only 25 compounds from each set which have excellent ADME properties or better than 95% of drugs property. However, the selected 25 derivatives of each set are based on the primary ADME prediction of the analogues and these compounds are further used for docking study to investigate the binding interaction between proteins and compounds. The molecular weight of the compounds from set 1 (**Table 1**) shows that most of the compounds have acceptable molecular weight. The human oral absorption prediction is based on

quantitative linear progression model. Designed compounds from set 1 has a good oral absorption in gastro intestine. So it can be stated from the prediction of the oral absorption results that the compounds have oral absorption between 25 to 80% can serve as a good qualitative model for human oral absorption. The log BB for blood/brain is found good in most of the compounds. However, few compounds have lower log BB value than standard value. The log HERG (log IC₅₀) values of all the selected compounds is below the standard value (-5) which shows that the lower is HERG value, the lesser is the blockage of K⁺ ion channels. The prediction of non-active transport, the PCaco descriptor are used which have value of more than 25. Here, the selected 25 compounds have an acceptable PCaco value more than 50. The predicted log K_h of the compounds are in the range which shows that the compounds have good protein binding affinity. Moreover, the van der Waals polar surface area and aqueous solubility of selected compounds are very good which shows that the compounds have good water solubility which is the primary need of oral medication. The polar surface area of few compounds is higher which indicated that these compounds can be poor at permeating cell membranes.

The molecular weight of compounds from set have acceptable range accept few compounds which have higher molecular weight but these compounds have good value in other descriptors. The percentage human oral absorption of the selected compounds have value in the acceptable range. Compound 22 from set 2 (**Table 2**) have less than 25% human oral absorption. All the compounds have good log BB value which found active in CNS system. Most of the compounds have acceptable log HERG value. Most of the compounds have higher than 500 PCaco value. All the selected compounds from set 2 have acceptable log K_h, PSA and log S value which indicate that these compounds which consider excellent drug-like compounds. The compounds from set 3 (**Table 3**) have favourable molecular weight and the human oral absorption. The log BB value of set 3 is

excellent than the standard value which is high in active CNS. The HERG drug binding of compounds are found better. The PCaco value of compounds is found to be potent with acceptable range and can be have good cell permeability. The polar surface area of the compounds is higher than 100 and the solubility of these compounds is less than -6 which can stated as significant range for drug like compounds. Moreover, The PKhsa value of the set 3 is less than 1.5 which is acceptable.

The selected compounds of set 4 (**Table 4**) also have good predicted ADME properties. The molecular weight of the compounds does not exceed the standard range. The human oral absorption in gastro intestine of the compounds is higher than 80% which indicate that the compounds will finely absorbs in intestine. The blood/brain barrier range of the set 4 is below 1.5. The compounds have an acceptable range of log HERG prediction. The PCaco permeability of the compounds of set 4 is higher than 500 which is excellent for drug like compounds. The aqueous solubility and polar surface area value of the compounds is in the range except the aqueous solubility of the compound 2, 6, 11, 18, 19, 20, 21, 23, 24 and 25 is lower. The ADME or pharmacokinetic properties of the compounds are very important to serve as a drug or medicine. The observed result of principal descriptors and ADME from set 1, set 2, set 3 and set 4 are very close to the drug-like compounds and can be develop as good inhibitor. The compounds which have good ADME properties are further subjected for docking study to investigate the binding affinity of the compounds against Enoyl-ACP reductase.

3.2 Docking Study

In order to validate the novel function of benzimidazole and 4*H*-pyran derivatives, it was thought important to study the interaction between 25 selected designed molecules with protein of *Mycobacterium Tuberculosis* Enoyl-ACP reductase (Oxidoreductase) using

computational docking methodology. The docking study was done on the known active site of four different proteins 2B37, 1QG6 4TZK and 4TZZ. This proteins belongs to H₃₇Rv strain of MTB which will help to identify the best molecule which may have good inhibitory action against *Mycobacterium Tuberculosis*. For this purpose, Schrodinger Glide program was used and the designed molecules were docked by the crystal structure of MTB Enoyl-ACP reductase (PDB: 2B37, 1QG6, 4TZK, 4TZY). To validate docking results, known native ligands of the protein and standard drug of MTB were also docked in the binding site of the receptor. The docking analysis of the designed compounds was also done as four different sets and each set was docked in to the four different proteins to identify the potent ligand. The docking results of the designed compounds are given in **Table 5**, **Table 6**, **Table 7** and **Table 8** for each set with all the protein. The docking score represents the ligand binding free energy with the receptor while glide van der Waals energy represents the attraction between molecule and receptor with either covalent or ionic bonding.

Table 5. Docking scores and binding energies of 25 lead molecules from Set 1.

PDB Code	2B37		1QG6		4TZK		4TZZ	
Compound	DS*	Gevdw*	DS*	Gevdw*	DS*	Gevdw*	DS*	Gevdw*
1	-8.873	-43.404	-10.317	-50.361	-11.239	-50.607	-9.917	-47.332
2	-8.871	-51.63	-9.582	-48.885	-11.027	-52.369	-9.524	-45.376
3	-8.400	-53.764	-9.518	-50.697	-10.975	-53.04	-9.514	-41.358
4	-8.215	-52.997	-9.518	-50.697	-10.748	-45.533	-8.924	-50.815
5	-8.215	-52.997	-9.272	-49.146	-10.748	-45.533	-8.921	-48.17
6	-8.163	-40.581	-9.272	-49.146	-10.68	-52.561	-8.866	-53.282
7	-8.163	-40.581	-8.832	-55.725	-10.408	-52.254	-8.695	-42.753
8	-8.111	-46.872	-8.708	-53.951	-10.116	-53.177	-8.686	-53.856
9	-8.058	-51.305	-8.428	-54.665	-10.116	-53.177	-8.636	-51.279

10	-8.058	-51.305	-8.428	-54.665	-10.116	-53.177	-8.521	-53.832
11	-8.04	-58.443	-8.097	-50.671	-10.116	-53.177	-8.521	-53.832
12	-8.04	-58.443	-8.097	-50.671	-10.105	-42.3	-8.382	-46.732
13	-7.84	-45.975	-8.069	-48.282	-10.095	-48.426	-8.343	-44.814
14	-7.84	-45.975	-8.004	-54.457	-10.023	-42.651	-8.343	-44.814
15	-7.835	-58.709	-7.927	-52.083	-9.89	-55.091	-8.269	-40.643
16	-7.8	-50.958	-7.881	-48.595	-9.635	-59.34	-8.232	-38.552
17	-7.799	-58.258	-7.881	-48.595	-9.542	-49.631	-8.232	-38.552
18	-7.737	-50.411	-7.851	-52.624	-9.542	-49.631	-8.224	-54.121
19	-7.736	-47.213	-7.851	-52.624	-9.473	-50.045	-8.088	-47.234
20	-7.718	-50.701	-7.786	-46.452	-9.451	-47.578	-8.088	-47.234
21	-7.718	-50.701	-7.739	-52.711	-9.368	-57.464	-8.013	-49.655
22	-7.699	-59.148	-7.707	-46.607	-9.272	-49.335	-8.013	-49.655
23	-7.592	-49.782	-7.677	-48.793	-9.238	-61.115	-7.984	-36.339
24	-7.481	-48.244	-7.677	-48.793	-9.158	-42.096	-7.984	-36.339
25	-7.423	-50.246	-7.645	-49.977	-9.095	-51.256	-7.953	-38.901

Docking result of set 1 suggest that these compounds have potent binding affinity with all the proteins. Compound **1** (1-(1-(2-(2-(1*H*-imidazol-2-yl)hydrazinyl)-2-oxoethyl)-4,5-dihydroxy-6-(trifluoromethyl)-1*H*-benzo[d]imidazol-2-yl)-3-phenylurea) have significant docking score with the proteins 2B37, 1QG6, 4TZK and 4TZZT at -8.873, -10.317, -11.239 and -9.917, respectively. Moreover, the docking score is increased in the case of 2B37 and 4TZK. Rest of the compounds have also displayed potency against *Mycobacterium Tuberculosis* Enoyl-ACP reductase with interesting docking energies. The interaction of compound **1** with the proteins are given in **Figure 1**. It was observed that the compound have bonded with the 1QG6 receptor with three hydrogen and one aromatic

bond. The side chain (N'-(2H-tetrazol-5-yl)propionohydrazide) of the compound have two hydrogen bond with residue ILE 194 and THR 196 (Figure 1 a) while the substituted hydroxyl group on benzimidazole have bonded with one hydrogen bond with TYR 158 (**Figure 1 a**). The aromatic bond of ligand is bonded well with receptor PHE 97 (**Figure 1 a**). In the case of protein 2B37 we observed that there is seven hydrogen bonding interactions between ligand and receptor at -8.873 docking score. Side chain of ligand have two hydrogen bond with residue GLY 93 (**Figure 1 b**) and THR 194 (**Figure 1b**). The main benzimidazole moiety have five hydrogen bond with the residue VAL 65, CYS 63, GLN 40 (**Figure 1b**) and two hydrogen bond with GLY 93 (**Figure 1 b**). Furthermore, the hydrogen bonding in 4TZK was found at residue MET 98 (**Figure 1c**) with side chain and GLY 96 (**Figure 1 c**) with benzimidazole. However, there is only two hydrogen and one aromatic bond was seen in the protein 4TZZ but the docking score was very impressive. The side chain of the ligand have one hydrogen bond with the residue MET 98 (fig.1 d) and benzimidazole moiety have hydrogen bond with GLY 96 (fig.1 d) and aromatic interaction with the residue PHE 97.

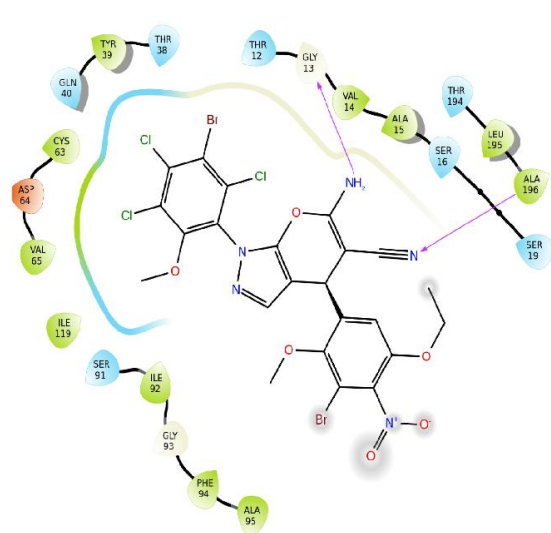


Table 6. Docking scores and binding energies of 25 lead molecules from Set 2.

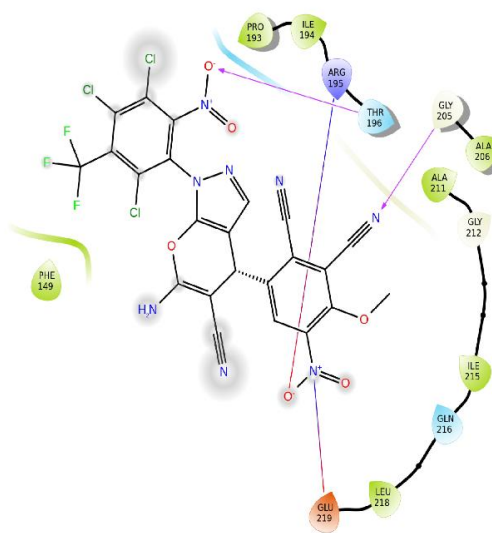
PDB Code	2B37		1QG6		4TZK		4TZZ	
Compounds	DS*	Gevdw*	DS*	Gevdw*	DS*	Gevdw*	DS*	Gevdw*
1	-6.918	-49.323	-7.744	-53.927	-10.232	-52.803	-9.495	-53.195
2	-6.659	-46.788	-7.687	-54.691	-9.999	-51.471	-9.31	-37.477
3	-6.4	-45.118	-7.375	-50.266	-9.465	-54.447	-9.139	-41.58
4	-6.317	-51.328	-7.365	-52.976	-9.443	-45.911	-8.877	-39.462
5	-6.284	-46.628	-7.361	-53.37	-9.42	-42.033	-8.742	-32.202
6	-6.219	-49.578	-7.171	-47.627	-9.335	-52.67	-8.639	-53.411
7	-6.191	-42.324	-7.128	-49.522	-9.29	-48.338	-8.618	-49.237
8	-6.142	-45.827	-7.12	-48.674	-9.174	-47.05	-8.45	-49.581
9	-6.11	-47.03	-7.083	-51.113	-9.125	-36.981	-8.418	-42.077
10	-6.098	-47.795	-7.052	-47.956	-9.124	-55.873	-8.349	-53.669
11	-6.057	-43.315	-7.048	-50.368	-9.099	-52.735	-8.34	-50.533
12	-6.043	-47.099	-7.046	-50.338	-8.909	-39.804	-8.335	-49.871
13	-6.026	-47.448	-7.022	-51.425	-8.896	-54.768	-8.329	-42.909
14	-6.013	-48.84	-6.971	-49.424	-8.864	-51.048	-8.329	-37.406
15	-6.006	-48.121	-6.97	-50.131	-8.846	-49.402	-8.225	-42.672
16	-6.002	-46.793	-6.937	-50.096	-8.835	-52.428	-8.112	-35.401
17	-5.996	-50.188	-6.93	-48.464	-8.822	-54.387	-8.059	-41.529
18	-5.981	-47.422	-6.914	-50.044	-8.815	-54.844	-8.015	-43.202
19	-5.979	-49.398	-6.901	-50.292	-8.736	-51.694	-7.998	-37.431
20	-5.976	-45.652	-6.847	-46.952	-8.736	-45.932	-7.967	-54.918
21	-5.972	-48.088	-6.798	-50.466	-8.722	-56.607	-7.961	-40.257
22	-5.967	-47.224	-6.796	-51.005	-8.66	-51.212	-7.919	-39.942
23	-5.963	-46.905	-6.79	-49.867	-8.655	-49.296	-7.865	-52.436
24	-5.945	-48.456	-6.784	-49.954	-8.635	-53.996	-7.77	-39.685
25	-5.917	-49.959	-6.752	-51.287	-8.632	-47.362	-7.74	-38.218

Here, in the case of series of compound from set 2 is based on 4*H*-pyran moiety and the designed derivatives have different substituted aldehyde and phenyl hydrazine. Moreover, the docking result against each protein have a different binding score due to different binding affinity of the compounds against receptor. The study revealed that the result from docking study of set 2 support the significant of the compounds and may be get a good biological activity against *Mycobacterium Tuberculosis*. In the series of set 2, compound 1 have a 2-bromo, 1,3,4-trichloro 5-methoxyethane substitution while aromatic aldehyde have a 1-bromo,4-ethoxyethane, 1-methoxyethane 4-nitro substitutions. This compound have formed two hydrogen bond between free NH₂ of pyran and Gly13 (**Figure 2 a**) residue of protein 2B37 at -6.918 docking score. The compound 1 with 1,3,4-trichloro,2-trifloromethane,5-nitro substation on phenyl hydrazine and 1,2-dinitrile, 4-methoxyethane, 5-nitro substations on aromatic hydrogen have ability to bind strongly with the protein 1QG6. The docking result of Compound 1 with docking score -7.744 against the protein 1QG6 undergoes hydrogen bonding between interaction between the nitrile substitutions on aromatic aldehyde with Gly205 (**Figure 2b**) and between nitro substitution on phenyl hydrazine with THR 193 (**Figure 2 b**) residue. Interestingly, compound 1 (6-amino-1-(2-bromo-3,4,5-trichloro-6-nitrophenyl)-4-(3-bromo-5-ethoxy-2-fluoro-4-methoxyphenyl)-1,4-dihydropyrano[2,3-*c*]pyrazole-5-carbonitrile) which have 3-bromo,1-flouro,4-methoxyethane, 5-ethoxyethane substitutions on aromatic aldehyde and 2-bromo, 1,2,3-trichloro, 5-nitro substitutions on phenyl hydrazine have increased its docking score against protein 4TZK. However, the compound formed only one hydrogen bond between nitrile substitution and Tyr158 (**Figure 2c**) residue with docking score -10.232. Furthermore, in the case of protein 4TZZ, compound 1 with substitution of 2-bromo, 1,3,4-trichloro, 5-diethoxyethane on phenyl hydrazine and substitution of 1-flouro, 3-

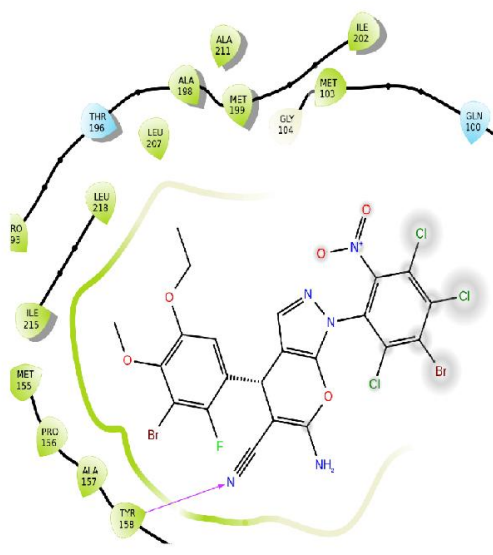
methoxymethane,2-nitrile, 4-nitro on aromatic aldehyde have a docking score -9.495 and found to form hydrogen bond between nitrogen of nitrile and Tyr158 (**Figure 2d**) residue of protein 4TZT.



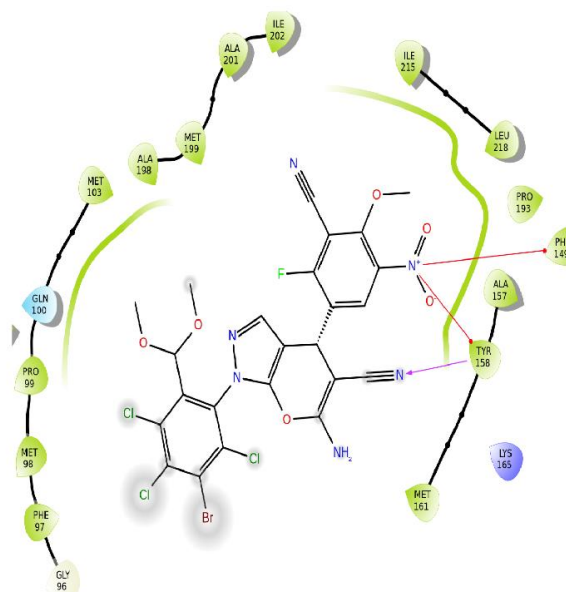
(a) Binding interaction of Compound 1 with protein 1QG6



(b) Binding interaction of Compound 1 with protein 2B37



(c) Binding interaction of Compound 1 with protein 4TZK



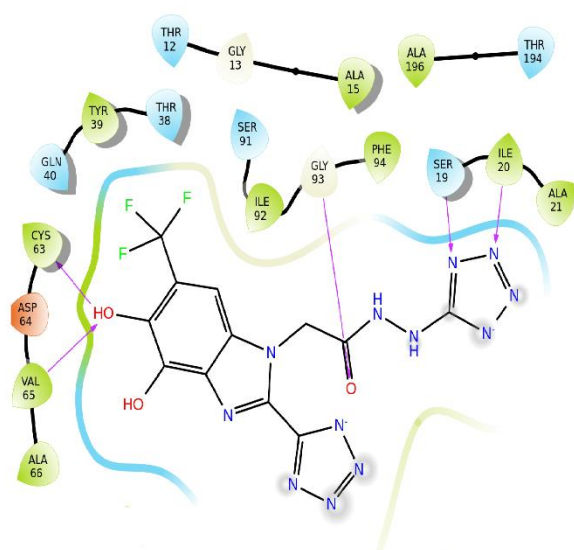
(d) Binding interaction of Compound 1 with protein 4TZT

Figure 2. Biding interactions of compounds 1 of set 2 within the pocket of receptors.

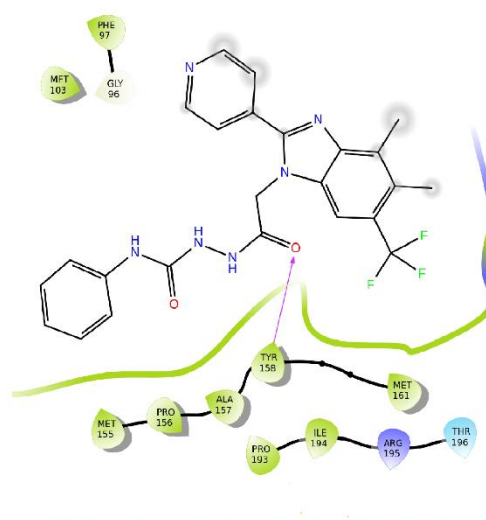
Table 7. Docking scores and binding energies of 25 lead molecules from Set 3.

Code	2B37		1QG6		4TZK		4Tzt	
Compounds	DS*	Gevdw*	DS*	Gevdw*	DS*	Gevdw*	DS*	Gevdw*
1	-8.97	-49.642	-9.011	-40.007	-11.795	-49.495	-11.549	-41.382
2	-8.97	-49.642	-9.011	-40.007	-11.795	-49.495	-11.549	-41.382
3	-8.97	-49.642	-8.396	-41.472	-11.795	-49.495	-11.313	-42.915
4	-8.97	-49.642	-8.396	-41.472	-11.795	-49.495	-11.313	-42.915
5	-8.933	-58.525	-8.396	-41.472	-11.549	-46.703	-11.089	-45.376
6	-8.933	-58.525	-8.396	-41.472	-11.549	-46.703	-11.089	-45.376
7	-8.933	-58.525	-7.609	-50.392	-11.533	-56.329	-10.976	-44.812
8	-8.933	-58.525	-7.609	-50.392	-11.533	-56.329	-10.976	-44.812
9	-8.884	-57.499	-7.609	-50.392	-11.239	-55.311	-10.976	-44.812
10	-8.884	-57.499	-7.609	-50.392	-11.239	-55.311	-10.976	-44.812
11	-8.884	-57.499	-7.573	-42.139	-11.239	-55.311	-10.322	-40.597
12	-8.884	-57.499	-7.573	-42.139	-11.239	-55.311	-10.322	-40.597
13	-8.65	-45.493	-7.548	-38.429	-10.866	-37.915	-10.322	-40.597
14	-8.65	-45.493	-7.548	-38.429	-10.866	-37.915	-10.322	-40.597
15	-8.646	-41.668	-7.548	-38.429	-10.865	-46.454	-10.25	-52.126
16	-8.646	-41.668	-7.548	-38.429	-10.865	-46.454	-10.25	-52.126
17	-8.646	-41.668	-7.393	-41.248	-10.865	-46.454	-10.25	-52.126
18	-8.646	-41.668	-7.393	-41.248	-10.865	-46.454	-10.25	-52.126
19	-8.505	-51.012	-7.358	-39.696	-10.865	-46.454	-9.834	-48.674
20	-8.505	-51.012	-7.358	-39.696	-10.865	-46.454	-9.834	-48.674
21	-8.505	-51.012	-7.358	-39.696	-10.865	-46.454	-9.834	-48.674
22	-8.505	-51.012	-7.358	-39.696	-10.865	-46.454	-9.834	-48.674
23	-8.505	-51.012	-7.333	-51.805	-10.776	-44.61	-9.808	-40.528
24	-8.505	-51.012	-7.333	-51.805	-10.776	-44.61	-9.808	-40.528
25	-8.505	-51.012	-7.333	-51.805	-10.776	-44.61	-9.808	-40.528

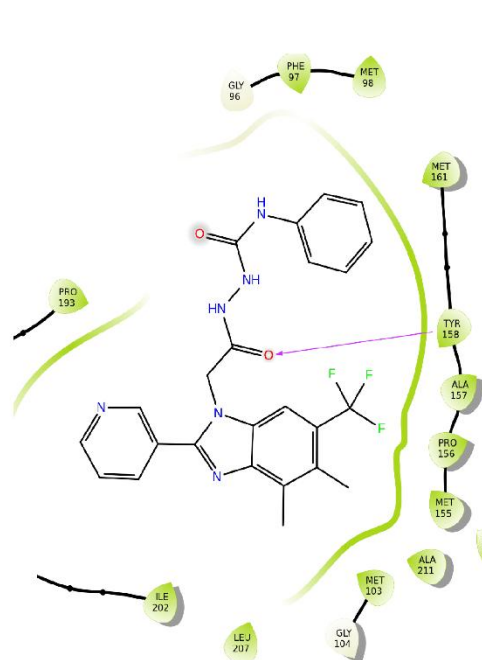
Compound 1 from series of set 3 form a five hydrogen bond with protein 2B37 with moderate binding energy (-8.970). The docking energies of set 3 with the receptors are given in table 3 and the binding interaction of the compound with receptors are given in **Figure 3**. Hydroxy substitution on Compound 1 (2-(4,5-dihydroxy-2-(1H-tetrazol-5-yl)-6-(trifluoromethyl)-1H-benzo[d]imidazol-1-yl)-N'-(1H-tetrazol-5-yl)acetohydrazides) shows two hydrogen bonding with the residue CYS 63 and VAL 65 (fig. 3 a).. The nitrogen on tetrazole ring have a formed two nitrogen bond with the residue Ser19 and Ile20 (**Figure 3a**). Moreover, complex of compound 1 (2-(2-(4,5-dimethyl-2-(pyridin-4-yl)-6-(trifluoromethyl)-1H-benzo[d]imidazol-1-yl)acetyl)-N-phenylhydrazinecarboxamide) with receptor 1QG6 have a good binding energy and formed one hydrogen bond between oxygen and residue Tyr158 (**Figure 3b**). We have found that docked complex between protein 4TZK and compound 1 (2-(2-(4,5-dimethyl-2-(pyridin-3-yl)-6-(trifluoromethyl)-1H-benzo[d]imidazol-1-yl)acetyl)-N-phenylhydrazinecarboxamide) have forms high binding energy (-11.795) and hydrogen bonding between oxygen and residue Tyr158 (**Figure 3c**). Additionally, the complex of compound 1 (2-(5-(tert-butyl)-6-methyl-2-(pyridin-2-yl)-4-(trifluoromethyl)-1H-benzo[d]imidazole-1-yl)-N'-(1H-imidazol-2-yl)acetohydrazides) and protein 4TZT have also good binding energy (-11.549) and found form two hydrogen bond between nitrogen of imidazole and nitrogen of amide with residue MET 98 (fig.3 d).



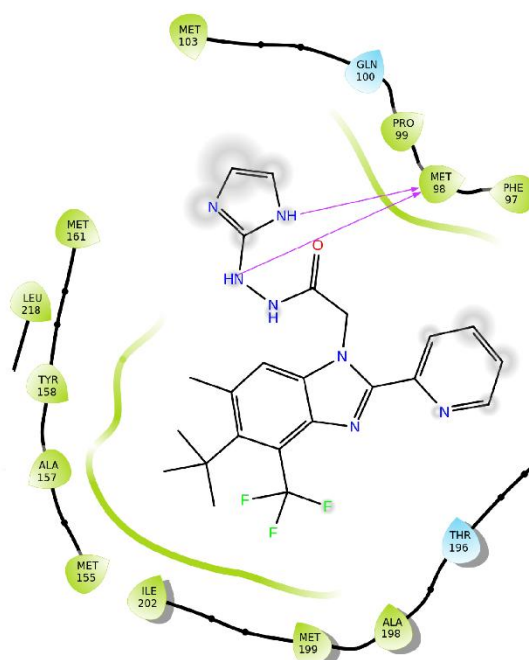
(a) Binding interaction of compound 1 with protein 1QG6



(b) Binding interaction of compound 1 with protein 2B37



(c) Binding interaction of compound 1 with protein 4TZK



(d) Binding interaction of compound 1 with protein 4TZT

Figure 3. Biding interactions of compounds 1 of set 3 within the pocket of receptors.

Table 8. Docking scores and binding energies of 25 lead molecules from Set 4.

PDB Code	2B37		1QG6		4TZK		4TZZ	
Compounds	DS*	Gevdw*	DS*	Gevdw*	DS*	Gevdw*	DS*	Gevdw*
1	-9.222	-60.562	-8.857	-40.743	-9.026	-59.457	-8.116	-37.991
2	-9.219	-59.537	-8.643	-52.496	-8.857	-52.616	-7.936	-51.989
3	-8.963	-57.353	-8.443	-59.173	-8.594	-57.394	-7.914	-62.853
4	-8.61	-51.523	-8.267	-62.666	-8.478	-51.812	-7.793	-59.241
5	-8.59	-58.405	-7.975	-53.713	-8.411	-61.323	-7.765	-56.353
6	-8.506	-62.948	-7.835	-32.359	-8.319	-60.166	-7.724	-53.471
7	-8.446	-58.63	-7.701	-68.914	-8.099	-66.014	-7.654	-53.064
8	-8.334	-61.783	-7.646	-58.077	-8.039	-46.218	-7.647	-58.353
9	-8.317	-56.293	-7.598	-69.069	-8.006	-48.313	-7.563	-51.718
10	-8.311	-55.75	-7.537	-51.579	-7.99	-59.531	-7.46	-48.056
11	-8.281	-58.35	-7.48	-42.229	-7.937	-42.07	-7.409	-48.03
12	-8.171	-61.308	-7.474	-56.149	-7.913	-41.423	-7.405	-53.51
13	-8.111	-65.013	-7.376	-68.713	-7.855	-49.417	-7.34	-61.478
14	-8.054	-56.3	-7.296	-51.443	-7.805	-67.5	-7.118	-56.633
15	-8.019	-52.772	-7.145	-57.387	-7.802	-63.939	-7.045	-52.979
16	-7.95	-58.207	-7.053	-54.721	-7.762	-55.189	-7.034	-50.503
17	-7.872	-60.68	-7.039	-69.785	-7.705	-40.958	-7.018	-49.104
18	-7.847	-55.492	-7.035	-67.037	-7.677	-53.365	-6.978	-45.449
19	-7.825	-56.846	-7.034	-65.781	-7.672	-48.962	-6.942	-43.929
20	-7.812	-60.968	-6.974	-59.066	-7.645	-54.195	-6.893	-50.922
21	-7.785	-58.092	-6.968	-60.601	-7.412	-54.112	-6.87	-52.686
22	-7.713	-55.296	-6.918	-57.178	-7.398	-38.485	-6.668	-54.501
23	-7.71	-57.462	-6.894	-57.52	-7.397	-48.732	-6.613	-44.593
24	-7.668	-57.767	-6.89	-62.75	-7.393	-55.433	-6.61	-43.671
25	-7.666	-46.419	-6.878	-27.967	-7.353	-54.043	-6.553	-41.485

The obtain result from docking study of set 4 suggests that the compounds of set 4 have different binding affinity with each protein. The docking energies of the selected compounds from series set 4 against receptors are given in table 3 and the hydrogen bonding of compounds with amino acids are visualized in figure 4. In the series of set 4, benzimidazole moiety is attached with the substituted benzothiazole and 4-qoumarin derivatives. Here, benzothiazole and benzimidazole are substituted with different electron withdrawing and electron donating functional group. Compound 1 (2-(7-bromo-4,6-bis(dimethoxymethyl)-2-(2-oxo-2*H*-chromen-3-yl)-1*H*-benzo[d]imidazol-1-yl)-N-(6-chloro-7-(dimethoxymethyl)-5-methoxybenzo[d]thiazol-2-yl)acetamide) have a good docking score -9.222 against 2B37 receptor, substitution of 1-bromo, 2-4 (1,1 dimethoxyethne) on benzimidazole moiety while benzothiazole have 2-chloro, 1-ethoxyethene, 3-methoxyethane. Compound 1 is found to form a four hydrogen bond with the 2B37 receptor. The two hydrogen bond is formed between the oxygen of benzothiazole with residue Ala196 and Ser19 (**Figure 4 a**). Furthermore, the receptor Gly93 (**Figure 4a**) form two hydrogen bond with nitrogen of benzothiazole ring and receptor PHE 94 form aromatic interaction with 4-qoumarin ring. In the case of receptor 1QG6, compound 1 (N-(6,7-dichloro-5-methoxybenzo[d]thiazol-2-yl)-2-(4-(dimethoxymethyl)-6-fluoro-7-methoxy-2-(2-oxo-2*H*-chromen-3-yl)-1*H*-benzo[d]imidazol-1-yl)acetamide) with - 8.857 docking score is able to form a one hydrogen bond with the residue Tyr158 (**Figure 4b**).

Moreover, compound 1 (2-(7-chloro-4-(dimethoxymethyl)-6-methoxy-2-(2-oxo-2*H*-chromen-3-yl)-1*H*-benzo[d]imidazol-1-yl)-N-(6,7-dichloro-5-(dimethoxymethyl)benzo[d]thiazol-2-yl)acetamide) which have 1-chloro, 2-ethoxyethane, 4-dimethoxyethane substitution on benzimidazole and 1,2-dichloro, 3-dimethoxyethane on

benzothiazole have a good docking score in the case of protein 4TZK. It was observed that the compound increased the docking score -9.026 against 4TZK and formed two hydrogen bond where one hydrogen bond between residue Met98 (**Figure 4 c**) with oxygen atom on 4-qoumarin and other hydrogen bond between Gly96 (**Figure 4c**) with nitrogen atom in linkage. Compound 1 (2-(5-chloro-4-ethoxy-2,7-dimethoxy-1H-benzo[d]imidazol-1-yl)-N-(7-chloro-5-(dimethoxymethyl)-6-methoxybenzo[d]thiazol-2-yl)acetamide) which have highest docking score (-8.116) against the protein 4TZZ have a 1-chloro, 2-methoxyethan, 3-dimethoxyethane substitution on benzothiazole and 2-chloro, 4-methoxymethane, 1-methoxyethan substitution on benzimidazole and 4-qoumarin were replaced with methoxy group. This compound is found to form one hydrogen bond between the atom oxygen with residue Met98 (**Figure 4d**) and aromatic bond with the residue Phe349 (**Figure 4d**).

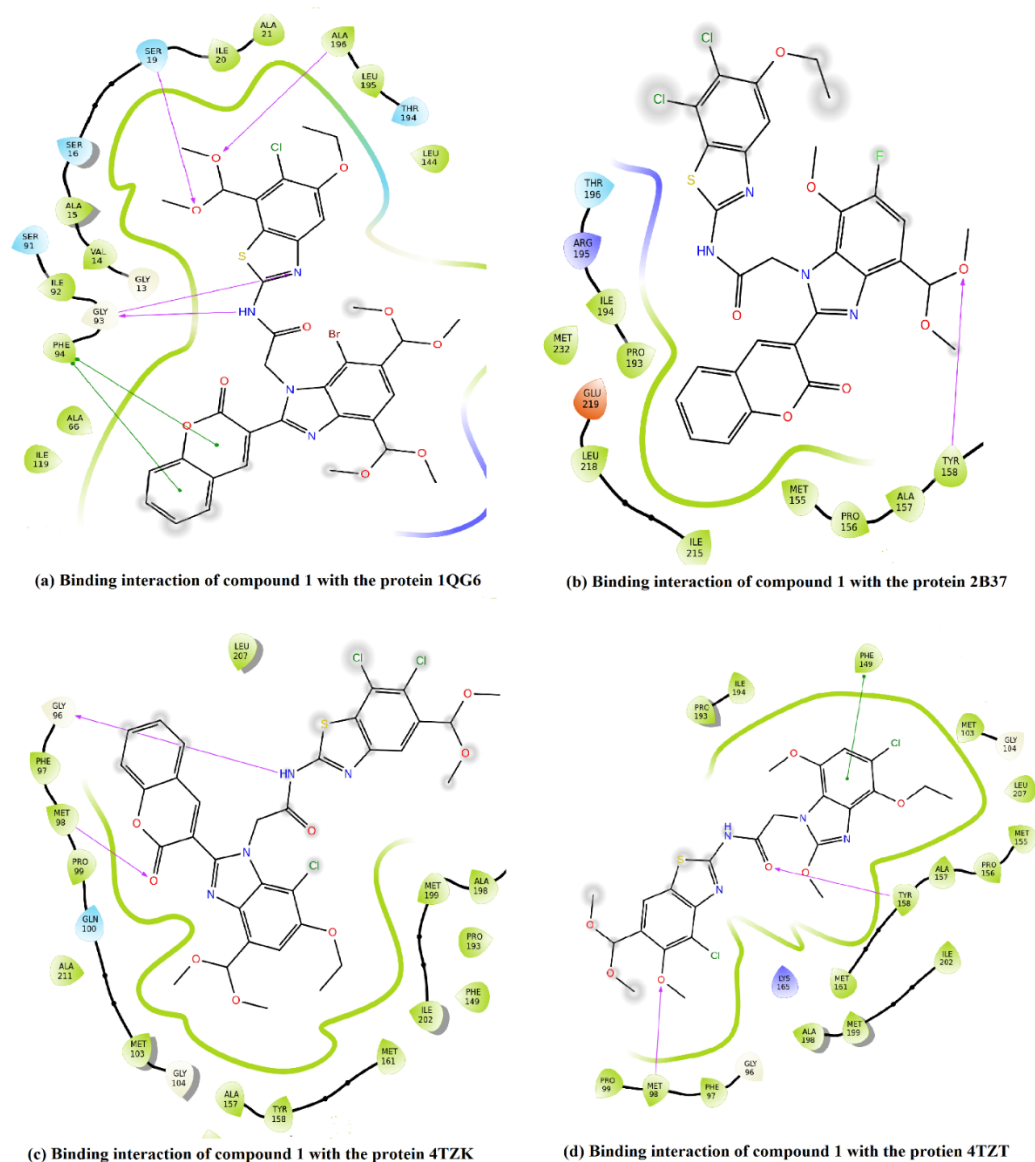


Figure 4. Binding interactions of compounds from set 4 within the pocket of receptors

From the docking result, we observed that the selected designed analogues depicted excellent *In silico* inhibition activity against four different proteins from *Mycobacterium Tuberculosis* Enoyl-ACP reductase. However, each derivative have different binding energy with different protein but basic moiety is benzimidazole and 4*H*-pyran. The best derivative could be differentiate with the help of given figures. Observed result suggest that the proposed benzimidazole and 4*H*-pyran derivative have better binding affinity than

standard and triclosan derivative. This analogues could be further developed as anti-bacterial drug after the synthesis.

3.3 Pharmacophore hypothesis development

The common pharmacophore hypothesis was generated using molecular docking post-processing module. The pharmacophore was developed for single ligand in each set (Series of set 1,2,3,4) which have highest docking score against particular receptor in different set of ligands. Here, from the docking study we have selected four different ligand for pharmacophore generation from each set. Ligand 1 (1-(1-(2-(2-(1H-imidazol-2-yl)hydrazinyl)-2-oxoethyl)-4,5-dihydroxy-6-(trifluoromethyl)-1H-benzo[d]imidazol-2-yl)-3-phenylurea) from set 1, which have highest docking score (-11.239) against protein 4TZK, ligand 1 (6-amino-1-(2-bromo-3,4,5-trichloro-6-nitrophenyl)-4-(3-bromo-5-ethoxy-2-fluoro-4-methoxyphenyl)-1,4-dihydropyrano[2,3-c]pyrazole-5-carbonitrile) from set 2 which have highest docking score (-10.232) against protein 4TZK, ligand 1 (2-(2-(4,5-dimethyl-2-(pyridin-3-yl)-6-(trifluoromethyl)-1H-benzo[d]imidazol-1-yl)acetyl)-N-phenylhydrazinecarboxamide) from set 3 which have highest docking score (-11.795) against protein 4TZK and the ligand 1 (2-(7-bromo-4,6-bis(dimethoxymethyl)-2-(2-oxo-2H-chromen-3-yl)-1H-benzo[d]imidazol-1-yl)-N-(6-chloro-7-(dimethoxymethyl)-5-methoxybenzo[d]thiazol-2-yl)acetamide) from set 4 which have highest docking score (-9.222) against protein 2B37 were selected for pharmacophore generation.

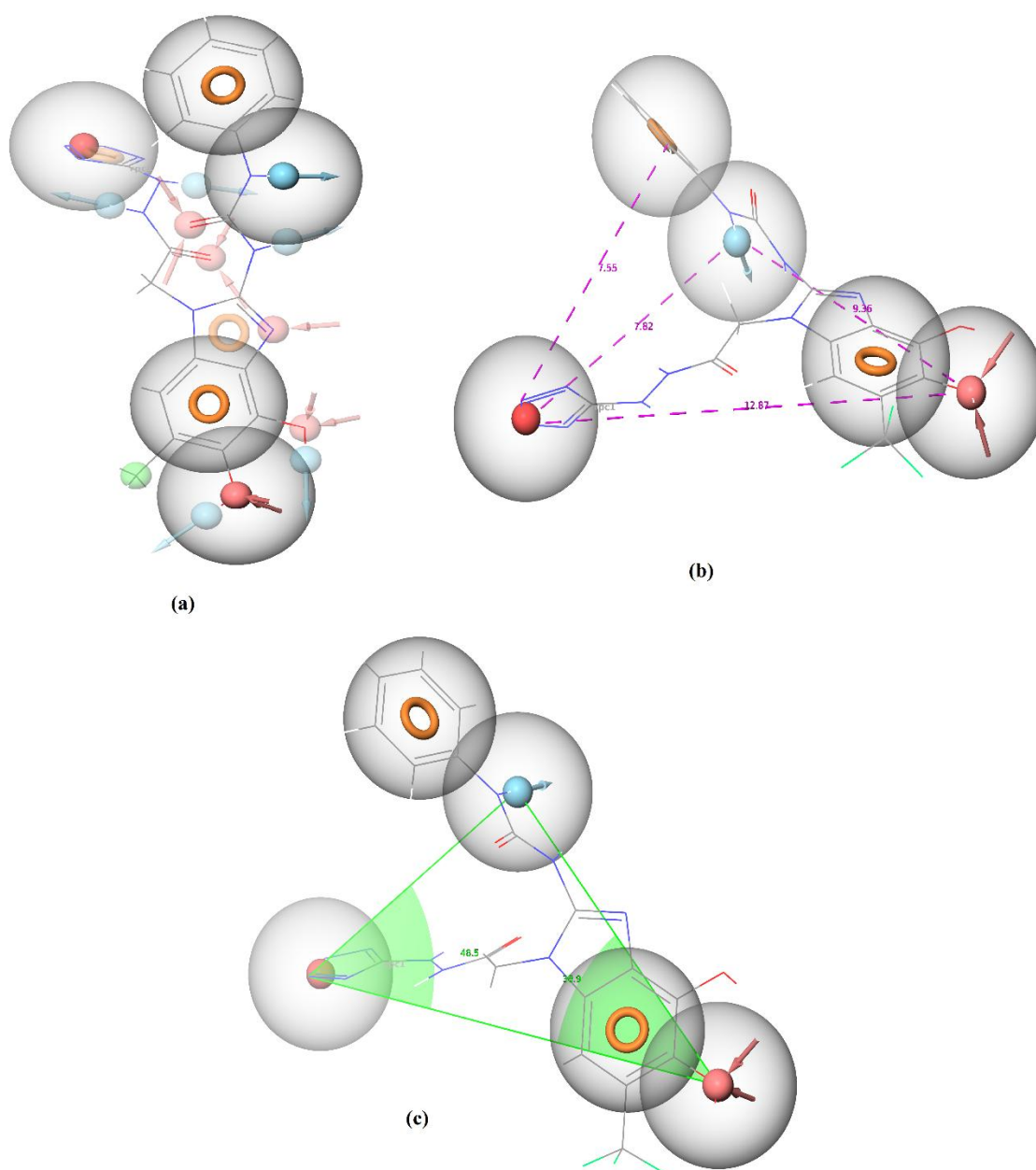


Figure 5. (a) Selected pharmacophore and generated pharmacophore of ligand 1 from set 1. (b) Pharmacophore hypothesis and distance between sites. (c) Generated angle between pharmacophore sites. All the distance and angle are in $^{\circ}$ A unit

Table 9. Predicted pharmacophore result of ligand 1 from set 1 with different pharmacophore hypothesis

Hypothesis	Survival score	Site score	Vector score	Volume Score	Selectivity score	Matched Ligand Sites	Fitness score
ADNRR	5.146	0.903	0.998	0.857	2.088	A(4) D(10) N(13) R(16) R(17)	2.757
ADNRR	5.134	0.887	0.999	0.857	2.091	A(4) D(10) N(13) R(14) R(17)	2.742
DDRRR	5.13	0.902	0.977	0.857	2.094	D(6) D(7) R(15) R(16) R(17)	3
AAANR	5.127	0.864	0.999	0.857	2.107	A(3) A(4) A(5) N(13) R(17)	2.719
DHNRR	5.124	0.798	0.998	0.857	2.171	D(10) H(12) N(13) R(16) R(17)	2.652
AHNRR	5.124	0.783	0.998	0.857	2.186	A(3) H(12) N(13) R(16) R(17)	2.638
AAHNR	5.123	0.786	0.999	0.857	2.18	A(3) A(4) H(12) N(13) R(17)	3
AAHNR	5.123	0.777	0.998	0.857	2.19	A(3) A(5) H(12) N(13) R(17)	3
AADNR	5.122	0.889	0.998	0.857	2.077	A(4) A(5) D(10) N(13) R(17)	3
AAHNR	5.122	0.776	0.997	0.857	2.192	A(3) A(5) H(12) N(13) R(16)	3
AANR	4.648	0.866	0.999	0.857	1.626	A(3) A(4) N(13) R(17)	2.722
ADNR	4.641	0.899	0.999	0.857	1.586	A(4) D(10) N(13) R(17)	3
AAAN	4.627	0.852	0.998	0.857	1.62	A(3) A(4) A(5) N(13)	2.706
AANR	4.624	0.863	0.998	0.857	1.605	A(1) A(4) N(13) R(17)	2.718
AANR	4.623	0.883	0.998	0.857	1.584	A(4) A(5) N(13) R(17)	2.738
AAAN	4.621	0.835	0.998	0.857	1.63	A(1) A(3) A(4) N(13)	2.69
AANR	4.612	0.848	0.998	0.857	1.608	A(3) A(5) N(13) R(17)	2.703
AAHN	4.608	0.753	0.998	0.857	1.7	A(3) A(5) H(12) N(13)	3
AAHN	4.603	0.763	0.999	0.857	1.683	A(3) A(4) H(12) N(13)	3
AAHN	4.601	0.743	0.998	0.857	1.703	A(1) A(3) H(12) N(13)	3

The generated pharmacophore of ligand from set 1 are shown in **Figure 5** and the result are displayed in **Table 9**. Here, the different hypothesis was generated but the selected hypothesis is shown in figure was selected based on highest survival score. The generated pharmacophore have five features with highest survival score (5.146) to bind with the protein 4TZK. The two aromatic rings required for the hydrophobic interaction

within the pocket namely R16 and R17 together with one acceptor (A4), one donor (D10) and one negative (N13) site. In the case of ligand 1 from set 2 with highest docking score against receptor 4TZK, the generated pharmacophore are shown in figure 6 and the predicted pharmacophore results are presented in table 10. The selected hypothesis have five features with highest survival and fitness score 5.581 and 2.998 respectively. The generated hypothesis have three hydrogen bonding feature namely H10, H11 and H13 along with one aromatic ring (R19) and one hydrogen acceptor (A5) feature.

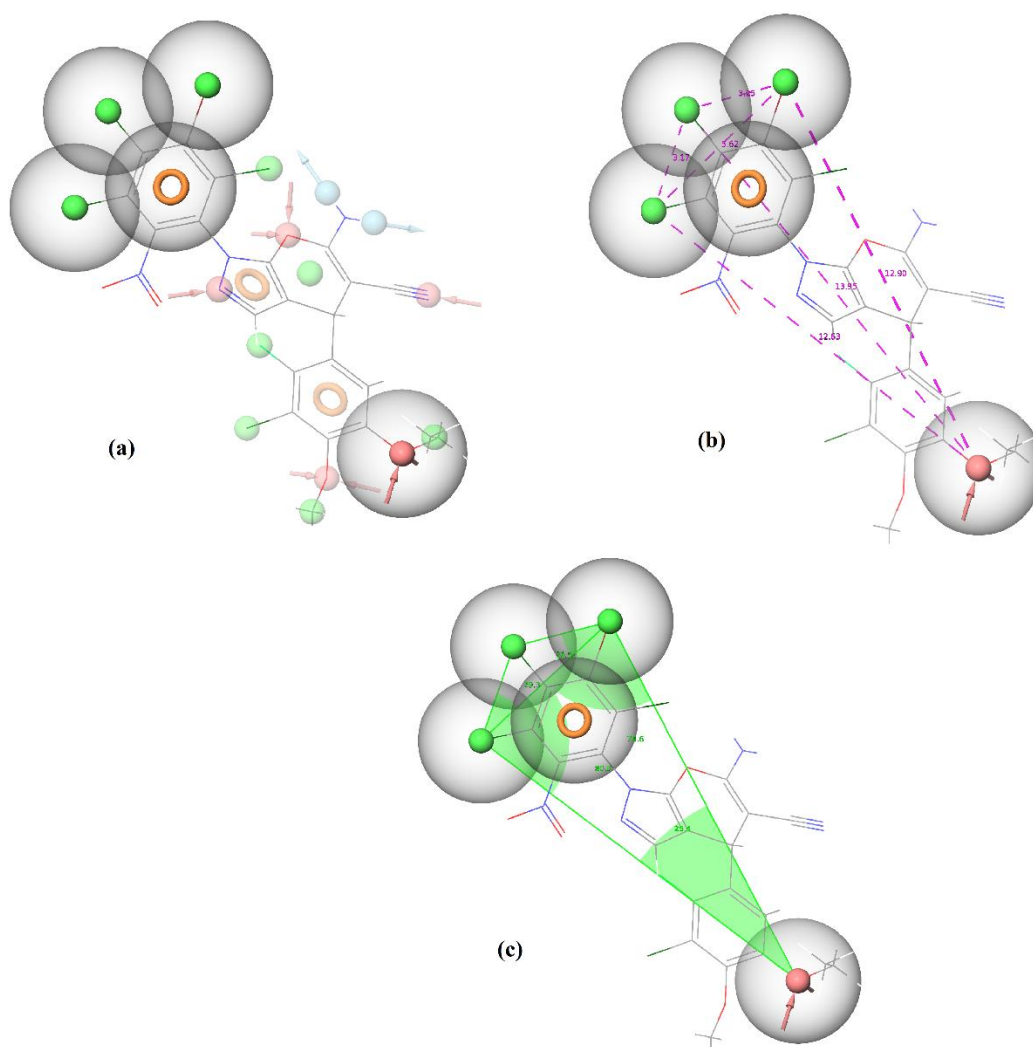


Figure 6. (a) Generated pharmacophore feature and selected pharmacophore feature of ligand 1 from set 2. (b) Pharmacophore hypothesis and distance between sites (c) angle between pharmacophore sites. All the distance and angle are in °A unit

Table 10. Predicted pharmacophore result of ligand 1 from set 2 with different pharmacophore hypothesis

Hypothesis	Survival Score	Site score	Vector score	Volume score	Selectivity score	Matched Ligand Sites	Fitness score
AHHHR	5.581	1	1	0.998	2.282	A(5) H(10) H(11) H(13) R(19)	2.998
AHHHR	5.581	1	1	0.998	2.282	A(5) H(10) H(11) H(13) R(19)	2.998
AAHHR	5.57	1	1	0.998	2.271	A(4) A(5) H(11) H(13) R(19)	2.997
AHHHR	5.563	1	1	0.998	2.264	A(5) H(9) H(11) H(13) R(19)	2.998
AAHHH	5.559	1	1	0.998	2.261	A(4) A(5) H(10) H(11) H(13)	2.997
AAHHH	5.559	1	1	0.998	2.26	A(4) A(5) H(10) H(11) H(13)	2.997
AAHHR	5.558	1	1	0.998	2.259	A(4) A(5) H(11) H(13) R(19)	2.997
AHHHR	5.556	1	1	0.998	2.257	A(5) H(10) H(11) H(13) R(19)	2.998
AAHHH	5.552	1	1	0.998	2.253	A(4) A(5) H(10) H(11) H(13)	2.997
AAHHH	5.551	1	1	0.998	2.253	A(4) A(5) H(10) H(11) H(13)	2.997
AHHR	4.978	1	1	0.998	1.679	A(5) H(11) H(13) R(19)	2.998
AHHR	4.97	1	1	0.998	1.671	A(5) H(11) H(13) R(19)	2.998
AHHR	4.968	1	1	0.998	1.669	A(5) H(11) H(13) R(19)	2.998
AHHR	4.96	1	1	0.998	1.661	A(5) H(10) H(11) R(19)	2.998
AAHH	4.952	1	1	0.998	1.654	A(4) A(5) H(11) H(13)	2.997
AHHR	4.946	1	1	0.998	1.647	A(4) H(10) H(11) R(19)	3
AHHR	4.943	1	1	0.998	1.644	A(5) H(11) H(13) R(19)	3
AHHR	4.94	1	1	0.998	1.642	A(5) H(10) H(13) R(19)	2.998
AHHR	4.94	1	1	0.998	1.642	A(5) H(10) H(13) R(19)	2.998
AAHH	4.94	1	1	0.998	1.641	A(4) A(5) H(11) H(13)	2.997

Furthermore, the ligand 1 from set 3 which also have highest docking score against the receptor 4TZK have generated five feature AHHHR hypothesis with highest survival

(5.507) and fitness score (3). The generated pharmacophore are shown in figure 7 and predicted pharmacophore are shown in **Table 11**. The ligand 1 from set 3 have found to generated five feature pharmacophore, where three hydrogen bonding namely H8, H9 and H10 together with one hydrogen acceptor (A4) and one aromatic ring (R12). This pharmacophore feature have supported the ligand 1 to bound strongly within the pocket of protein 4TZK and able to generate highest docking score. Additionally, in the case of ligand 1 from set 4, the generated pharmacophore are presented in figure 8 and the predicted pharmacophore results are given in **Table 12**. The generated pharmacophore hypothesis have a five features with highest fitness (2.657) and survival score (5.24), where two aromatic reigns which required for the hydrophobic interaction with the binding site of protein 2B37 namely R18 and R20.

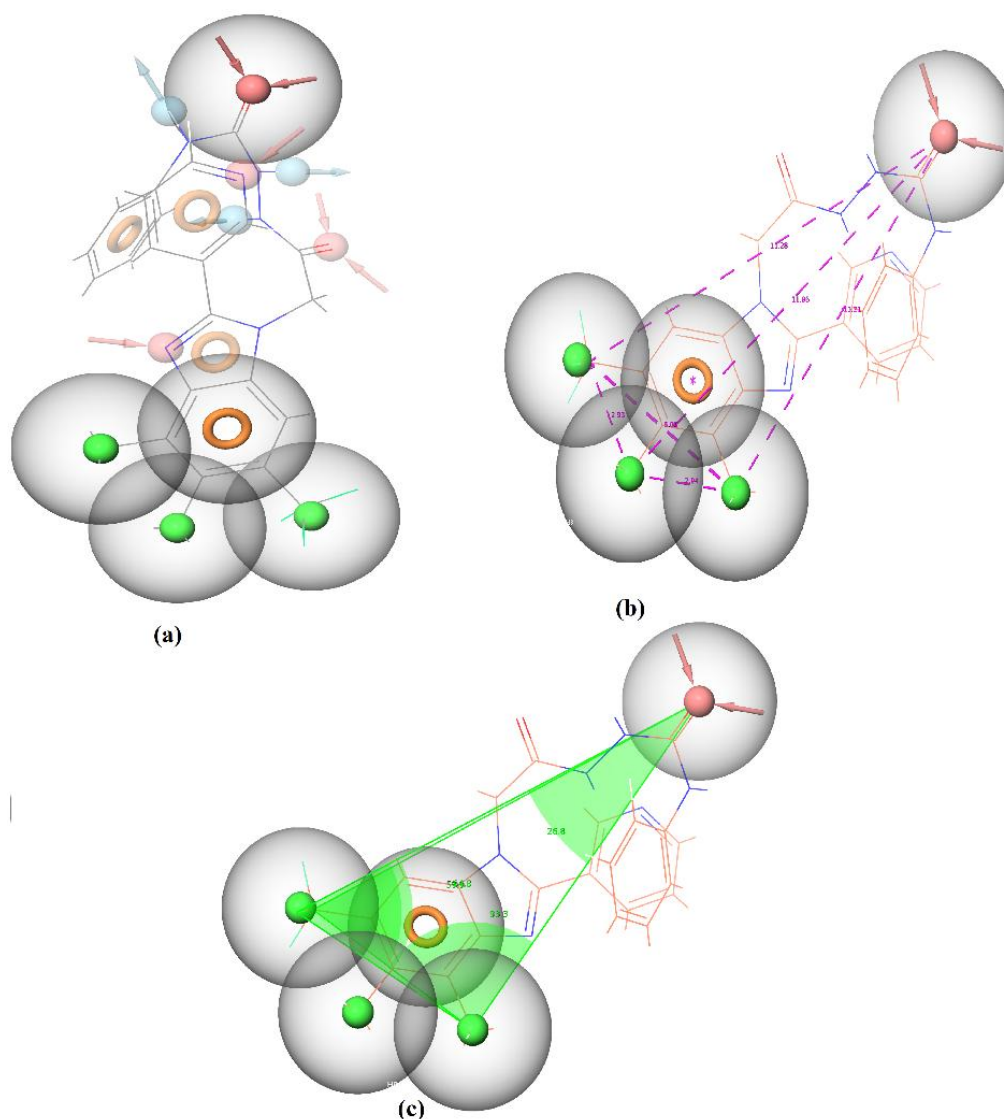


Figure 7. (a) Generated pharmacophore feature and selected pharmacophore feature of ligand 1 from set 3. (b) Pharmacophore hypothesis and distance between sites (c) angle between pharmacophore sites. All the distance and angle are in $^{\circ}$ A unit

The rest of feature involving two hydrogen bonding (H14, H16) and one hydrogen acceptor (A4) feature. This comparative pharmacophore hypothesis development study also supports and suggests our prediction regarding the minimum pharmacophore features required in ligands to behave as *Mycobacterium Tuberculosis* inhibitor and it will helpful in screening large database as development of new antibacterial agents in future.

Table 11. Predicted pharmacophore result of ligand 1 from set 3 with different pharmacophore hypothesis

Hypothesis	Survival score	Site score	Vector score	Volume score	Selectivity score	Matched Ligand Sites	Fitness score
AHHHR	5.507	1	1	1	2.206	A(4) H(8) H(9) H(10) R(12)	3
DHHRR	5.497	1	1	1	2.196	D(7) H(8) H(9) R(11) R(12)	3
DDHHR	5.491	1	1	1	2.19	D(5) D(7) H(8) H(10) R(12)	3
DDHHR	5.487	1	1	1	2.186	D(5) D(7) H(8) H(9) R(12)	3
DHHRR	5.482	1	1	1	2.181	D(5) H(8) H(9) R(11) R(12)	3
AHHRR	5.473	1	1	1	2.172	A(4) H(8) H(10) R(11) R(12)	3
DDHHR	5.472	1	1	1	2.171	D(5) D(7) H(9) H(10) R(12)	3
DHHRR	5.471	1	1	1	2.17	D(7) H(8) H(9) R(12) R(13)	3
AHHR	4.923	1	1	1	1.622	A(4) H(8) H(10) R(12)	3
AHHR	4.909	1	1	1	1.608	A(4) H(8) H(9) R(12)	3
DHHR	4.902	1	1	1	1.601	D(7) H(8) H(10) R(12)	3
DHHR	4.9	1	1	1	1.599	D(7) H(8) H(9) R(12)	3
AHHR	4.89	1	1	1	1.589	A(4) H(9) H(10) R(12)	3
DHHR	4.89	1	1	1	1.588	D(5) H(8) H(9) R(12)	3
DHHR	4.886	1	1	1	1.585	D(7) H(9) H(10) R(12)	3
AHHR	4.885	1	1	1	1.584	A(4) H(8) H(10) R(11)	3
AHHR	4.881	1	1	1	1.58	A(4) H(8) H(9) R(11)	3
DHHRR	5.48	1	1	1	2.179	D(7) H(9) H(10) R(11) R(12)	3
DHHR	4.887	1	1	1	1.586	D(5) H(8) H(10) R(12)	3
DHHRR	5.487	1	1	1	2.186	D(7) H(8) H(10) R(11) R(12)	3

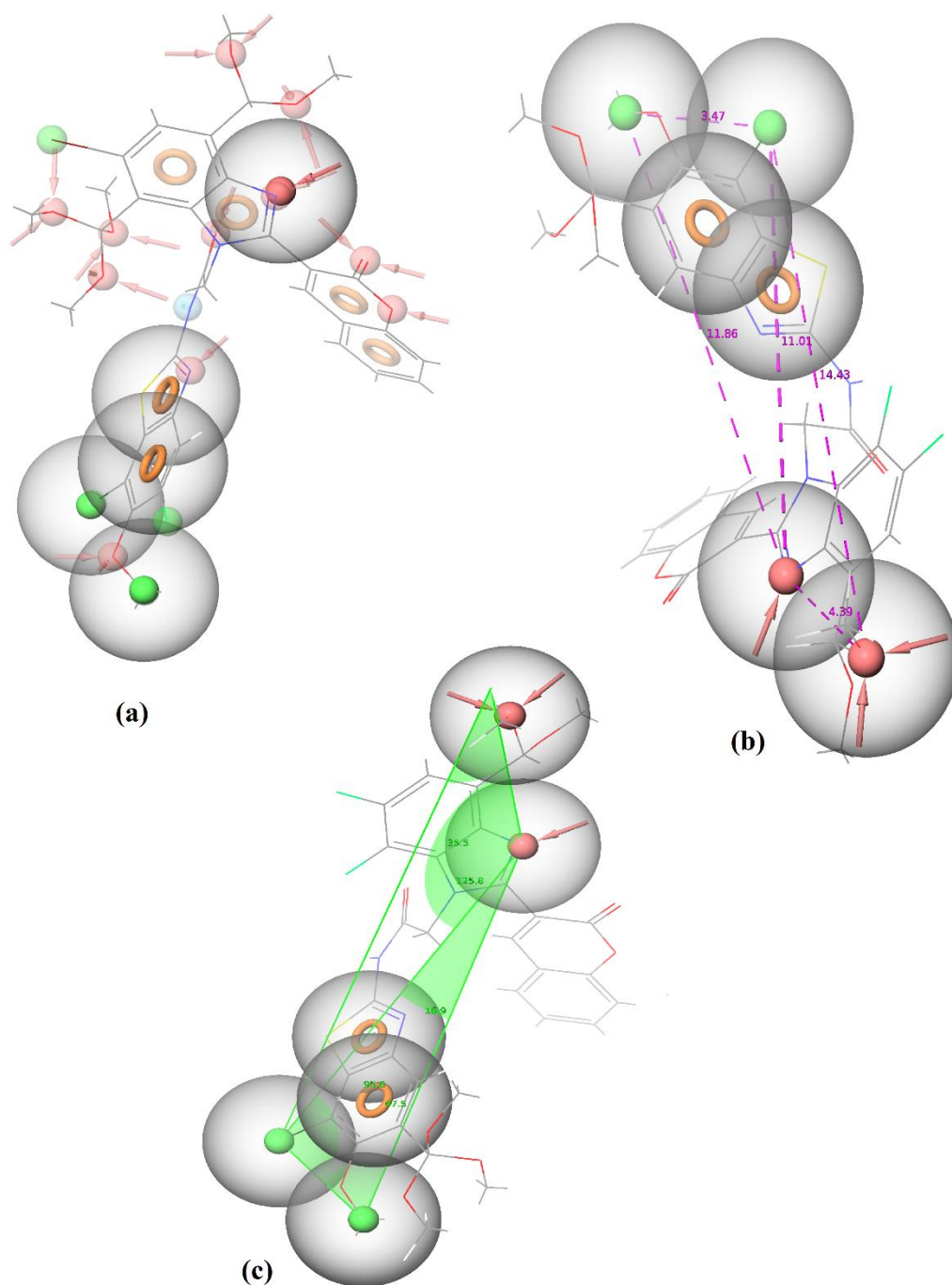


Figure 8. (a) Selected pharmacophore and generated pharmacophore of ligand 1 from set 3. (b) Pharmacophore hypothesis and distance between sites. (c) Generated angle between pharmacophore sites. All the distance and angle are in ° Å unit

Table 12. Predicted pharmacophore result of ligand 1 from set 4 with different pharmacophore hypothesis

Hypothesis	Survival score	Site score	Vector score	Volume score	Selectivity score	Matched Ligand Sites	Fitness score
AHHRR	5.24	0.945	0.972	0.741	2.282	A(4) H(14) H(16) R(18) R(20)	2.657
AHHRR	5.223	0.968	1	0.793	2.161	A(1) H(14) H(16) R(18) R(20)	2.761
AAHHR	5.216	0.927	0.975	0.746	2.267	A(4) A(11) H(14) H(16) R(20)	2.648
AHHRR	5.215	0.958	1	0.793	2.163	A(10) H(14) H(16) R(18) R(20)	2.751
AAHHR	5.209	0.915	0.975	0.74	2.278	A(4) A(10) H(14) H(16) R(20)	2.63
AHHRR	5.207	0.927	0.973	0.749	2.256	A(4) H(14) H(16) R(20) R(22)	2.65
AHHRR	5.201	0.965	1	0.667	2.268	A(4) H(14) H(16) R(18) R(20)	3
AAHHR	5.198	0.962	1	0.793	2.142	A(1) A(10) H(14) H(16) R(20)	2.755
ADHHR	5.221	0.918	0.971	0.744	2.286	A(4) D(12) H(14) H(16) R(20)	2.633
AHHRR	5.196	0.97	1	0.793	2.132	A(1) H(14) H(16) R(20) R(22)	2.764
AHHR	4.639	0.965	1	0.794	1.58	A(1) H(14) H(16) R(18)	2.758
AHHR	4.627	0.988	1	0.792	1.546	A(9) H(14) H(16) R(20)	3
AHHR	4.626	0.945	0.957	0.737	1.686	A(4) H(14) H(16) R(18)	2.639
AHHR	4.638	0.965	1	0.793	1.579	A(11) H(14) H(16) R(20)	2.758
AHHR	4.659	0.96	1	0.792	1.606	A(10) H(14) H(16) R(20)	2.752
AHHR	4.631	0.955	1	0.793	1.582	A(10) H(14) H(16) R(18)	2.748
AHHR	4.673	0.974	1	0.792	1.606	A(1) H(14) H(16) R(20)	2.766
AHHR	4.642	0.975	1	0.666	1.7	A(4) H(14) H(16) R(20)	3
HHRR	4.628	0.983	1	0.79	1.555	H(14) H(16) R(18) R(20)	2.772
AHHR	4.664	0.954	0.958	0.738	1.712	A(4) H(14) H(16) R(20)	2.651

4.0 Conclusion

The focal point of the current work was the development of new biologically active scaffold based on benzimidazole and 4*H*-pyran clubbed with coumarin, isoniazid and phenyl hydrazine and aromatic aldehyde derivatives. This compact system was developed with hope of generating new bioactive chemical entities that could be useful as potent anti-bacterial and anti-tuberculosis agents. Enoyl-ACP reductase of the type II fatty acid synthase (FAS-II) is major component of mycobacterial cell wall which involved the biosynthesis of mycolic acid. Mycolic acid is main component of mycobacteria and due to this Enoyl-ACP reductase enzyme is interesting target for novel Anti-tuberculosis drug development. In this present study, a library of more than 50,000 compounds from each set was developed with help of enumeration module in maestro. Compounds which are clubbed with isoniazid, coumarin and derivatives of 4*H*-pyran have shown grater selectivity and potency towards *Mycobacterium Tuberculosis* Enoyl-ACP reductase enzyme.

By employing a combination of ADME, docking and pharmacophore study calculations, novel potent hits to inhibit Enoyl-ACP reductase were identified with the points for consideration for designing of Enoyl-ACP reductase inhibitor. The ADME study revealed that the designed analogues showed better pharmacokinetic properties than 95% drug molecules. It is clear from the molecular docking study that, most of the compounds exhibited excellent binding energy with all the four proteins and showed strong binding affinity against receptor. Additionally, selected compounds exhibited greater binding energies against the protein 4TZK. The comparative pharmacophore study was done with the highest binding energy scoring compounds from each set. The pharmacophore study shown that the predicted hypothesis have the minimum pharmacophore features which was required for the ligand molecules to behave as anti-tuberculosis inhibitor. Furthermore, the

similarity of selected target structures also suggest that there is possibility of being targeted by different group of compounds. Here, our proposed inhibitors in future could be either used combination with standard drug or alone which can together act interactively more effective, active and have different mode of action cure Tuberculosis.

References

1. http://www.who.int/tb/publications/global_report/en/2018
2. Appunni S, Rajisha PM, Rubens M, Chandana S, Singh HN, Swarup V. Computational biology and chemistry. 2017; 67:200-4.
3. Ràfols C, Bosch E, Ruiz R, Box KJ, Reis M, Ventura C, Santos S, Araújo ME, Martins F. Journal of Chemical & Engineering Data. 2011; 57(2):330-8.
4. Mantu D, Antoci V, Moldoveanu C, Zbancioc G, Mangalagiu II. Journal of enzyme inhibition and medicinal chemistry. 2016; 31(sup2):96-103.
5. Gong JX, He Y, Cui ZL, Guo YW. Phosphorus, Sulfur, and Silicon and the Related Elements. 2016; 191(7):1036-41.
6. Kazimierczuk Z, Andrzejewska M, Kaustova J, Klimešova V. European journal of medicinal chemistry. 2005; 40(2):203-8.
7. Stanley SA, Grant SS, Kawate T, Iwase N, Shimizu M, Wivagg C, Silvis M, Kazyanskaya E, Aquadro J, Golas A, Fitzgerald M. ACS chemical biology. 2012; 7(8):1377-84.
8. Vasava MS, Bhoi MN, Rathwa SK, Shetty SS, Patel RD, Rajani DP, Rajani SD, Patel A, Pandya HA, Patel HD. Journal of Molecular Structure. 2019; 1181:383-402.
9. Shen J, Zhang W, Fang H, Perkins R, Tong W, Hong H. InBMC bioinformatics. BioMed Central. 2013; 14(14): S6
10. Muchmore, S. W.; Hajduk, P. Current Opinion in Drug Discovery & Development. 2003; 6: 544–549.
11. Jorgensen, W. L. Science (Washington, DC, U. S.) 2004; 303:1813-1818.
12. Jain A, Mondal R. FEMS Immunology & Medical Microbiology. 2008; 53(2):145-50.

13. Quemard A, Sacchettini JC, Dessen A, Vilcheze C, Bittman R, Jacobs Jr WR, Blanchard JS. *Biochemistry*. 1995; 34(26):8235-41.
14. Dessen A, Quemard A, Blanchard JS, Jacobs WR, Sacchettini JC. *Science*. 1995; 267(5204):1638-41.
15. Briken V, Porcelli SA, Besra GS, Kremer L. *Molecular microbiology*. 2004; 53(2):391-403.
16. Zhang Y, Mitchison D. *The international journal of tuberculosis and lung disease*. 2003; 7(1):6-21.
17. Konno K, Feldmann FM, McDermott W. *American Review of Respiratory Disease*. 1967; 95(3):461-9.
18. Hartmann, G.; Honikel, K. O.; Knußel, F.; Nüesch, J. *Biochim.Biophys. Acta* 1967; 145: 843.
19. Salam NK, Nuti R, Sherman W. *Journal of chemical information and modelling*. 2009; 49(10):2356-68.

Chapter: 3

Synthesis, Characterization, in vitro biological evaluation and in silico study of N-(benzo[d]thiazol-2-yl)-2-(2-(2-oxo-2H-chromen-3-yl)-1H-benzo[d]imidazol-1-yl)acetamide derivatives

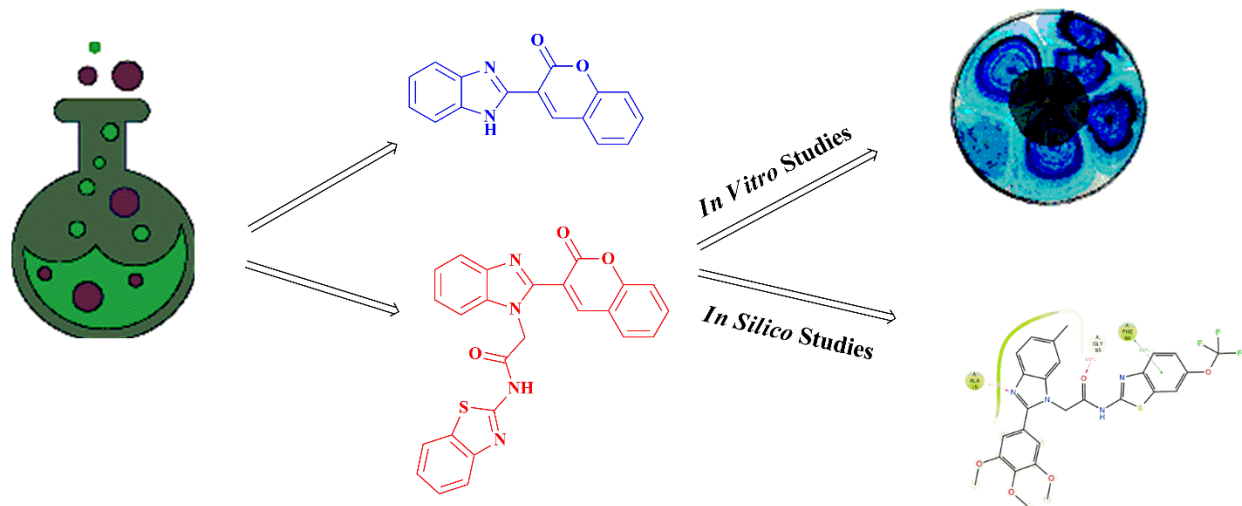


Table of Contents

1.0 Introduction	183
2.0 Methods and Materials	187
2.1 Chemistry	187
2.1.1 Synthesis of 3-(1 <i>H</i> -benzo[d]imidazol-2-yl)-2 <i>H</i> -chromen-2-one (4a-i).	187
2.1.2 Synthetic procedure of N-(benzo[d]thiazol-2-yl)-2-chloroacetamide (7a-d).....	190
2.1.2 General synthetic procedure of N-(benzo[d]thiazol-2-yl)-2-(2-(2-oxo-2 <i>H</i> -chromen-3-yl)-1 <i>H</i> -benzo[d]imidazol-1-yl)acetamide (8a-f).	191
2.2 Biological assay.....	197
2.2.1 <i>In vitro</i> anti-bacterial activity	197
2.2.2 <i>In vitro</i> anti-tuberculosis activity and MDR-TB study.....	198
2.2.3 <i>In vitro</i> anti-malarial and anti-fungal activity.....	198
2.3 Computational Study.....	199
2.3.1 ADMET property prediction	199
2.3.2 Molecular Docking.....	199
2.3.4 Molecular Dynamics.....	200
3.0 Result and Discussion	202
3.1 Chemistry	202
3.2 Biological assay.....	207
3.2.1 <i>in vitro</i> anti-bacterial activity	208

3.2.2 <i>In vitro</i> anti-tuberculosis activity and MDR-TB study.....	209
3.2.3 <i>In vitro</i> anti-malarial and anti-fungal activity.....	209
3.3 Computational Study.....	211
3.3.1 ADME property prediction.....	211
3.3.2 Molecular Docking Study.....	213
3.3.3 Molecular dynamics Study	216
4.0 Conclusion.....	221
References.....	223

Summary:

In an attempt to find new agents to fight against mycobacterial infection and act as good Enoyl-ACP reductase inhibitors, we have synthesized new benzimidazole-coumarin-benzothiazole clubbed series of 3-(1*H*-benzo[d]imidazol-2-yl)-2*H*-chromen-2-one (**4a-i**) and N-(benzo[d]thiazol-2-yl)-2-(2-(2-oxo-2*H*-chromen-3-yl)-1*H*-benzo[d]imidazol-1-yl)acetamide (**8a-f**, **9b**) derivatives. The newly synthesized compounds were characterized by different spectroscopic method. The compounds were further subjected to in vitro anti-bacterial activity against gram-positive and gram-negative bacteria. After the primary anti-bacterial evaluation, the compounds were screened for their anti-tuberculosis and MDR-TB potency. Most of the compounds exhibited promising anti-bacterial, anti-tuberculosis and MDR-TB activity. Furthermore, the compounds were analysed for ADME properties and showed potential as oral drug candidates. The binding interactions of synthesized compounds at the active site of Enoyl-ACP reductase with four different protein (InhA) was explored using molecular docking studies. Additionally, the stability of docked complex of ligand **9b** with protein 1QG6 were determined by molecular dynamic simulation analysis. The result from the present study clearly identified some selective, specific and novel Enoyl-ACP reductase (InhA) inhibitors against H₃₇Rv strain and resistant strain *Mycobacterium Tuberculosis*.

1.0 Introduction

Tuberculosis is caused by a bacteria called *Mycobacterium Tuberculosis*, TB still remain major cause of death among the infectious disease globally [1]. Millions of people die every years due to this deadly disease and it is estimated that between 2000 to 2020, approximately 36 million will die, a billion of people will be infected and more than 150 million people will get sick of Tuberculosis. This is also leading cause of death amongst people with HIV-positive [2]. The cell wall of mycobacterium tuberculosis deserve better attention due to the remarkable molecular complexity and uniqueness among all prokaryotes [3]. The mycobacterium cell wall contains mycolic acid as core constituent which is essential for the integrity of cell wall. Numerous enzymes are involved in the biosynthesis of mycolic acid. However, NADH-dependent Enoyl-acyl carrier protein reductase (InhA) encoded by *InhA* gene is primary target in mycobacterium tuberculosis, which is involved in the catalytic reduction in the biosynthesis of long chain trans-2-Enoyl-ACPin the type II fatty acid [4]. Isoniazid is the potent drug which inhibit the *InhA* by blocking the cell wall of mycobacterium, but the increased resistance of this enzyme against Isoniazid arises from mutations in *KatG* [5], which activate the Isoniazid for the inhibition of the enzyme. To overcome this problem, new molecules that directly target *InhA* and bypass the activation step by *KatG* are promising drug candidates for combating multidrug-resistant strains of *Mycobacterium tuberculosis*. The emergence of bacterial resistance against two milestone anti-tubercular drugs, Isoniazid and rifampicin is the biggest threat in TB treatment. The current TB treatment is 6 to 9 months lengthy process and involves a combination of 3-4 drugs. Due to the resisted prophylaxis of microbes and the longer medication therapy than other pathogens, infectious microbial disease remain a pressing problem worldwide [6]. In the current era, threat of multi-drug resistance, extensively drug resistance and totally drug resistance microorganism have reached alarming level in many

countries around the world including India. To shorten this long-treatment period and to target multidrug-resistance tuberculosis strains there is burning need of novel drugs with new mode of action.

In this direction, numerous attempts to, the benzimidazoles still remain as one of the most significant and versatile class of molecule for the development of novel structural prototype in the search for more effective anti-bacterial agents against microbes [7-13] as a result benzimidazole is useful substructures for further molecular investigation. Benzimidazole and its derivatives are very useful subunits or intermediates for the development of new pharmaceutically or biologically important molecules [14]. Moreover, the substituted benzimidazole derivatives are found to have a numerous medicinal applications such as antibacterial and anti-tubercular agents [15], anti-allergic activity [16], anti-HIV inhibitors and anti-viral effect [17], anti-parasitic active compounds [18], anti-hypertensive agents [19], cardiotonic compounds [20], anti-ulcer analogues [21], anti-inflammatory analogues [22], anti-oxidant analogues [23], anti-protozoal agents [24], anti-diabetic agents [25], anticonvulsant agents [26], anti-inflammatory agents [27].

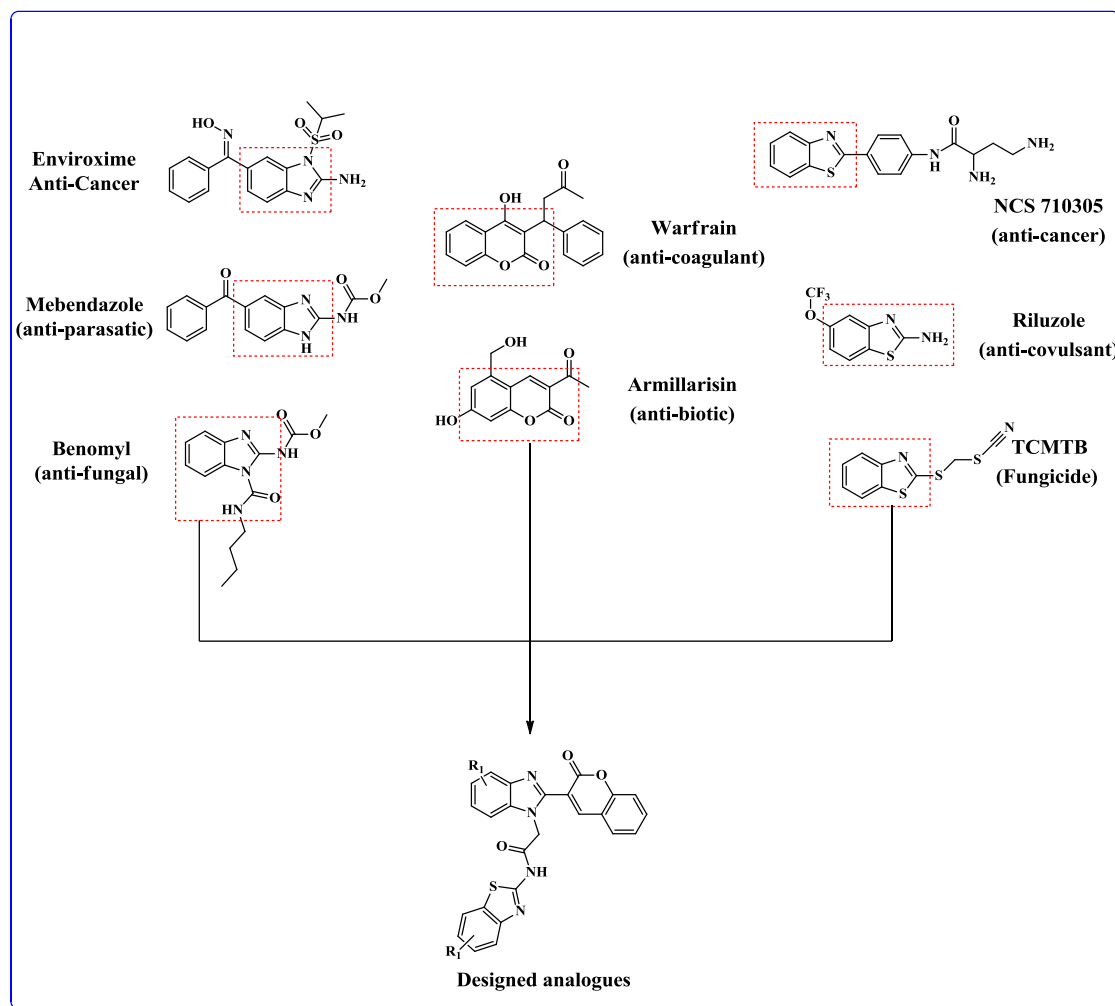


Figure 1. Designed strategy for the targeted molecules

In addition, due to the presence of coumarin in naturally occurring products and their wide-range applications in medicinal chemistry and agrochemicals, Coumarin and its derivatives are another potent moiety having a wide range of significant compounds [28-31]. Further, Coumarin nucleus able to produce an exclusive class of compounds, which exhibit a numerous therapeutic activities including anti-tuberculosis, antimicrobial, antioxidant, anti-inflammatory, antitumor and antiviral [32-35]. Despite several attempts in search for more effective compounds, coumarin still remains as one of the most important component among the molecules in medicinal chemistry and drug discovery. To develop novel molecules, most of hybrid molecules have been reported including both coumarin

and benzimidazole moieties [36]. However, there are rare examples are known for coumarin- benzimidazole hybrids biologically active compounds.

On the other hand, several compounds carrying benzothiazole ring system have been validated to be effective to possess promising anti-tuberculosis activity [37], therefore, many benzothiazole derivatives are screened for their in vitro anti-tuberculosis activity [38] using BACTEC methodology protocol and the molecules were found to exhibit tremendous inhibition (88-99 %) at MIC value of 6.25 $\mu\text{g/mL}$ against mycobacterium tuberculosis. Moreover, current literature survey revealed that the benzothiazole derivatives are developed with progressive findings about the different biological activities [39]. Additionally, benzothiazole is a versatile heterocyclic molecule having high potential for the development of new chemical entities for the treatment of cancer, CNS and infectious diseases [40].

In view of the above consideration and our previous computational work (**Chapter 2, Set 4**), present work was undertaken as an attempt to explore the biological significance of these compounds by hybridization method. Here we reported the synthesis, characterization, biological screening and in silico study of the 3-(1*H*-benzo[d]imidazol-2-yl)-2*H*-chromen-2-one (**4a-4i**) and N-(benzo[d]thiazol-2-yl)-2-(2-(2-oxo-2*H*-chromen-3-yl)-1*H*-benzo[d]imidazol-1-yl)acetamide (**8a-8f**, **9a**). The characterization of the synthesized compounds was done using ^1H and ^{13}C -NMR spectroscopy while in vitro biological screening was evaluated against bacterial strain, Tuberculosis H₃₇Rv strain, MDR-TB, malarial parasites and fungal strain to examine the ability of the compounds to inhibit the strains. Furthermore, due to lack of enzymatic study, the *In-silico* computational study was carried out in Schrodinger software. The ADME study was done to check the drug-like properties of the compounds while compounds were docked in the active site of

well-known target Enoyl-ACP reductase to investigate the binding affinity of the molecules within the active site of the receptor.

2.0 Methods and Materials

2.1 Chemistry

All the chemicals, reagents and solvents were acquired from commercial suppliers and were used in the reaction without further purification. The targeted compounds were synthesis using conventional method. The reaction progress was monitored via analytical thin layer chromatography (TLC). The TLC plate was silica gel coated aluminum sheets (silica gel G60 F₂₅₄, Merck) and visualized by UV radiation and different spray reagent. Melting points of the synthesized compounds were determined by automated melting point apparatus (MPA- Optimelt) and are uncorrected. ¹H and ¹³C NMR spectra were run on Bruker 500 and 125 MHz NMR spectroscopy by using DMSO-*d*₆ as solvent. The chemical shifts were expressed in parts per million (δ ppm) relative to TMS (internal reference), J values are given in hertz (Hz). Mass spectra was recorded on Advion Expression CMS, USA, with electro-spray ionization (ESI) was used as an ion source and ethanol: formic acid: water were used as a mobile phase. An elemental analysis were performed on vario MICRO cube, elemental CHNS analyzer (Serial Number: 15084053).

2.1.1 Synthesis of 3-(1*H*-benzo[d]imidazol-2-yl)-2*H*-chromen-2-one (4a-i).

The mixture of substituted benzene-1,2-diamine (**1a-i**) (1eq.), 2-oxo-2*H*-chromene-3-carboxylic acid (**2**) (1 eq.) or 3,4,5-trimethoxybenzaldehyde (**3**) (1 eq.) were taken in a flat bottom flask with Methanol and 4*N* HCl [41]. The reaction mixture was further refluxed for 3-4 hours and different derivatives are shown in **Table 1**. The progress of reaction was monitored by TLC and confirm by consumption of starting materials. After complementation of the reaction, the reaction mixture was allowed to cool at room temperature. Due to the acidic media of reaction mixture, it was further treated with sodium bicarbonate to neutralize the reaction mixture and precipitate out the product. The mixture

was filtered continuously by giving a wash of cold water. The obtained crude was purified by simple crystallization method to get the targeted product **3-(1*H*-benzo[d]imidazol-2-yl)-2*H*-chromen-2-one (4a-i) (5b)**.

2.2.1.1. 3-(1*H*-benzo[d]imidazol-2-yl)-2*H*-chromen-2-one (4a).

Light yellow solid, m.p. 242-246°C.; Anal. Calc. for C₁₆H₁₀N₂O₂ (%): C, 73.27; H, 3.84; N, 10.68; O, 12.20; Found: C, 73.19; H, 3.76; N, 10.48%; ¹H NMR (500 MHz, DMSO): δ; 8.17 (s, 1H), 7.67 (s, 1H), 7.61 (d, *J* = 16.1 Hz, 2H), 7.44 (s, 1H), 7.27 - 7.17 (m, 4H), 4.86 (s, 1H).; ¹³C NMR (125 MHz, DMSO): δ; 165.98, 154.13, 151.54, 139.18, 137.69, 137.50, 132.87, 129.57, 125.01, 123.62, 123.33, 120.60, 118.49, 117.14, 115.12, 108.78.; ESI-MS: *m/z* Calculated 262.26, found [*m/z*] [M+H]⁺ 263.1.

2.2.1.2. 3-(6-methyl-1*H*-benzo[d]imidazol-2-yl)-2*H*-chromen-2-one (4b).

Light brown solid, m.p. 248-252°C.; Anal. Calc. for C₁₇H₁₂N₂O₂ (%): C, 73.90; H, 4.38; N, 10.14; O, 11.58%. Found: C, 73.82; H, 4.39; N, 10.06%; ¹H NMR (500 MHz, DMSO): δ; 8.14 (s, 1H), 7.61 (d, *J* = 0.4 Hz, 2H), 7.41 (d, *J* = 21.1 Hz, 2H), 7.15 (d, *J* = 18.5 Hz, 2H), 7.08 (s, 1H), 5.02 (s, 1H), 2.28 (s, 3H).; ¹³C NMR (125 MHz, DMSO): δ; 165.98, 154.13, 151.54, 139.18, 137.02, 135.90, 230.01, 117.04, 133.31, 132.87, 129.57, 125.01, 123.19, 120.60, 113.78, 108.78, 21.21.

2.2.1.3. 3-(3*H*-imidazo[4,5-*b*]pyridin-2-yl)-2*H*-chromen-2-one (4c).

Dark brown solid, m.p. 240-245°C.; Anal. Calc. for C₁₅H₉N₃O₂ (%): C, 68.44; H, 3.45; N, 15.96; O, 12.16%. Found: C, 68.40; H, 3.38; N, 15.29%; ¹H NMR (500 MHz, DMSO): δ; 8.39 (s, 1H), 8.25 (s, 1H), 7.88 (s, 1H), 7.69 (s, 1H), 7.50 (s, 1H), 7.36 (s, 1H), 7.26 (d, *J* = 2.3 Hz, 2H), 4.91 (s, 1H).; ¹³C NMR (125 MHz, DMSO): δ; 165.98, 158.92, 154.13, 150.12, 142.18, 139.18, 132.87, 131.56, 129.57, 126.17, 125.01, 122.01, 120.60, 117.14, 108.78.

2.2.1.4. 3-(6-fluoro-1*H*-benzo[d]imidazol-2-yl)-2*H*-chromen-2-one (4d).

Yellowish solid, m.p. 251-254°C.; Anal. Calc. for C₁₆H₉FN₂O₂ (%): C, 68.57; H, 3.24; F, 6.78; N, 10.00; O, 11.42%. Found: C, 68.60; H, 3.17; N, 9.76%; ¹H NMR (500 MHz, DMSO): δ; 8.12 (s, 1H), 7.61 (s, 1H), 7.50 (d, *J* = 8.1 Hz, 2H), 7.39 (s, 1H), 7.15 (d, *J* = 17.7 Hz, 2H), 7.01 (s, 1H), 5.10 (s, 1H).; ¹³C NMR (125 MHz, DMSO): δ; 165.98, 154.64, 154.13, 151.54, 139.18, 138.50, 134.31, 132.87, 129.57, 125.01, 120.60, 119.56, 117.14, 115.65, 108.78, 99.42.

2.2.1.5. 3-(5-benzoyl-1*H*-benzo[d]imidazol-2-yl)-2*H*-chromen-2-one (4e).

Dark yellow solid, m.p. 258-262°C.; Anal. Calc. for C₂₃H₁₄N₂O₃ (%): C, 75.40; H, 3.85; N, 7.65; O, 13.10%. Found: C, 74.89; H, 3.80; N, 7.62%; ¹H NMR (500 MHz, DMSO) δ 8.16 (s, 1H), 8.08 (s, 1H), 7.76 (s, 1H), 7.63 (dd, *J* = 35.1, 4.3 Hz, 4H), 7.41 (d, *J* = 6.3 Hz, 2H), 7.37 - 7.31 (m, 2H), 7.16 (d, *J* = 4.3 Hz, 2H), 5.07 (s, 1H).; ¹³C NMR (125 MHz, DMSO): δ; 195.76, 165.98, 154.13, 152.06, 139.18, 138.40, 137.92, 136.39, 132.87, 131.92, 131.11, 129.57, 129.11, 128.72, 128.45, 128.05, 125.01, 122.51, 120.62, 117.14, 111.35, 108.78.

2.2.1.6. 3-(6-bromo-3*H*-imidazo[4,5-*b*]pyridin-2-yl)-2*H*-chromen-2-one (4f).

Light orange solid, m.p. 254-258°C.; Anal. Calc. for C₁₅H₈BrN₃O₂ (%): C, 52.66; H, 2.36; Br, 23.35; N, 12.28; O, 9.35%. Found: C, 51.88; H, 2.19; N, 12.17%; ¹H NMR (500 MHz, DMSO): δ; 8.54 (s, 1H), 8.33 (s, 1H), 8.24 (s, 1H), 7.69 (s, 1H), 7.50 (s, 1H), 7.26 (d, *J* = 1.8 Hz, 2H), 4.82 (s, 1H).; ¹³C NMR (125 MHz, DMSO): δ; 165.98, 159.28, 154.13, 144.49, 140.43, 139.18, 133.77, 132.87, 129.57, 127.67, 125.01, 120.60, 118.44, 117.14, 108.78.

2.2.1.8. 3-(7-methyl-1*H*-benzo[d]imidazol-2-yl)-2*H*-chromen-2-one (4g).

Brown solid, m.p. 247-251°C.; Anal. Calc. for $C_{17}H_{12}N_2O_2$ (%): C, 73.90; H, 4.38; N, 10.14; O, 11.58%. Found: C, 72.71; H, 4.30; N, 10.07%; 1H NMR (500 MHz, DMSO): δ ; 8.17 (s, 1H), 7.63 (s, 1H), 7.45 (d, J = 14.5 Hz, 2H), 7.18 (t, J = 8.0 Hz, 3H), 7.08 (s, 1H), 4.79 (s, 1H), 2.58 (s, 3H); ^{13}C NMR (125 MHz, DMSO): δ ; 165.98, 154.13, 149.40, 139.18, 138.35, 137.44, 132.87, 129.57, 125.00, 124.62, 124.32, 120.60, 117.14, 114.32, 108.78, 18.24.

2.2.1.9. 3-(5,6-dichloro-1*H*-benzo[d]imidazol-2-yl)-2*H*-chromen-2-one (4h).

Light brown solid, m.p. 256-261°C.; Anal. Calc. for $C_{16}H_8Cl_2N_2O_2$ (%): C, 58.03; H, 2.43; Cl, 21.41; N, 8.46; O, 9.66%. Found: C, 58.06; H, 2.27; N, 8.38%; 1H NMR (500 MHz, DMSO): δ ; 8.14 (s, 1H), 7.76 (s, 1H), 7.61 (s, 1H), 7.56 (s, 1H), 7.40 (s, 1H), 7.15 (d, J = 17.4 Hz, 2H), 5.11 (s, 1H); ^{13}C NMR (125 MHz, DMSO): δ ; 165.98, 154.13, 152.06, 139.18, 136.91, 136.21, 132.87, 129.57, 127.06, 126.56, 125.01, 120.60, 117.40, 117.14, 114.69, 108.78.

2.2.1.10. 3-(6-chloro-1*H*-benzo[d]imidazol-2-yl)-2*H*-chromen-2-one (4i).

Light orange solid, m.p. 253-258°C.; Anal. Calc. for $C_{16}H_9ClN_2O_2$ (%): C, 64.77; H, 3.06; Cl, 11.95; N, 9.44; O, 10.78%. Found: C, 63.92; H, 3.11; N, 9.08%; 1H NMR (500 MHz, DMSO): δ ; 8.14 (s, 1H), 8.02 (s, 1H), 7.78 (s, 1H), 7.61 (s, 1H), 7.40 (d, J = 10.3 Hz, 2H), 7.34 (d, 1H), 7.12 (d, 1H), 5.28 (s, 1H); ^{13}C NMR (125 MHz, DMSO): δ ; 165.98, 154.13, 151.54, 139.18, 138.15, 136.83, 132.87, 130.77, 129.57, 125.01, 122.06, 120.60, 119.26, 117.14, 113.39, 108.78.

2.1.2 Synthetic procedure of N-(benzo[d]thiazol-2-yl)-2-chloroacetamide (7a-d).

The equivalent amount of substituted 2-amino benzothiazole (**6a-d**) (1 eq.) was treated with chloro acetyl chloride in dry acetone using anhydrous potassium dichromate at 0-5 °C for 1-2 hours. The completion of reaction was checked by TLC and visualized under UV lamp. After completion of the reaction, solvent was extracted by rotatory pump

to get the dry crude. Crude product (**7a-d**) was further used in next step without any purification.

2.1.2 General synthetic procedure of N-(benzo[d]thiazol-2-yl)-2-(2-(2-oxo-2H-chromen-3-yl)-1H-benzo[d]imidazol-1-yl)acetamide (**8a-f**).

The synthesized mixture **4a-i** (3.35 mmol, 1 eq.), **7a-d** (3.35mmol, 1eq.), potassium tert-butoxide (2 eq.) and Pd(OAc)₂ (10% mol) in DMF solvent were taken in oven dried flat bottom flask. The reaction mixture was stirred 100 °C in nitrogen atmosphere for 8-10 hours. The reaction mixture was continuously monitored by TLC. After the completion of reaction the mixture was cooled at room temperature, poured in ice water and extracted with ethyl acetate. The combined extracts were dried over MgSO₄ and filtered out. The filtered was concentrated under reduced pressure and was purified by column chromatography using Ethyl acetate: Hexane mixture as an eluent to get the targeted product N-(benzo[d]thiazol-2-yl)-2-(2-(2-oxo-2H-chromen-3-yl)-1H-benzo[d]imidazol-1-yl)acetamide (**8a-f**).

2.1.2.1. N-(benzo[d]thiazol-2-yl)-2-(2-(2-oxo-2H-chromen-3-yl)-1H-benzo[d]imidazol-1-yl)acetamide (**8a**).

Dark brown solid, m.p. 286-290°C.; Anal. Calc. for C₂₅H₁₆N₄O₃S (%): C, 66.36; H, 3.56; N, 12.38; O, 10.61; S, 7.09%. Found: C, 66.25; H, 3.41; N, 11.76%.; ¹H NMR (500 MHz, DMSO): δ; 9.02 (s, 1H), 8.24 (d, 1H), 7.96 (s, 1H), 7.73 (s, 2H), 7.71 (d, *J* = 6.7 Hz, 2H), 7.62 (d, *J* = 27.7 Hz, 2H), 7.56 (d, 2H), 7.41 (t, *J* = 12.7 Hz, 2H), 7.21 (dd, *J* = 6.6, 4.5 Hz, 2H), 5.06 (d, *J* = 16.7 Hz, 1H).; ¹³C NMR (125 MHz, DMSO): δ; 168.17, 163.00, 156.70, 154.13, 153.43, 151.38, 139.17, 136.73, 134.41, 132.87, 132.09, 129.57, 125.53, 125.01, 124.56, 122.95, 122.86, 122.66, 121.34, 120.60, 120.06, 118.71, 117.14, 112.91, 112.32, 47.60.; ESI-MS: m/z Calculated 452.48, found [m/z] [M+H]⁺ 453.3.

2.1.2.2. N-(6-methoxybenzo[d]thiazol-2-yl)-2-(2-(2-oxo-2*H*-chromen-3-yl)-3*H*-imidazo[4,5-*b*]pyridin-3-yl)acetamide (8b).

Blackish solid, m.p. 291-294°C.; Anal. Calc. for C₂₅H₁₇N₅O₄S (%): C, 62.10; H, 3.54; N, 14.48; O, 13.24; S, 6.63%. Found: C, 62.17; H, 3.23; N, 14.12%; ¹H NMR (500 MHz, DMSO): δ; 8.98 (s, 1H), 8.74 (d, 1H), 8.04 (s, 1H), 7.93 (d, 2H), 7.77 (s, 1H), 7.67 (d, 1H), 7.47 (d, *J* = 8.5 Hz, 2H), 7.34 (d, *J* = 4.2 Hz, 2H), 7.19 (d, 1H), 5.00 (s, 2H), 3.78 (s, 3H). ¹³C NMR (125 MHz, DMSO): δ; 168.17, 163.00, 154.13, 153.43, 153.20, 150.82, 149.20, 147.65, 142.26, 138.02, 134.42, 132.87, 132.09, 129.57, 127.17, 125.01, 120.60, 120.40, 119.02, 117.14, 113.83, 112.91, 108.79, 56.04, 44.19.

2.1.2.3. N-(benzo[d]thiazol-2-yl)-2-(6-fluoro-2-(2-oxo-2*H*-chromen-3-yl)-1*H*-benzo[d]imidazol-1-yl)acetamide (8c).

Dark yellowish solid, m.p. 283-288°C.; Anal. Calc. for C₂₅H₁₅FN₄O₃S (%): C, 63.82; H, 3.21; F, 4.04; N, 11.91; O, 10.20; S, 6.82%. Found: C, 63.71; H, 3.10; N, 11.59%; ¹H NMR (500 MHz, DMSO): δ; 9.16 (s, 1H), 8.24 (s, 1H), 8.08 (d, *J* = 30.0 Hz, 2H), 7.70 – 7.63 (m, 3H), 7.49 - 7.40 (m, 3H), 7.20 (d, *J* = 3.0 Hz, 2H), 7.00 (s, 1H), 5.50 (s, 1H), 5.08 (s, 1H). ¹³C NMR (125 MHz, DMSO): δ; 168.17, 163.00, 156.70, 154.13, 153.43, 151.38, 137.44, 136.02, 134.41, 132.87, 132.09, 129.57, 125.53, 125.01, 122.86, 121.34, 120.61, 118.71, 117.14, 116.25, 112.91, 99.11, 47.60.

2.1.2.4. N-(benzo[d]thiazol-2-yl)-2-(5-benzoyl-2-(2-oxo-2*H*-chromen-3-yl)-1*H*-benzo[d]imidazol-1-yl)acetamide (8d).

Brown solid, m.p. 298-302°C.; Anal. Calc. for C₃₂H₂₀N₄O₄S (%): C, 69.05; H, 3.62; N, 10.07; O, 11.50; S, 5.76%. Found: C, 68.37; H, 3.58; N, 9.88%; ¹H NMR (500 MHz, DMSO): δ; 9.12 (s, 1H), 8.19 (d, 2H), 8.10 (s, 1H), 8.05 - 7.87 (d, 1H), 7.87 - 7.80 (m, 2H), 7.63 (dd, *J* = 8.9 Hz, 2H), 7.50 (d, 2H), 7.41 (dd, *J* = 10.3 Hz, 2H), 7.37 - 7.30 (m, 3H), 7.19 (d, *J* = 5.7 Hz, 2H), 4.97 (s, 2H). ¹³C NMR (125 MHz, DMSO): δ; 195.76, 168.17,

163.00, 156.97, 154.13, 153.43, 151.38, 146.35, 141.63, 137.96, 134.41, 132.87, 132.09, 131.92, 130.25, 129.57, 128.72, 128.05, 127.53, 125.47, 125.01, 122.86, 121.64, 121.34, 120.60, 118.71, 117.14, 112.91, 108.62, 47.60.

2.1.2.5. N-(benzo[d]thiazol-2-yl)-2-(7-methyl-2-(2-oxo-2H-chromen-3-yl)-1H-benzo[d]imidazol-1-yl)acetamide (8e).

Brown solid, m.p. 289-293°C.; Anal. Calc. for C₂₆H₁₈N₄O₃S (%): C, 66.94; H, 3.89; N, 12.01; O, 10.29; S, 6.87 Found: C, 66.86; H, 3.64; N, 11.68%; ¹H NMR (500 MHz, DMSO): δ; 9.21 (s, 1H), 8.18 (s, 1H), 7.97 (d, *J* = 14.3 Hz, 2H), 7.62 (s, 1H), 7.47 (s, 1H), 7.45 - 7.37 (m, 3H), 7.20 - 7.12 (m, 3H), 7.04 (s, 1H), 5.29 (s, 1H), 4.87 (s, 1H), 2.31 - 2.27 (m, 3H); ¹³C NMR (125 MHz, DMSO): δ; 168.17, 163.00, 156.25, 154.13, 153.43, 151.38, 138.91, 136.05, 134.41, 132.87, 132.09, 129.57, 128.95, 125.01, 124.49, 122.95, 122.84, 122.66, 121.34, 120.60, 118.71, 117.14, 116.14, 112.91, 48.58, 18.02.

2.1.2.6. N-(6-ethoxybenzo[d]thiazol-2-yl)-2-(6-methyl-2-(2-oxo-2H-chromen-3-yl)-1H-benzo[d]imidazol-1-yl)acetamide (8f).

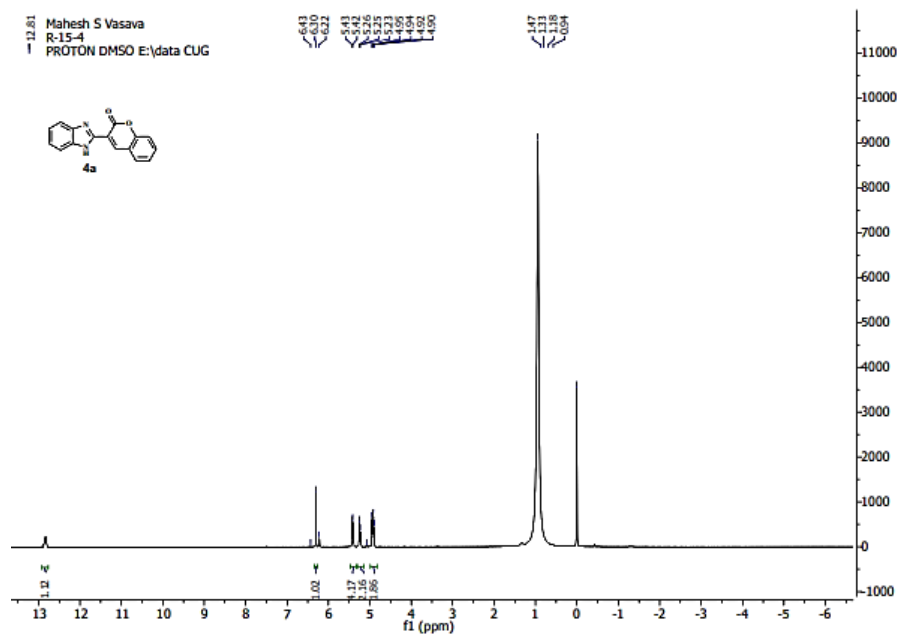
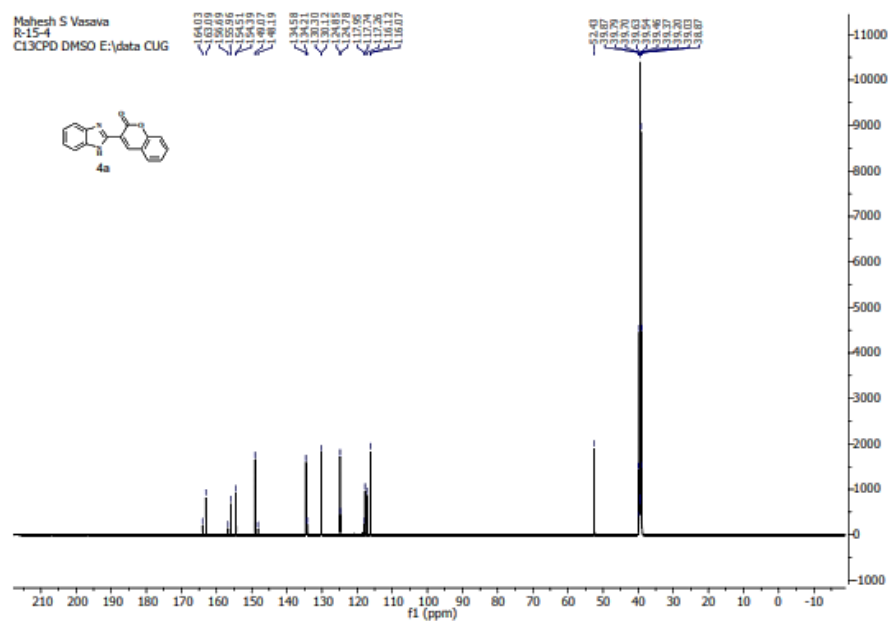
Light brown solid, m.p. 285-290°C.; Anal. Calc. for C₂₈H₂₂N₄O₄S (%): C, 65.87; H, 4.34; N, 10.97; O, 12.53; S, 6.28 Found: C, 65.28; H, 4.21; N, 10.47%; ¹H NMR (500 MHz, DMSO): δ; 9.67 (s, 1H), 8.11 (d, *J* = 35.8 Hz, 2H), 7.76 (s, 1H), 7.71 (s, 1H), 7.56 (d, *J* = 17.4 Hz, 2H), 7.39 (s, 1H), 7.26 - 7.11 (m, 3H), 7.09 (s, 1H), 4.96 (s, 2H), 4.09 - 3.97 (m, 2H), 2.36 (s, 3H), 1.41 - 1.37 (m, 3H). ¹³C NMR (125 MHz, DMSO): δ; 168.17, 163.00, 156.70, 154.13, 153.43, 153.18, 149.61, 138.77, 137.22, 135.27, 134.31, 132.87, 132.09, 129.57, 125.01, 124.58, 120.64, 119.82, 117.14, 113.95, 112.91, 110.30, 110.10, 63.99, 47.60, 21.21, 13.83.

2.1.3 General procedure for the synthesis of 2-(6-methyl-2-(3,4,5-trimethoxyphenyl)-1*H*-benzo[d]imidazol-1-yl)-N-(6-(trifluoromethoxy)benzo[d]thiazol-2-yl)acetamide (9a):

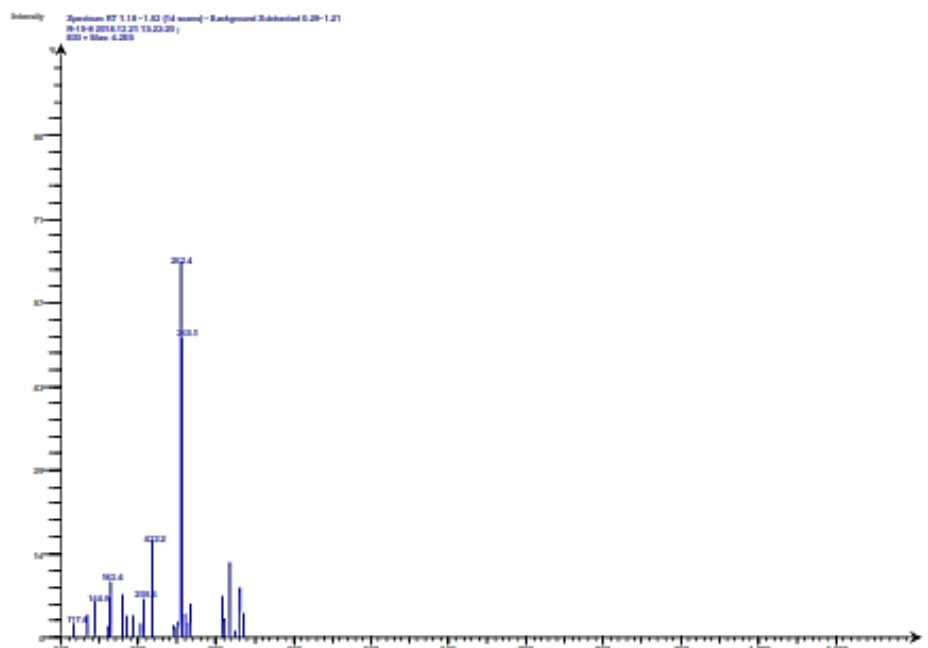
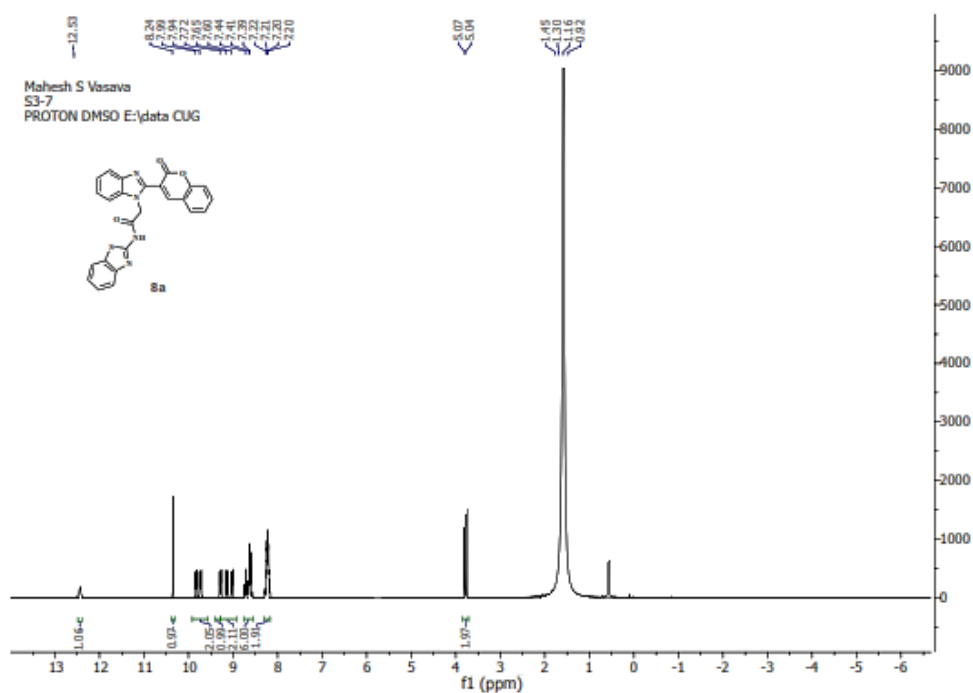
The compound **9a** was synthesized as mentioned in the synthetic procedure for **8a-f**. However, in this reaction, synthesized compound **5b** was used instead of **4a-i** with **7a-d** (3.35mmol, 1eq.), potassium tert-butoxide (2 eq.) and Pd(OAc)₂ (10% mol) in DMF solvent. The crud product was extracted and purified as mentioned in the above method to obtain the desired product 2-(6-methyl-2-(3,4,5-trimethoxyphenyl)-1*H*-benzo[d]imidazol-1-yl)-N-(6-(trifluoro methoxy) benzo[d] thiazol-2-yl)acetamide (**9a**).

2.1.3.1. 2-(6-methyl-2-(3,4,5-trimethoxyphenyl)-1*H*-benzo[d]imidazol-1-yl)-N-(6-(trifluoromethoxy)benzo[d]thiazol-2-yl)acetamide (9a).

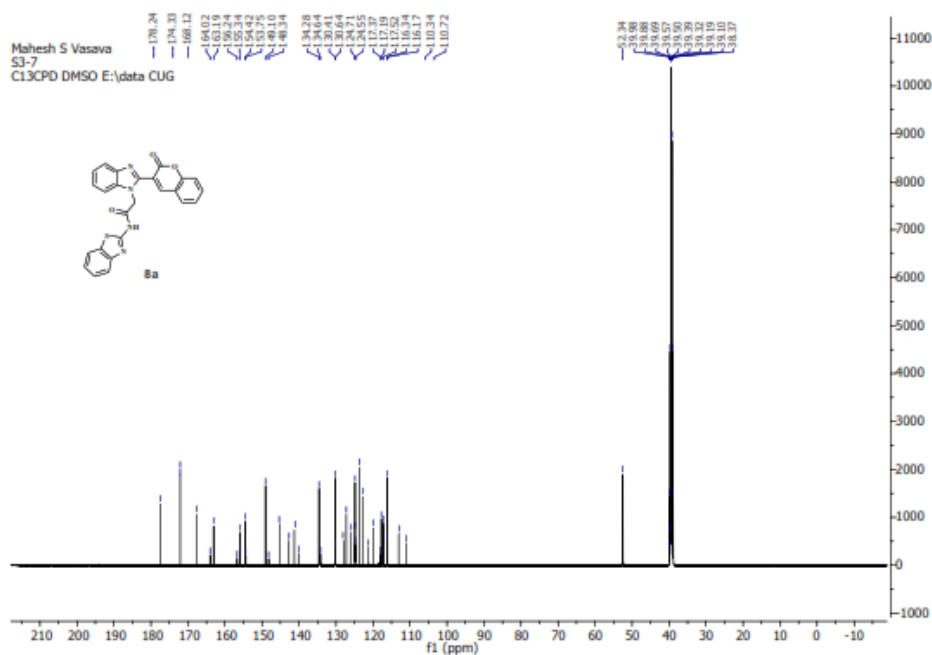
Dark yellowish solid, m.p. 295-300°C.; Anal. Calc. for C₂₇H₂₃F₃N₄O₅S (%): C, 56.64; H, 4.05; F, 9.95; N, 9.79; O, 13.97; S, 5.60%; Found: C, 55.86; H, 3.98; N, 9.56%; ¹H NMR (500 MHz, DMSO): δ; 9.04 (s, 1H), 7.99 (s, 1H), 7.90 (s, 1H), 7.76 (s, 1H), 7.58 (s, 1H), 7.11 (d, *J* = 3.4 Hz, 2H), 7.02 - 6.98 (d, 2H), 5.09 (d, *J* = 17.4 Hz, 2H), 3.86 (s, 9H), 2.36 (s, 3H); ¹³C NMR (125 MHz, DMSO): δ; 168.17, 153.43, 150.57, 150.03, 149.82, 147.86, 141.64, 138.77, 137.22, 135.27, 129.76, 127.33, 124.58, 120.69, 118.42, 116.76, 114.4, 106.33, 110.60, 110.30, 60.65, 56.89, 56.58, 46.91, 21.21.

2.1.4 ^1H NMR spectra of compound 4a.2.1.5 ^{13}C NMR spectra of compound 4a.

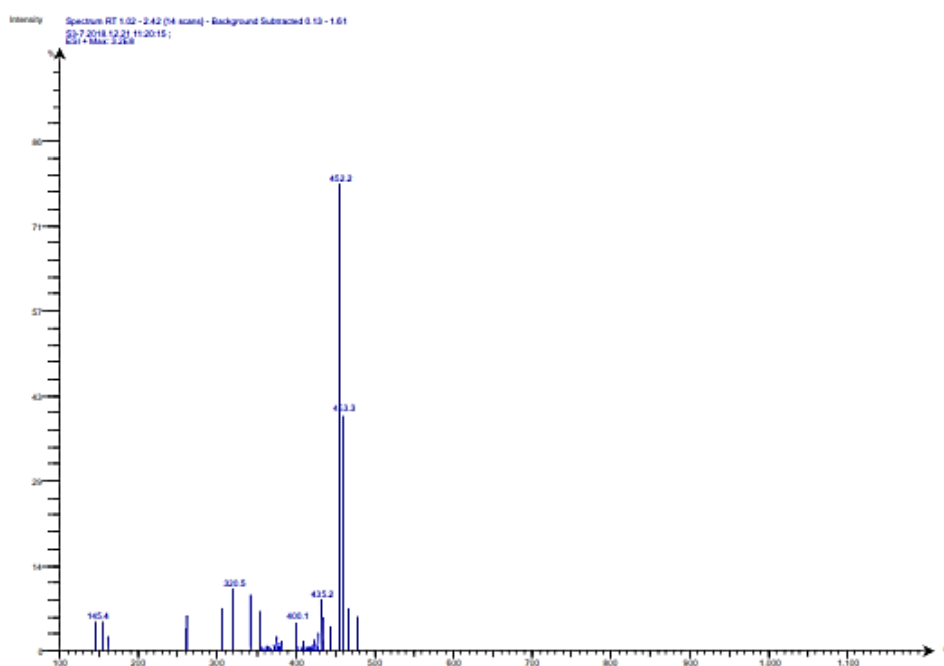
2.1.6 Mass spectra of compound 4a.

2.1.7 ^1H NMR spectra of compound 8a.

2.1.8 ^{13}C NMR spectra of compound 8a.



2.1.9 Mass spectra of compound 8a.



2.2 Biological assay

2.2.1 In vitro anti-bacterial activity

The *In vitro* anti-bacterial activity of synthesized compounds were performed against four different bacterial strains (*E. coli* MTCC 443, *P. aeruginosa* MTCC 1688, *S.*

aureus MTCC 96, *S. pyogenus* MTCC 442) and compared with standard drugs Ampicillin, Chloramphenicol and Ciprofloxacin. This activity was performed in accordance with method in Patel et al. and Mungra et al. The highest dilution showing at least 99% inhibition has taken as MIC value [42].

2.2.2 *In vitro* anti-tuberculosis activity and MDR-TB study

The anti-tuberculosis screening of the synthesized compounds was carried out using method described by Patel et al. and Mungra et al. [42]. The MIC of test compound was taken as < 20 colonies or no development of colonies occurred at the concentration. The *M. tuberculosis* H₃₇Rv strain was tested with standard drug isoniazid for the comparison intense. The multi-drug resistance tuberculosis activity of the synthesized compounds against *M. tuberculosis* H₃₇Rv. (MDR-TB strain was collected from National Institute for Research in Tuberculosis, Chennai, Tamil Nadu, and India). (The strain was identified by phenotype and genotype).

2.2.3 *In vitro* anti-malarial and anti-fungal activity

The *in vitro* anti-malarial activity of all the synthesized compounds was carried out in 96 well micro titre plates according to the micro assay protocol of Rieckmann et. al. (1978) with minor modification. The culture of plasmodium falciparum strain were maintained in medium RPMI 1640 supplemented with 25mM HEPES, 1% D-glucose, 0.23% NaHCO₃ and 10% heat inactivated human serum. The asynchronous parasite of plasmodium falciparum were synchronized after 5% D-sorbitol treatment to obtain only the ring stage parasitized cells. For carrying out the assay, Primary stage of parasitemia of 0.9 to 1.4% at 4% haematocrit in total volume of 200 µL of medium RPMI-1640 was determined by Jaswant Singh Bhattacharya (JSB) staining to assess the percentage parasitemia rings and uniformly maintained with 50% RBCs (O +ve). The culture plates were incubated 37° C in a candle jar. After 36 to 40 hours incubation, thin bloods near from each well were prepared and stand with JSB strain. The slides were microscopically

observed to record maturation of the ring stage parasites into trophozoites and schizonts in the presence of different concentrations of the test agents. The test concentration which inhibited the complete maturation into schizonts was recorded as the IC₅₀. Chloroquine and quinine were used as a reference drugs.

Furthermore, the antifungal activity of all the synthesized compounds were performed on three fungal strains (*A. clavatus* MTCC 1323, *C. albicans* MTCC 227 and *A. niger* MTCC 282) using the agar dilution method. Ampicillin, Ciprofloxacin, and Chloramphenicol were used as standard control drugs for antibacterial activity, whereas Nystatin and Greseofulvin were used as standard drugs for antifungal activity.

2.3 Computational Study

2.3.1 ADMET property prediction

A set of ADMET-related properties of the synthesized compounds were predicted by using Qikprop programs (Schrödinger, LLC, New York, NY, 2015) [43-44]. *LigPrep* module were used to prepare the compounds and were utilized for the calculation of pharmacokinetic parameters by *QikProp* module. The program *QikProp* generates physically relevant descriptors, and uses them to perform ADMET predictions and utilizes the method of Jorgensen [45] to calculate pharmacokinetic properties and descriptors.

2.3.2 Molecular Docking

The potential binding mode and the binding interaction of the ligand with Enoyl-ACP reductase (oxidoreductase) have been investigated by using Maestro 10.7 Schrödinger, LLC, New York, NY, 2012. The 3D structures of all the compounds were obtained using Marvin suites and saved as SDF file. The 3D crystal structures of Enoyl-ACP reductase (oxidoreductase) from *Mycobacterium tuberculosis* (PDB ID: 1QG6, 2NSD, 4TZK, 4TZZ) were retrieved from the protein data bank (www.rcsb.org). The protein was chosen based on structure similarity of ligands, resolution and expression system. Moreover, the protein organism is *Mycobacterium Tuberculosis* (H37Rv Strain)

which is encourage us to do the docking in the active site of this protein. The ligand with the lowest energy, correct Lewis structure, tautomers and ionization states ($\text{pH } 7.0 \pm 2.0$) for each of the ligands were generated and optimized with default settings were prepared for molecular docking using *Ligprep* module of Schrödinger. The OPLS_2005 [43] force field were used for computing partial atomic charges. The proteins were prepared for docking using Protein Preparation Wizard module in Maestro. Bond order and formal charges were assigned and hydrogen atoms were added to the crystal structure. Further to refine the structure OPLS-2005 force field parameter was used to alleviate steric clashes. The receptor grid, which was generated using Glide 5.8 (Maestro, Schrödinger, LLC, New York, NY, 2012) with default settings for all parameters. An approximately large grid size was preferred to include all active site residues involved in substrate binding. The Glide extra-standard precision (XP) mode was used for docking of the generated receptor grid file along with all prepared ligand conformers. Default settings were retained for the scoring and refinement.

2.3.4 Molecular Dynamics

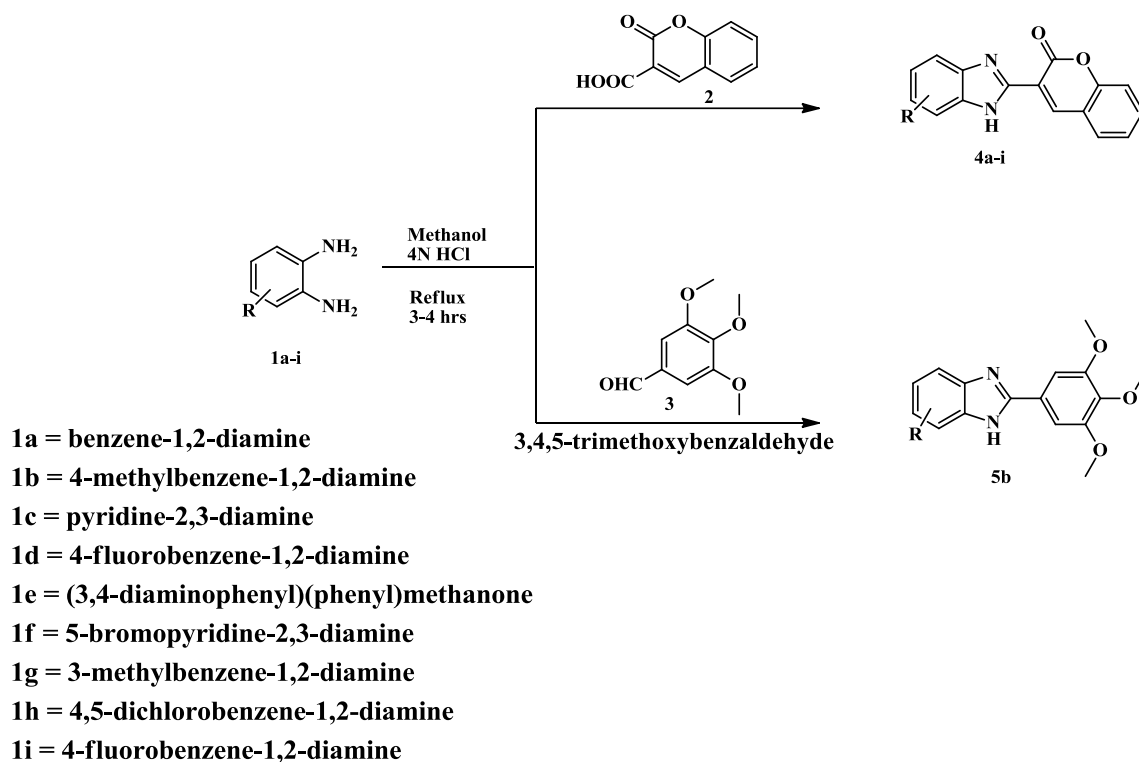
The natural dynamics on different timescales of docked complex of compound **9b** and protein, thermal average of the molecular properties of complex is carried with the help of molecular dynamics (MD) stimulation. MD simulations have been conducted with Desmond [43-44] program, as implemented Schrödinger Materials Science Suite 2015-4 [46]. OPLS_2005 [43] force field with NPT ensemble class have been used, while pressure and temperature were set to 1.0325 bar and 300 K, respectively. The system was modelled by placing one NATPB (5-[(4-nitrophenyl)acetamido]-2-(4-tert-butylphenyl)benzoxazole) molecule into the cubic box with around 3000 water molecules and the simulation time was set to 10 ns cut off radius was set to 12 Å, pressure to 1.0325 bar, while temperature was set to 300 K. In all cases when Desmond was used, input and output files were manipulated

by Maestro graphical user interface application of Schrödinger Materials Science Suite
2015-4.

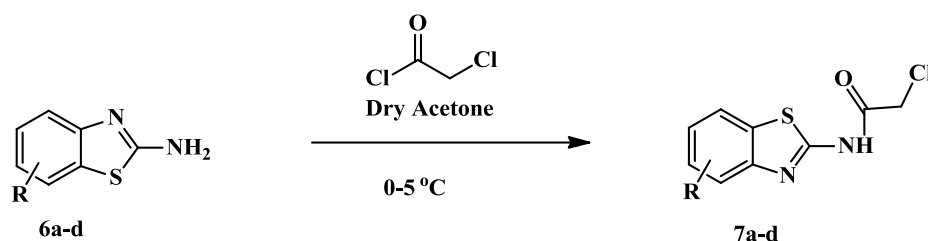
3.0 Result and Discussion

3.1 Chemistry

The targeted benzimidazole-incorporated coumarin, benzothiazole analogues were prepared from commercially available chemicals and the synthetic routes were outlined in **Scheme 1, 2 and 3**. 3-(1*H*-benzo[d]imidazol-2-yl)-2*H*-chromen-2-one (**4a-i**) (**5b**) which is required as starting material for the synthesis of targeted compound **8a-f** and **9b** were synthesis by condensation reaction between substituted benzene-1,2-diamine (**1a-i**) and 2-oxo-2*H*-chromene-3-carboxylic acid (**2**) or 3,4,5-trimethoxybenzaldehyde (**3**) using 4*N* HCl and Methanol as solvent (**Scheme 1**). On the other hand, substituted 2-amino benzothiazole (**6a-d**) with chloro acetyl chloride in the presence of anhyd. potassium carbonate in dry acetone gave N-(benzo[d]thiazol-2-yl)-2-chloroacetamide (**7a-d**) (**Scheme 2**) which was used as second starting material for the synthesis of compound **8a-f** and **9b**. The reaction between 3-(1*H*-benzo[d]imidazol-2-yl)-2*H*-chromen-2-one (**4a-i**) (**5b**) and N-(benzo[d]thiazol-2-yl)-2-chloroacetamide (**7a-d**) in the presence of potassium tert-butoxide and Pd(OAc)₂ catalyst in DMF solvent with 8-10 hrs stirring, resulted in the formation of N-(benzo[d]thiazol-2-yl)-2-(2-(2-oxo-2*H*-chromen-3-yl)-1*H*-benzo[d]imidazol-1-yl)acetamide (**8a-f**) (**9b**) (**Scheme 3**). Here, we have attempted to synthesize targeted compounds by using simple basic condition but the reaction was unsuccessful to produce the desired product as a result the special condition was required. The purity of the compounds was monitored by TLC plate and the synthesized compounds were characterized by spectral data analysis. The structure of synthesized derivatives along with melting point and the isolated percentage yield are presented in **Table 1**.

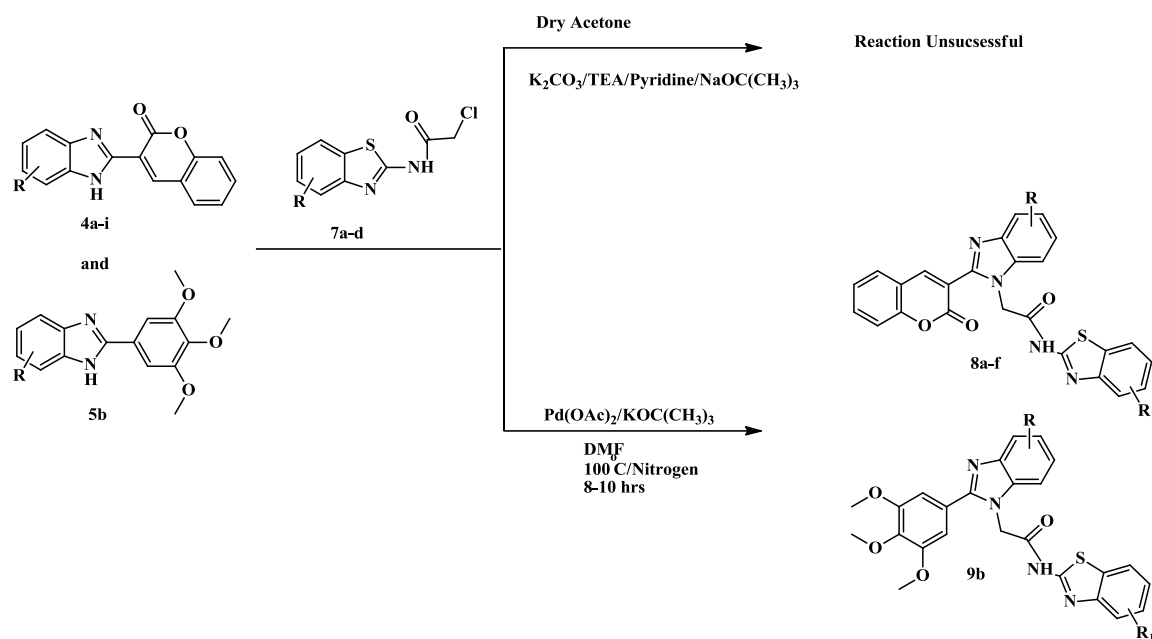


Scheme 1. Synthetic pathways for the synthesis of targeted compounds **4a-I** and **5b**.



- 6a = benzo[d]thiazol-2-amine
6b = 6-ethoxybenzo[d]thiazol-2-amine
6c = 6-methoxybenzo[d]thiazol-2-amine
6d = 6-(trifluoromethoxy)benzo[d]thiazol-2-amine

Scheme 2. Synthetic pathways for the synthesis of targeted compounds **7a-d**.

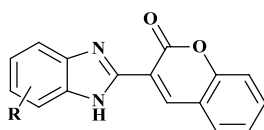
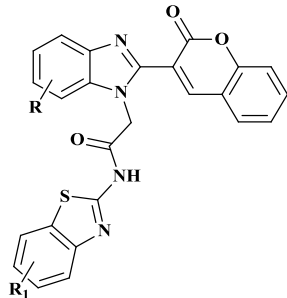


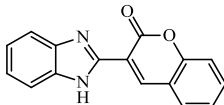
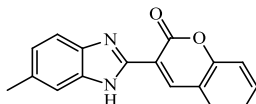
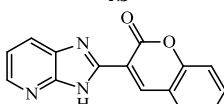
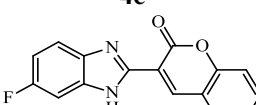
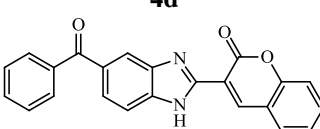
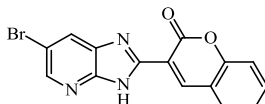
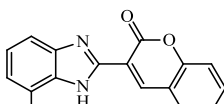
Scheme 3. Synthetic pathways for the synthesis of targeted compounds **8a-f** and **9b**.

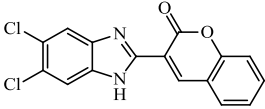
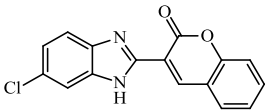
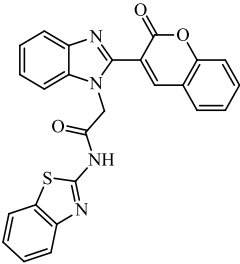
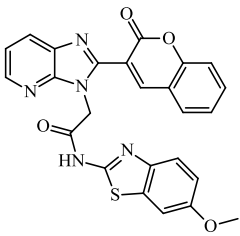
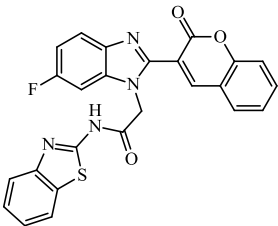
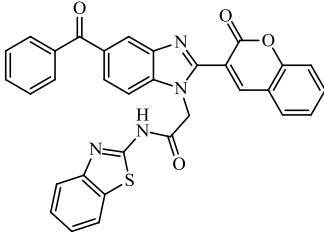
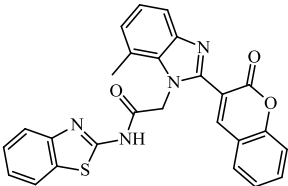
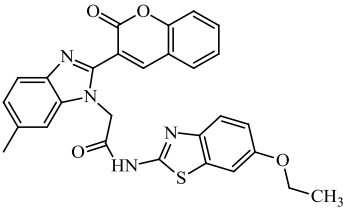
In the 1H NMR spectra, compound **4a** gave singlets at 4.86 ppm assigned to the -NH proton linked to the coumarin moiety which confirm the formation benzimidazole molecule. The signals between 7.67 to 7.17 confirm the two benzene ring of the compound **4a**. The ^{13}C NMR chemical shift of the neighbor carbons of -NH in compound **4a** were observed at 139.18 and 132.87 ppm. Signals at 165.98 ppm was observed due to the presence of carbonyl carbon presence in the coumarin moiety. Both the benzene ring appeared at 123.62, 123.33, 120.60, 118.49, 117.14, 115.12 ppm. Further, the 1H NMR spectrum of targeted compound **8a** also confirm the formation of the structure. Signal at 9.02 ppm confirmed the presence of -NH proton from amide linkage between benzothiazole and benzimidazole. The signal of N-CH₂ proton was observed in downfield shift, which were slight higher due to the strong electron-withdrawing ability of nitrogen atom in benzimidazole ring. In the ^{13}C NMR, The carbonyl carbons of amide linkage and coumarin moiety were appeared 165.00 and 160.70 ppm, respectively. Signal at 172.17 ppm appeared due to the presence of carbon near to sulfur and nitrogen in benzothiazole moiety.

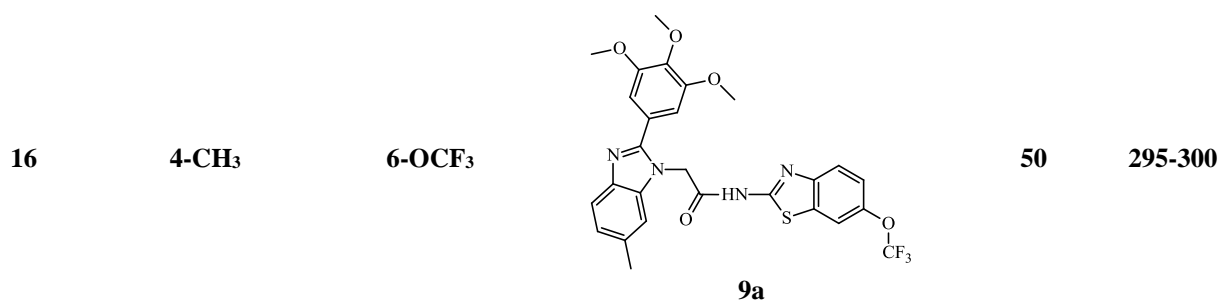
Moreover, all the other three ring aromatic protons and carbons observed at the appropriate chemical shifts and integral values.

Table 1. The substituent information for the synthesized compounds 4a-I, 8a-f and 9b along with the details of isolated yield and melting point.

					
4a-i			8a-f, 9b		

Entry	R	R ₁	Product	Yield ^a %	MP °C
1	H	-	 4a	62	242-246
2	4-CH ₃	-	 4b	58	248-252
3	Pyridine	-	 4c	56	240-245
4	4-F	-	 4d	69	251-254
5	Phenyl methanone	-	 4e	47	258-262
6	5-Br pyridine	-	 4f	53	254-258
7	3-CH ₃	-	 4g	70	247-251

8	4,5- Cl	-	 <p>4h</p>	57	256-261
9	4-Cl	-	 <p>4i</p>	66	253-258
10	H	H	 <p>8a</p>	63	286-290
11	Pyridine	6-OCH ₃	 <p>8b</p>	47	291-294
12	4-F	H	 <p>8c</p>	65	283-288
13	Phenyl methanone	H	 <p>8d</p>	56	298-302
14	3-CH ₃	H	 <p>8e</p>	44	289-293
15	4-CH ₃	6-OCH ₂ CH ₃	 <p>8f</p>	51	285-290



^a Isolated yield

3.2 Biological assay

3.2.1 *In vitro* anti-bacterial activity

The newly synthesized analogues **4a-I**, **8a-f** and **9b** were evaluated for their *in vitro* anti-bacterial activity against gram +ve bacteria ((*Staphylococcus aureus*, *Bacillus pumillus*) and Gram -ve bacteria (*Pseudomonas aeruginosa*, *Escherichia coli*) and the results are recorded by measuring the zone of inhibition at minimum inhibitory concentration (MIC). The anti-bacterial activity results are summarized in Table 2. Compound **4a** (62.5, 100, 50, 100 µg/mL), **4f** (125, 50, 25, 12.5 µg/mL), **4g** (50, 100, 62.5, 125 µg/mL), **8b** (62.5, 250, 100, 62.5 µg/mL), **8c** (62.5, 25, 50, 12.5 µg/mL) and **9b** (50, 25, 125, 12.5 µg/mL) shows good bacterial inhibition against *E. coli*, *P. aeruginosa*, *S. aureus* and *S. pyogenes* compared with the standard drugs. Moreover, analogue **8a** shows potent activity at MIC value 25 µg/mL particularly against *E. coli* as compared to standard drug. In addition, Compound **8f** displayed significant MIC value 12.5 µg/mL against *E. coli* which was far better than standard drug. Compound **4b** also showed good anti-bacterial activity at MIC value 62.5 µg/mL against *E. coli* as compared to standard drug Ampicillin. The result revealed that, above discussed compound have the ability to inhibit the bacterial growth and may be further develop as good anti-bacterial agents.

Table 2. *In vitro* anti-bacterial, anti-tuberculosis and MDR-TB screening result of synthesized compounds.

Entry	Compound code	Anti-Bacterial				Anti-Tuberculosis	MDR-TB ^c MIC µg/mL
		Gram-negative ^a		Gram-positive ^b		H ₃₇ RV ^c MIC µg/mL	
		E.C. MIC µg/mL	P.A. MIC µg/mL	S.A. MIC µg/mL	S.P. MIC µg/mL		
1	4a	62.5	100	50	100	25	62.5
2	4b	62.5	100	125	250	50	125
3	4c	250	100	125	125	12.5	25
4	4d	125	100	500	250	125	250
5	4e	100	125	250	125	500	1000
6	4f	125	50	25	12.5	125	250
7	4g	50	100	62.5	125	500	1000
8	4h	125	250	125	50	100	125
9	4i	100	250	100	100	250	500
10	8a	25	100	250	125	250	500
11	8b	62.5	250	100	62.5	50	100
12	8c	62.5	25	50	12.5	62.5	100
13	8d	125	250	100	125	100	125
14	8e	100	125	500	250	500	>1000
15	8f	12.5	100	100	250	125	250
16	9b	50	25	125	12.5	25	125
17	Ampicillin	100		250	100	-	-
18	Chloramphenicol	50	50	50	50	-	-
19	Ciprofloxacin	25	25	50	50	-	-
20	Isoniazid	-	-	-	-	0.20	-

^a Ec: *Escherichia coli* (MTCC-443); Pa: *Pseudomonas aeruginosa* (MTCC-1688).^b Sa: *Staphylococcus aureus* (MTCC-96), Sp: *Streptococcus pyogenes* (MTCC-442).^c Minimum inhibitory concentration against H₃₇Rv strain of M. Tuberculosis and Multi Drug-Resistance Tuberculosis (µg/mL).

3.2.2 *In vitro* anti-tuberculosis activity and MDR-TB study

The observed result of the synthesized compounds from primary anti-bacterial screening encourage us to go for the *in vitro* anti-tuberculosis and MDR-TB evaluation for the synthesized compounds. The anti-tuberculosis activity was performed on H₃₇Rv strain and the MDR-TB activity was performed on clinically isolated Isoniazid resistant strain.

Table 2 displayed the significant effects of compounds against tuberculosis strain and the

MIC values are given in $\mu\text{g/mL}$. From the data table, it was observed that compounds **4c** exhibited excellent anti-tuberculosis activity with MIC value $12.5 \mu\text{g/mL}$. Moreover, compounds **9b** and **4a** showed potent activity with MIC value $25 \mu\text{g/mL}$ against tuberculosis strain. Compound **4b** and **8b** exerted better anti-tuberculosis activity at MIC value $50 \mu\text{g/mL}$. Additionally, compound **8c** found to have good anti-tuberculosis activity at MIC value $62.5 \mu\text{g/mL}$. Rest of the compounds have demonstrated moderate to poor anti-tuberculosis activity. Furthermore, the in vitro MDR-TB activity of the synthesized compounds are summarized in **Table 2**. Among all the tested compounds, most interesting activity was found for compound **4c** ($25 \mu\text{g/mL}$) against the resisted strain. Compound **4a** showed promising activity at MIC value $62.5 \mu\text{g/mL}$. Anti-bacterial, anti-tuberculosis and MDR-TB activities indicates that some of the derivatives possessed a broad spectrum of activity against tested strain and these molecules may be developed as good anti-tubercular agents in future.

3.2.3 In vitro anti-malarial and anti-fungal activity

The newly synthesized compounds **4a-I**, **8a-f** and **9b** were subjected for their *in vitro* anti-malarial activity against *Plasmodium falciparum* by measuring the IC_{50} value ($\mu\text{g/mL}$) as summarized in **Table 3**, respectively. Among all the tested compounds, compounds **4c**, **4f**, **4i**, **8f** and **9b** showed good anti-malarial activity comparable to the standard drugs Chloroquine and Quinine. Compound **9b** and **4c** being the most active analogues with IC_{50} 0.21 and $0.23 \mu\text{g/mL}$ and compound **4g** the least active with IC_{50} $2.20 \mu\text{g/mL}$. Moreover, compounds **4f**, **4i** and **8f** were found to have significant activity with IC_{50} value 0.42, 0.36 and $0.46 \mu\text{g/mL}$, respectively. The remaining compounds showed moderate to good activity against the pathogen.

Table 3. *In vitro* anti-Malarial, anti-Fungal screening result of synthesized compounds.

Entry	Compound	Anti-Malarial		Anti-Fungal	
		P. Falciparum	C. Albicans	A. Niger	A. Clavatus
		µg/mL (mean IC50)	MTCC 227 µg/mL	MTCC 282 µg/mL	MTCC 1323 µg/mL
1	4a	0.75	500	>1000	>1000
2	4b	1.40	500	250	250
3	4c	0.23	1000	1000	>1000
4	4d	0.90	500	>1000	>1000
5	4e	0.70	500	500	1000
6	4f	0.42	500	500	500
7	4g	2.20	>1000	500	500
8	4h	1.50	>1000	500	250
9	4i	0.36	250	500	1000
10	8a	2.06	1000	1000	1000
11	8b	1.65	250	500	500
12	8c	0.85	250	1000	>1000
13	8d	2.02	500	250	500
14	8f	0.46	1000	250	500
15	8e	1.50	500	250	500
16	9b	0.21	1000	500	1000
17	Quinine	0.268	500	1000	1000
18	Chloroquine	0.02	-	-	-
19	Nystatin	-	100	100	100
20	Greseofulvin	-	100	100	100

^a; *Plasmodium falciparum*, ^b; *Candida albicans* ^c; *Aspergillus niger*, ^d; *Aspergillus clavatus*

Additionally, to determine the anti-fungal activity, the synthesized compounds were subject to evaluate the anti-fungal activity against *Candida albicans*, *Aspergillus niger* and *Aspergillus clavatus* and the results are shown in **Table 3**. Compound **4i**, **8b** and **8c** showed acceptable anti-fungal activity at MIC value 250 µg/mL against *Candida albicans*. Further, analogues **4b**, **8d**, **8f** and **8e** shows moderate activity against *A. niger* and *A. clavatus*. Remaining compounds demonstrated moderate to poor anti-fungal activity against the pathogen.

3.3 Computational Study

3.3.1 ADME property prediction

Compound which combines potency with an admirable absorption, distribution, metabolism, excretion and toxicity (ADMET) properties is define as a promising lead molecule. The *in silico* pharmacokinetic (ADME) properties of synthesized compounds were determined by using QikProp tool in Maestro, Schrodinger software. Here, total seven different parameters were predicted to investigate the drug-like properties of compounds such as Percent human oral absorption (>80% - high & <25% - poor), QPlog BB (-3.0 - 1.5), QPlog HERG (below -5), QPPCaco (<25 poor, >500 great), QPlog Kh_{sa} (-1.5 - 1.5), PSA (70 - 200 Å) and QPlog S (-6.5 - 5).

Table 4. Predicted ADME parameters for synthesized compounds.

Entry	Compound Code	Percent human oral absorption (>80% - high & <25% - poor)	QPlog BB (-3.0 - 1.5)	QPlog HERG (below -5)	QPPCaco (<25 poor, >500 great)	QPlog Kh _{sa} (-1.5 - 1.5)	PSA (70 - 200 Å)	QPlog S (-6.5 - 5)
1	4a	100	-0.236	-5.736	1428.06	0.216	62.460	-4.181
2	4b	100	-0.265	-5.725	1429.063	0.394	62.462	-4.600
3	4c	91.96	-0.489	-5.549	766.334	-0.087	75.552	-3.402
4	4d	100	-0.130	-5.629	1428.357	0.263	62.455	-4.426
5	4e	100	-0.895	-7.104	568.242	0.452	88.938	-5.525
6	4f	95.388	-0.333	-5.535	766.527	0.067	75.549	-4.291
7	4g	100	-0.182	-5.667	1693.27	0.384	61.354	-4.497
8	4h	100	0.047	-5.62	1429.342	0.461	62.463	-5.101
9	4i	100	-0.082	-5.693	1428.721	0.345	62.456	-4.832
10	8a	100	-0.624	-7.513	1025.347	0.442	101.784	-6.202
11	8b	100	-1.014	-7.539	607.287	0.219	124.744	-6.204
12	8c	100	-0.520	-7.387	1023.914	0.483	101.814	-6.561
13	8d	77.384	-1.332	-8.667	426.784	0.689	126.537	-7.681
14	8e	100	-0.752	-7.360	777.463	0.575	98.906	-6.678
15	8f	84.098	-0.923	-7.816	968.27	0.744	104.861	-7.859

3.0 RESULT AND DISCUSSION

16	9b	100	-0.319	-6.830	2012.811	1.093	93.499	-8.882
17	AMP	17.342	-1.300	-0.709	1.298	-0.929	139.523	-1.512
18	CHL	66.552	-1.398	-2.693	71.218	-0.808	120.365	-1.984
19	CIP	48.492	-0.671	-3.248	12.952	0.023	98.960	-3.793
20	ETH	57.536	-0.326	-5.581	58.030	-0.754	69.477	0.551
21	INH	66.83	-0.844	-3.588	275.34	-0.752	81.524	-0.051
22	PYR	67.422	-0.720	-3.224	294.381	-0.818	78.425	-0.541

AMP; Ampicilline, CHL;Chloromphenicol, CIP; Ciprofloxacin, ETH;Ethambutol, INH; Isoniazid, PYR; Pyrizinamide

The predicted result provides range for comparing the properties of molecules with 95% known drug molecules. The predicted ADME properties the synthesized compounds are summarized in **Table 4**. It was observed from the result that all the compounds have achieved acceptable range of ADME profile. Compound **8d** have an oral human absorption at 77.384 which is between the ranges of known drugs. However, all the other molecules have high percentage of human oral absorption. Further, the blood/brain barrier partition coefficient of the molecules were found between 0.047 to -1.332 which not exceed the acceptable value. It indicate that these molecules have very low susceptibility to cross the BB barrier, in this manner molecules are decreased the chance of CNS related toxicity. The caco-2 cell permeability predicted value (above 500) also supports the oral absorption of molecules. The parameter HERG is define as log IC₅₀ of K⁺ channel blockage and the predicted values were found below -5 which indicate that the blockage of K⁺ channel ion is less. The primary need of oral absorption of any molecule is water solubility and this ability was predicted by two parameter as PSA and log S which can be define as polar surface area and water solubility, respectively. The predicted values of PSA and log S were found between the ranges of 95% drug molecules which support the good water solubility of the molecules.

3.3.2 Molecular Docking Study

The *in silico* molecular docking study is useful and widely used method to investigate the binding modes of small molecules into the active site of protein receptor. Due to the important role of Enoyl-ACP reductase enzyme in the cell wall synthesis of *Mycobacterium Tuberculosis*, we aimed to choose as target for docking study with four different 3d crystal structure of protein (PDB ID; 1QG6, 2B37, 4TZK, 4TZZ) and was retrieved from RSCB protein databank. In our research, molecular docking study was performed between all the synthesized compounds and selected target receptor to understand the binding modes and binding affinity. The predicted docking energies of synthesized compounds against four different proteins are summarized in **Table 5**.

Table 5. Docking energies of synthesized compounds against targeted receptor

PDB; 1QG6			PDB; 2NSD			PDB; 4TZK			PDB; 4TZZ		
Code	DS*	GE*	Code	DS*	GE*	Code	DS*	GE*	Code	DS*	GE*
9b	-8.443	-71.823	8b	-11.258	-55.524	8c	-9.035	-42.930	8f	-8.751	-47.933
8d	-8.452	-60.509	4h	-10.109	-46.767	4a	-8.480	-44.414	AMP	-8.625	-50.352
8a	-7.095	-50.652	4c	-10.333	-49.131	CHL	-8.420	-48.709	4b	-8.759	-45.687
4c	-7.061	-61.751	4d	-9.853	-41.52	4c	-8.418	-55.680	CHL	-8.295	-54.071
8b	-6.541	-59.768	4i	-9.889	-44.323	AMP	-8.554	-51.692	4c	-8.599	-42.085
8c	-6.310	-62.061	4a	-9.476	-46.703	4b	-8.776	-43.053	4a	-8.174	-42.682
8f	-6.242	-68.993	4b	-9.706	-33.991	8f	-8.385	-45.550	4d	-8.659	-43.515
AMP	-6.221	-55.874	4g	-9.692	-44.817	4g	-7.996	-53.229	4h	-8.040	-44.373
INH	-5.806	-26.349	4f	-9.704	-43.214	4d	-8.230	-40.946	4g	-8.437	-42.36
4h	-5.778	-43.456	CHL	-8.998	-52.839	4i	-8.200	-38.954	8d	-8.101	-44.885
4e	-6.206	-55.417	9b	-7.849	-64.592	4f	-8.100	-43.785	8c	-7.647	-50.568
CHL	-5.633	-45.517	CIP	-8.689	-50.409	8d	-7.801	-64.531	4f	-7.874	-44.724
CIP	-5.711	-38.169	8e	-7.295	-49.83	4h	-7.744	-44.889	8a	-7.183	-47.494
4i	-5.853	-43.885	AMP	-7.018	-45.525	8a	-7.594	-52.993	4e	-7.456	-42.79

3.0 RESULT AND DISCUSSION

4b	-5.599	-40.810	IINH	-6.354	-32.868	4e	-7.130	-44.197	CIP	-7.924	-41.721
4g	-5.569	-45.675	8c	-5.498	-53.998	CIP	-7.652	-38.762	INH	-5.577	-27.301
4a	-5.058	-43.954	4e	-5.450	-55.115	8e	-7.779	-50.137	8b	-5.524	-56.881
8e	-5.185	-46.711	PYR	-4.472	-29.88	INH	-4.091	-33.264	8e	-4.643	-48.682
4d	-5.061	-41.449	8a	-4.351	-47.896	PYR	-3.775	-30.172	9b	-5.077	-50.452
ETH	-4.947	-29.049	8f	-4.185	-56.666	ETH	-4.477	-32.853	4i	-4.053	-55.012
4f	-4.900	-46.693	ETH	-3.535	-33.152	8b	-1.990	-59.588	PYR	-3.978	-23.934
PYR	-4.398	-26.404	8d	-4.675	-26.885	9b	-2.783	-53.460	ETH	-1.711	-28.126

DS; Docking score, DE; Glide energy, Amp; Ampicilline, INH; Isoniazid, Chl; Chloromphenicol, Cip; Ciprofloxacin, Pyr; Pyrizinamid, Eth; Ethambutol

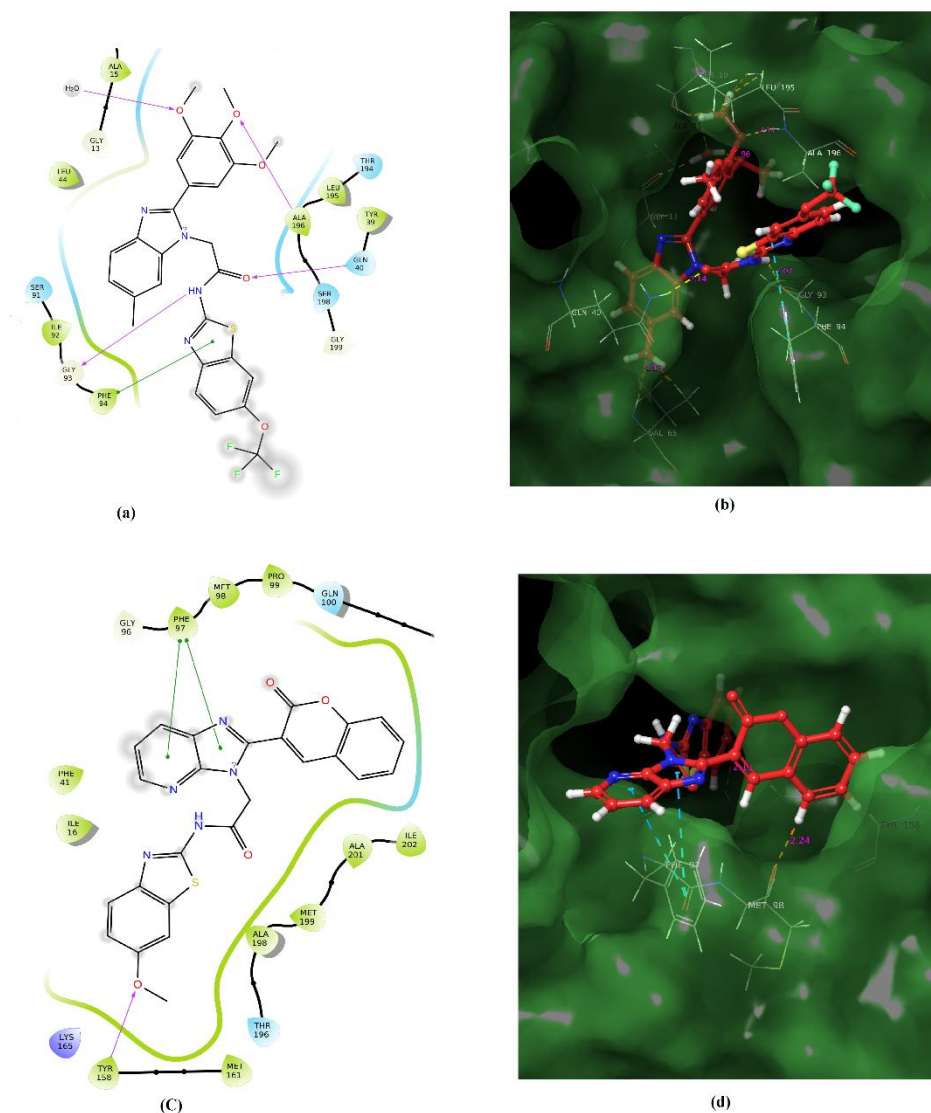


Figure 2. (a) 2d and (b) 3d docked representation of compound **9b** at the active site of protein 1QG6. (c) 2d and (d) 3d representation of compound **8a** at the active site of protein 2NSD.

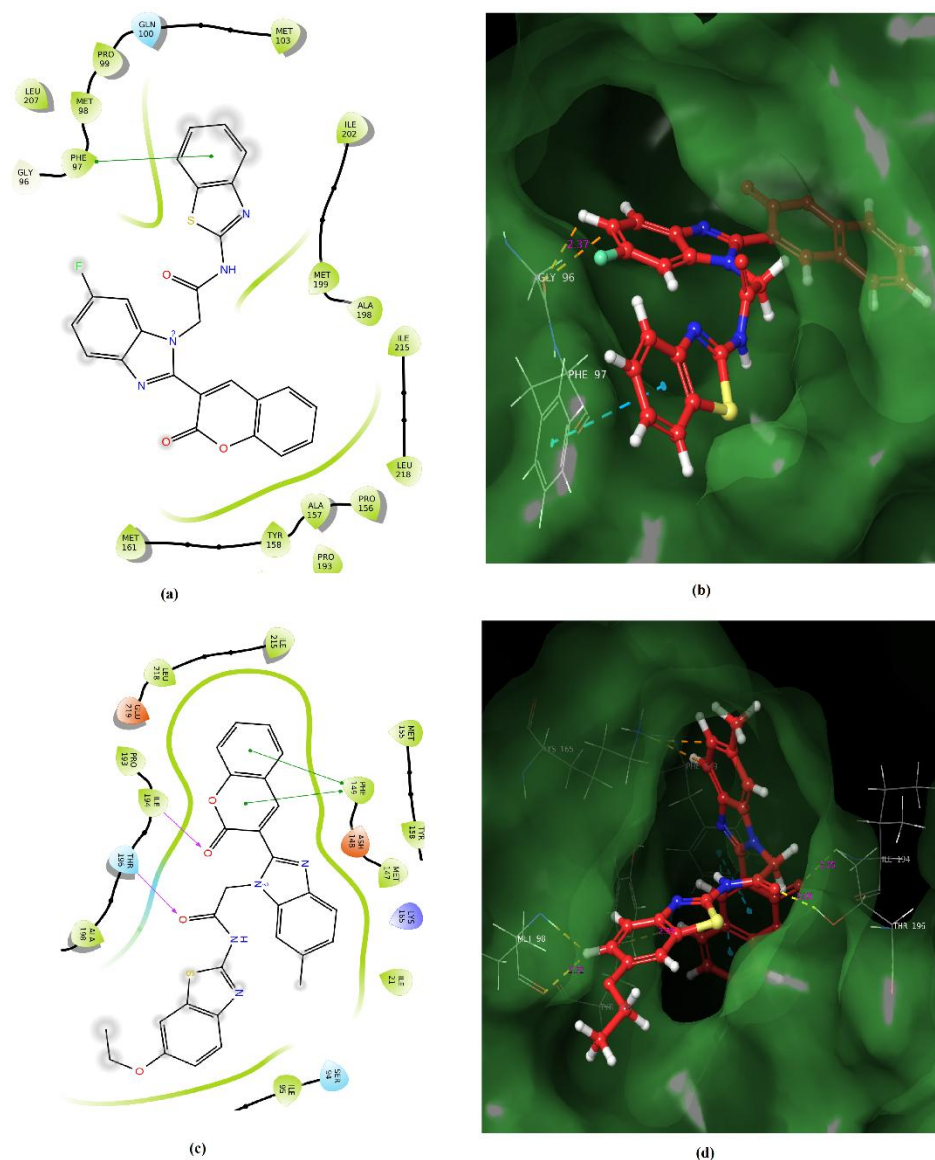


Figure 3. (a) 2d and (b) 3d representation of compound **8c** at the active site of protein 4TZK. (c) 2d and (d) 3d representation of compound **8f** at the active site of protein 4TZZ.

The binding interaction between lowest glide scoring compounds and proteins are illustrated in **Figure 2 and 3**. As shown in **Figure 2(a) (b)**, Analogue **9b** was found to generate four hydrogen bond with amino acid residue Ala196, Gln40, Gly93 and water molecule against receptor 1QG6 at docking score -8.443. Two aromatic ring contact of compound **8b** was generated with amino acid residue Phe97 against protein 2NSD at lowest docking score -11.258 (**Figure 2 (c) (d)**). Further, compound **8c** have displayed lowest docking score (-9.035) against receptor 4TZK which indicates the highest binding affinity

of compounds towards target receptor. However, compound **8c** have found to generate only one ring contact with amino acid residue Phe97 (**Figure 3 (a) (b)**). **Figure 3 (c) (d)** demonstrate the four binding interaction of compound **8f** with target receptor 4TZT at docking score -8.751. The hydrogen binding interaction of compound **8f** was found with amino acid residue Ile194 and Thr196. The two ring contact of coumarin moiety from compound **8f** was generated with amino acid residue Phe194. In addition, rest of the compounds have also showed potent binding affinity with lowest docking score towards selected target receptor (Enoyl-ACP reductase from *Mycobacterium Tuberculosis*) with different protein crystal structure. Most of the compounds displays significant potency to inhibit the Enoyl-ACP reductase and can be further developed as good anti-tuberculosis agents.

3.3.3 Molecular dynamics Study

The molecular dynamics simulation of energy minimised docked complex of compound **9b** with Enoyl-ACP reductase protein encoded with 1QG6 was carried out within the active site of the receptor. After the docking studies, Molecular dynamic simulation was performed in a polar solution environment. The RMSD (root mean square deviation) of the backbone atoms was used to evaluate the overall stability of the system under simulation. The RMSD values of the backbone system computed against the structure of ligand **9b** is shown in **Figure 4 (c)**. The figure suggests that the RMSD of the protein backbone is stable over the progress of the MD simulation and remain constant after 2 ns, with an average fluctuation of two RMSD. **Figure 4 (a) and (b)** demonstrate the binding interaction between amino acid residue and ligand **9b**. Figures revealed that amino acid residue Gly93 and Ala15 shows maximum hydrogen bonding with ligand **9b** with stability of 93% and 60 %, respectively. Moreover, amino acid residue Phe94 shows aromatic ring interaction more than 80% with ligand **9b**. The Root Mean Square Fluctuation (RMSF) is

useful for characterizing local changes along the protein chain and characterizing changes in the ligand atom positions. On the plot in **Figure 4 (d)**, peaks indicate areas of the protein that fluctuate the most during the simulation. Typically it was observe that the tails (N- and C-terminal) fluctuate more than any other part of the protein. Secondary structure elements like *alpha* helices and *beta* strands are usually more rigid than the unstructured part of the protein, and thus fluctuate less than the loop regions. In the **Figure 4 (f)**, the 'Fit Ligand on Protein' line shows the ligand fluctuations, with respect to the protein. The protein-ligand complex is first aligned on the protein backbone and then the ligand RMSF is measured on the ligand heavy atoms. A timeline representation of the interactions and contacts (H-bonds, Hydrophobic, Ionic, Water bridges) summarized in **Figure 4 (e)**. The top panel shows the total number of specific contacts the protein creates with the ligand over the course of the MD simulation. The bottom panel shows which residues interact with the ligand in each trajectory frame. Some residues make more than one specific contact with the ligand, which is represented by a darker shade of orange, according to the scale to the right of the plot.

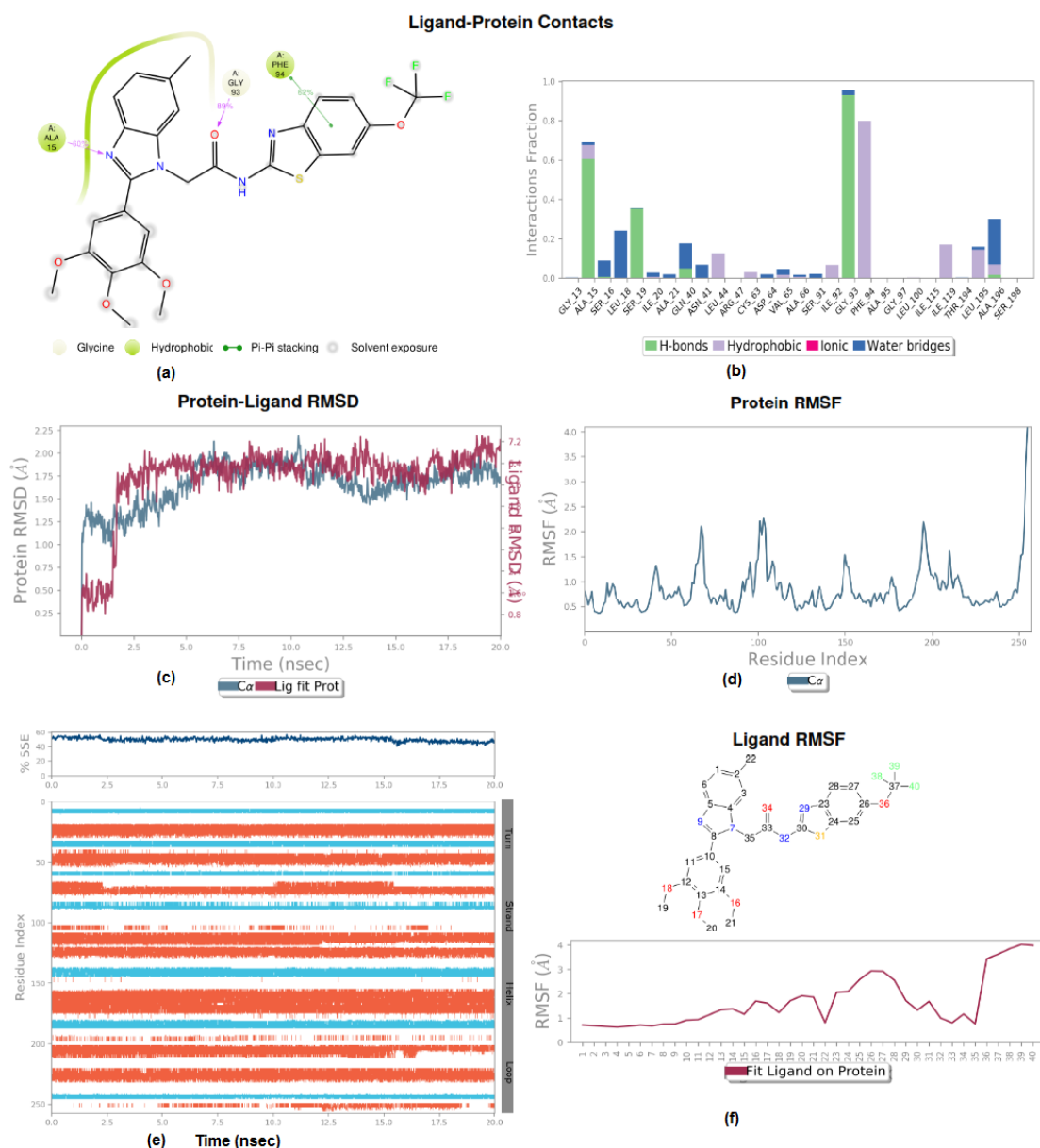


Figure 4. Analysis of the molecular dynamics simulations of ligand 9b and protein 1QG6. (a) 2d representation of protein-ligand interaction; (b) Detailed informative plot of interaction between ligand-receptor; (c) The root mean square deviation (RMSD) of protein-ligand backbone; (d) The protein RMSF for side chain atom; (e) A timeline representation of the interactions and contacts between ligand-protein during simulation; (f) The Ligand Root Mean Square Fluctuation (L-RMSF).

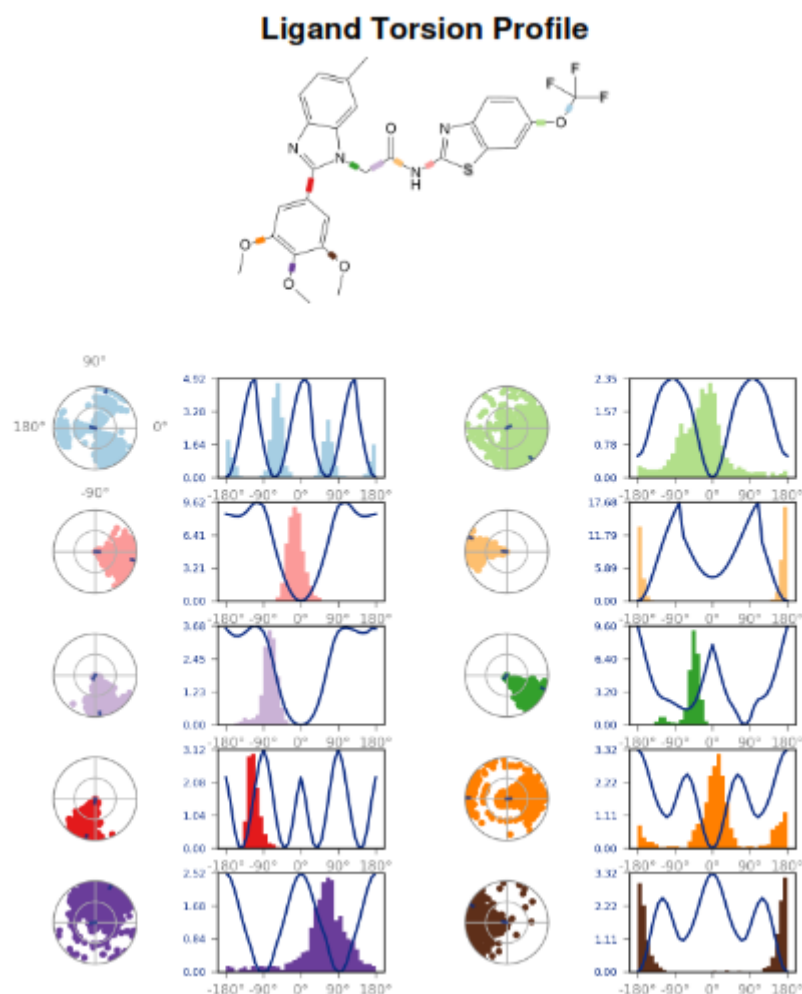


Figure 5. The ligand torsions plot summarizes the conformational evolution of every rotatable bond (RB) in the ligand during the MD simulation trajectory

In the **Figure 5**, the ligand torsions plot summarizes the conformational evolution of every rotatable bond (RB) in the ligand during the MD simulation (0.00 through 20.00 nsec). The top panel in figure shows the 2d schematic of a ligand with color-coded rotatable bonds. Each rotatable bond torsion is accompanied by a dial plot and bar plots of the same color. Radial plots describe the conformation of the torsion throughout the course of the simulation. The beginning of the simulation is in the centre of the radial plot and the time evolution is plotted radially outwards. The bar plots summarize the data on the dial plots, by showing the probability density of the torsion. If torsional potential information is available, the plot also shows the potential of the rotatable bond by summing the potential

of the related torsions. The values of the potential are on the left Y-axis of the chart, and are expressed in kcal/mol. Looking into the histogram and torsion relationship may give insight the conformational strain the ligand undergoes to maintain a protein-bound confirmation. In consequence, molecular dynamic simulation was efficiently utilized to understand the role of the active site that overcomes under normal biological environments in the better interpretation of the biological activity.

4.0 Conclusion

In the present study, we designed and synthesized benzimidazole-coumarin-benzothiazole based derivatives as possible anti-tubercular analogues and characterized by spectroscopy technique. We observed promising anti-bacterial activity in the case of compounds **4a**, **4f**, **4g**, **8a**, **8b**, **8c**, **8f** and **9b** against gram-negative bacteria. Compounds **4a**, **4f**, **4g**, **8b**, **8c** and **9b** exhibit significant anti-bacterial efficacy against gram-positive bacteria. Due to the strong ability of the compounds as bacterial growth inhibitor, we further subjected these compounds to determine their anti-tubercular and MDR-TB activity. From the anti-tuberculosis activity, Compound **4c**, **4a** and **9b** showed potent activity with MIC value **12.5**, **25** and **25** $\mu\text{g/mL}$, respectively. Additionally, compound **4b** and **8b** also displayed good anti-tubercular activity with MIC value **50** $\mu\text{g/mL}$. In the case of MDR-TB activity, compound **4c** which have only hybridization of benzimidazole-coumarin moiety have surprised us with the significant MDR-TB activity with MIC value **25** $\mu\text{g/mL}$. Compound **4a** demonstrate acceptable MDR-TB activity with MIC value **62.5** $\mu\text{g/mL}$. However, the in vitro findings have some limitation and could not reveal that the binding interaction of ligand within the target. Due to this reason, we have subjected the synthesized compounds for *in silico* molecular docking analysis to improve the reliability and accuracy of the biological targets for better understanding of the drug-receptor binding interaction and binding efficiency. The molecular docking study was carried out with four different proteins of mycobacterial Enoyl-ACP reductase (InhA) enzyme to find out the potency of compounds as InhA inhibitors. Docking result revealed that, Compounds **9b**, **8d**, **8a** and **4c** shows good binding interaction with lower glide docking score against protein 1QG6. Compounds **8b**, **4h**, **4c** and **4d** found to have good binding interaction with lower docking score against protein 2NSD. Furthermore, Compounds **8c** and **4a** against 4TZK and compounds **8f** and **4b** against 4TZZ demonstrated better binding affinity as

compared to standard drug candidates. Furthermore, Molecular dynamic study revealed that the docked complex of ligand **9b** and protein 1QG6 have stable binding interaction between ligand and amino acid residue of the receptor. In addition, the ADME pharmacokinetics properties of the synthesized compounds were determined by QikProp module and their values were found to be within appreciable range of 95% drug molecules. Our findings could represent a novel lead analogues for further development as lead candidates. It is realized that this study provides improved anti-tubercular agents as enoyl reductase inhibitors and may further develop as good anti-tubercular agents in future. Further this novel findings has thrown light on how a simple benzimidazole-coumarin hybridization can lead to a potential moiety to develop a novel drug candidates.

References

1. Kishore N, Mishra BB, Tripathi V, Tiwari VK. *Fitoterapia*. 2009; 80(3):149-63.
2. P. Smith, A. Moss, in: B. Bloom (Ed.), *Epidemiology of Tuberculosis*. ASM Press. Washington, DC; 1994: 47.
3. Alderwick LJ, Harrison J, Lloyd GS, Birch HL. *Cold Spring Harbor perspectives in medicine*. 2015; 5(8):a021113.
4. Marrakchi H, Laneelle MA, Daffé M. *Chemistry & biology*. 2014; 21(1):67-85.
5. Zhang Y, Heym B, Allen B, Young D, Cole S. *Nature*. 1992; 358(6387):591.
6. Shingalapur RV, Hosamani KM, Keri RS. *European journal of medicinal chemistry*. 2009; 44(10):4244-8.
7. B.C. Bishop, E.T.J. Chelton, A.S. Jones, *Biochem. Pharmacol.* 13 (1964) 751e754.
8. Habib NS, Soliman R, Ashour FA, El-Taiebi M. *Die Pharmazie*. 1997; 52(11):844-7.
9. Tunçbilek M, Göker H, Ertan R, Eryigit R, Kendi E, Altanlar N. *Archiv der Pharmazie*. 1997; 330(12):372-6.
10. Göker H, Kuş C, Boykin DW, Yildiz S, Altanlar N. *Bioorganic & medicinal chemistry*. 2002; 10(8):2589-96.
11. Ansari KF, Lal C. *European journal of medicinal chemistry*. 2009; 44(10):4028-33.
12. Deng X, Mani NS. *European Journal of Organic Chemistry*. 2010; 2010(4):680-6.
13. Mohamed BG, Hussein MA, Abdel-Alim AA, Hashem M. *Archives of pharmacal research*. 2006; 29(1):26-33.
14. Verma N, Singh RB, Srivastava S, Dubey P. *Journal of chemical and pharmaceutical research*. 2016; 8:365-74.
15. Rathee PS, Dhankar R, Bhardwaj S, Gupta M, Kumar R. *Journal of Applied Pharmaceutical Science*. 2011; 1(10):14.

16. Nakano H, Inoue T, Kawasaki N, Miyataka H, Matsumoto H, Taguchi T, Inagaki N, Nagai H, Satoh T. Chemical and pharmaceutical bulletin. 1999; 47(11):1573-8.
17. Fonseca T, Gigante B, Marques MM, Gilchrist TL, De Clercq E. Bioorganic & medicinal chemistry. 2004; 12(1):103-12.
18. Serafin B, Borkowska G, Głowczyk J, Kowalska I, Rump S. Polish journal of pharmacology and pharmacy. 1989; 41(1):89-96.
19. Bethke T, Brunkhorst D, der Leyen HV, Meyer W, Nigbur R, Scholz H. Naunyn-Schmiedeberg's archives of pharmacology. 1988; 337(5):576-82.
20. Khan FR, Asnani AJ. International Journal of Research in pharmaceutical and biomedical sciences. 2011; 2(2):695-700.
21. Al-Douh MH, Sahib HB, Osman H, Hamid SA, Salhimi SM. Asian Pacific Journal of Cancer Prevention. 2012; 13(8):4075-9.
22. Aydin S, Beis R, Can ÖD. Die Pharmazie-An International Journal of Pharmaceutical Sciences. 2003; 58(6):405-8.
23. Kazimierczuk Z, Upcroft JA, Upcroft P, Górska A, Starosciak B, Laudy A. Acta Biochimica Polonica-English Edition. 2002; 49(1):185-96.
24. Zarguil A, Saadouni M, Boukhris S, Habbadi N, Hassikou A, Souizi A. Mediterranean Journal of Chemistry. 2011; 1(1):30-7.
25. Tushar M, Kaneria DM, Kapse GK, Gaikwad TV, Sarvaiya JA. International Journal of Pharmaceutical Research Scholars. 2013: 90-8.
26. Thakurdesai PA, Wadodkar SG, Chopade CT. Pharmacologyonline. 2007; 1:314-29.
27. Shadia AG. Shweekar and Naemel EI. Arch. Pharma Chem Life science. 2011; 11:255-63.

28. Egan D, O'kenney R, Moran E, Cox D, Prosser E, Thornes RD. Drug metabolism reviews. 1990; 22(5):503-29.
29. Nawrot-Modranka J, Nawrot E, Graczyk J. European journal of medicinal chemistry. 2006; 41(11):1301-9.
30. Karalı N, Kocabalkanlı A, Gürsoy A, Ateş Ö. Il Farmaco. 2002; 57(7):589-93.
31. Cacic M, Trkovnik M, Cacic F, Has-Schon E. Molecules. 2006; 11(2):134-47.
32. Fylaktakidou KC, Hadjipavlou-Litina DJ, Litinas KE, Nicolaides DN. Current pharmaceutical design. 2004; 10(30):3813-33.
33. Roskopf F, Kraus J, Franz G. Die Pharmazie. 1992; 47(2):139-42.
34. Hwu JR, Singha R, Hong SC, Chang YH, Das AR, Vliegen I, De Clercq E, Neyts J. Antiviral Research. 2008; 77(2):157-62.
35. Patel RV, Kumari P, Rajani DP, Chikhaliya KH. Medicinal Chemistry Research. 2013; 22(1):195-210.
36. Neyts J, Clercq ED, Singha R, Chang YH, Das AR, Chakraborty SK, Hong SC, Tsay SC, Hsu MH, Hwu JR. Journal of medicinal chemistry. 2009; 52(5):1486-90.
37. Bhusari KP, Khedekar PB, Umathe SN, Bahekar RH, Rao AR. Indian Journal of Heterocyclic Chemistry. 2000; 9(3):213-6.
38. Hegde VS, Kolavi GD, Lamani RS, Khazi IA. Journal of Sulfur Chemistry. 2006; 27(6):553-69.
39. Rana A, Siddiqui N, Khan S. Indian Journal of Pharmaceutical Sciences. 2007; 69(1).
40. Sharma PC, Sinhmar A, Sharma A, Rajak H, Pathak DP. Journal of enzyme inhibition and medicinal chemistry. 2013; 28(2):240-66.
41. Gund DR, Tripathi AP, Vaidya SD. European Journal of Chemistry. 2017; 8(2):149-54.

42. Patel RV, Patel PK, Kumari P, Rajani DP, Chikhaliya KH. European journal of medicinal chemistry. 2012; 53:41-51.
43. Banks JL, Beard HS, Cao Y, Cho AE, Damm W, Farid R, Felts AK, Halgren TA, Mainz DT, Maple JR, Murphy R. Journal of computational chemistry. 2005; 26(16):1752-80.
44. Shivakumar D, Williams J, Wu Y, Damm W, Shelley J, Sherman W. Journal of chemical theory and computation. 2010; 6(5):1509-19.
45. QikProp, Technical Information (2.1).
46. Schrödinger Release 2015-4: Desmond Molecular Dynamics System, version 4.4, D. E. Shaw Research, New York, NY 2015.

Chapter: 4

Synthesis, Characterization, biological application and in silico study of novel N'-(2-(1H-benzo[d]imidazol-1-yl)acetyl)nicotinohydrazide derivatives

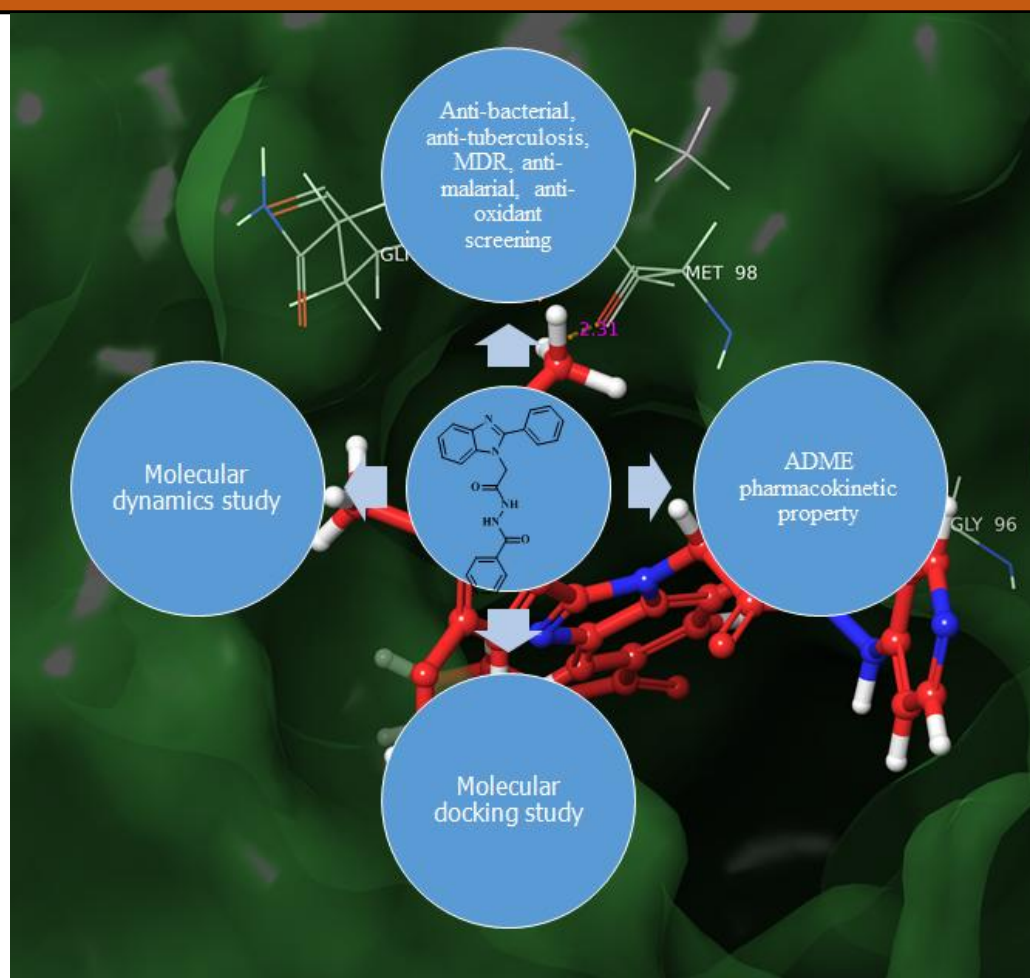


Table of Contents

1.0 Introduction	227
2.0 Methods and Materials	232
2.1 Chemistry	232
2.1.1 Synthesis of 2-phenyl-1 <i>H</i> -benzo[d]imidazole (D1-D16)	232
2.1.2 Synthesis of 1 <i>H</i> -benzo[d]imidazole (DD1-DD4).....	232
2.1.3 General synthetic procedure of ethyl 2-(1 <i>H</i> -benzo[d]imidazol-1-yl)acetate (E1-E16 & EE1-EE4)	233
2.1.4 Synthetic procedure of N'-(2-(1 <i>H</i> -benzo[d]imidazol-1-yl)acetyl)isonicotinohydrazide (GG1-GG2):.....	233
2.2 Biological assay.....	243
2.2.1 <i>In vitro</i> anti-bacterial activity	243
2.2.2 <i>In vitro</i> anti-tuberculosis activity and MDR-TB study.....	243
2.2.3 <i>In vitro</i> anti-malarial and anti-fungal activity.....	243
2.2.4. Anti-Oxidant activity protocol.....	244
2.3 Computational Study.....	245
2.3.1 ADMET property prediction	245
2.3.2 Molecular Docking	246
2.3.4 Molecular Dynamics.....	246
3.0 Result and Discussion	247
3.1 Chemistry	247

3.2 Biological assay.....	253
3.2.1 <i>In vitro</i> anti-bacterial activity	253
3.2.2 <i>In vitro</i> anti-tuberculosis activity and MDR-TB study.....	254
3.2.3 <i>In vitro</i> anti-malarial activity	256
3.2.4. Anti-Oxidant activity	258
3.3 Computational Study.....	261
3.3.1 ADMET property prediction	261
3.3.2 Molecular Docking Study.....	263
3.3.3 Molecular dynamics Study	267
4.0 Conclusion	271
References.....	273

Summary:

The main aim of this present study was to synthesized new substituted benzimidazole derivatives hybridized with nicotinic hydrazide to investigate the pharmacological activity of these newly compounds such as anti-bacterial, anti-tubercular, MDR-TB, anti-malarial and anti-oxidant activity for possible drug design in future. The synthesis of compounds **G1-16**, **GG1-4** was achieved by condensation of ethyl 2-(1*H*-benzo[d]imidazol-1-yl)acetate (**E1-E16** & **EE1-EE4**) with nicotinic hydrazide. The structure of newly synthesized compounds was determined via elemental analytical data, ¹H and ¹³C NMR spectroscopy, mass spectroscopy method. The outcome of the findings from *in vitro* biological activity revealed that compounds **G5**, **G6**, **G7**, **G8**, **G14**, **GG2** and **GG4** are the most active derivatives with lowest MIC values. Furthermore, the *in silico* computational study of the synthesized compounds was carried out to investigate the ADME properties, protein-ligand binding interaction and the stability of the docked complex. The ADME properties of the compounds suggest that most of the compounds have drug-like properties. The molecular docking study was performed against Enoyl-acp reductase enzyme with four different PDB. (1QG6, 2NSD, 4TZK, 4TZZ). Compound **G6** against 1QG6, **GG4** against 2NSD and **G7** against 4TZK and 4TZZ have shown strong binding affinity with lowest binding energy. The stability of the docked complex of ligand (**G7**) - receptor (4TZK) was investigated with help of molecular dynamics simulation. All the *in vitro* screening and *in silico* study prediction suggest that nicotinic hydrazide along with benzimidazole derivatives can be a potent inhibitor of Enoyl-acp reductase with ability to modulate the target in comparatively smaller dose. Hence, these synthesized derivatives is likely to become a good lead molecules for the development of effective anti-tubercular agents in future.

1.0 Introduction

Tuberculosis (TB) is a deadliest bacterial infection, caused by a bacteria named *Mycobacterium tuberculosis* which is commonly spread through the air. The *Mycobacterium tuberculosis* was first identified by Robert Koch in 1882, which can mainly attack the lungs, however it can also affect the other body parts [1]. According to the global TB report published by WHO in 2018, TB is one of the top 10 causes of death and the leading cause from a single infectious agent (above HIV/AIDS), globally. Millions of people continue to fall sick with TB every year. TB caused an approximate 1.3 million deaths among HIV-negative people and there were an additional 300000 deaths from TB among HIV-positive people in 2017. Worldwide, the best estimate is that 5.8 million men, 3.2 million women and 1.0 million children get sick with TB, more than 10.0 million people developed TB disease in 2017 [2].

The increased emergence of multi-drug resistant, extensively drug resistance strains of *Mycobacterium tuberculosis* and the emergence of new TB cases, the increased incidence of TB associated with viral infections and the adverse effects of first- and second-line anti-TB medicine have led to renewed research interest for the new anti-TB analogues [3]. In recent times, totally drug resistance tuberculosis (TDR) a more dangerous and completely incurable form of tuberculosis has also been reported in Iran, Italy and more recently in India [3-7]. TDR-TB strain has been demonstrated to be resistant to all the first line, second line and third line anti-TB agents. Hence, there is an urgent need to develop novel anti-TB agents with novel mode of action, which are synthetically possible, have less side effects and shorter duration of the treatment of TB. Although, numerous new analogues are currently in different stages of clinical trials [8-13], only two new drug Bedaquiline (**1**) and Delamanid (**2**) has been recently approved by FDA for the treatment against drug resistant

tuberculosis [3]. From 2016, the End TB Strategy was implemented to end the global threat of TB. The strategy assists as a blueprint for countries to decrease the number of TB deaths by 90% by 2030 [12]. Therefore, the re-emergence of this deadliest disease prompt the synchronized need to develop novel anti-tuberculosis and anti-microbial drug candidate in order to fight against different drug resistance.

In the search of new medicinally important analogues, Isoniazid derivatives have been found to have significant anti-tuberculosis activities [14-19]. Isoniazid (INH) (**3**) isonicotinic hydrazide, a pro-drug is one of the milestone, first-line clinically approved drugs for the treatment of TB. Isoniazid gets activated by a catalase-peroxidase enzyme commonly known as KatG in mycobacteria. The activated form of isoniazid reacts non-enzymatically against coenzymes, NAD and NADP⁺⁺ to form isonicotinoyl-NAD(P) complex [20-23], which interact with the enoyl-acyl carrier protein (ACP) reductase known as InhA. The enzyme, InhA supports in the synthesis of mycolic acid for the development of cell wall of mycobacteria. Therefore, Isoniazid inhibits the mycobacterial Enoyl-acyl carrier protein reductase. InhA is the clinically validated target in the mycolic acid synthetic pathway in *Mycobacterium Tuberculosis*. Last few years have witnessed the synthesis of a number of lipophilic derivatives of Isoniazid and few of them have shown significant *in-vitro* anti-mycobacterial activity [24-28]. Furthermore, LL-3858 (**4**) which is developed by Lupin Limited, is an Isoniazid derivative. It has shown potent anti-bacterial activity against both drug sensitive and multidrug resistant TB [39]. The effectiveness LL-3858 was studied in Phase I clinical trial and have shown the potential of treating pulmonary tuberculosis patients [30]. The mechanism of action of LL-3858 is still unknown. At present, this analogue is in the initial stage of phase II clinical trial for the Tuberculosis treatment [31]. In addition, a number of anti-tubercular drug candidates such as Ftivazid (**5**), Verazide (**6**), Salinazide (**7**) and Opiniazide (**8**) are isonicotinic acid hydrazides derivatives [32-34].

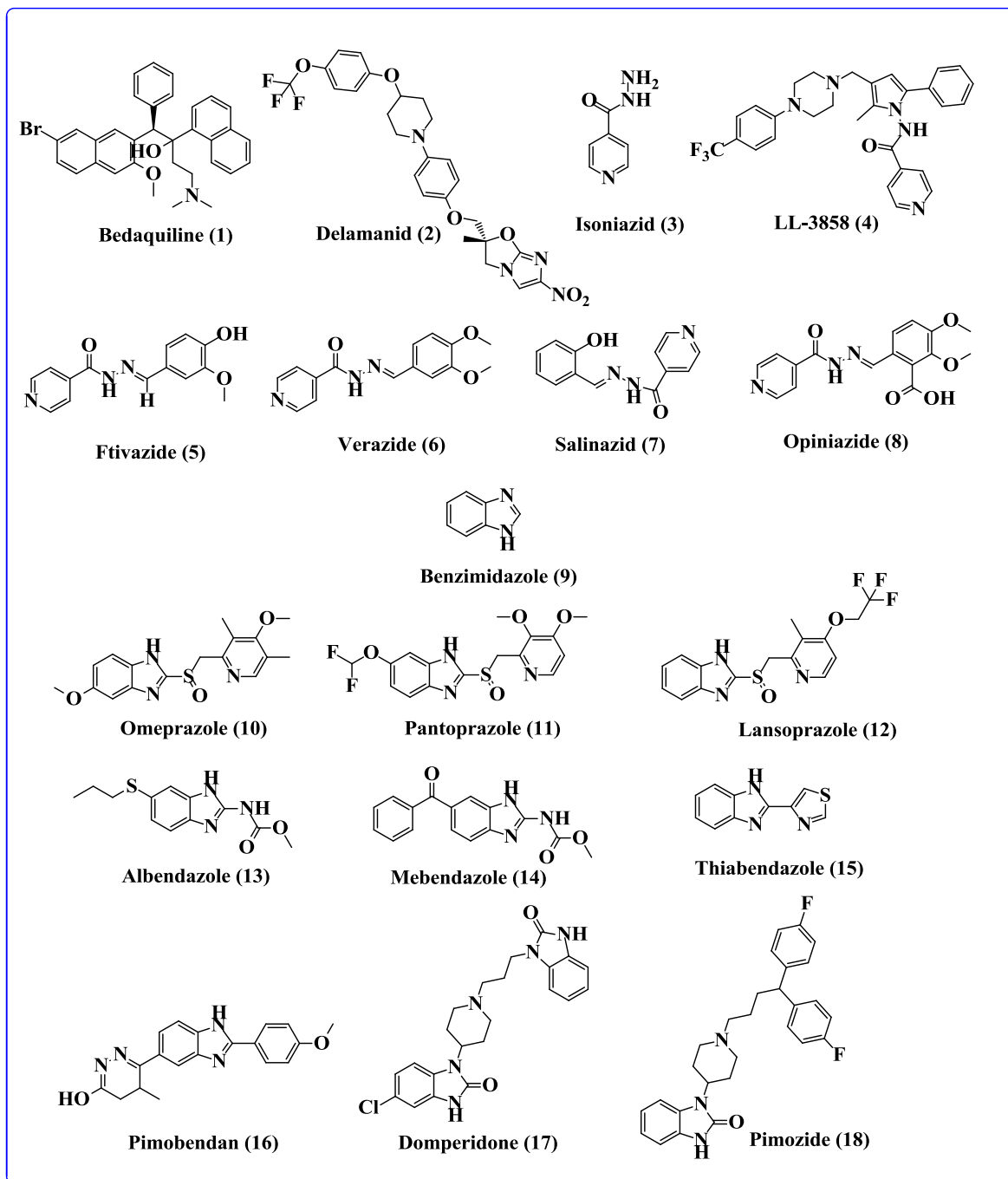


Figure 1. Structure of important drugs based on Isoniazid and benzimidazole motif.

Meanwhile, the medically important pharmacophore benzimidazole (9) molecule is a versatile heterocycle possessing a wide spectrum of biological activity including antimicrobial [35-38], antiproliferative [39], anti-diabetic [40], anti-inflammatory [41], spasmolytic [42], anti-viral [43] and anti-hypertensive [44] activities. Benzimidazole motif

is also found in a variety of naturally occurring compounds for example, vitamin B12 and its derivatives and benzimidazole is structurally similar to purine bases. Benzimidazoles derivatives are broadly used as drug candidates such as, Omeprazole (**10**), Pantoprazole (**11**), Lansoprazole (**12**); proton pump inhibitor [45], Albendazole (**13**), Mebendazole (**14**), Thiabendazole (**15**); antihelmintic [46], Pimobendan (**16**); Ionodilator [47] Domperidone (**17**); antidopaminergic [48-49] and Pimozide (**18**); antipsychotic [50]. This broad biological importance of benzimidazole molecule, encourage us to develop a new class of compounds based on benzimidazole with different substitution.

A modern trend for the drug design and drug development is the concept of multi-target ‘intramolecular’ hybridization of molecules [51-53]. According to this approach, new hybrid drug candidates should combine different pharmacophore at more than one target providing an advantage when treatment is aimed specially for drug-resistant infection. Hydrazine-derived analogues create an important class of potential anti-TB agents, given that the hydrazine-based pharmacophore Isoniazid is an unvarying anti-tuberculosis pyridine-based drug candidate [55-56]. In our continuous program in the search of new, effective, powerful and safe isoniazid derivatives, we decided to construct a new class of an attractive anti-tubercular agents, designing by hybridization between isonizotinic hydrazide and benzimidazole derivatives.

The present study is a part of our ongoing efforts towards the development of novel anti-TB agents with different mode of action and better biological activity. In a previous study (**Chapter 2**), we have designed and screened number of new compounds based on benzimidazole and nicotinic hydrazide scaffold. However, we have selected only 25 compounds from the *in silico* screening according to the results obtain from ADME and docking study. Motivated by this findings, we aimed to synthesize two different sets of N'-(2-(2-phenyl-1*H*-benzo[d]imidazol-1-yl)acetyl)isonicotinohydrazide (**G1-G16**) and

(**GG1-GG4**) by reaction between compound **E1-E16** & **EE1-EE4** and nicotinic hydrazied in absolute alcohol . However, due to unavailability of synthetic protocol for some designed compounds we have made few changes to synthesize the targeted compounds which selected from previous study. For the synthesis of compounds **G1-G16** and **GG1-GG4**, compounds 2-phenyl-1*H*-benzo[d]imidazole (**D1-D16**) was synthesized first by reaction between o-phenylenediamine, aromatic aldehyde and carboxylic derivative using methanol and 4N HCl. The compound **D1-D16** than further treated with ethyl chloroacetate in the presence of dry acetone at 0-5°C temperature to get the ethyl 2-(1*H*-benzo[d]imidazol-1-yl)acetate (**E1-E16** & **EE1-EE4**) derivatives.

The synthesized compounds were characterized by mass spectrometer, ¹H and ¹³C NMR spectroscopy. It is noteworthy that no attention was paid to explore the antibacterial and anti-tuberculosis activities for the targeted scaffold, so far. Therefore, the synthesized derivatives **G1-G16** and **GG1-GG4** not only were evaluated for their anti-tuberculosis and anti-bacterial activity, but also assessed for their anti-malarial and MDR-TB activities. Also, the anti-oxidant of the most active compounds were tested by DPPH, NO and H₂O₂ methods. Additionally, due to the few changes in the molecules and for the validation of our previous study (**Chapter 2**), we have performed ADME, docking and molecular dynamics study of the synthesized compounds against the active site of the NADH-dependent Enoyl-acyl Carrier Protein reductase (Enoyl-ACP reductase) encoded by the *Mycobacterium* gene *InhA* *Mycobacterium tuberculosis* oxidoreductase enzyme using four different PDB. (PDB ID: 1QG6, 2NSD, 4TZK, 4TZZ).

2.0 Methods and Materials

2.1 Chemistry

All the chemicals and solvents were purchased from commercial source and were used in the reaction without further purification. Synthesis of the desired products were carried out using conventional method. Melting points were determined by automated melting point system (MPA- Optimelt) and were uncorrected. The completion of the reactions was checked by TLC (thin layer chromatography). The TLC is silica gel coated aluminum sheets (silica gel G60 F₂₅₄, Merck) which was visualized by UV radiation and various spray reagent. Elemental analysis were performed on vario MICRO cube, elemental CHNS analyser (Serial Number: 15084053). ¹H and ¹³C NMR spectra were run on Bruker 400 and 100 MHz NMR spectrometer respectively, using DMSO-*d*₆ as solvents. The chemical shifts were expressed in parts per million (δ ppm) with TMS as internal reference. J values are given in hertz (Hz). Mass spectra was recorded on Advion Expression CMS, USA, with electro-spray ionization (ESI) was used as an ion source and ethanol: formic acid: water was used as a mobile phase.

2.1.1 Synthesis of 2-phenyl-1H-benzo[d]imidazole (D1-D16).

Compounds D1-D16 was synthesized according to reported procedure by Mariappan G *et al.* [57].

2.1.2 Synthesis of 1H-benzo[d]imidazole (DD1-DD4).

Compounds D1-D16 was synthesized according to reported procedure by Prajapati BK *et al.* [58].

2.1.3 General synthetic procedure of ethyl 2-(1*H*-benzo[d]imidazol-1-yl)acetate (E1-E16 & EE1-EE4).

Compounds E1-E16 and EE1-EE4 was synthesized according to reported procedure by Brand-Williams W *et al.* [59].

2.1.4 General procedure for the synthesis of N'-(2-(2-phenyl-1*H*-benzo[d]imidazol-1-yl)acetyl)isonicotinohydrazide (G1-G16):

An equimolar mixture of nicotinic hydrazide (**F1.2**) (1.0 eq.) and the appropriate ethyl 2-(1*H*-benzo[d]imidazol-1-yl)acetate derivatives (E1-E16) (1.0 eq.) in absolute ethyl alcohol (15 mL) was taken in 100 mL flat bottom flask. The reaction mixture was refluxed for 3-4 hours on hot magnetic plate. The progress of the reaction was observed by TLC analysis. After the completion of reaction, the reaction mixture allowed cool at room temperature and poured into ice cold water with continues stirring. The solid thus obtained was filtered, dried and recrystallize from appropriate solvent to get desired compound N'-(2-(2-phenyl-1*H*-benzo[d]imidazol-1-yl)acetyl)isonicotinohydrazide derivatives (**G1-G16**) with good practical yield (45-82%).

2.1.4.1 N'-(2-(2-(4-nitrophenyl)-1*H*-benzo[d]imidazol-1-yl)acetyl)isonicotinohydrazide (G1).

Dark yellow solid, m.p. 243-249°C.; Anal. Calc. for C₂₁H₁₆N₆O₄ (%): C, 60.57; H, 3.87; N, 20.18; O, 15.37%. Found- C, 59.49; H, 3.30; N, 19.73%; ¹H NMR (400 MHz, DMSO): δ; 8.95 - 8.79 (m, 2H), 8.27 - 8.13 (m, 2H), 7.98 - 7.86 (m, 2H), 7.86 - 7.71 (m, 2H), 7.67 (d, J = 10.8 Hz, 2H), 7.29 (d, J = 13.9 Hz, 2H), 6.27 (s, 1H), 5.28 (s, 1H), 5.12 (s, 1H), 4.92 (s, 1H); ¹³C NMR (100 MHz, DMSO): δ; 169.14, 166.90, 154.11, 151.19, 150.79, 145.92, 139.99, 139.17, 136.73, 135.89, 127.37, 126.98, 125.82, 125.60, 124.50, 123.24, 122.92, 120.06, 112.32, 46.50. ESI-MS: m/z Calculated 416.25, found [m/z] [M+H]⁺417.08.

2.1.4.2 2N'-(2-(2-(4-bromophenyl)-6-methyl-1*H*-benzo[d]imidazol-1-yl)acetyl)isonicotinohydrazide (G2).

Brown solid, m.p. 267-271°C.; Anal. Calc. for C₂₂H₁₈BrN₅O₂ (%): C, 56.91; H, 3.91; Br, 17.21; N, 15.08; O, 6.89%. Found- C, 56.85; H, 3.62; N, 14.83%; ¹H NMR (400 MHz, DMSO) δ 8.97 - 8.82 (m, 4H), 7.78 (s, 2H), 7.77 - 7.67 (m, 6H), 7.11 (s, 1H), 5.18 (s, 1H), 4.94 (s, 1H), 2.30 - 2.26 (m, 3H).; ¹³C NMR (100 MHz, DMSO): δ; 169.14, 166.90, 154.11, 151.19 - 150.79, 139.99, 138.77, 137.22, 135.27, 134.50, 132.65, 132.44, 128.20, 127.98, 124.58, 123.22, 122.83, 121.51, 120.69, 110.30, 46.50, 21.21.

2.1.4.3 N'-(2-(5,6-dichloro-2-(4-nitrophenyl)-1*H*-benzo[d]imidazol-1-yl)acetyl)isonicotinohydrazide (G3).

Yellow solid, m.p. 274-279°C.; Anal. Calc. for C₂₁H₁₄Cl₂N₆O₄ (%): C, 51.98; H, 2.91; Cl, 14.61; N, 17.32; O, 13.19%. Found- C, 52.12; H, 2.58; N, 17.18%; ¹H NMR (400 MHz, DMSO): δ; 9.04 - 8.89 (m, 2H), 8.41 - 8.27 (m, 2H), 7.94 - 7.78 (m, 4H), 7.77 (s, 1H), 7.61 (s, 1H), 6.65 (s, 1H), 4.94 (d, *J* = 16.3 Hz, 2H).; ¹³C NMR (100 MHz, DMSO): δ; 169.14, 166.90, 154.51, 151.19, 150.79, 145.92, 139.99, 137.45, 135.89, 133.22, 127.60, 127.38, 127.28, 126.98, 125.82, 125.60, 123.22, 122.83, 120.02, 114.67, 46.50.

2.1.4.4 N'-(2-(5,6-dichloro-2-(4-nitrophenyl)-1*H*-benzo[d]imidazol-1-yl)acetyl)nicotinohydrazide (G4).

Light brown solid, m.p. 273-279°C.; Anal. Calc. for C₂₁H₁₄Cl₂N₆O₄ (%): C, 51.98; H, 2.91; Cl, 14.61; N, 17.32; O, 13.19%. Found- C, 52.09; H, 2.85; N, 17.36%; ¹H NMR (400 MHz, DMSO): δ; 9.10 (s, 1H), 8.80 (s, 1H), 8.37 - 8.23 (m, 2H), 8.06 (s, 1H), 7.91 - 7.79 (m, 2H), 7.75 (d, *J* = 16.7 Hz, 2H), 7.53 (s, 1H), 7.10 (s, 1H), 7.02 (s, 1H), 4.97 (d, *J* = 17.8 Hz, 2H).; ¹³C NMR (100 MHz, DMSO): δ; 169.14, 168.05, 154.51, 150.91, 149.45, 145.92,

137.52, 135.89, 133.22, 132.64, 127.60, 127.38, 127.28, 126.98, 125.82, 125.60, 122.68, 120.02, 114.67, 46.50.

2.1.4.5 N'-(2-(6-methyl-2-(3,4,5-trimethoxyphenyl)-1H-benzo[d]imidazol-1-yl)acetyl)isonicotinohydrazide (G5).

Light brown solid, m.p. 257-261°C.; Anal. Calc. for C₂₅H₂₅N₅O₅ (%): C, 63.15; H, 5.30; N, 14.73; O, 16.82%. Found- C, 63.20; H, 5.02; N, 14.34%.; ¹H NMR (400 MHz, DMSO) δ 8.99 - 8.84 (m, 2H), 8.73 (s, 1H), 7.90 - 7.73 (m, 3H), 7.61 (s, 1H), 7.55 (s, 1H), 7.11 (s, 1H), 7.02 - 6.98 (m, 2H), 5.15 (s, 1H), 5.02 (s, 1H), 3.89 - 3.85 (m, 6H), 3.85 - 3.81 (m, 3H), 2.34 - 2.30 (m, 3H).; ¹³C NMR (100 MHz, DMSO): δ; 169.14, 166.90, 153.11, 151.19, 150.79, 150.03, 149.82, 141.64, 139.99, 138.77, 137.22, 135.27, 127.33, 124.58, 123.22, 122.83, 120.69, 111.00, 110.60, 110.30, 60.65, 56.89, 56.58, 46.50, 21.21.

2.1.4.6 N'-(2-(6-methyl-2-(3,4,5-trimethoxyphenyl)-1H-benzo[d]imidazol-1-yl)acetyl)nicotinohydrazide (G6).

Yellow solid, m.p. 258-260°C.; Anal. Calc. for C₂₅H₂₅N₅O₅ (%): C, 63.15; H, 5.30; N, 14.73; O, 16.82%. Found- C, 62.75; H, 5.26; N, 14.50%.; ¹H NMR (400 MHz, DMSO): δ; 9.01 (s, 1H), 8.74 (s, 1H), 8.68 (s, 1H), 8.14 (s, 1H), 7.64 (s, 1H), 7.53 (d, *J* = 18.2 Hz, 2H), 7.12 (s, 1H), 7.00 - 6.96 (m, 2H), 6.69 (s, 1H), 5.10 (d, *J* = 7.5 Hz, 2H), 3.89 - 3.85 (m, 3H), 3.83 - 3.79 (m, 6H), 2.39 - 2.35 (m, 3H).; ¹³C NMR (100 MHz, DMSO): δ; 169.14, 168.05, 153.11, 150.91, 150.03, 149.82, 149.45, 141.64, 138.77, 137.58, 137.22, 135.27, 132.64, 127.33, 124.58, 122.68, 120.69, 111.00, 110.60, 110.30, 60.65, 56.89, 56.58, 46.50, 21.21.

2.1.4.7 2-(5-benzoyl-2-(3,4,5-trimethoxyphenyl)-1H-benzo[d]imidazol-1-yl)-N'-(pyridin-4-yl)acetohydrazides (G7).

Brown, m.p. 282-287°C.; Anal. Calc. for $C_{30}H_{27}N_5O_5$ (%): C, 67.03; H, 5.06; N, 13.03; O, 14.88%. Found- C, 66.79; H, 4.96; N, 12.43%.; 1H NMR (400 MHz, DMSO): δ ; 8.43 - 8.28 (m, 2H), 8.07 (s, 1H), 7.78 (s, 1H), 7.74 - 7.61 (m, 3H), 7.44 (s, 1H), 7.39 - 7.33 (m, 2H), 7.01 - 6.97 (m, 2H), 6.54 (s, 1H), 6.46 - 6.31 (m, 2H), 5.09 (s, 1H), 5.04 (s, 1H), 3.94 (s, 1H), 3.88 - 3.82 (m, 9H).; ^{13}C NMR (100 MHz, DMSO): δ ; 195.76, 170.56, 156.69, 153.58, 152.15, 151.75, 150.03, 149.82, 141.63, 137.96, 131.92, 129.11, 128.72, 128.45, 128.05, 127.53, 127.33, 125.41, 121.64, 111.00, 110.60, 108.62, 108.32, 107.93, 60.65, 56.89, 56.58, 46.50.

2.1.4.8 N'-(2-(2-(4-nitrophenyl)-1H-benzo[d]imidazol-1-yl)acetyl)isonicotinohydrazide (G8).

Light yellow solid, m.p. 242-248°C.; Anal. Calc. for $C_{21}H_{16}N_6O_4$ (%): C, 60.57; H, 3.87; N, 20.18; O, 15.37%. Found- C, 61.13; H, 3.82; N, 20.21%.; 1H NMR (400 MHz, DMSO): δ ; 8.94 - 8.80 (m, 2H), 8.28 - 8.13 (m, 2H), 7.99 - 7.85 (m, 2H), 7.64 (dd, $J = 15.0, 9.6$ Hz, 4H), 7.31 (s, 1H), 7.26 (s, 1H), 6.68 (s, 1H), 6.38 (s, 1H), 5.14 (s, 1H), 5.07 (s, 1H).; ^{13}C NMR (100 MHz, DMSO): δ ; 169.14, 166.90, 154.11, 151.19, 150.79, 145.92, 139.99, 139.17, 136.73, 135.89, 127.37, 126.98, 125.82, 125.60, 124.50, 123.24, 122.92, 120.06, 112.32, 46.50.

2.1.4.9 N'-(2-(7-methyl-2-(4-nitrophenyl)-1H-benzo[d]imidazol-1-yl)acetyl)isonicotinohydrazide (G9).

Dark brown solid, m.p. 245-249°C.; Anal. Calc. for $C_{22}H_{18}N_6O_4$ (%): C, 61.39; H, 4.22; N, 19.53; O, 14.87%. Found- C, 60.81; H, 3.98; N, 18.72%.; 1H NMR (400 MHz, DMSO): δ ; 9.06 - 8.90 (m, 2H), 8.34 - 8.20 (m, 2H), 7.91 - 7.73 (m, 4H), 7.54 (s, 1H), 7.22 (s, 1H), 7.13 (d, $J = 4.4$ Hz, 2H), 6.68 (s, 1H), 5.17 (s, 1H), 4.77 (s, 1H), 2.43 - 2.39 (m, 3H).; ^{13}C NMR (100 MHz, DMSO): δ ; 169.14, 166.90, 154.23, 151.19, 150.79, 145.92, 139.99,

138.91, 136.05, 135.89, 128.95, 127.37, 126.98, 125.82, 125.60, 124.49, 123.23, 122.93, 116.14, 47.67, 18.02.

2.1.4.10 N'-(2-(7-methyl-2-(4-nitrophenyl)-1*H*-benzo[d]imidazol-1-yl)acetyl)nicotinohydrazide (G10).

Dark brown solid, m.p. 245-250°C.; Anal. Calc. for C₂₂H₁₈N₆O₄ (%): C, 61.39; H, 4.22; N, 19.53; O, 14.87%. Found- C, 61.47; H, 4.17; N, 19.23%; ¹H NMR (400 MHz, DMSO): δ; 9.10 (s, 1H), 8.79 (s, 1H), 8.39 - 8.25 (m, 2H), 8.14 (s, 1H), 7.98 - 7.83 (m, 2H), 7.53 (d, *J* = 0.8 Hz, 2H), 7.21 (s, 1H), 7.09 (d, *J* = 29.8 Hz, 2H), 6.68 (s, 1H), 5.22 (s, 1H), 4.76 (s, 1H), 2.33 - 2.29 (m, 3H); ¹³C NMR (100 MHz, DMSO): δ; 169.14, 168.05, 154.23, 150.91, 149.45, 145.92, 138.91, 137.58, 136.09, 135.97, 132.64, 128.95, 127.37, 126.98, 125.82, 125.60, 124.49, 123.04, 122.68, 116.14, 47.67, 18.02.

2.1.4.11 N'-(2-(2-(4-chlorophenyl)-7-methyl-1*H*-benzo[d]imidazol-1-yl)acetyl)isonicotinohydrazide (G11).

Brown solid, m.p. 257-262°C.; Anal. Calc. for C₂₂H₁₈ClN₅O₂ (%): C, 62.93; H, 4.32; Cl, 8.44; N, 16.68; O, 7.62%. Found- C, 62.75; H, 4.34; N, 16.31%; ¹H NMR (400 MHz, DMSO): δ; 9.04 - 8.89 (m, 2H), 8.30 (s, 1H), 7.90 - 7.75 (m, 4H), 7.74 - 7.59 (m, 2H), 7.59 - 7.43 (m, 2H), 7.43 - 7.38 (m, 1H), 7.19 (s, 1H), 4.79 (s, 2H), 2.06 (s, 3H); ¹³C NMR (100 MHz, DMSO): δ; 169.14, 166.90, 154.23, 151.19, 150.79, 139.99, 138.91, 136.05, 134.34, 132.68, 129.93, 129.53, 128.95, 128.44, 128.23, 124.49, 123.23, 122.93, 116.14, 47.67, 18.02.

2.1.4.12. N'-(2-(6-bromo-2-(3,4,5-trimethoxyphenyl)-3*H*-imidazo[4,5-*b*]pyridin-3-yl)acetyl)isonicotinohydrazide (G12).

Dark brown solid, m.p. 274-279°C.; Anal. Calc. for C₂₃H₂₁BrN₆O₅ (%): C, 51.03; H, 3.91; Br, 14.76; N, 15.52; O, 14.78%. Found- C, 50.89; H, 3.81; N, 15.19%; ¹H NMR (400 MHz,

DMSO): δ ; 9.77 (s, 1H), 9.07 - 8.93 (m, 2H), 8.81 (s, 1H), 8.26 (s, 1H), 8.15 (s, 1H), 7.95 - 7.80 (m, 2H), 7.17 - 7.13 (m, 2H), 5.24 (s, 1H), 5.07 (s, 1H), 3.89 - 3.85 (m, 6H), 3.84, 3.80 (m, 3H).; ^{13}C NMR (100 MHz, DMSO): δ ; 169.14, 166.90, 151.19, 150.79, 150.03, 149.82, 149.11, 148.21, 142.94, 141.64, 139.99, 139.82, 129.30, 127.33, 123.22, 122.83, 114.98, 111.00, 110.60, 60.65, 56.89, 56.58, 43.76.

2.1.4.13 N'-(2-(6-bromo-2-(3,4,5-trimethoxyphenyl)-3H-imidazo[4,5-b]pyridin-3-yl)acetyl)nicotinohydrazide (G13).

Light brown solid, m.p. 274-278°C.; Anal. Calc. for $\text{C}_{23}\text{H}_{21}\text{BrN}_6\text{O}_5$ (%): C, 51.03; H, 3.91; Br, 14.76; N, 15.52; O, 14.78%. Found- C, 51.62; H, 3.60; N, 14.88%.; ^1H NMR (400 MHz, DMSO): δ ; 9.20 (s, 1H), 9.06 (s, 1H), 8.95 (s, 1H), 8.81 (s, 1H), 8.26 (s, 1H), 8.19 (s, 1H), 7.53 (s, 1H), 7.13 - 7.09 (m, 2H), 6.86 (s, 1H), 4.98 (d, $J = 0.9$ Hz, 2H), 3.89 - 3.85 (m, 6H), 3.84 - 3.80 (m, 3H).; ^{13}C NMR (100 MHz, DMSO): δ ; 169.14, 168.05, 150.91, 150.03, 149.82, 149.45, 149.11, 148.21, 142.94, 141.64, 139.82, 137.58, 132.64, 129.30, 127.33, 122.68, 114.98, 111.00, 110.60, 60.65, 56.89, 56.58 (m), 43.76.

2.1.4.14 4-(1-(2-(2-isonicotinoylhydrazinyl)-2-oxoethyl)-6-methyl-1H-benzo[d]imidazol-2-yl)benzoic acid (G14).

Light yellow solid, m.p. 253-259°C.; Anal. Calc. for $\text{C}_{23}\text{H}_{19}\text{N}_5\text{O}_4$ (%): C, 64.33; H, 4.46; N, 16.31; O, 14.90%. Found- C, 64.28; H, 4.13; N, 16.47%.; ^1H NMR (400 MHz, DMSO): δ ; 10.48 (s, 1H), 8.99 - 8.85 (m, 2H), 8.59 (s, 1H), 8.21 - 8.07 (m, 2H), 7.86 - 7.78 (m, 4H), 7.63 (s, 1H), 7.56 (s, 1H), 7.09 (d, $J = 30.2$ Hz, 2H), 5.10 (d, $J = 19.1$ Hz, 2H), 2.39 - 2.35 (m, 3H).; ^{13}C NMR (100 MHz, DMSO): δ ; 169.14, 168.95, 166.90, 154.11, 151.19, 150.79, 139.99, 138.77, 137.22, 136.52, 135.27, 131.59, 131.20, 128.47, 128.17, 127.95, 124.58, 123.22, 122.83, 120.69, 110.30, 46.50, 21.21.

2.1.4.15 4-(6-methyl-1-(2-(2-nicotinoylhydrazinyl)-2-oxoethyl)-1H-benzo[d]imidazol-2-yl)benzoic acid (G15).

Dark orange solid, m.p. 254-259°C.; Anal. Calc. for C₂₃H₁₉N₅O₄ (%): C, 64.33; H, 4.46; N, 16.31; O, 14.90%. Found- C, 64.14; H, 4.08; N, 15.96%; ¹H NMR (400 MHz, DMSO): δ; 11.02 (s, 1H), 9.13 (s, 1H), 8.74 (s, 1H), 8.59 (s, 1H), 8.18 - 8.10 (m, 3H), 7.90 - 7.76 (m, 2H), 7.64 (s, 1H), 7.56 (s, 1H), 7.51 (s, 1H), 7.12 (s, 1H), 6.96 (s, 1H), 5.10 (d, *J* = 11.4 Hz, 2H), 2.39 - 2.35 (m, 3H).; ¹³C NMR (100 MHz, DMSO): δ; 169.14, 168.95, 168.05, 154.11, 150.91, 149.45, 138.77, 137.58, 137.22, 136.52, 135.27, 132.64, 131.59 - 131.20, 128.47, 128.17 - 127.95, 124.58, 122.68, 120.69, 110.30, 46.50, 21.21.

2.1.4.16 4-(1-(2-(2-nicotinoylhydrazinyl)-2-oxoethyl)-1H-benzo[d]imidazol-2-yl)benzoic acid (G16).

Light brown solid, m.p. 247-251°C.; Anal. Calc. for C₂₂H₁₇N₅O₄: C, 63.61; H, 4.12; N, 16.86; O, 15.41%. Found- C, 62.71; H, 4.24; N, 16.03%; ¹H NMR (400 MHz, DMSO): δ; 10.52 (s, 1H), 8.87 (s, 1H), 8.74 (s, 1H), 8.56 (s, 1H), 8.27 (s, 1H), 8.20 - 8.07 (m, 2H), 7.90 - 7.75 (m, 2H), 7.66 (s, 1H), 7.60 (s, 1H), 7.50 (s, 1H), 7.30 (s, 1H), 7.25 (s, 1H), 7.07 (s, 1H), 5.13 (s, 1H), 5.08 (s, 1H).; ¹³C NMR (100 MHz, DMSO): δ; 169.14, 168.95, 168.05, 154.11, 150.91, 149.45, 139.17, 137.58, 136.73, 136.52, 132.64, 131.59, 131.20, 128.47, 128.17, 127.95, 124.50, 123.05, 122.68, 120.06, 112.32, 46.50.

2.1.3 Synthetic procedure of N'-(2-(1H-benzo[d]imidazol-1-yl)acetyl)isonicotinohydrazide (GG1-GG2):

An equimolar mixture of nicotinic hydrazide (**F1.2**) (1.0 eq.) and the appropriate ethyl 2-(1H-benzo[d]imidazol-1-yl)acetate derivatives (**EE1-EE4**) (1.0 eq.) in absolute ethyl alcohol (15 mL) was taken in 100 mL flat bottom flask. The reaction mixture was refluxed for 3-4 hours on hot magnetic plate. The progress of the reaction was observed by

TLC analysis. After the completion of reaction, the isolation of yield performed same as compound G1-G16 to get compounds GG1-GG4 (of **N'-(2-(1*H*-benzo[d]imidazol-1-yl)acetyl)isonicotinohydrazide**).

2.1.3.1. N'-(2-(6-methyl-2-(4-propoxyphenyl)-1*H*-benzo[d]imidazol-1-yl)acetyl)isonicotinohydrazide (GG1).

Dark brown solid, m.p. 253-258°C.; Anal. Calc. for C₂₅H₂₅N₅O₃ (%): C, 67.70; H, 5.68; N, 15.79; O, 10.82%. Found- C, 67.81; H, 5.48; N, 15.60%.; ¹H NMR (400 MHz, DMSO): δ; 9.00 - 8.85 (m, 2H), 8.21 (s, 2H), 7.89 - 7.71 (m, 2H), 7.56 (d, *J* = 9.4 Hz, 2H), 7.12 (s, 2H), 7.10 - 6.99 (m, 2H), 5.11 (s, 2H), 3.99 - 3.95 (m, 2H), 2.41 - 2.37 (m, 3H), 1.85 - 1.81 (m, 2H), 1.02 - 0.98 (m, 3H).; ¹³C NMR (100 MHz, DMSO): δ; 169.14, 166.90, 159.23, 154.11, 151.19, 150.79, 139.99, 138.77, 137.22, 135.27, 128.06, 127.72, 127.32, 124.58, 123.22 - 122.83, 120.69, 115.21, 115.00, 110.30, 71.73, 46.50, 21.28, 10.62.

2.1.3.2 N'-(2-(6-methyl-2-(2-oxo-2*H*-chromen-3-yl)-1*H*-benzo[d]imidazol-1-yl)acetyl)isonicotinohydrazide (GG2).

Light yellow solid, m.p. 291-295°C.; Anal. Calc. for C₂₅H₁₉N₅O₄ (%): C, 66.22; H, 4.22; N, 15.44; O, 14.11%. Found- C, 66.82; H, 4.30; N, 15.23%.; ¹H NMR (400 MHz, DMSO): δ; 9.01 - 8.86 (m, 2H), 8.15 (s, 1H), 7.95 - 7.80 (m, 2H), 7.79 (d, *J* = 8.0 Hz, 2H), 7.62 (s, 1H), 7.53 (d, *J* = 4.0 Hz, 2H), 7.42 (s, 1H), 7.18 (d, *J* = 1.9 Hz, 2H), 7.09 (s, 1H), 4.88 (s, 2H), 2.32 - 2.28 (m, 3H).; ¹³C NMR (100 MHz, DMSO): δ; 169.14, 166.90, 163.00, 156.70, 154.13, 151.19, 150.79, 139.99, 138.77, 137.22, 135.27, 132.87, 132.09, 129.57, 125.01, 124.58, 123.22, 122.83, 120.64, 117.14, 112.91, 110.30, 46.82, 21.21.

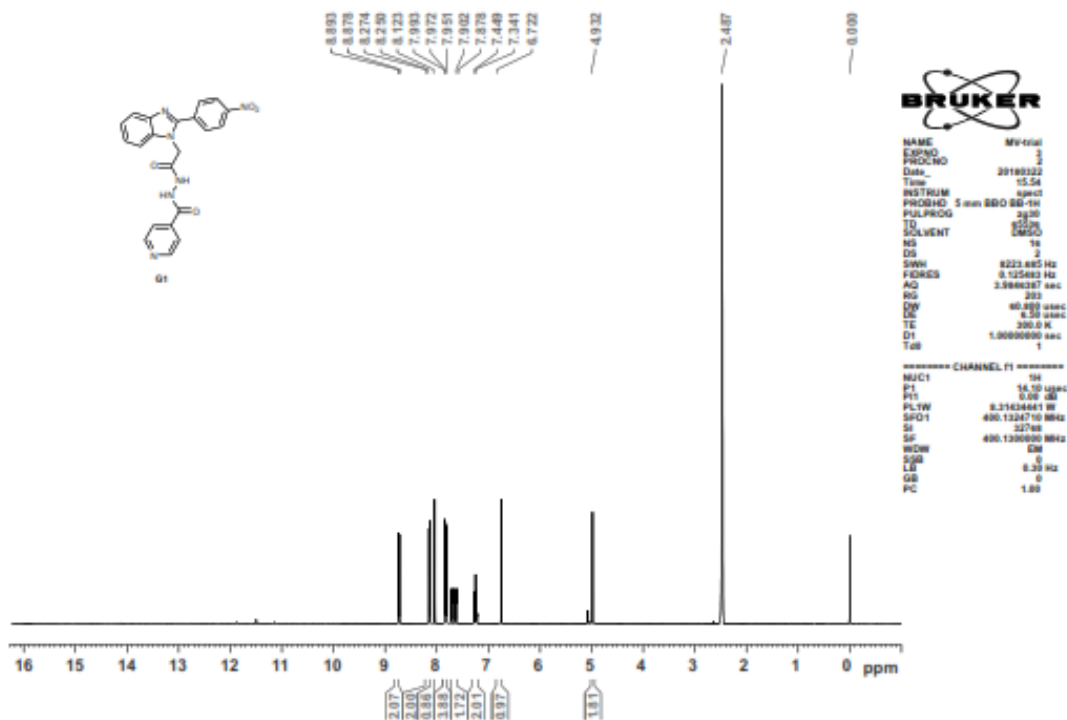
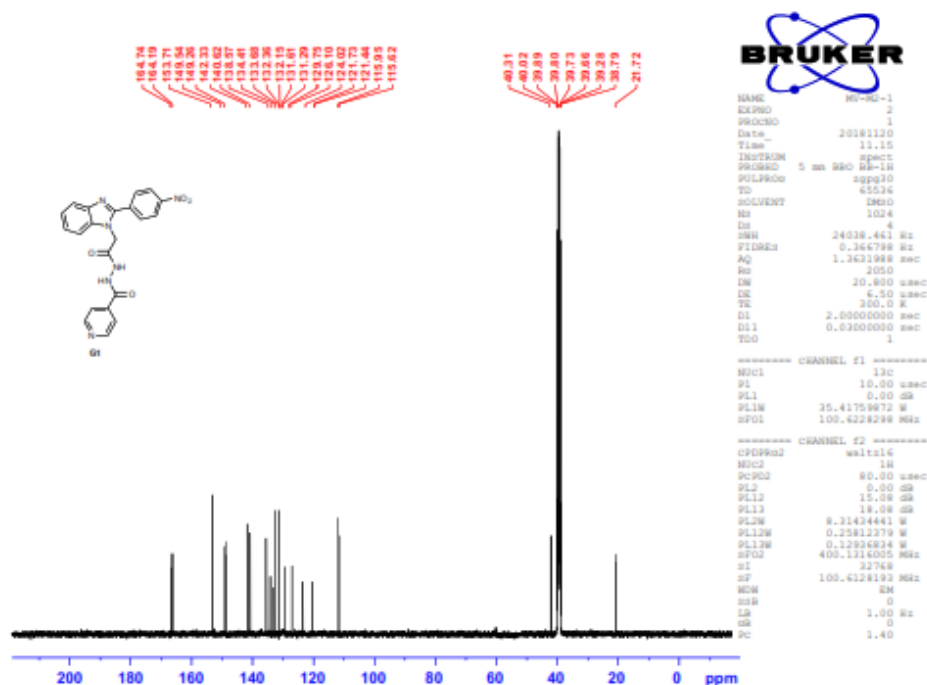
2.1.3.3 N'-(2-(6-methyl-2-(2-oxo-2H-chromen-3-yl)-1H-benzo[d]imidazol-1-yl)acetyl)nicotinohydrazide (GG3).

Brown solid, m.p. 292-295°C.; Anal. Calc. for C₂₅H₁₉N₅O₄ (%): C, 66.22; H, 4.22; N, 15.44; O, 14.11%. Found- C, 65.90; H, 4.25; N, 15.20%; ¹H NMR (400 MHz, DMSO): δ; 8.88 (s, 1H), 8.74 (s, 1H), 8.15 (s, 1H), 7.93 (s, 1H), 7.62 (s, 2H), 7.62 - 7.44 (m, 8H), 4.97 (s, 2H), 2.10 (s, 3H).; ¹³C NMR (100 MHz, DMSO): δ; 169.14, 168.05, 163.00, 156.70, 154.13, 150.91, 149.45, 138.77, 137.58, 137.22, 135.27, 132.87, 132.64, 132.09, 129.57, 125.01, 124.58, 122.68, 120.64, 117.14, 112.91, 110.30, 46.82, 21.21.

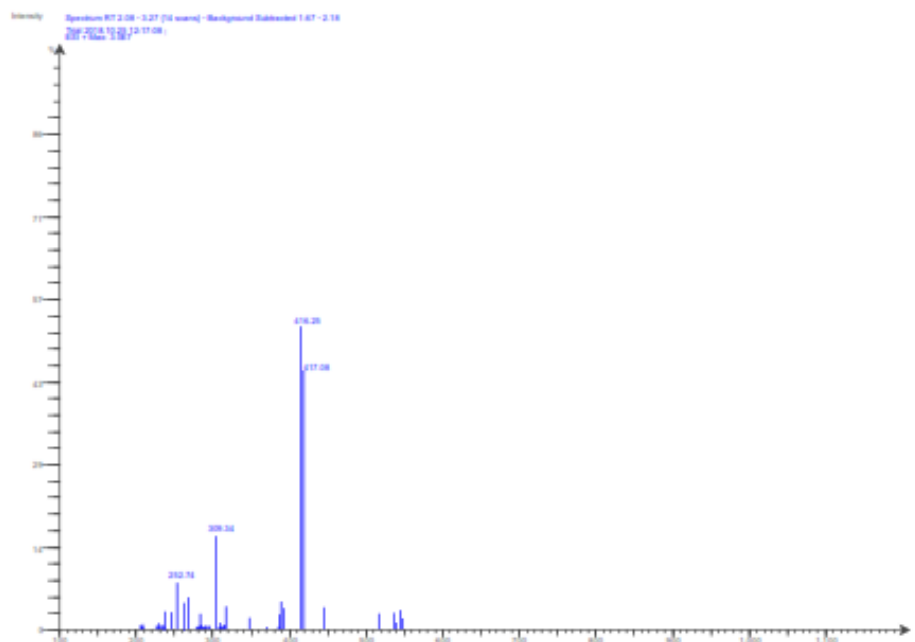
2.1.3.4 N'-(2-(6-bromo-2-(pyrazin-2-yl)-3H-imidazo[4,5-b]pyridin-3-yl)acetyl)isonicotinohydrazide (GG4).

Dark orange solid, m.p. 273-278°C.; Anal. Calc. for C₁₈H₁₃BrN₈O₂ (%): C, 47.70; H, 2.89; Br, 17.63; N, 24.72; O, 7.06%. Found- C, 48.09; H, 2.67; N, 24.49%; ¹H NMR (400 MHz, DMSO): δ; 9.35 (s, 1H), 9.02 (s, 1H), 9.00 - 8.84 (m, 3H), 8.70 - 8.54 (m, 3H), 8.21 (s, 1H), 7.88 - 7.73 (m, 2H), 5.25 (s, 1H), 5.21 (s, 1H).; ¹³C NMR (100 MHz, DMSO): δ; 169.14, **166.90**, 151.20, 150.79, 148.21, 147.80, 143.37, 142.96, 141.73, 139.99, 139.82, 129.30, 123.22, 122.83, 114.98, 43.76.

2.0 METHODS AND MATERIALS

2.1.4 ^1H NMR Spectrum of synthesized compound G12.1.5 ^{13}C NMR Spectrum of synthesized compound G1

2.1.5 Mass spectrum of synthesized compound G1



2.2 Biological assay

2.2.1 *In vitro* anti-bacterial activity

The *in vitro* anti-bacterial activity of synthesized compounds were performed against four different bacterial strains (*E. coli* MTCC 443, *P. aeruginosa* MTCC 1688, *S. aureus* MTCC 96, *S. pyogenus* MTCC 442) and compared with standard drugs according to method described in **Chapter 3**.

2.2.2 *In vitro* anti-tuberculosis activity and MDR-TB study

The anti-tuberculosis screening of the synthesized compounds was carried out using method described in **Chapter 3**.

2.2.3 *In vitro* anti-malarial and anti-fungal activity

The *in vitro* anti-malarial activity of all the synthesized compounds was carried out in 96 well micro titre plates according to the micro assay protocol described in **Chapter 3**.

2.2.4. Anti-Oxidant activity protocol

In this study, we used three different methods (DPPH, NO, H₂O₂) to evaluate the anti-oxidant activity of the compounds because anti-oxidant scavenging effect should not be determined on a single test protocol. The selected compounds were dissolved in DMSO to prepare a series of concentrations for the anti-oxidant scavenging activity and compared with standard compound in all methods.

2.2.4.1 DPPH method

The % DPPH scavenging activity of the compounds **G5**, **G8**, **G14** and **GG4** were evaluated in vitro according to the protocol described by Brand Williams *et al.* [60]. In order to evaluate the anti-oxidant potential of the test samples by free radical scavenging protocol, the variation in the optical density of DPPH radicals was monitored. 24 mg DPPH was dissolved in 100 mL Methanol and stored at 20 °C to prepare a stock solution. 100 µl of compound and 3 ml aliquot of the stock solution was mixed at different concentrations shown in **Table 3**. Further, the reaction mixer was incubated for 15 min in dark room at room temperature. The percentage of DPPH scavenging effect was calculated by equation given below;

$$\% \text{ scavenging activity of DPPH radical} = ([A_0 - A_1] / A_0) \times 100$$

Where, A₀ is the absorbance of the control and A₁ is the absorbance of the sample.

2.2.4.2 NO method

The specific synthesis of nitric oxide generates a nitrite ion in biological tissue. The sodium nitroprusside is decomposed in aqueous solution and produce nitrite ion at biological pH, nitrite ion reacts with oxygen to produce stable nitrate and nitrite, the quantities of these ions can be determined using Griess reagent [61]. 10 mM solution of sodium nitroprusside was taken 2 mL and dissolved in 0.5 mL phosphate buffer saline with

pH 7.4 is mixed with 0.5 mL of compound at various concentrations given in **Table 4**. The mixer was then incubated for 150 min at 25 °C. 0.5 mL of the incubated solution was withdrawn and mixed with Griess reagent (1 mL of sulphanic acid and 0.33% in 20% glacial acetic acid was mixed with 1 mL of naphthylethylenediamine dichloride, 0.1% w/v). The mixture was further incubated for 30 min and the absorbance was measured at 546 nm. The percentage nitric oxide radical inhibition was calculated using following equation;

$$\% \text{ inhibition of NO radical} = ([B_0 - B_1] / B_0) \times 100$$

Where, B_0 is the absorbance of the control and B_1 is the absorbance of the sample.

2.2.4.3 H₂O₂ method

The percentage H₂O₂ scavenging activity of the compounds were assessed according to the procedure described by Ruch *et al.* [62] The 40 mM solution of hydrogen peroxide was prepared in phosphate buffer (50 mM, pH = 7.4). 20 to 60 mg/mL compound was dissolved in distilled water and the solution was added to the solution of hydrogen peroxide. The absorbance of the reaction mixer was measured at 230 nm. The percentage H₂O₂ scavenging activity of the compounds was calculated by given equation.

$$\% \text{ inhibition of NO radical} = ([C_0 - C_1] / C_0) \times 100$$

Where, C_0 is the absorbance of the control and C_1 is the absorbance of the sample.

2.3 Computational Study

2.3.1 ADMET property prediction

A set of ADMET-related properties of the synthesized compounds were predicted by using Qikprop programs (Schrödinger, LLC, New York, NY, 2015) according to method described in **Chapter 2**.

2.3.2 Molecular Docking

The potential binding mode and the binding interaction of the ligand with Enoyl-ACP reductase (oxidoreductase) (PDB; 1QG6, 2NSD, 4TZK, 4TZZ) have been investigated by using Maestro, Schrödinger, LLC, New York, NY, 2012. The investigation of docking scores and energies was predicated using method described in **Chapter 2**.

2.3.4 Molecular Dynamics

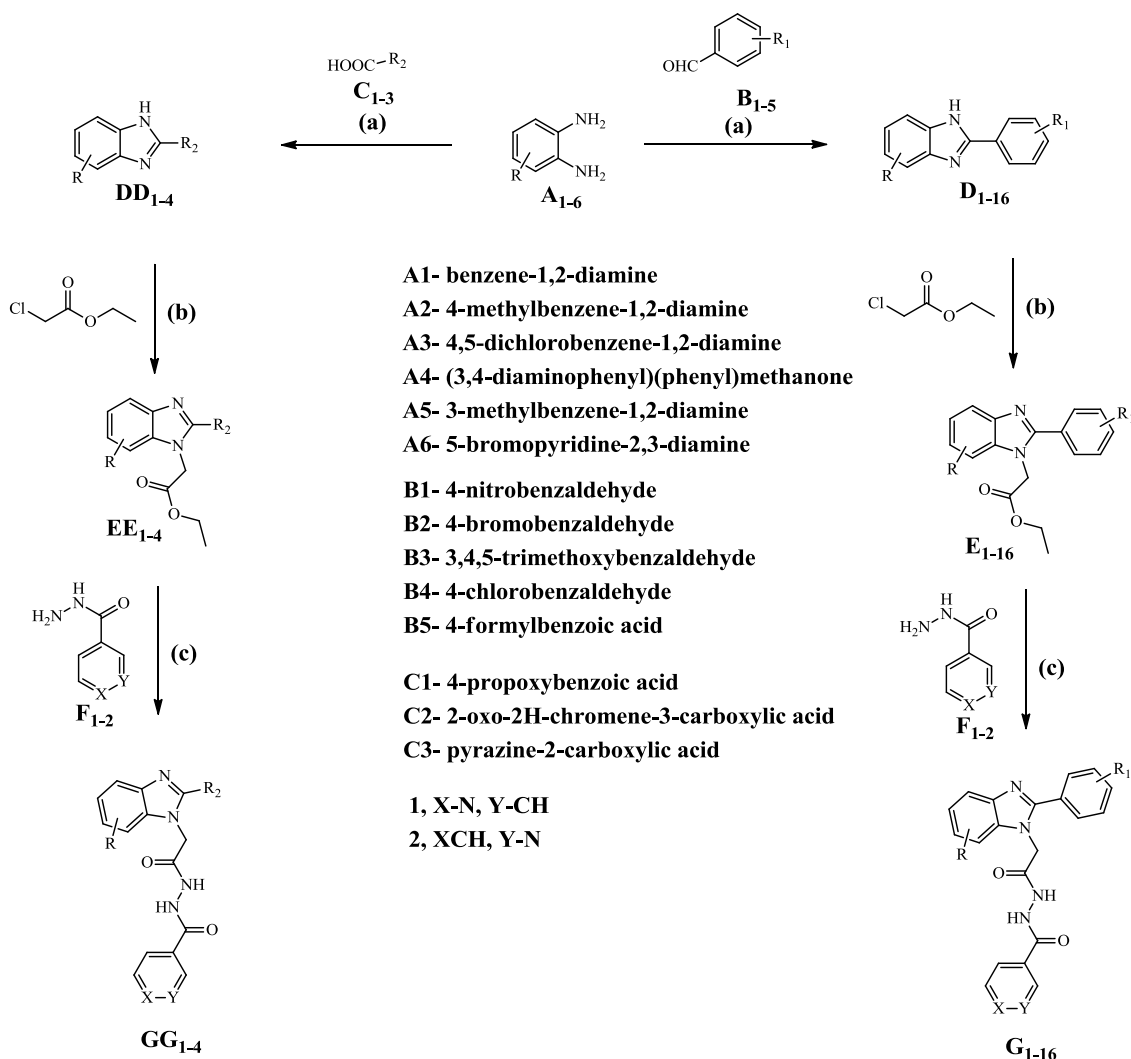
The molecular dynamics on 10 ns of the complex of ligand G7 with protein 4TZK was carried out with the help of molecular dynamics (MD) stimulation module, Desmond-GPU in maestro according to the procedure mentioned in **Chapter 3**.

3.0 Result and Discussion

3.1 Chemistry

The synthetic strategy for preparing the targeted N'-(2-(2-phenyl-1*H*-benzo[d]imidazol-1-yl)acetyl)isonicotinohydrazide (**G1-G16**) from nicotinic hydrazide (**F1-2**) and ethyl 2-(1*H*-benzo[d]imidazol-1-yl)acetate derivatives (**E1-E16**) was illustrated in **Scheme 1** and the synthesized derivatives with isolated yield is demonstrated in **Table 1**. The synthesis of the targeted compounds **G1-G16** and **GG1-GG4** is required three successive synthetic reaction. These reaction was synthesized by using reported synthetic protocol. In the first step we have synthesized compound substituted benzimidazole derivatives (**D1-D16**) by reaction between o-phenylenediamine (**A1-A6**) and substituted aldehyde (**B1-B5**), carboxylic acid derivative (**C1-C3**) using Methanol as solvent in the presence of 4N HCl with very good yield. The second step was done by treating ethyl chloroacetate with **D1-D16** to get **E1-E16**, **EE1-EE4** with good yield. This was followed by condensation of **E1-E16**, **EE1-EE4** and nicotinic hydrazide in absolute ethyl alcohol to yield the desired final compounds **G1-G16** and **GG1-GG4** (**Scheme 1**).

3.0 RESULT AND DISCUSSION



Reaction condition; (a). 4N HCl, Methanol, Reflux (b). Dry Acetone, 0-5°C Anhyd. K_2CO_3 (c). Ethanol, Reflux

Scheme 1. Schematic representation of the synthetic route of desired product G(1-16) and GG(1-4).

The newly synthesized compounds (**G1-G16**, **GG1-GG4**) was characterized by ^1H and ^{13}C -NMR spectroscopy method. In the ^1H -NMR spectrum of compound G1, the signals at 8.95 - 8.79 and 8.27 - 8.13 ppm were assigned for amide (-NH) protons. The -CH protons for pyridine ring appears at 7.98 - 7.86 and 7.86 - 7.71 ppm. The aromatic proton of benzimidazole motif and benzene ring was assigned at 7.86 - 7.71, 7.67, 7.29 and 6.27 ppm.

The signal of methylene -CH₂ was appear at the 4.92 ppm value. Furthermore, from the ^{13}C

NMR spectra, it was observed that the carbons of pyridine were observed at 150.79, 139.99 and 125.60 ppm. Whereas the carbon from amide (-C=O) was assigned at 169.14 and 166.90 ppm. The aliphatic carbon (-C-H) from the compound **G1** was observed at 46.50 ppm. The peaks at 154.11, 145.92, 135.89, 120.06 and 112.32 ppm was appeared for the carbon from benzimidazole motif. This data from the spectroscopic method validate the structure of the targeted compounds.

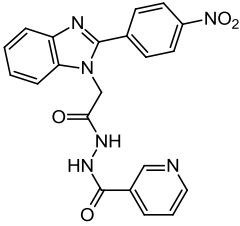
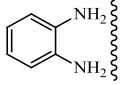
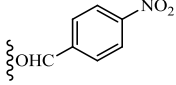
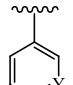
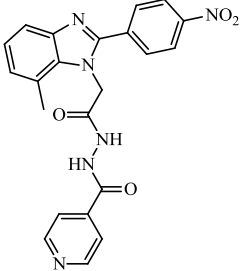
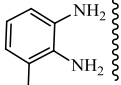
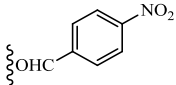
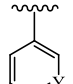
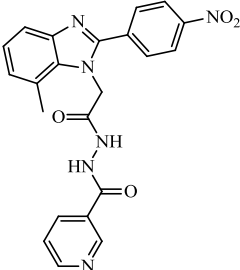
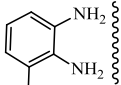
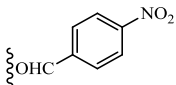
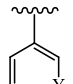
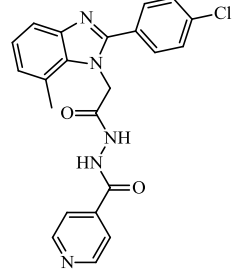
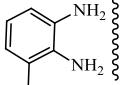
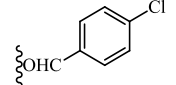
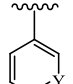
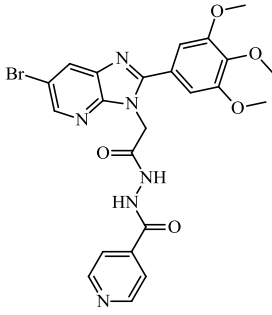
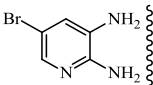
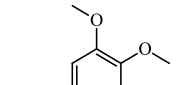
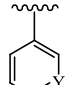
Table 1. The substituent details for the synthesized compounds G(1-16), GG(1-4) along with the details of melting point and isolated yield.

	G1 - G16		GG1 - GG4				
Entry	Compound	R	R ₁ & R ₂	R ₃	MW	MP	% Yield ^a
1					416.39	283-289	62
	G1	A1	R₁; B1	X-N, Y-CH			
2					464.31	294-271	52
	G1	A2	R₁; B2	X-N, Y-CH			

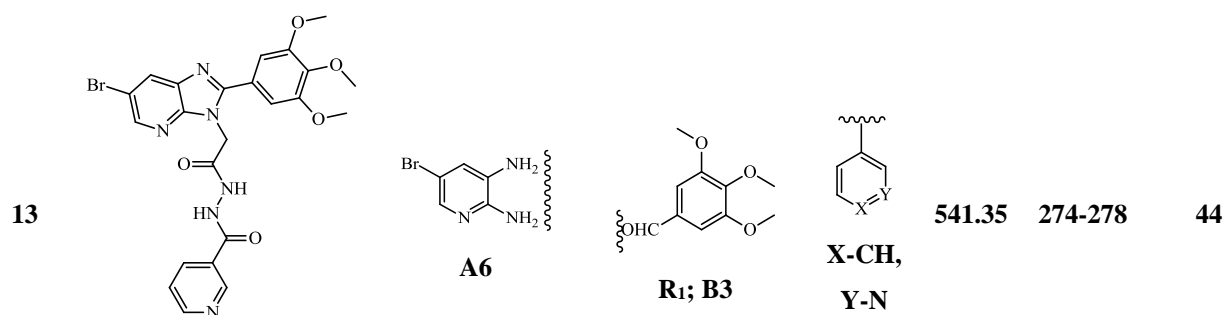
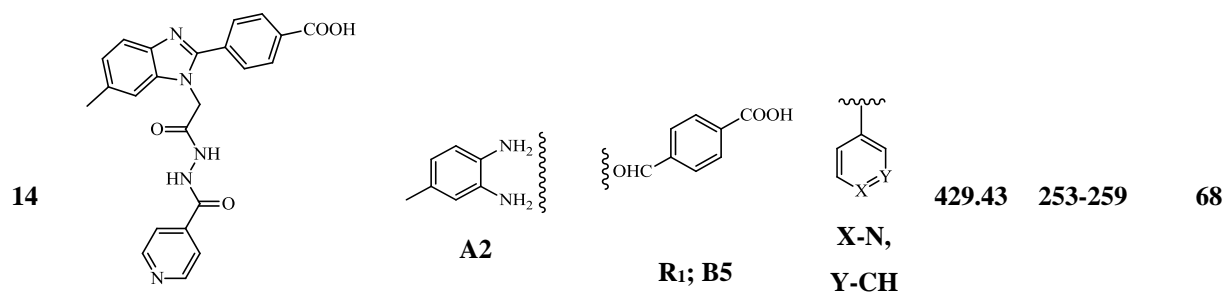
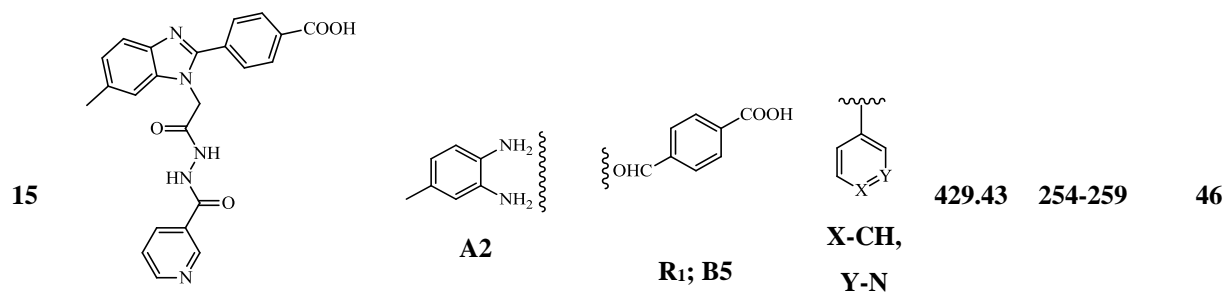
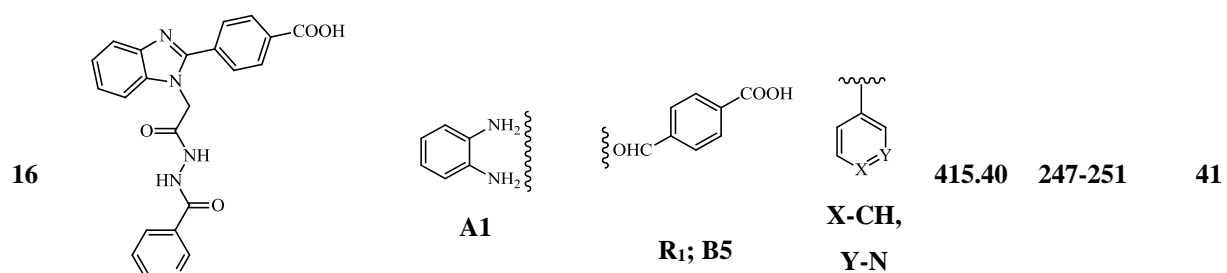
3.0 RESULT AND DISCUSSION

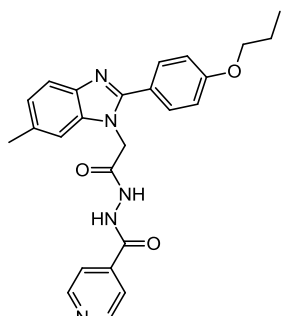
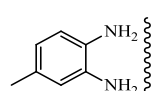
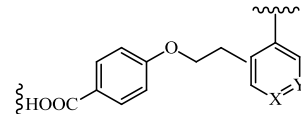
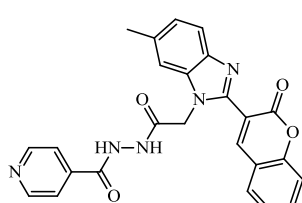
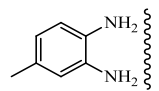
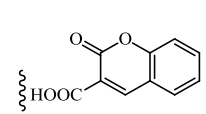
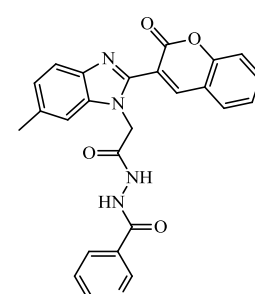
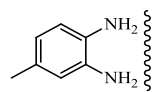
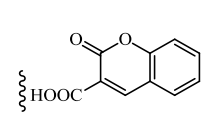
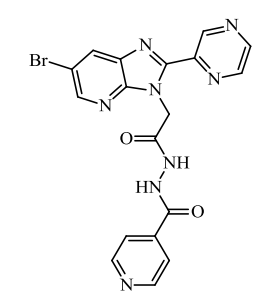
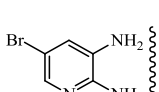
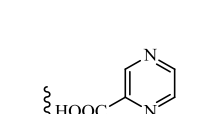
3					484.05	274-279	48
	G3	A3	R₁; B₁	X-N, Y-CH			
4					484.05	273-279	61
	G4	A3	R₁; B	X-CH, Y-N			
5					475.50	257-261	43
	G5	A2	R₁; B₃	X-N, Y-CH			
6					475.50	258-260	50
	G6	A2	R₁; B₃	XCH, Y-N			
7					537.57	282-287	67
	G7	A4	R₁; B₃	X-N, Y-CH			

3.0 RESULT AND DISCUSSION

8	 <p>G8</p>	 <p>A1</p>	 <p>R₁; B1</p>	 <p>X-CH, Y-N</p>	416.39	242-248	70
9	 <p>G9</p>	 <p>A5</p>	 <p>R₁; B1</p>	 <p>X-N, Y-CH</p>	430.42	245-249	63
10	 <p>G10</p>	 <p>A5</p>	 <p>R₁; B1</p>	 <p>X-CH, Y-N</p>	430.42	245-250	61
11	 <p>G11</p>	 <p>A5</p>	 <p>R₁; B4</p>	 <p>X-N, Y-CH</p>	419.86	257-262	55
12	 <p>G12</p>	 <p>A6</p>	 <p>R₁; B3</p>	 <p>X-N, Y-CH</p>	541.35	274-279	43

3.0 RESULT AND DISCUSSION

**G13****G14****G15****G16**

17				443.50	253-258	54
	GG1					
18				453.45	291-295	60
	GG2					
19				453.45	292-295	58
	GG3					
20				553.25	273-278	64
	GG4					

^a Isolated yield

3.2 Biological assay

3.2.1 *In vitro* anti-bacterial activity

All the synthesized compounds were subjected to anti-bacterial evaluation by determining minimum inhibitory concentration (MIC) on gram-positive and gram-negative

bacteria (*Escherichia coli* (MTCC-443), *Pseudomonas aeruginosa* (MTCC-1688), *Staphylococcus aureus* (MTCC-96), and *Streptococcus pyogenes* (MTCC-442)) and the results are summarized in **Table 2**, the result were compared with standard drug such as Ampicillin, Ciprofloxacin and Chloramphenicol.

In this primary evaluation, we observed that, most of the compounds have potential to inhibit the bacterial growth. Compound **G8** and **G14** strongly inhibit the *E. Coli* bacterial growth at MIC value 12.5 µg/mL. Further, analogue **G6** and **GG4** have displayed potent inhibiting potency towards *E. coli* (MIC= 25 µg/mL), while the compounds **G5** and **G7** also found to have a significant efficacy to inhibit the *E. coli* bacteria at MIC 50 µg/mL. Compound **GG4** have shown superior inhibition efficacy against *P. aeruginosa* at MIC 12.5 µg/mL. Compounds **G6**, **G8**, **G10**, **G12** and **G16** have displayed favourable activity against *P. aeruginosa* at MIC 50 µg/mL of each. However, rest of the compounds shows moderate activity against *P. aeruginosa*. In the case of *S. aureus* bacteria, compound **G6** and **G8** showed the best growth inhibitory activity with MIC value 25 µg/mL. Compound **G1**, **G14**, **GG1** and **GG4** inhibited the bacteria the *S. aureus* with MIC value 50, 62.5, 62.5 and 62.5 µg/mL, respectively. In addition, Compound **G5**, **G10**, **G14** and **G7** demonstrated acceptable anti-bacterial effect against *S. pyogenes* with MIC value 50, 50, 50 and 62.5 µg/mL, respectively. Here, compound **G1** have proven the efficiency to inhibit the bacteria *S. pyogenes* as compared to standard drug at MIC value 12.5 µg/mL.

3.2.2 *In vitro* anti-tuberculosis activity and MDR-TB study

The observed result from the primary biological screening of anti-bacterial evaluation encourage us to go for the next ant-tuberculosis study. Hence, the targeted compounds **G1-G16**, **GG1-GG4** were *in vitro* evaluated for their anti-tubercular activity against *Mycobacterium tuberculosis* H₃₇Rv using the Lowenstein-Jensen method and the

minimum inhibitory concentration is summarized in **Table 2**. Among the tested nicotinohydrazide derivatives, compound G8 emerged as the most potent number with significant anti-tuberculosis activity with a MIC value of 12.5 µg/mL. Compound **G14** and **G6** also able to have a potent activity with a MIC value of 25 µg/mL. In addition, analogue **G1**, **G5**, **G9**, **GG2** and **GG4** enhance good anti-tuberculosis activity with a MIC value at 50 µg/mL. Furthermore, Compound **G3**, **G10** and **GG1** were found moderate activity against H37Rv strain with a MIC value 62.5 µg/mL. All the reaming compounds were found to demonstrate reasonable activity at MIC value 100 to 500 µg/mL.

Table 2. *In vitro* anti-bacterial, anti-tuberculosis and MDR-TB screening result of synthesized compounds.

Entry	Compound Code	Anti-Bacterial				Anti-Tuberculosis	MDR-TB ^c MIC μg/mL
		Gram-negative ^a		Gram-positive ^b		H ₃₇ RV ^c MIC μg/mL	
		E.C. MIC μg/mL	P.A. MIC μg/mL	S.A. MIC μg/mL	S.P. MIC μg/mL		
1	G1	100	100	50	12.5	50	500
2	G2	100	125	100	100	100	250
3	G3	62.5	100	250	250	62.5	125
4	G4	100	125	250	500	100	125
5	G5	50	100	125	50	50	100
6	G6	25	50	25	100	25	100
7	G7	50	125	100	62.5	50	62.5
8	G8	62.5	50	25	100	12.5	62.5
9	G9	250	125	500	250	50	125
10	G10	100	50	125	50	62.5	250
11	G11	500	250	250	125	100	250
12	G12	12.5	50	100	125	500	1000
13	G13	100	125	250	250	100	100
14	G14	12.5	100	62.5	50	25	250
15	G15	125	62.5	500	250	100	250
16	G16	100	50	125	100	100	100
17	GG1	100	250	62.5	100	62.5	100
18	GG2	250	500	250	250	50	125

3.0 RESULT AND DISCUSSION

19	GG3	125	100	125	100	50	100
20	GG4	25	12.5	62.5	500	12.5	125
25	Ampicillin	100		250	100	-	-
26	Chloramphenicol	50	50	50	50	-	-
27	Ciprofloxacin	25	25	50	50	-	-
38	Isoniazid	-	-	-	-	0.20	-

^a Ec: *Escherichia coli* (MTCC-443); Pa: *Pseudomonas aeruginosa* (MTCC-1688).

^b Sa: *Staphylococcus aureus* (MTCC-96), Sp: *Streptococcus pyogenes* (MTCC-442).

^c Minimum inhibitory concentration against H₃₇Rv strain of *M. Tuberculosis* and Multi Drug-Resistance *Tuberculosis* (µg/mL).

Additionally, all the synthesized compounds further screened for MDR-TB INH-resistant clinically isolated strain. The observed result was summarized in **Table 2**. It was observed from the data table that, analogues **G7** and **G8** have an acceptable activity against MDR-TB strain with a MIC value 62.5 µg/mL. The rest of the compounds showed comparatively poor biological activity against MDR-TB strain. The *in vitro* poorer efficiency of the synthesized compounds against the strain may be not suitable to laboratory environments and different media, which may affect the effectiveness of certain inhibitors and demonstrated poor effect against the strain.

3.2.3 *In vitro* anti-malarial activity

The anti-malarial activity of all the synthesized analogues were evaluated against *Plasmodium falciparum* and the result are presented in IC₅₀ values in microgram (**Table 3**). The result of anti-malarial activity revealed that compounds **GG4** and **G14** have a potency to inhibit the growth of the organism with IC₅₀ value 0.37 and 0.48, µg/mL, respectively. Further, compound **G5**, **G12**, **GG2** and **G2** exhibited moderate activity as revealed from their IC₅₀ value 0.57, 0.63, 0.68 and 0.69 µg/mL, respectively. Rest of the compounds displayed poor activity against *P. falciparum* organism.

Additionally, the *in vitro* antifungal activity of the newly synthesized compounds were determined against *C. albicans*, *A. niger* and *A. clavatus*, the observed results are

presented in minimum inhibitory concentration and are given in **Table 3**. The screening result indicate that, among the tested compounds, **G14** and **GG4** showed significant antifungal activity against *C. clbicans* with MIC value 50 and 25 $\mu\text{g/mL}$, respectively. Compound **G5** against *A. niger* and compound **GG4** have demonstrated potent activity against *A. clavatus* with MIC value 100 $\mu\text{g/mL}$ which is comparable with standard drugs. All other compounds showed less inhibition and were less active against fungal microorganism. In general, among the tested compounds most of the compounds have better anti-malarial and anti-fungal activity and comparable with the activity of standard drugs.

Table 3. *In vitro* anti-malarial, anti-fungal screening result of synthesized compounds.

Entry	Compound	Anti-malarial		Anti-fungal	
		<i>P. falciparum</i>	<i>C. albicans</i>	<i>A. niger</i>	<i>A. clavatus</i>
		$\mu\text{g/mL}$ (mean IC50)	MTCC 227 $\mu\text{g/mL}$	MTCC 282 $\mu\text{g/mL}$	MTCC 1323 $\mu\text{g/mL}$
1	G1	0.94	500	1000	1000
2	G2	0.69	250	500	500
3	G3	1.30	250	500	250
4	G4	2.10	250	1000	1000
5	G5	0.57	100	100	500
6	G6	0.67	500	>1000	>1000
7	G7	1.36	1000	1000	1000
8	G8	2.08	100	>1000	>1000
9	G9	1.32	500	500	1000
10	G10	1.98	>1000	1000	>1000
11	G11	2.25	250	500	1000
12	G12	0.63	250	500	1000
13	G13	1.36	500	1000	>1000
14	G14	0.48	50	>1000	1000
15	G15	1.36	500	1000	>1000
16	G16	1.32	250	500	500
17	GG1	2.12	500	1000	500
18	GG2	0.68	500	500	1000

3.0 RESULT AND DISCUSSION

19	GG3	2.54	250	500	1000
20	GG4	0.37	25	1000	100
25	Quinine	0.268	500	1000	1000
26	Chloroquine	0.02	-	-	-
27	Nystatin	-	100	100	100
28	Greseofulvin	-	100	100	100

^a; *Plamodium falciparum*, ^b; *Candida albicans* ^c; *Aspergillus niger*, ^d; *Aspergillus clavatus*

3.2.4. Anti-Oxidant activity

Oxidation reaction can generate free radicals in human body which lead to chain reaction that may damage the cells of host organism. Antioxidant compounds play an important role as a health protecting factor by terminate the chain reaction. The naturally occurring antioxidants like Vitamin C, Vitamin E, phenolic acid, carotenes, phytet and phytoestrogens have been recognized as having the significance to reduce the risk of disease cause by oxidation. Compounds **G5**, **G8**, **G14** and **GG4** have shown significant anti-tuberculosis and MDR-TB activity and encourage us to go for further screening. Hence, these compounds were subjected to screen anti-oxidant activity using DPPH (1,1-diphenyl-2-picrilhydrazyl), NO (Nitric oxide) and H₂O₂ (Hydrogen peroxide) methods. The DPPH radical is stable scavenging model to evaluate the anti-oxidant activity, thereby it's extensively used to evaluate the anti-oxidant activity. DPPH can accept electron or hydrogen radical due to the stability of the radical and thus be converted in to stable, diamagnetic molecule. The selected compounds displayed significant antioxidant activity against all the methods. The evaluated antioxidant activity using DPPH radical was illustrated in **Table 4**, **Figure 2**. The hydrogen donating activity of the compounds was measured using DPPH radicals and demonstrated significant association could be found between the concentration of novel molecule and the percentage of inhibition. From the result table, it was observed that when compounds shows better activity as compared to

ascorbic acid (Standard). However, when the concentration was increased the activity of the compounds were decreased slightly. Compound **G14** was found to have superior antioxidant activity as compared to Standard compound ($IC_{50} = 7.5$) with IC_{50} value 6.04.

Table 4. *In vitro* % DPPH scavenging activity of the compounds.

Sample Code	Concentration ($\mu\text{g/ml}$)					IC_{50} Value
	0	25	50	75	100	
G5	41.09	68.91	78.07	88.88	96.36	9.02
G8	39.64	72.62	84.66	90.72	95.00	9.00
G14	43.8	76.21	81.97	90.11	97.32	6.04
GG4	38.04	66.47	75.09	87.76	93.14	10.03
Control (Ascorbic acid)	40.21	75.19	80.66	89.04	91.73	7.5

Table 5. *In vitro* % NO scavenging activity of the compounds.

Sample Code	Concentration ($\mu\text{g/ml}$)					IC_{50} Value
	0	25	50	75	100	
G5	33.95	41.08	53.84	65	79.42	43.00
G8	39.77	48.34	64.31	77.46	86.11	28.05
G14	32.48	55.67	63.84	73.08	92.37	18.00
GG	41.85	55.49	68.9	79.31	93.14	15.05
Control (Ascorbic acid)	42	51.73	60.18	79.31	90.21	21.05

Table 6. *In vitro* % H_2O_2 scavenging activity of the compounds.

Sample Code	Concentration ($\mu\text{g/ml}$)					IC_{50} Value
	0	25	50	75	100	
G5	41.09	49.66	57.94	73.58	90.31	25.08
G8	42.84	51.88	61.00	76.82	91.08	19.08
G14	41.36	57.33	71.08	84.19	93.78	12.05
GG4	43.61	51.84	56.17	69.04	91.84	18.00
Control (Ascorbic acid)	40.11	47.35	61.94	80.77	88.91	30.00

3.0 RESULT AND DISCUSSION

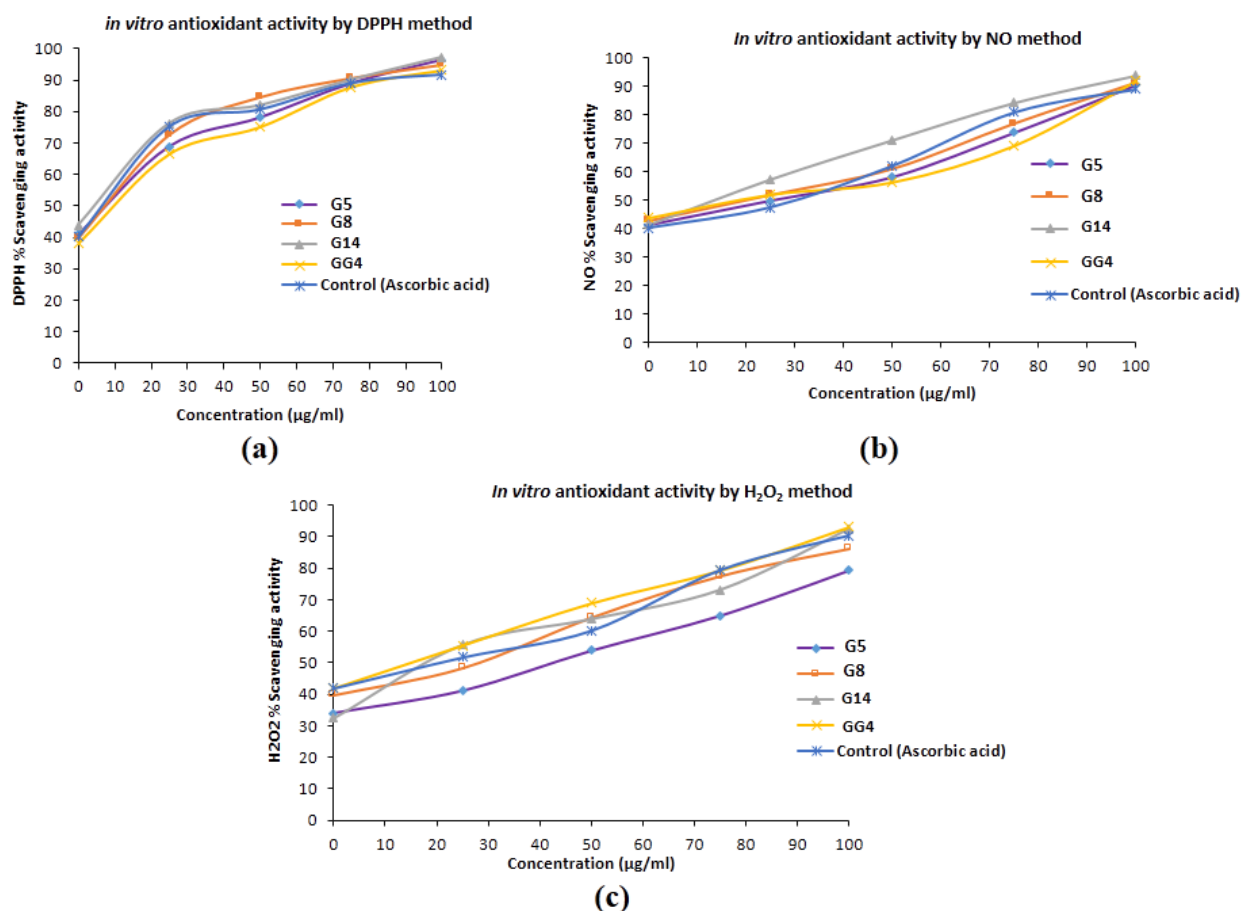


Figure 2. The effect of the compounds toward (a) DPPH, (b) NO and (c) H₂O₂ scavenging.

The nitric oxide method has been extensively used to evaluate the effectiveness of the free radical scavenging on various antioxidant analogues. Nitric oxide produced due to decomposition of sodium nitroprusside in aqueous media which interacts with oxygen at biological pH to produce nitrite ions. The nitrite ions were subjected to diazotization followed by azo coupling reaction to generate an azo dye and the absorption band was measured at 540 nm. The NO scavenging activity of the compounds are shown in **Table 5**, **Figure 2**. The observed result revealed that the activity of the compounds were increased while increasing concentration of dosage. Compounds **G14** (IC₅₀ = 18) and **GG4** (IC₅₀ = 15.05) demonstrated significant anti-oxidant activity as compared to standard compound

($IC_{50} = 21.05$) using NO scavenging method. Furthermore, Hydrogen peroxide radicals can damage DNA in the body by initiating lipid peroxidation which occurs by decomposition of H_2O_2 into oxygen and water. The hydrogen peroxide scavenging activity of the screened compounds are shown in **Table 6, Figure 2**. The analogue **G5** ($IC_{50} = 25.08$), **G8** ($IC_{50} = 19.08$) **G14** ($IC_{50} = 12.05$) and **GG4** ($IC_{50} = 18$) are found to have excellent H_2O_2 scavenging activity as compared to standard compound ($IC_{50} = 30$). The anti-oxidant study of the compounds suggest that these compounds have potent anti-oxidant activity and will be used as good anti-oxidant analogues in future.

3.3 Computational Study

3.3.1 ADMET property prediction

It has been analyzed the physically significant descriptors [65] and the pharmaceutically relevant properties of the synthesized compounds to validate our previous study (**Chapter 2**). The ADME properties of compound is thumb to evaluate a drug-like properties, in other words, to determine if a chemical compound has a certain biological activity and pharmacological properties that would likely make it an orally active drug in humans. The ADME properties were calculated for the compounds using QikProp module in maestro. The predicted pharmacokinetics properties of the targeted compounds are given in the **Table 7**. It was observed from the result table, the percentage human oral absorption in GI was observed between the range of 25 - 80% and above. The log BB is stand for blood /brain which found in the range of 95% drugs.

Table 7. Predicted ADME parameters for synthesized compounds.

Entry	Compound Code	Percent human oral absorption (>80% – high & <25% – poor)	QPlog BB (-3.0 – 1.5)	QPlog HERG (below -5)	QPPCaco (<25 poor, >500 great)	QPlog Kh _{sa} (-1.5 – 1.5)	PSA (70 – 200 Å)	QPlog S (-6.5 – 5)
1	agoG1	75.38	-2.289	-7.164	56.95	0.272	150.067	-5.587
2	bhoG2	100	-1.047	-7.136	461.904	0.65	104.93	-6.985
3	cgoG3	80.404	-2.115	-7.052	54.082	0.504	149.807	-7.04
4	cgpG4	80.368	-2.105	-7.023	54.192	0.501	149.967	-7.007
5	bioG5	100	-1.474	-6.849	455.795	0.512	127.732	-6.653
6	bipG6	100	-1.491	-6.884	449.078	0.499	127.974	-6.664
7	DioG7	83.89	-1.683	-7.188	349.32	0.426	128.217	-6.337
8	agpG8	75.876	-2.226	-6.372	64.446	0.287	151.067	-5.685
9	egoG9	80.189	-2.375	-7.598	67.484	0.498	145.57	-6.626
10	egpG10	78.417	-2.096	-6.806	73.473	0.336	146.159	-5.556
11	EjoG11	100	-0.899	-6.966	574.166	0.536	100.609	-6.425
12	fioG12	69.11	-1.447	-6.815	336.807	0.238	140.222	-6.469
13	fipG13	70.349	-0.997	-5.75	532.453	0.035	135.56	-4.913
14	bkoG14	64.856	-2.5	-5.305	41.48	0.138	154.167	-6.056
15	bkpG15	64.96	-2.494	-5.307	41.623	0.137	154.205	-6.053
16	akpG16	63.178	-2.415	-5.385	41.652	-0.013	154.318	-5.474
17	BloGG1	100	-1.554	-7.565	450.757	0.78	112.533	-7.472
18	bmoGG2	91.612	-1.418	-7.307	297.339	0.273	141.416	-5.866
19	bmpGG3	91.726	-1.413	-7.314	300.874	0.272	141.312	-5.868
20	fnoGG4	79.544	-1.434	-6.829	185.516	-0.396	137.738	-4.581
21	Isoniazid	66.83	-0.844	-3.588	275.34	-0.752	81.524	-0.051
22	Ampicillin	17.342	-1.3	-0.709	1.298	-0.929	139.523	-1.512
23	Ciprofloxacin	48.492	-0.671	-3.248	12.952	0.023	98.96	-3.793
24	Ethambutol	57.536	-0.326	-5.581	58.03	-0.754	69.477	0.551
25	Pyrazinamide	67.422	-0.72	-3.224	294.381	-0.818	78.425	-0.541

The log HERG (log IC₅₀) for the synthesized derivatives are found better than the standard compounds. The IC₅₀ represent the concentration of a drug that is required for 50% inhibition in vitro. The decreased value of logHERG indicates that the blockage of K⁺ ion channels is lower. Further, the caco permeability of the synthesized compounds was found great with the value of 25 -500 in nm/sec. The logK_{hsa} (serum protein binding) was found good as compared with 95% of drug range in most of the derivatives. The polar surface area and aqueous solubility of the targeted compounds were assessed the synthesized derivatives were found to be decreasing the acceptable range indicating incomplete solubility of the synthesized compounds which can be further enhanced using solubility enhancers. The value of ADME prediction of synthesized derivatives are closer to the drug-like properties.

3.3.2 Molecular Docking Study

All the synthesized derivatives **G1-G16**, **GG1-GG4** were docked in the active pocket of Enoyl-ACP reductase protein using four different PDB (1QG6, 2NSD, 4TZK, 4TZZ) to evaluate their binding efficiency. The motivation behind this was to investigate and predict the anti-tubercular activity of the compounds. The docking energies of the compounds against four different proteins are given in the **Table 8**. The results suggest that, the synthesized compounds have shown good binding affinity against receptor, which is superior to standard drug. The binding interaction of the ligand which have higher docking score against each protein are illustrated in **Figure 3 and 4**. As depicted in **Figure 4 (a) (b)**, compound G6 have found to generate three hydrogen bond with residue Gln40 (2.93 Å), Ala196 (2.21 Å) and Gly93 (1.56 Å) with lowest docking score (-7.316) against protein 1QG6.

Table 8. Binding energy of Compounds with target protein (kcal/mol).

PDB; 1QG6			PDB; 2NSD			PDB; 4TZK			PDB; 4TZZ		
Code	DS*	GE*	Code	DS*	GE*	Code	DS*	GE*	Code	DS*	GE*
G6	-7.316	-56.541	GG4	-6.914	-58.662	G7	-9.583	-66.311	G7	-8.052	-66.065
G12	-6.922	-63.12	GG2	-6.528	-53.219	GG3	-8.264	-56.276	GG2	-7.986	-49.612
G2	-6.88	-60.173	Isoniazid	-6.354	-32.868	GG1	-6.45	-54.49	GG3	-7.173	-53.499
G7	-6.758	-63.239	G6	-5.914	-53.473	G13	-6.282	-54.389	Isoniazid	-5.576	-27.301
G5	-6.638	-68.984	G14	-5.907	-55.98	G1	-6.273	-45.681	G1	-5.483	-47.349
G16	-6.632	-59.111	G16	-5.848	-57.497	G12	-6.252	-54.287	G5	-5.274	-54.201
G13	-6.55	-58.692	G7	-5.84	-39.507	G2	-5.644	-41.817	GG4	-5.07	-55.771
G3	-6.423	-62.15	GG1	-5.573	-55.418	G3	-5.571	-54.025	G6	-5.054	-52.484
G11	-6.276	-58.614	G5	-5.523	-44.93	G16	-5.455	-46.34	G13	-4.897	-52.813
G1	-6.199	-59.299	G12	-5.485	-52.1	G15	-5.362	-54.092	G15	-4.852	-50.427
G10	-6.108	-57.411	G4	-5.408	-51.694	GG2	-5.355	-57.3	G10	-4.672	-47.358
G4	-6.08	-60.072	G15	-5.343	-55.693	G14	-5.269	-53.378	G14	-4.615	-49.652
GG3	-5.943	-59.882	G2	-5.226	-41.589	G6	-5.176	-52.396	G12	-4.587	-46.574
GG1	-5.937	-53.97	G1	-5.094	-45.492	G10	-5.134	-51.307	GG1	-4.583	-52.77
G9	-5.896	-53.816	G8	-4.961	-47.954	G11	-5.1	-44.871	G4	-4.105	-50.887
Isoniazid	-5.805	-26.349	G3	-4.747	-42.773	G4	-5.02	-53.924	Pyrazinamide	-3.978	-23.934
GG2	-5.502	-58.582	G13	-4.551	-53.444	GG4	-5.016	-53.914	G16	-3.826	-47.771
G14	-5.494	-61.74	Pyrazinamide	-4.472	-29.88	G9	-4.316	-44.692	G9	-3.717	-50.429
GG4	-5.301	-58.054	GG3	-4.461	-50.934	Isoniazid	-4.09	-33.264	G2	-3.643	-45.144
G15	-5.12	-54.825	G11	-4.191	-49.867	Pyrazinamide	-3.775	-30.172	G8	-3.264	-44.14
Ethambutol	-4.769	-29.049	G9	-3.727	-55.093	Ethambutol	-3.678	-32.853	G11	-3.226	-44.595
Pyrazinamide	-4.398	-26.404	G10	-3.562	-47.483	G8	-3.269	-42.551	G3	-3	-47.16
G8	-2.987	-53.858	Ethambutol	-3.357	-33.152	G5	-2.537	-55.002	Ethambutol	-1.533	-28.126

*Where, DS: Docking Score, GE: Glide Energy (Modified Coulomb-Van der Waals energy),

The amide linkage in compound G6 able to generate two hydrogen bond with residue Gly93 and Gln40. Compound GG4 with docking score -6.914 forms hydrogen bonding with residue Met98 (2.35 Å) against protein 2NSD (**Figure 4 (c) (d)**). As illustrated in figure, Isoniazid contain -NH in analogue G7 makes a hydrogen bonding interaction with amino acid residue Gly96 with distance of 2.07 Å with lowest docking score -9.583 against protein 4TZK. Further, the compound G7 have found to generate aromatic ring contact with amino acid residue Tyr158 (**Figure 5 (a) (b)**).

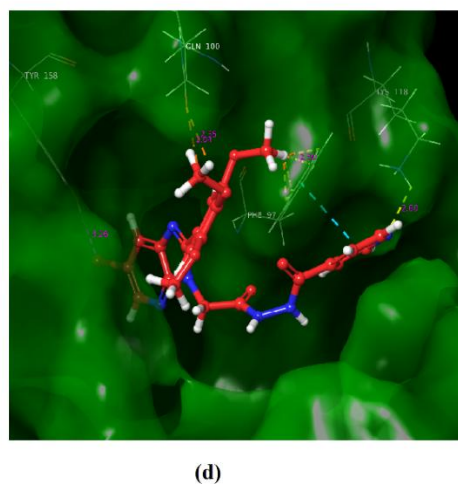
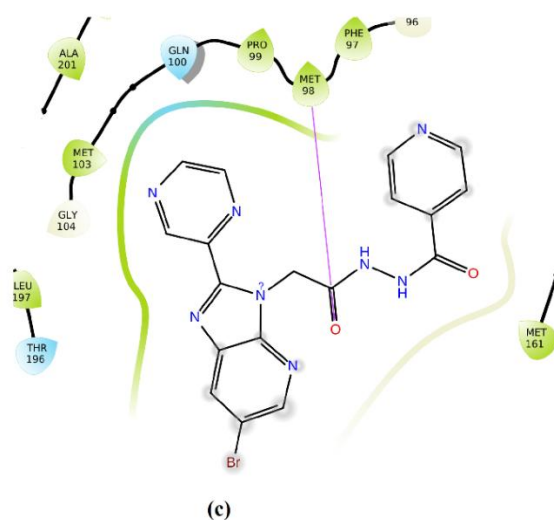
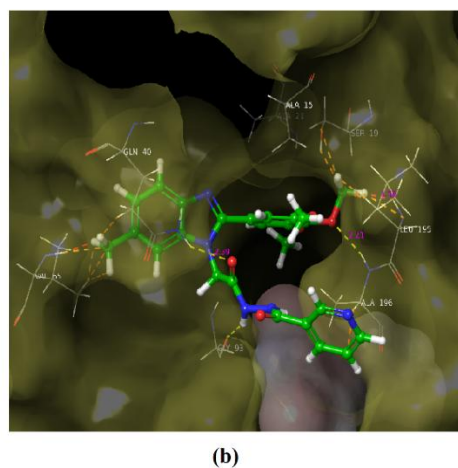
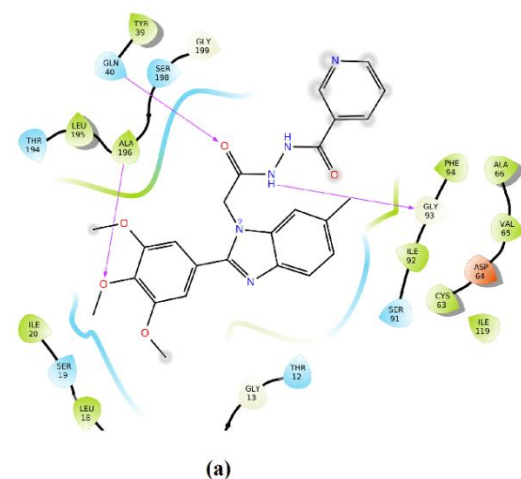


Figure 3. (a) 2d and (b) 3d docked representation of compound G6 at the active site of protein 1QG6. (c) 2d and (d) 3d representation of compound GG4 at the active site of protein 2NSD.

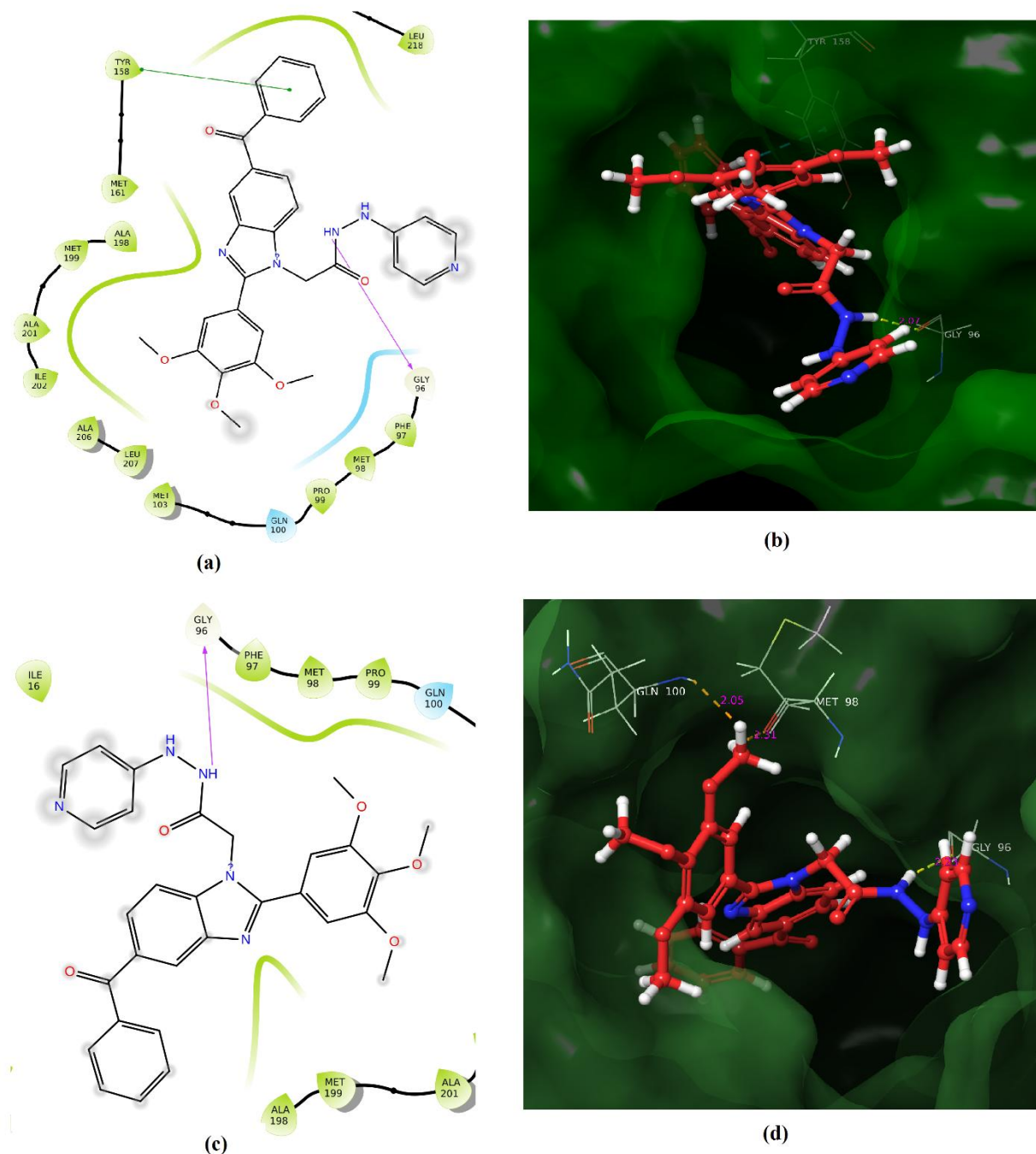


Figure 4. (a) 2d and (b) 3d representation of compound G7 at the active site of protein 4TZK. (c) 2d and (d) 3d representation of compound G7 at the active site of protein 4TZT.

In the case of protein 4TZT, the compound G7 was shown lowest binding energy and docking score (-8.052). The compound G7 have shown hydrogen bonding with amino acid residue Gly96 with distance of 2.05 Å (**Figure 5 (c) (d)**). Additionally, rest of the compounds also displayed potent binding affinity with all the protein target against Enoyl-ACP reductase enzyme from *Mycobacterium tuberculosis*. From the observed result, it can be stated that the *in vitro* activity of these compounds also support the *in silico* docking study. These compounds shows the potential to act as Enoyl-ACP reductase inhibitors and also as anti-tuberculosis agents.

3.3.3 Molecular dynamics Study

The docked protein (PDB: 4TZK) complexes of the ligand (G7) were subjected to 10 ns MD simulation. The RMSD value of the ligand with the protein complex is represented in **Figure 5 (a)**, which indicates that binding interactions pattern was quite higher between 2 to 3 ns after that it goes lower. However, the RMSD of the complex goes constant higher after 6 ns. For getting suggestion about the local changes along the protein chain, the RMSF value of the residues for the ligand-receptor complex are shown in **Figure 5 (c)**. The fluctuation between backbone and complex are shown in the **Figure 5 (f)**, which indicates that there was slight changes observed by time interval of 6 ns.

3.0 RESULT AND DISCUSSION

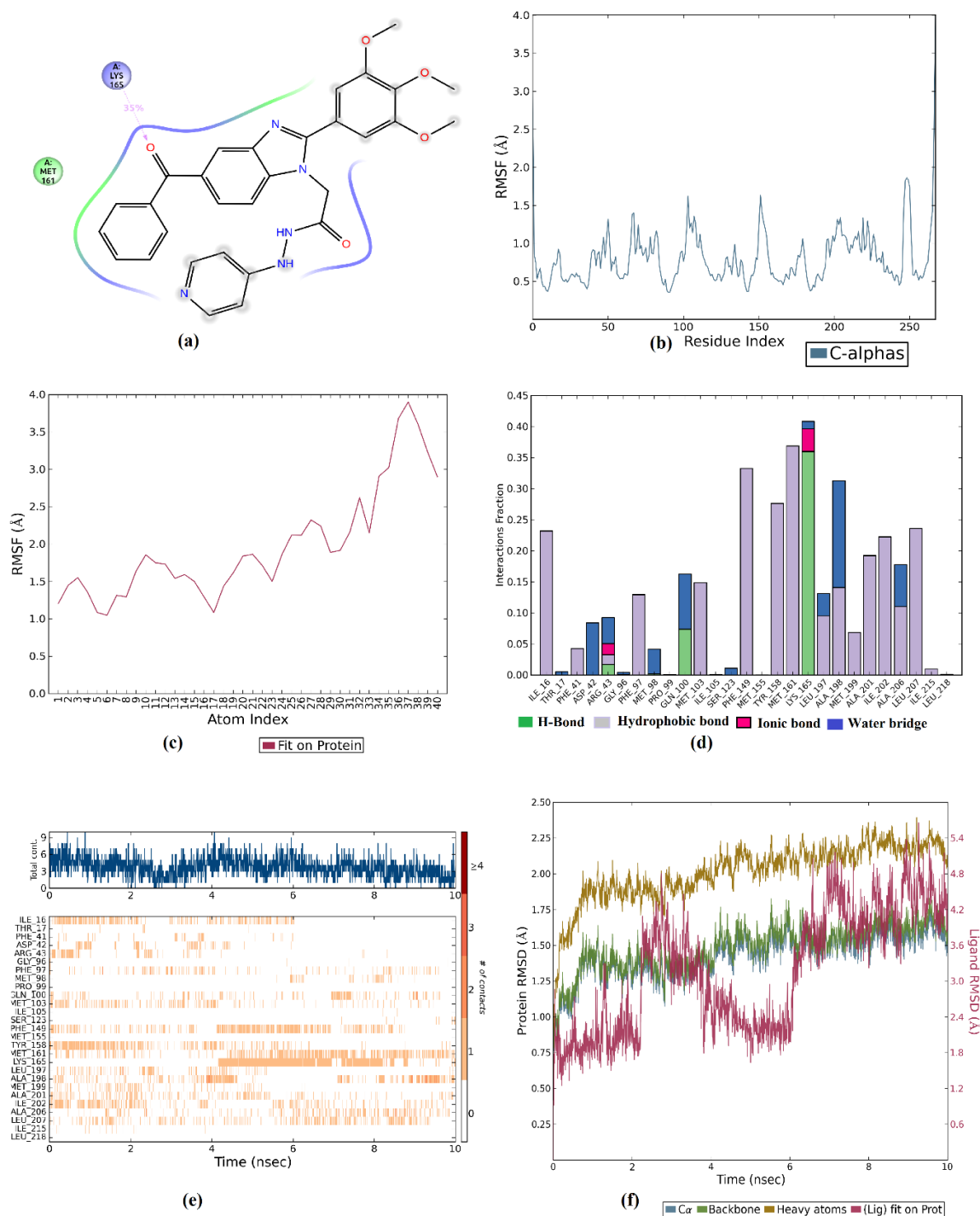


Figure 5. (a) Amino acid-ligand interaction (b) RMSF of receptor-ligand (c) RMSF of ligand (d) amino-acid residue-ligand interaction (e) Timeline representation of receptor-ligand (f) RMSD of protein-ligand over a period of 10 ns of docked complex of protein 4TZK and ligand G7.

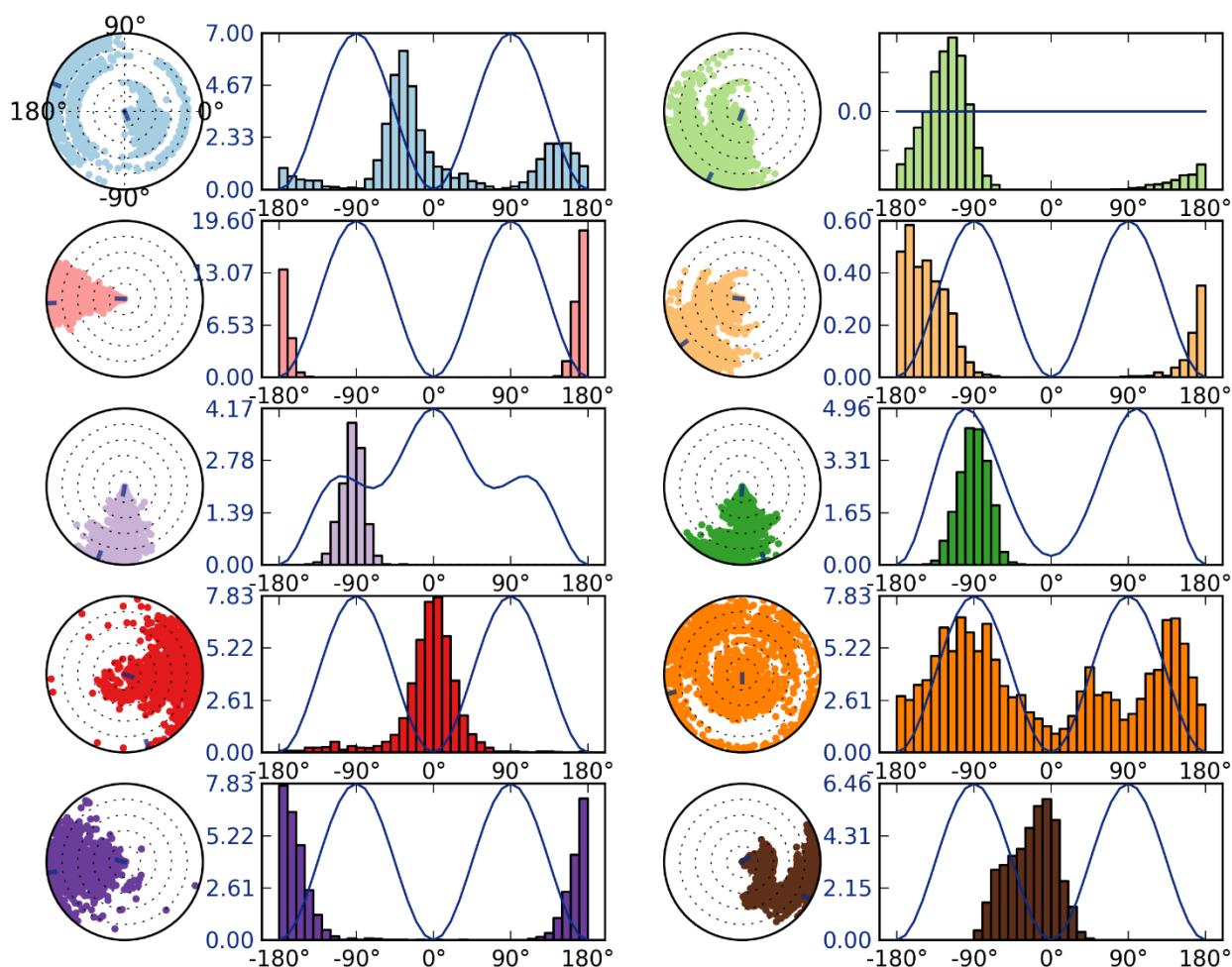


Figure 6. Plot and radial representation of ligand (G7) torsion showing rotatable bond over a time period of 10 ns.

The amino acids residues involved for ligand-protein interactions throughout the MD simulation were shown in **Figure 5 (d)**. The figure revealed that the docked complex displays many prominent hydrophobic interactions with residue Ile16, Phe97, Met103, Phe149, Tyr158, Met161, Ala201, Ile202 and Leu207 which are only maintained their interaction above 0.25 interaction fraction of the total simulation time. However, the ligand-receptor complex shows that there is a prominent Hydrogen bond with Gln100 and Lys165 along with hydrophobic, ionic and water interaction respectively. The torsional degrees of freedom in the ligand given by rotational bonds were investigated to understand the

dynamics associated with the ligand-receptor complex. Each rotatable bond torsion is accompanied by a dial plot and bar plots of the same color which are shown in **Figure 6**. Further, a total of ten rotatable bonds have been observed in the analogue **G7**. Ultimately the molecular dynamics study suggest that the capabilities of to act as anti-tuberculosis agents. Computational study indicates that compounds were found to be better inhibitors for protein as compared to standard drug. The present study revealed that the targeted compounds have a strong binding affinity towards Enoyl-ACP reductase protein for plausible anti-tuberculosis activity.

4.0 Conclusion

The synthesis of targeted compounds were performed with good yields from commercially available reagents, solvents and chemicals. All the synthesized derivatives were characterized by ^1H NMR and ^{13}C NMR spectroscopy method. Furthermore, the synthesized compounds subjected to anti-bacterial, anti-tuberculosis, MDR-TB and anti-malarial screening. In relation to the pharmacological activity, it was observed that analogue **G5**, **G6**, **G7**, **G8**, **G14**, **GG2** and **GG4** exhibited a significant anti-tubercular activity against H₃₇Rv. Moreover, compound **G7** and **G8** have shown acceptable MIC value **62.5 $\mu\text{g/mL}$** against INH resistant MDR-TB strain. The observed result suggest that these analogues have a potent anti-tuberculosis activity. Additionally, compounds **GG4** and **G14** have satisfactory anti-malarial activity against *P. falciparum* organism with IC₅₀ value **0.37** and **0.48 $\mu\text{g/mL}$** , respectively. Compound **GG4** and **G14** found significant anti-fungal activity against *C. albicans* with MIC value **50 $\mu\text{g/mL}$** which is better than standard drug (MIC = 100 $\mu\text{g/mL}$). The anti-oxidant scavenging activity of the compounds **G5**, **G8**, **G14** and **GG4** were evaluated by three different (DPPH, NO, H₂O₂) and compared with standard compound (Ascorbic acid). These compounds found to have better percentage inhibition against all the free radical methods as compared to standard compound. The problem of delivery across the many membranes enveloping the different bacteria could be a reason for the poor activity of some of these synthesized analogues. However, the potent compounds found from the biological, it is also possible that some of these compounds have other targets too and will be show good inhibition.

On the other hand, the ADME pharmacokinetics properties were predicted using QikProp module and the predicted result were found to have properties like 95 % drug molecules. The binding interaction and binding energies of the synthesized ligands were

4.0 CONCLUSION

predicted by molecular docking study against Enoyl-ACP reductase enzyme from *Mycobacterium tuberculosis* with four different protein (PDB ID; 1QG6, 2NSD, 4TZK, 4TZT). From the result, compounds **G6** (-7.316 kcal/mol against 1QG6), **GG4** -6.194 kcal/mol against 2NSD) and **G7** (-9.583 against 4TZK, -8.052 against 4TZT kcal/mol) shows strong binding with receptor as compared to isoniazid. Furthermore, the molecular dynamic simulation at 10 ns was performed to check the stability of the complex of ligand (**G7**) with protein 4TZK. The result form the MD simulation suggest that the stability of the complex remain constant till 6 ns and after that it increased slightly.

In conclusion, various study in the literature provide evidence of an endless search for new anti-Tuberculosis agents among the isonicotinohydrazide/nicotinohydrazide and benzimidazole derivatives. The results described in this study are favourable and suggest further development and optimization of these INH hybrid and nitrogen-nitrogen-containing indole analogues which may act as Enoyl-ACP reductase inhibitors.

References

1. Vasava MS, Bhoi MN, Rathwa SK, Borad MA, Nair SG, Patel HD. Indian Journal of Tuberculosis. 2017; 64(4):252-75.
2. https://www.who.int/tb/publications/global_report/tb18_ExecSum_web_4Oct18.pdf?ua=1.
3. Vasava MS, Nair SG, Rathwa SK, Patel DB, Patel HD. Indian Journal of Tuberculosis. 2018.
4. Velayati AA, Masjedi MR, Farnia P, Tabarsi P, Ghanavi J, ZiaZarifi AH, Hoffner SE. Chest. 2009; 136(2):420-5.
5. K. Rowland, Nature News (2012).
6. Loewenberg S. The Lancet. 2012; 379(9812):205.
7. Fauci AS, NIAID Tuberculosis Working Group. The Journal of infectious diseases. 2008; 197(11):1493-8.
8. Ahirrao P. Mini reviews in medicinal chemistry. 2008; 8(14):1441-51.
9. <http://www.newtbdrugs.org/pipeline.php>.
10. Villemagne B, Crauste C, Flipo M, Baulard AR, Deprez B, Willand N. European journal of medicinal chemistry. 2012; 51:1-6.
11. Ginsberg AM. Tuberculosis. 2010; 90(3):162-7.
12. Cole ST, Riccardi G. 2011; 14(5):570-6.
13. Maccari R, Ottana R, Vigorita MG. Bioorganic & medicinal chemistry letters. 2005; 15(10):2509-13.
14. Sinha N, Jain S, Tilekar A, Upadhyaya RS, Kishore N, Jana GH, Arora SK. Bioorganic & medicinal chemistry letters. 2005; 15(6):1573-6.
15. Mohamad S, Ibrahim P, Sadikun A. Tuberculosis. 2004; 84(1-2):56-62.

16. Maccari R, Ottana, R.; Bottari, B.; Rotondo, E.; Vigorita, MG. *Bioorganic & Medicinal Chemistry Letters*. 2004; 14:5731.
17. Bottari B, Maccari R, Monforte F, Ottana R, Vigorita MG, Bruno G, Nicolo F, Rotondo A, Rotondo E. *Bioorganic & medicinal chemistry*. 2001; 9(8):2203-11.
18. Slayden RA, Barry III CE. *Microbes and Infection*. 2000; 2(6):659-69.
19. Maccari R, Ottana R, Monforte F, Vigorita MG. *Antimicrobial agents and chemotherapy*. 2002; 46(2):294-9.
20. Manjashetty TH, Yogeeswari P, Sriram D. *Bioorganic & medicinal chemistry letters*. 2011; 21(7):2125-8.
21. Ramani AV, Monika A, Indira VL, Karyavardhi G, Venkatesh J, Jeankumar VU, Manjashetty TH, Yogeeswari P, Sriram D. *Bioorganic & medicinal chemistry letters*. 2012; 22(8):2764-7.
22. Hearn MJ, Cynamon MH, Chen MF, Coppins R, Davis J, Kang HJ, Noble A, Tussekine B, Terrot MS, Trombino D, Thai M. *European journal of medicinal chemistry*. 2009; 44(10):4169-78.
23. Vavříková E, Polanc S, Kočevár M, Horváti K, Bősze S, Stolaříková J, Vávrová K, Vinšová J. *European journal of medicinal chemistry*. 2011; 46(10):4937-45.
24. Vavříková E, Polanc S, Kočevár M, Košmrlj J, Horváti K, Bősze S, Stolaříková J, Imramovský A, Vinšová J. *European journal of medicinal chemistry*. 2011; 46(12):5902-9.
25. Boechat N, Ferreira VF, Ferreira SB, Ferreira MD, da Silva FD, Bastos MM, Costa MD, Lourenço MC, Pinto AC, Krettli AU, Aguiar AC. *Journal of medicinal chemistry*. 2011; 54(17):5988-99.
26. De P, Koumba Yoya G, Constant P, Bedos-Belval F, Duran H, Saffon N, Daffé M, Baltas M. *Design, Journal of medicinal chemistry*. 2011; 54(5):1449-61.

27. Sinha N, Jain S, Tilekar A, Upadhayaya RS, Kishore N, Jana GH, Arora SK. Bioorganic & medicinal chemistry letters. 2005; 15(6):1573-6.
28. <http://www.ctri.nic.in/Clinicaltrials/pmaindet2.php?trialid=922>.
29. <http://www.newtbdugs.org/project.php?id=155>
30. Nayyar A, Monga V, Malde A, Coutinho E, Jain R. Bioorganic & medicinal chemistry. 2007; 15(2):626-40.
31. Nayyar A, Jain R. Current medicinal chemistry. 2005; 12(16):1873-86.
32. Fu LM, Shinnick TM. Journal of Infection. 2007; 54(3):277-84.
33. Güven ÖÖ, Erdoğan T, Göker H, Yıldız S. Bioorganic & medicinal chemistry letters. 2007; 17(8):2233-6.
34. Dolzhenko AV, Chui WK, Dolzhenko AV, Chan LW. Journal of fluorine chemistry. 2005; 126(5):759-63.
35. He Y, Yang J, Wu B, Risen L, Swayze EE. Bioorganic & medicinal chemistry letters. 2004; 14(5):1217-20.
36. Kucukbay H, Durmaz R, Orhan E, Gunal S. IL Farmaco. 2003; 58: 431-437.
37. Chen CH, Chien MH, Kuo ML, Chou CT, Lai JJ, Lin SF, Thummanagoti S, Sun CM. Journal of combinatorial chemistry. 2009; 11(6):1038-46.
38. Ramanatham V, Vaidya S. D, Kumar S. B. V, Bhise U. N, Bhirud S. B, Mashelkar U. C. Eur. J. Med. Chem., 43, 2008; 43:986-995.
39. Stevenson C, Davies RJ. Chemical research in toxicology. 1999; 12(1):38-45.
40. Gabriel N. V, Hermenegilda M. D, Francisco A. C, Ismael L. R., Rafael V. M, Omar M. M, Samuel E. S. Bioorganic & Medicinal Chemistry Letters. 2006; 16: 4169-4173.

41. Rao A, Chimirri A, De Clercq E, Monforte AM, Monforte P, Pannecouque C, Zappalà M. *Il Farmaco*. 2002; 57(10):819-23.
42. Kumar JR, Jawahar L, Pathak DP. *Journal of Chemistry*. 2006; 3(4):278-85.
43. Razdan B., *Medicinal Chemistry*, 1St ed., Vol I , CBS Publisher, New Delhi, 2010, 335-337.
44. Satoskar RS, Bhandarkar SD, Ainapure SS, *Pharmacology and Pharmacotherapeutics*, Bombay, 14th ed., Vol-II, Popular Prakashan, Bombay, 1995; 716-719.
45. Alamgir M, Black DS, Kumar N. In *Bioactive Heterocycles III* 2007 (pp. 87-118). Springer, Berlin, Heidelberg.
46. <http://en.wikipedia.org/wiki/Domperidone>
47. Awadallah AM, Seppelt K, Shorafa H. *Tetrahedron*. 2006; 62(33):7744-6.
48. <http://en.wikipedia.org/wiki/Pimozide>
49. Friedland G. *Current infectious disease reports*. 2007;9(3):252.
50. Koul A, Arnoult E, Lounis N, Guillemont J, Andries K. *Nature*. 2011; 469(7331):483.
51. Tomioka H. *Current Pharmaceutical Design*. 2014; 20(27):4305-6.
52. Manjunatha UH, Smith PW. *Bioorganic & medicinal chemistry*. 2015; 23(16):5087-97.
53. Dai R, Wilson DJ, Geders TW, Aldrich CC, Finzel BC. *ChemBioChem*. 2014; 15(4):575-86.
54. Ellis S, Kalinowski DS, Leotta L, Huang ML, Jelfs P, Sintchenko V, Richardson DR, Triccas JA. *Molecular pharmacology*. 2014; 85(2):269-78.
55. Negi VJ, Sharma AK, Negi JS, Ram V. *International Journal of Pharmaceutical Chemistry*. 2012; 4:100-9.

56. Gund DR, Tripathi AP, Vaidya SD. European Journal of Chemistry. 2017; 8(2):149-54.
57. Mariappan G, Hazarika R, Alam F, Karki R, Patangia U, Nath S. Arabian Journal of Chemistry. 2015; 8(5):715-9.
58. Prajapati BK, Sen DD. American Journal of Advanced Drug Delivery. 2013; 1(1):151-9.
59. Brand-Williams W, Cuvelier ME, Berset CL. LWT-Food science and Technology. 1995; 28(1):25-30.
60. Marcocci L, Maguire JJ, Droylefaix MT, Packer L. Biochemical and biophysical research communications. 1994; 201(2):748-55.
61. Ruch RJ, Cheng SJ, Klaunig JE. Carcinogenesis. 1989; 10(6):1003-8.
62. Duffy EM, Jorgensen WL. Journal of the American Chemical Society. 2000; 122(12):2878-88.

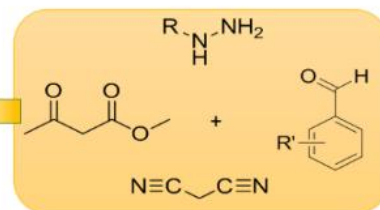
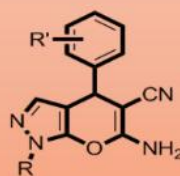
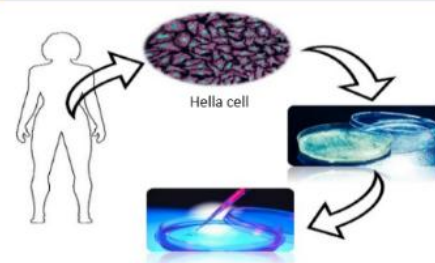
Chapter: 5

Synthesis, Characterization, in vitro biological evaluation and in silico study of novel 2-amino-3-cyano-4H-pyrans derivatives

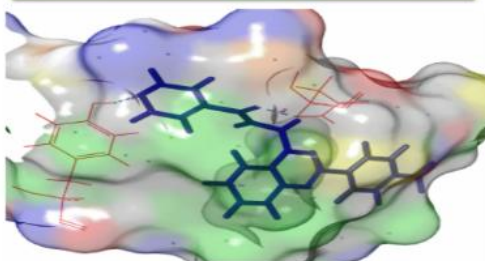
Biological Screening



Cytotoxicity Study



Molecular Docking



Molecular Dynamics

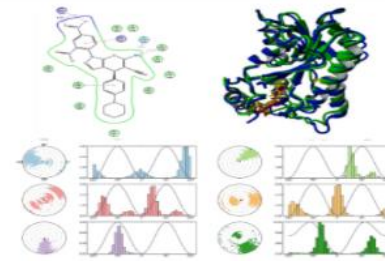


Table of Contents

1.0 Introduction	279
2.0 Methods and Materials	282
2.1 Chemistry.....	282
2.1.1 Synthesis of 4-(piperidin-1-yl) benzaldehyde derivatives (6a-6b).....	282
2.1.2 General procedure for the synthesis of 6-amino-1-(2,4-dinitrophenyl)-4- phenyl-1,4 dihydropyrano[2,3-c]pyrazole-5-carbonitrile derivatives (5a-5u).....	282
2.1.3. Synthesis of 6-amino-1-(2,4-dinitrophenyl)-4-(4-(piperidin-1-yl)phenyl)-1,4- dihydropyrano[2,3-c]pyrazole-5-carbonitrile derivatives (7a-7b).....	294
2.2 Biological assay.....	301
2.2.1 <i>In vitro</i> anti-bacterial activity	301
2.2.2 <i>In vitro</i> anti-tuberculosis activity and MDR-TB study.....	301
2.2.3 <i>In vitro</i> anti-malarial and anti-fungal activity.....	301
2.2.4 Cytotoxicity assay protocol	301
2.3 Computational Study.....	301
2.3.1 ADMET property prediction	301
2.3.2 Molecular Docking	302
2.3.4 Molecular Dynamics.....	302
3.0 Results and Discussion	303
3.1 Chemistry	303

3.2 Biology	311
3.2.1 <i>In vitro</i> anti-bacterial activity	311
3.2.3 <i>In vitro</i> anti-tuberculosis activity and MDR-TB study.....	313
3.2.4 <i>In vitro</i> anti-malarial activity and anti-fungal activity.....	314
3.2.5 Cytotoxicity assay.....	315
3.3 Computational Study.....	317
3.3.1 ADMET property prediction	317
3.3.2 Molecular docking.....	319
3.3.3 Molecular Dynamics.....	325
4.0 Conclusion.....	330
Reference.....	332

Summary:

In the present study, a series of pharmaceutically important, highly effective, simple kind of functionalized 6-amino-1-(2,4-dinitrophenyl)-4-phenyl-1,4-dihydropyrano[2,3-c]pyrazole-5-carbonitrile derivatives (**5a-5u**) have been synthesized through multicomponent reaction between various substituted aromatic aldehyde derivative (**4a-4u**), 2, 4-dinitrophenyl hydrazine (**1**), ethyl acetoacetate (**2**) and malononitrile (**3**) in the presence of SnCl₂ as a prompt catalyst using both microwave irradiation method as well as conventional method. The structure of synthesized compounds were confirmed by various spectroscopic methods such as ¹H-NMR, ¹³C-NMR, IR, Mass analysis and elemental analysis. All the synthesized compounds were subjected *in vitro* antibacterial, anti-tuberculosis screening and cytotoxicity MTT assay. *In vitro* biological study revealed that the synthesized compound **5a**, **7a** and **8a** are showing good anti-bacterial and anti-tuberculosis activity. The *in silico* study of ADME pharmacokinetic properties were also predicted for synthesized compounds for checking their bioavailability. Furthermore, molecular docking study of synthesized compounds with Enoyl-ACP reductase (oxidoreductase) was carried out to find out the binding affinity of compounds. Docking study demonstrated that compound **7b** and **7a** possessed superior binding affinity with target enzyme by strong hydrogen bonding. We have also carried out molecular dynamics simulation to check the stability of docked complex, conformational changes and primary molecular interaction.

1.0 Introduction

The treatment of infectious diseases that are predominantly endemic into the developing countries, it requires simple medications that can be produced in large quantities at low cost. Tuberculosis (TB) is most dangerous infectious disease which causes maximum fatality by subverting the immune system of the human host due to its long and wide association with humans and is often regarded as a successful pathogen [1]. According to the WHO report 2017, one-third of the world population is potentially infected with TB and millions of new cases occur worldwide every year [2].

There are many drugs available for TB in market, among them, Isoniazid (INH), Rifampicin, Pyrazinamide, and Ethambutol are four milestones in the treatment of TB for more than 50 years. Isoniazid is pro-drug which activate by the mycobacterial catalyse peroxidase (KatG), which inhibit the Enoyl-ACP reductase of the mycobacterial fatty-II type acid. It involved in the biosynthesis of mycolic acid eventually leading to cell death [3-4]. Studies have confirmed that the front-line anti-TB drugs such as INH and Ethionamide is primary targeting InhA gene [3]. Freundlich *et al.* revealed that potent triclosan derivatives that inhibit InhA in the nanomolar range with minimum inhibitory concentrations of 5–10 µg/mL [5]. Additionally, several compounds have been reported, such as arylamides derivatives [6], pyrrolidine carboxamide derivatives [7], pyrazole derivatives and indole-5-amides derivatives [8] which targeting InhA enzyme. However, the increasing prevalence of multi-drug-resistant TB (MDR-TB) and extensively drug-resistant TB (XDR-TB) decrease the effectiveness of these drugs against tuberculosis. Hence, to stop this infection, there is a burning requirement to develop inhibitors targeting InhA directly without prerequisite for activation [9].

Owing to the vast research on anti-tubercular activity, many synthesized heterocyclic compounds have efficiently displayed anti-tubercular activity. Current

literature is describing that the 4*H*-pyrans and pyran-annulated heterocyclic scaffolds have drawn considerable interest in medicinal chemistry from the last several years [10-16]. Figure 1 represents some of the bioactive pyran-annulated heterocyclic compounds which are good antibacterial agents. Various studies have indicated 4*H*-pyran derivatives display a potent activity against mycobacterium [17-29] as well as anticancer [20], cytotoxic [21], anti-inflammatory [22], anti-HIV [23-24], antimalarial [25], anti-hyperglycemic, and anti-dyslipidemic [26], anti-neurodegenerative disorders like Alzheimer's, Parkinson disease, Huntington's disease [27], and many more [28-39]. Furthermore, substituted 4*H*-pyran derivatives have encouraged increasing roles in synthetic methodologies to promising compounds in the field of medicinal [30], pigment industries [31], agrochemical and cosmetics [32]. Keeping this knowledge in mind, organic chemists have develop shortest synthetic routes to synthesize these heterocyclic compounds.

Nowadays, the most straightforward method for the synthesis of various heterocyclic compounds involves a three-component reaction or multi-component reaction to avoid the setbacks such as time-consuming reaction, low yields, toxicity of the chemicals, harmful organic solvents, dynamic reaction conditions and strenuous work-up. Additionally, Microwave-assisted synthesis is one of the most prominent method increasing its importance in the field of organic synthetic chemistry [33]. As compared to conventional heating, microwave irradiation method is much faster and provides higher practical yield in many organic synthesis [34]. Due to this advantage, this technique is widely used in the organic synthetic chemistry. In context to the already existing literature [35-45], we decided to use a simple, rapid, and effective one-pot MCR methodology to synthesize the targeted compounds.

In this current study, our aim was to synthesize new structural moieties under microwave irradiation and conventional heating. The 1,4-dihydropyrano[2,3-c]pyrazole derivatives synthesized by the reaction between substituted aldehyde derivatives, ethyl acetoacetate, malononitrile and 2,4-dinitrophenyl hydrazine using SnCl_2 as a rapid catalyst under solvent-free condition with good practical yields. All the synthesised compounds were screened for their anti-bacterial, anti-tuberculosis activity against various bacterial strain and cytotoxic activity against HeLa cell line.

In addition, the ADME pharmacokinetic properties of synthesized compounds have been studied for gaining preliminary information concerning their possibly drug-like profile. Moreover, based on the favourable *in vitro* antimicrobial results and by considering NADH-dependent Enoyl-Acyl Carrier Protein reductase (Enoyl-ACP reductase) as the target receptor, Molecular docking and molecular dynamics studies were performed against the active site of the NADH-dependent Enoyl-Acyl Carrier Protein reductase (Enoyl-ACP reductase) encoded by the *Mycobacterium* gene *inhA* *Mycobacterium tuberculosis* oxidoreductase enzyme.

2.0 Methods and Materials

2.1 Chemistry

All the chemicals and solvents were purchased from commercial source and were used in the reaction without further purification. Synthesis of the desired product was carried out using conventional and microwave irradiation (CEM Discover microwave system, Model No. 908010; Make up CEM Matthews, Inc, USA) methods. Melting points were determined by automated melting point system (MPA- Optimelt) and were uncorrected. The completion of the reactions was checked by thin layer chromatography (TLC). It is silica gel coated aluminium sheets (silica gel G60 F₂₅₄, Merck) which was visualized by UV radiation and various spray reagent. Elemental analysis were performed on vario MICRO cube, elemental CHNS analyser (Serial Number: 15084053). The IR spectra (in KBr pellets) were recorded on a Perkin-Elmer 377 spectrophotometer with absorption in cm⁻¹. ¹H and ¹³C NMR spectra were run on Bruker 400 and 100 MHz NMR spectrometer respectively, using DMSO-*d*₆ as solvents. The chemical shifts were expressed in parts per million (δ ppm) with TMS as internal reference. J values are given in hertz (Hz). Mass spectra was recorded on Advion Expression CMS, USA, with electro-spray ionization (ESI) was used as an ion source and ethanol: formic acid: water was used as a mobile phase. Column Chromatography with 60-120 mesh size of silica gel was used to purify the synthesized compounds.

2.1.1 Synthesis of 4-(piperidin-1-yl) benzaldehyde derivatives (6a-6b):

To a stirred solution of 4-fluoro aldehyde (**5g**) (1.0 eq.) in Methanol was added piperidine (1.0 eq.) and anhydrous Potassium carbonate (10 mol %) at room temperature. The resulting reaction mixture was heated at 130 °C for 20h. The progress of reaction was monitored by TLC plate. The reaction mixture was cooled at room temperature and then

poured it into ice cold water and kept for 24h. The solid product was precipitated out, filtered it using vacuum filtration and washed with hot water. The crude material was crystallized with Methanol to get pure compounds *4-(piperidin-1-yl) benzaldehyde derivatives 6a-6b* with good practical yield.

2.1.2 General procedure for the synthesis of 6-amino-1-(2,4-dinitrophenyl)-4-phenyl-1,4 dihydropyrano[2,3-c]pyrazole-5-carbonitrile derivatives (5a-5u):

2.1.2.1. Microwave irradiation method (Method A)

An equimolar mixture of 2,4-dinitrophenyl hydrazine (**1**) (1.0 eq.), ethyl acetoacetate (**2**) (1.0 eq.), malononitrile (**3**) (1.0 eq.), aldehyde derivatives (**4**) (1.0 eq.) in the presence of SnCl₂ (10 mol %) as a catalyst was irradiated in microwave (CEM Discover microwave) at 180 W for 10-20 min. The progress of the reaction was continuously observed by TLC analysis. After the consumption of the starting material, the reaction mixture was cooled at room temperature and poured into ice cold water and extracted with ethyl acetate (2 x 30 mL). The organic layer was dried with anhydrous Na₂SO₄, and the solvent was evaporated under reduced pressure. The crude material was purified through column chromatography using 20% Ethyl acetate in Hexane as an eluent to get desired compound 6-amino-1-(2,4-dinitrophenyl)-4-phenyl-1,4dihydropyrano[2,3-c]pyrazole-5-carbonitrile derivatives (**5a-5u**) with good practical yield (61-89%).

2.1.2.2. Conventional Method (Method B)

All the reaction mixtures were taken same as mention in Method A in 50 ml FBF (Flat Bottomed Flask) in the presence of SnCl₂ (10 mol %) as a catalyst. The reaction mixture was stirred at 80 °C for appropriate time mentioned in Table 1. The progress of the reaction was observed by TLC analysis. After the completion of reaction, the reaction mixture was allowed to cool at room temperature and poured into ice cold water and

extracted with ethyl acetate (2 x 30 mL). The organic layer was dried with anhydrous Na₂SO₄, and the solvent was evaporated under reduced pressure. The crude product (**5a-5u**) were then dried and further purified in to column chromatography using 20 % (v/v) Ethyl acetate: Hexane mixture as an eluent which resulted in 54-81 % yield of the final product.

2.1.2.3. 6-amino-1-(2,4-dinitrophenyl)-4-phenyl-1,4-dihydropyrano[2,3-c]pyrazole-5-carbonitrile (**5a**).

Brownish red solid, m.p. 240-243 °C.; Anal. Calc. for C₁₉H₁₂N₆O₅: C, 56.44; H, 2.99; N, 20.78; O, 19.78%. Found- C, 55.85; H, 2.34; N, 20.16%.; IR ν_{max} (KBr) cm⁻¹: 3323 (N-H_{str}), 3106 (C-H_{Aromatic, str}), 1613 (C=C_{str}), 2249 (-CN), 1023 (C-O_{str}), 1514, 1346 (N-O_{str}).; ¹H NMR: (400 MHz, DMSO): δ : 9.642 (s, 1H), 8.936-8.921 (d, J = 6 Hz, 1H), 8.471 (s, 2H), 8.150-8.142 (d, J = 3.2 Hz, 1H), 7.900 (s, 1H), 7.572-7.567 (d, J = 2 Hz, 2H), 7.358 (s, 1H), 7.317-7.313 (d, J = 1.6 Hz, 2H), 4.656 (s, 1H).; ¹³C NMR: (100 MHz, DMSO): δ : 174.91, 151.30, 145.86, 142.19, 139.87, 137.22, 135.31, 129.72, 129.46, 128.23, 128.10, 127.35, 125.29, 125.08, 119.78, 117.92, 116.89, 60.18, 28.14; ESI-MS: m/z Calculated 404.34, found [m/z] [M+H]⁺405.1.

2.1.2.4. (E)-6-amino-1-(2,4-dinitrophenyl)-4-styryl-1,4-dihydropyrano[2,3-c]pyrazole-5carbonitrile (**5b**).

Yellow solid, m.p. 248-251 °C.; Anal. Calc. for C₂₁H₁₄N₆O₅: C, 58.61; H, 3.28; N, 19.53; O, 18.59%. Found- C, 57.69; H, 3.10; N, 18.83%.; IR ν_{max} (KBr) cm⁻¹: 3417 (N-H_{str}), 2955 (C-H_{Aromatic, str}), 1686 (C=C_{str}), 2349 (-CN), 1270 (C-O_{str}), 1596, 1349 (N-O_{str}).; ¹H NMR: (400 MHz, DMSO): δ : 9.637 (s, 1H), 8.756 - 8.739 (s, J = 6.8 Hz 1H), 8.644 (s, 2H), 8.573 - 8.562 (d, J = 4.4 Hz, 1H), 7.958 (s, 1H), 7.635-7.620 (d, J = 6 Hz, 2H), 7.511-7.499 (d, J = 4.8 Hz, 1H), 7.480-7.469 (d, J = 4.4 Hz, 2H), 6.379-6.361 (s, J = 7.2 Hz, 1H), 6.035-

6.021 (d, $J = 5.6$ Hz, 1H), 4.357 (s, 1H).; ^{13}C NMR: (100 MHz, DMSO): δ ; 174.82, 152.01, 147.86, 142.97, 140.35, 136.24, 135.87, 131.02, 128.51, 128.48, 128.37, 128.04, 127.35, 127.02, 123.61, 127.02, 120.34, 119.76, 119.07, 118.65, 60.04, 28.17; ESI-MS: m/z Calculated 430.37, found $[m/z]$ $[\text{M}+\text{H}]^+$ 431.3.

2.1.2.5. 6-amino-4-(3-chlorophenyl)-1-(2,4-dinitrophenyl)-1,4-dihydropyrano[2,3-c]pyrazole-5-carbonitrile (5c).

Light yellow solid, m.p. 260-264 °C.; Anal. Calc. for $\text{C}_{19}\text{H}_{11}\text{ClN}_6\text{O}_5$: C, 52.01; H, 2.53; Cl, 8.08; N, 19.15; O, 18.23%. Found- C, 52.34; H, 2.24; N, 19.67%; IR ν_{max} (KBr) cm^{-1} : 3282 (N-H_{str}), 3093 (C-H_{Aromatic, str}), 1612 (C=C_{str}), 2192 (-CN), 1059 (C-O_{str}), 1512, 1344 (N-O_{str}).; ^1H NMR: (400 MHz, DMSO): δ ; 10.108 (s, 1H), 9.235-9.226 (d, $J = 3.6$ Hz, 1H), 8.982 (s, 2H), 8.834-8.821 (d, $J = 5.2$ Hz, 1H), 7.990 (s, 1H), 7.701-7.692 (d, $J = 3.6$ Hz, 2H), 7.508-7.490 (d, $J = 7.2$ Hz, 2H), 4.887 (s, 1H).; ^{13}C NMR: (100 MHz, DMSO): δ ; 174.62, 151.17, 146.43, 142.30, 140.79, 137.60, 137.21, 134.68, 129.73, 128.23, 127.88, 127.37, 125.62, 124.39, 120.03, 118.40, 117.79, 58.42, 26.54; ESI-MS: m/z Calculated 438.78 found, $[m/z]$ 438.2 $[\text{M}+\text{H}]^+$ 439.2.

2.1.2.6. 6-amino-4-(2,5-dimethoxyphenyl)-1-(2,4-dinitrophenyl)-1,4-dihydropyrano[2,3-c]pyrazole-5-carbonitrile (5d).

Brownish yellow solid, m.p. 286-289 °C.; Anal. Calc. for $\text{C}_{21}\text{H}_{16}\text{N}_6\text{O}_7$: C, 54.31; H, 3.47; N, 18.10; O, 24.12%. Found- C, 54.24; H, 3.31; N, 17.34%; IR ν_{max} (KBr) cm^{-1} : 3439 (N-H_{str}), 3076 (C-H_{Aromatic, str}), 1626 (C=C_{str}), 2352 (-CN), 1065 (C-O_{str}), 1525, 1381 (N-O_{str}).; ^1H NMR: (400 MHz, DMSO): δ ; 10.929 (s, 1H), 8.914-8.908 (d, $J = 2.4$ Hz, 1H), 8.589 (s, 2H), 8.432-8.420 (s, $J = 4.8$ Hz, 1H), 7.822 (s, 1H), 7.369 (s, 1H), 7.181-7.159 (d, $J = 8.8$ Hz, 1H), 7.066-7.052 (d, $J = 5.6$ Hz, 1H), 5.005 (s, 1H), 3.778 (s, 3H).; ^{13}C NMR: (100 MHz, DMSO): δ ; 175.35, 152.08, 151.62, 150.20, 144.78, 142.80, 139.83, 126.71, 124.63,

121.01, 117.90, 116.86, 115.32, 114.13, 113.67, 113.085, 60.64, 55.80, 54.58, 29.01; ESI-MS: m/z Calculated 464.39, found $[m/z]$ $[M+H]^+$ 465.2.

2.1.2.7. 6-amino-4-(2-chlorophenyl)-1-(2,4-dinitrophenyl)-1,4-dihydropyrano[2,3-c]pyrazole-5-carbonitrile (5e).

Brown solid, m.p. 260-264 °C.; Anal. Calc. for $C_{19}H_{11}ClN_6O_5$: C, 52.01; H, 2.53; Cl, 8.08; N, 19.15; O, 18.23%. Found- C, 52.42; H, 2.69; N, 19.40%; IR ν_{max} (KBr) cm^{-1} : 3425 (N-H_{str}), 2979 (C-H_{Aromatic, str}), 1595 (C=C_{str}), 2197 (-CN), 1060 (C-O_{str}), 1513, 1343 (N-O_{str}).; 1H NMR: (400 MHz, DMSO): δ ; 9.978 (s, 1H), 9.540-9.534 (d, $J=2.4$ Hz, 1H), 9.212 (s, 2H), 8.937-8.925 (s, $J = 4.8$ Hz, 1H), 7.962 (s, 1H), 7.802 (s, 1H), 7.404-7.398 (d, $J = 2.4$ Hz, 2H), 7.205-7.192 (d, $J = 5.2$ Hz, 2H), 4.895 (s, 1H).; ^{13}C NMR: (100 MHz, DMSO): δ ; 175.29, 152.00, 146.02, 143.77, 141.90, 39.68, 136.73, 131.90, 129.11, 128.48, 127.95, 126.64, 126.35, 124.51, 120.03, 117.64, 116.84, 58.97, 24.35; ESI-MS: m/z Calculated 438.78, found $[m/z]$ $[M+H]^+$ 439.3.

2.1.2.8. 6-amino-1-(2,4-dinitrophenyl)-4-(3-nitrophenyl)-1,4-dihydropyrano[2,3-c]pyrazole-5-carbonitrile (5f).

Yellow solid, m.p. 283-286 °C.; Anal. Calc. for $C_{19}H_{11}N_7O_7$: C, 50.79; H, 2.47; N, 21.82; O, 24.92%. Found- C, 51.24; H, 2.19; N, 21.32%; IR ν_{max} (KBr) cm^{-1} : 3316 (N-H_{str}), 3111 (C-H_{Aromatic, str}), 1619 (C=C_{str}), 2214 (-CN), 1030 (C-O_{str}), 1513, 1334 (N-O_{str}).; 1H NMR: (400 MHz, DMSO): δ ; 10.124 (s, 1H), 9.582-9.571 (d, $J=4.4$ Hz, 1H), 8.969 (s, 2H), 8.590-8.578 (d, $J = 4.8$ Hz, 1H), 8.504-8.496 (d, $J = 3.2$ Hz, 2H), 7.946 (s, 1H), 7.877-7.864 (d, $J = 5.2$ Hz, 2H), 4.681 (s, 1H).; ^{13}C NMR: (100 MHz, DMSO): δ ; 175.79, 151.14, 146.02, 145.82, 142.04, 140.60, 137.58, 136.43, 135.29, 133.82, 126.90, 123.73, 121.34, 120.15, 120.06, 119.83, 117.01, 59.42, 26.38; ESI-MS: m/z Calculated 449.33, found $[m/z]$ $[M+H]^+$ 450.1.

2.1.2.9. 6-amino-1-(2,4-dinitrophenyl)-4-(2-nitrophenyl)-1,4-dihydropyrano[2,3-c]pyrazole-5-carbonitrile (5g).

Yellow solid, m.p. 283-286 °C.; Anal. Calc. for C₁₉H₁₁N₇O₇: C, 50.79; H, 2.47; N, 21.82; O, 24.92%. Found- C, 50.19; H, 2.44; N, 21.17%; IR ν_{max} (KBr) cm⁻¹: 3313 (N-H_{str}), 2978 (C-H_{Aromatic, str}), 1597 (C=C_{str}), 2349 (-CN), 1088 (C-O_{str}), 1515, 1345 (N-O_{str}).; ¹H NMR: (400 MHz, DMSO): δ : 9.628 (s, 1H), 9.064-9.053 (d, *J* = 4.4 Hz, 1H), 8.8669 (s, 2H), 8.179-8.165 (d, *J* = 5.6 Hz, 1H), 8.342-8.312 (d, *J* = 12 Hz, 1H), 7.854-7.833 (d, *J* = 8.4 Hz, 1H), 7.546 (s, 1H), 7.530 (s, 1H), 7.461-7.455 (d, *J* = 2.4 Hz, 1H), 4.982 (s, 1H).; ¹³C NMR: (100 MHz, DMSO): δ : 176.28, 150.84, 150.05, 146.08, 141.62, 140.32, 137.82, 134.57, 133.34, 128.68, 127.10, 126.34, 123.93, 123.61, 119.83, 117.01, 116.30, 59.63, 25.67; ESI-MS: *m/z* Calculated 449.33, found [*m/z*] [M+H]⁺ 450.1.

2.1.2.10. 6-amino-1-(2,4-dinitrophenyl)-4-(furan-3-yl)-1,4-dihydropyrano[2,3-c]pyrazole-5-carbonitrile (5h).

Dark Red solid, m.p. 263-268 °C.; Anal. Calc. for C₁₇H₁₀N₆O₆: C, 51.78; H, 2.56; N, 21.31; O, 24.35%. Found- C, 50.91; H, 2.39; N, 21.67%; IR ν_{max} (KBr) cm⁻¹: 3330 (N-H_{str}), 3121 (C-H_{Aromatic, str}), 1625 (C=C_{str}), 2211 (-CN), 1180 (C-O_{str}), 1553, 1349 (N-O_{str}).; ¹H NMR: (400 MHz, DMSO): δ : 9.561 (s, 1H), 8.884-8.875 (d, *J* = 3.6 Hz, 1H), 8.585 (s, 2H), 8.382-8.371 (s, *J* = 4.4 Hz, 1H), 7.676 (s, 1H), 7.340-7.328 (d, *J* = 4.8 Hz, 2H), 6.453-6.442 (d, *J* = 4.4 Hz, 1H), 4.720 (s, 1H).; ¹³C NMR: (100 MHz, DMSO): δ : 175.14, 152.24, 148.07, 143.58, 143.29, 141.06, 140.47, 137.01, 127.68, 124.78, 120.09, 119.81, 118.97, 118.00, 109.71, 59.47, 22.59; ESI-MS: *m/z* Calculated 394.30, found [*m/z*] [M+H]⁺ 395.2.

2.1.2.11. 6-amino-1-(2,4-dinitrophenyl)-4-(pyridin-2-yl)-1,4-dihydropyrano[2,3-c]pyrazole-5-carbonitrile (5i).

Brownish Red Solid, m.p. 272-276 °C.; Anal. Calc. for C₁₈H₁₁N₇O₅: C, 53.34; H, 2.74; N, 24.19; O, 19.74%. Found- C, 54.25; H, 2.34; N, 23.52%; IR ν_{max} (KBr) cm⁻¹: 3063 (N-H_{str}), 2956 (C-H_{Aromatic, str}), 1628 (C=C_{str}), 2798 (-CN), 1123 (C-O_{str}), 1628, 1352 (N-O_{str}).; ¹H NMR: (400 MHz, DMSO): δ ; 9.534 (s, 1H), 8.970 (s, 1H), 8.813 (d, 2H), 8.452 (s, 1H), 8.180 (s, 1H), 7.821 (s, 1H), 7.590-7.582 (d, J = 3.2 Hz, 1H), 7.478-7.462 (d, J = 6.4 Hz, 1H), 6.594 (s, 1H), 4.565 (s, 1H).; ¹³C NMR: (100 MHz, DMSO): δ ; 172.85, 156.40, 150.35, 148.54, 147.03, 141.76, 141.02, 137.81, 136.38, 128.57, 124.78, 123.39, 120.47, 120.02, 118.71, 117.50, 59.05, 27.81; ESI-MS: m/z Calculated 405.324, found [m/z] [M+H]⁺ 406.1.

2.1.2.12. 6-amino-1-(2,4-dinitrophenyl)-4-(pyridin-4-yl)-1,4-dihydropyrano[2,3-c]pyrazole-5-carbonitrile (5j).

Red Solid, m.p. 272-275 °C.; Anal. Calc. for C₁₈H₁₁N₇O₅: C, 53.34; H, 2.74; N, 24.19; O, 19.74%. Found- C, 53.28; H, 2.65; N, 23.75%; IR ν_{max} (KBr) cm⁻¹: 3669 (N-H_{str}), 2777 (C-H_{Aromatic, str}), 1616 (C=C_{str}), 2354 (-CN), 1031 (C-O_{str}), 1533, 1359 (N-O_{str}).; ¹H NMR: (400 MHz, DMSO): δ ; 9.865 (s, 1H), 8.946-8.933 (s, J = 5.2 Hz, 1H), 8.265 (s, 2H), 8.255-8.247 (s, J = 3.2 Hz, 1H), 7.953-7.943 (d, J = 4 Hz, 2H), 7.440-7.426 (d, J = 5.6 Hz, 2H), 7.281 (s, 2H), 4.968 (s, 1H).; ¹³C NMR: (100 MHz, DMSO): δ ; 150.35, 149.79, 146.79, 146.12, 142.53, 140.58, 137.14, 127.83, 124.69, 124.27, 123.77, 120.35, 118.94, 118.06, 60.10, 28.90; ESI-MS: m/z Calculated 405.32, found [m/z] [M+H]⁺ 406.3.

2.1.3.13. 6-amino-4-(4-(dimethylamino)phenyl)-1-(2,4-dinitrophenyl)-1,4-dihydropyrano[2,3-c]pyrazole-5-carbonitrile (5k).

Brownish green solid, m.p. 275-279 °C.; Anal. Calc. for C₂₁H₁₇N₇O₅: C, 56.38; H, 3.83; N, 21.91; O, 17.88%. Found- C, 56.15; H, 3.11; N, 20.57%; IR ν_{max} (KBr) cm⁻¹: 3324 (N-H_{str}), 2986 (C-H_{Aromatic, str}), 1692 (C=C_{str}), 2208 (-CN), 1187 (C-O_{str}), 1522, 1356 (N-O_{str}). ¹H NMR: (400 MHz, DMSO): δ ; 9.513 (s, 1H), 8.834-8.824 (s, J = 4 Hz, 1H), 8.413 (s, 2H), 8.285-8.278 (d, J = 2.8 Hz, 1H), 7.880 (s, 1H), 7.385-7.374 (d, J = 4.4 Hz, 2H), 6.794-6.782 (d, J = 4.8 Hz, 2H), 4.571 (s, 1H) 2.9335 (s, 6H).; ¹³C NMR: (100 MHz, DMSO): δ ; 175.69, 151.12, 150.06, 145.67, 142.20, 139.92, 138.29, 129.11, 128.76, 127.08, 124.81, 124.51, 120.34, 117.70, 116.64, 112.83, 112.09, 60.49, 42.76, 42.7, 29.38; ESI-MS: m/z Calculated 447.40, found [m/z] [M+H]⁺ 448.3.

2.1.2.14. 6-amino-1-(2,4-dinitrophenyl)-4-(3,4,5-trimethoxyphenyl)-1,4-dihydropyrano[2,3-c]pyrazole-5-carbonitrile (5l).

Light orange solid, m.p. 296-298 °C.; Anal. Calc. for C₂₂H₁₈N₆O₈: C, 53.44; H, 3.67; N, 17.00; O, 25.89. Found- C, 53.20; H, 3.27; N, 17.13%; IR ν_{max} (KBr) cm⁻¹: 3312 (N-H_{str}), 3098 (C-H_{Aromatic, str}), 1621 (C=C_{str}), 2312 (-CN), 1135 (C-O_{str}), 1512, 1335 (N-O_{str}).; ¹H NMR: (400 MHz, DMSO): δ ; 9.328 (s, 1H), 8.871-8.846 (d, J = 10 Hz, 1H), 8.364 (s, 2H), 7.952 (s, 1H), 6.748-6.720 (d, J = 11.2 Hz, 1H), 6.671-6.654 (d, J = 6.8 Hz, 1H), 4.483 (s, 1H), 3.589 (s, 9H).; ¹³C NMR: (100 MHz, DMSO): δ ; 175.19, 151.75, 151.50, 150.18, 143.93, 142.76, 138.92, 125.68, 123.53, 121.13, 117.86, 116.37, 115.40, 114.34, 112.59, 112.21, 60.37, 54.76, 53.87, 29.21; ESI-MS: m/z Calculated 494.41, found [m/z] [M+H]⁺ 495.2.

2.1.2.15. 6-amino-1-(2,4-dinitrophenyl)-4-(4-fluorophenyl)-1,4-dihydropyrano[2,3-c]pyrazole-5-carbonitrile (5m).

Dark Brown solid, m.p. 254-257 °C.; Anal. Calc. for C₁₉H₁₁N₆O₅F: C, 54.03; H, 2.63; F, 4.50; N, 19.90; O, 18.94 %; found C, 54.32; H, 2.14; N, 19.02%; IR ν_{max} (KBr) cm⁻¹: 3325 (N-H_{str}), 3036-2028 (C-H_{Aromatic}), 1615 (C=C_{str}), 2230 (-CN), 1163 (C-O_{str}), 1511, 1377 (N-O_{str}); ¹H NMR: (400 MHz, DMSO): δ 10.034 (s, 1H), 9.358 - 9.341 (d, J = 6.8 Hz, 1H), 9.039 (s, 2H), 8.649 - 8.635 (d, J = 5.6 Hz, 1H), 7.967 (s, 1H), 7.161 - 7.140 (d, J = 8.4 Hz, 2H), 7.051 - 7.036 (d, J = 6 Hz, 2H), 4.562 (s, 1H); ¹³C NMR: (100 MHz, DMSO): δ 169.95, 158.82, 150.74, 145.90, 142.33, 140.39, 138.86, 130.84, 130.31, 129.38, 128.07, 124.19, 121.32, 118.81, 118.04, 116.41, 115.80, 59.95. 27.93; ESI-MS: m/z Calculated 422.33, found [m/z] [M+H]⁺ 423.5.

2.1.2.16. 6-amino-4-(4-chlorophenyl)-1-(2,4-dinitrophenyl)-1,4-dihydropyrano[2,3-c]pyrazole-5-carbonitrile (5n).

Brown solid, m.p. 260-265 °C.; Anal. Calc. for C₁₉H₁₁ClN₆O₅: C, 52.01; H, 2.53; Cl, 8.08; N, 19.15; O, 18.23%. Found- C, 52.38; H, 2.26; N, 19.55%; IR ν_{max} (KBr) cm⁻¹: 3317 (N-H_{str}), 2921 (C-H_{Aromatic, str}), 1615 (C=C_{str}), 2209 (-CN), 1180 (C-O_{str}), 1521, 1331 (N-O_{str}).; ¹H NMR: (400 MHz, DMSO): δ : 10.089 (s, 1H), 8.986-8.978 (s, J = 3.2 Hz, 1H), 8.692 (s, 2H), 8.495-8.482 (s, J = 5.2 Hz, 1H), 7.989 (s, 1H), 7.692-7.654 (d, J = 15.2 Hz, 2H), 7.492-7.480 (d, J = 4.8 Hz, 2H), 4.892 (s, 1H).; ¹³C NMR: (100 MHz, DMSO): δ : 170.31, 150.88, 145.89, 142.67, 140.39, 138.30, 132.35, 131.27, 130.65, 130.51, 127.55, 125.81, 125.32, 125.06, 120.32, 118.21, 117.73, 59.48, 28.38; ESI-MS: m/z Calculated 438.78, found [m/z] [M+H]⁺ 439.4.

2.1.2.17. 6-amino-4-(4-cyanophenyl)-1-(2,4-dinitrophenyl)-1,4-dihydropyrano[2,3-c]pyrazole-5-carbonitrile (5o).

Light yellow solid, m.p. 266-268 °C.; Anal. Calc. for C₂₀H₁₁N₇O₅: C, 55.95; H, 2.58; N, 22.84; O, 18.63%. Found- C, 53.89; H, 2.68; N, 21.38%; IR ν_{max} (KBr) cm⁻¹: 3443 (N-H_{str}), 3028 (C-H_{Aromatic, str}), 1696 (C=C_{str}), 2324 (-CN), 1124 (C-O_{str}), 1498, 1365 (N-O_{str}); ¹H NMR: (400 MHz, DMSO): δ : 9.724 (s, 1H), 8.954 - 8.942 (d, 1H), 8.571 (s, 2H), 8.336 - 8.321 (d, *J* = 6 Hz, 1H), 7.898 (s, 1H), 7.620-7.612 (d, *J* = 3.2 Hz, 2H), 7.589-7.560 (d, *J* = 11.6 Hz, 2H), 4.632 (s, 1H); ¹³C NMR: (100 MHz, DMSO): δ : 173.02, 152.02, 147.41, 142.30, 140.67, 137.39, 130.11, 129.76, 127.20, 124.17, 120.53, 118.95, 118.84, 117.91, 109.42, 109.13, 108.86, 59.40, 28.71; ESI-MS: *m/z* Calculated, 429.35 found [*m/z*] [M+H]⁺ 430.3.

2.1.2.18. 6-amino-1-(2,4-dinitrophenyl)-4-(3-hydroxyphenyl)-1,4-dihydropyrano[2,3-c]pyrazole-5-carbonitrile (5p).

Dark brown solid, m.p. 258-260 °C.; Anal. Calc. For C₁₉H₁₂N₆O₆: C, 54.29; H, 2.88; N, 19.99; O, 22.84%. Found- C, 54.75; H, 2.16; N, 19.34%; IR ν_{max} (KBr) cm⁻¹: 3313 (N-H_{str}), 3103 (C-H_{Aromatic, str}), 1620 (C=C_{str}), 2313 (-CN), 1085 (C-O_{str}), 1514, 1368 (N-O_{str}); ¹H NMR: (400 MHz, DMSO): δ_H (ppm) 9.859 (s, 1H), 9.158-9.135 (d, *J* = 9.2 Hz, 1H), 8.859 (s, 2H), 8.372-8.356 (d, *J* = 6.4 Hz, 1H), 7.759 (s, 1H), 7.251-7.236 (d, *J* = 6 Hz, 2H), 7.047 (s, 1H), 6.939-6.921 (d, *J* = 7.2 Hz, 1H), 5.051 (s, 1H), 4.667 (s, 1H); ¹³C NMR: (100 MHz, DMSO): δ : 171.83, 155.74, 150.62, 146.71, 142.10, 139.90, 137.52, 136.71, 129.87, 127.35, 124.17, 122.05, 120.32, 117.58, 113.43, 112.18, 59.52, 28.82; ESI-MS: *m/z* Calculated 420.34, found [*m/z*] [M+H]⁺ 421.1.

2.1.2.19. 6-amino-4-(4-bromophenyl)-1-(2,4-dinitrophenyl)-1,4-dihydropyrano[2,3-c]pyrazole-5-carbonitrile (5q).

Brown solid, m.p. 273-276 °C.; Anal. Calc. for C₁₉H₁₁BrN₆O₅: C, 47.22; H, 2.29; Br, 16.54; N, 17.39; O, 16.55%. Found- C, 48.42; H, 2.64; N, 17.11%. IR ν_{max} (KBr) cm⁻¹: 3314 (N-H_{str}), 2938 (C-H_{Aromatic, str}), 1596 (C=C_{str}), 2350 (-CN), 1126 (C-O_{str}), 1506, 1346 (N-O_{str}).; ¹H NMR: (400 MHz, DMSO): δ_H (ppm) 9.694 (s, 1H), 8.869-8.836 (d, J = 13.2 Hz, 1H), 8.574 (s, 2H), 8.352-8.330 (d, J = 8.8 Hz, 1H), 7.895 (s, 1H), 7.621-7.594 (d, J 10.8 = , 2H), 7.047 (s, 1H), 7.320-7.304 (d, J = 6.4 Hz, 2H), 4.835 (s, 1H). ¹³C NMR: (100 MHz, DMSO): δ ; 170.56, 151.67, 146.38, 143.16, 140.32, 138.04, 134.09, 132.70, 131.61, 131.27, 130.74, 127.36, 124.15, 120.48, 120.28, 118.43, 117.59, 59.87, 29.09; ESI-MS: m/z Calculated 483.23, found [m/z] [M+H]⁺ 483.5.

2.1.2.20. 6-amino-4-(5-bromo-2-hydroxyphenyl)-1-(2,4-dinitrophenyl)-1,4dihydropyrano[2,3-c]pyrazole-5-carbonitrile (5r).

Orange solid, m.p. 288-293 °C.; Anal. Calc. for C₁₉H₁₁BrN₆O₆: C, 45.71; H, 2.22; Br, 16.01; N, 16.83; O, 19.23%. Found- C, 45.22; H, 2.68; N, 16.20%. IR ν_{max} (KBr) cm⁻¹: 3387 (N-H_{str}), 2803 (C-H_{Aromatic, str}), 1598 (C=C_{str}), 2214 (-CN), 1127 (C-O_{str}), 1513, 1345 (N-O_{str}).; ¹H NMR: (400 MHz, DMSO): δ ; 9.361 (s, 1H), 8.670-8.651 (s, J = 7.6 Hz, 1H), 8.576 (s, 2H), 8.281-8.270 (s, J = 4.4 Hz, 1H), 8.148 (s, 1H), 7.873-7.861 (d, J = 4.8 Hz, 1H), 7.472-7.460 (d, J = 4.8 Hz, 2H), 6.363 (s, 1H), 5.827 (s, 1H).; ¹³C NMR: (100 MHz, DMSO): δ ; 172.24, 156.88, 151.23, 146.64, 142.21, 139.85, 137.22, 136.00, 126.94, 124.61, 122.45, 120.38, 119.55, 118.20, 117.58, 115.68, 114.79, 59.68, 26.76; ESI-MS: m/z Calculated 499.23, found [m/z] [M+H]⁺ 500.6.

2.1.2.21. 6-amino-1-(2,4-dinitrophenyl)-4-(4-nitrophenyl)-1,4-dihydropyrano[2,3-c]pyrazole-5-carbonitrile (5s).

Dark orange solid, m.p. 283-285 °C.; Anal. Calc. for C₁₉H₁₁N₇O₇: C, 50.79; H, 2.47; N, 21.82; O, 24.92%. Found- C, 50.33; H, 2.29; N, 21.08%. IR ν_{max} (KBr) cm⁻¹: 3281 (N-H_{str}), 3110 (C-H_{Aromatic, str}), 1612 (C=C_{str}), 2314 (-CN), 1137 (C-O_{str}), 1514, 1346 (N-O_{str}).; ¹H NMR: (400 MHz, DMSO): δ ; 9.584 (s, 1H), 8.727-8.703 (d, J = 9.6 Hz, 1H), 8.538 (d, 2H), 8.371-8.359 (d, J = 4.8 Hz, 1H), 8.247 (s, 1H), 7.773-7.762 (d, J = 4.4 Hz, 2H), 7.658-7.629 (d, J = 11.6 Hz, 2H), 4.594 (s, 1H).; ¹³C NMR: (100 MHz, DMSO): δ_c (ppm) 27.87, 59.62, 116.87, 118.03, 120.06, 123.79, 124.04, 124.91, 127.08, 130.22, 130.90, 136.83, 139.13, 140.60, 142.11, 145.95, 146.29, 151.37, 173.20.; ESI-MS: m/z Calculated 449.33, found [m/z] [M+H]⁺ 450.1.

2.1.2.22. 6-amino-4-(3,4-dimethoxyphenyl)-1-(2,4-dinitrophenyl)-1,4-dihydropyrano[2,3c]pyrazole-5-carbonitrile (5t).

Black solid, m.p. 286-289 °C.; Anal. Calc. for C₂₁H₁₆N₆O₇: C, 54.31; H, 3.47; N, 18.10; O, 24.12%. Found- C, 54.62; H, 3.27; N, 17.86%. IR ν_{max} (KBr) cm⁻¹: 3315 (N-H_{str}), 2975 (C-H_{Aromatic, str}), 1615 (C=C_{str}), 2215 (-CN), 1085 (C-O_{str}), 1511, 1379 (N-O_{str}).; ¹H NMR: (400 MHz, DMSO): δ ; 9.580 (s, 1H), 8.784-8.772 (s, J = 4.8 Hz, 1H), 8.264 (s, 2H), 7.97-7.963 (s, J = 2.8 Hz, 1H), 7.579 (s, 1H), 7.242-7.231 (s, J = 4.4 Hz, 1H), 6.817-6.790 (d, J = 10.8 Hz, 2H), 4.861 (s, 1H), 3.871 (s, 6H).; ¹³C NMR: (100 MHz, DMSO): δ ; 172.22, 151.12, 150.67, 146.24, 145.92, 142.29, 140.40, 136.87, 128.24, 128.07, 124.20, 122.31, 120.42, 117.92, 117.31, 113.12, 112.83, 60.09, 56.67, 55.82, 28.71; ESI-MS: m/z Calculated 464.39, found [m/z] [M+H]⁺ 465.2.

2.1.2.23. 6-amino-1-(2,4-dinitrophenyl)-4-(4-hydroxy-3-methoxyphenyl)-1,4-dihydropyrano[2,3-c]pyrazole-5-carbonitrile (5u).

Reddish brown solid, m.p. 278-283 °C.; Anal. Calc. for C₂₀H₁₄N₆O₇: C, 53.34; H, 3.13; N, 18.66; O, 24.87% Found- C, 52.74; H, 3.42; N, 18.17%; IR ν_{max} (KBr) cm⁻¹: 3313 (N-H_{str}), 3075 (C-H_{Aromatic, str}), 1622 (C=C_{str}), 2314 (-CN), 1134 (C-O_{str}), 1514, 1366 (N-O_{str}); ¹H NMR: (400 MHz, DMSO): δ ; 9.428 (s, 1H), 8.965-8.952 (d, *J* = 5.2 Hz, 1H), 8.689 (s, 2H), 8.224-8.204 (d, *J* = 8 Hz, 1H), 7.847 (s, 1H), 7.042-7.037 (d, *J* = 2 Hz, 1H), 6.748-6.725 (d, *J* = 9.2 Hz, 2H), 4.865 (s, 1H), 4.834 (s, 1H), 3.674 (s, 3H); ¹³C NMR: (100 MHz, DMSO): δ ; 171.22, 152.14, 148.05, 146.18, 145.23, 142.20, 140.00, 136.71, 129.04, 127.10, 124.26, 122.19, 120.21, 118.09, 117.66, 114.79, 112.82, 59.48, 55.91, 28.59; ESI-MS: *m/z* Calculated 450.36, found [*m/z*] [M+H]⁺ 451.6.

2.1.3. Synthesis of 6-amino-1-(2,4-dinitrophenyl)-4-(4-(piperidin-1-yl)phenyl)-1,4-dihydropyrano[2,3-c]pyrazole-5-carbonitrile derivatives (7a-7b):

An equimolar mixture of 2, 4-dinitrophenyl hydrazine (**1**) (1.0 eq.), ethyl acetoacetate (**2**) (1.0 eq.), malononitrile (**3**) (1.0 eq.) and aldehyde derivatives (**6a-6b**) (1.0 eq.) were taken into 50 ml FBF (Flat Bottomed Flask) in the presence of SnCl₂ (10 mol %) as a catalyst. The reaction mixture was stirred at 80 °C for appropriate time mentioned in **Table 1** and also heated at 180 W for 10-20 min under microwave irradiation. The isolation of yield performed same as **5a-5u** to get compound **7a-7b**.

2.1.3.1. 6-amino-1-(2,4-dinitrophenyl)-4-(4-morpholinophenyl)-1,4-dihydropyrano[2,3-c] pyrazole-5-carbonitrile (7a).

Dark brown solid, m.p. 302-304 °C.; Anal. Calc. for C₂₃H₁₉N₇O₆: C, 56.44; H, 3.91; N, 20.03; O, 19.61%. Found- C, 55.76; H, 3.82; N, 20.34%; IR ν_{max} (KBr) cm⁻¹: 3284 (N-H_{str}), 2804 (C-H_{Aromatic, str}), 1599 (C=C_{str}), 2216 (-CN), 1060 (C-O_{str}), 1469, 1381 (N-O_{str});

^1H NMR: (400 MHz, DMSO): δ : 9.921 (s, 1H), 8.854 (s, 2H), 8.630 (s, 1H), 7.834-7.811 (d, J = 9.2 Hz, 1H), 7.756-7.738 (d, J = 7.2 Hz, 1H), 7.223-7.201 (d, J = 8.8 Hz, 2H), 7.051-7.031 (d, J = 8 Hz, 2H), 4.131 (s, 1H), 3.818-3.806 (t, J = 4.8 Hz, 4H), 3.402-3.364 (t, J = 15.2 Hz, 4H).; ^{13}C NMR: (100 MHz, DMSO): δ : 169.08, 151.80, 149.47, 144.49, 144.41, 141.54, 137.11, 129.41, 129.07, 128.11, 124.27, 123.80, 121.92, 116.63, 115.90, 112.19, 111.94, 65.87, 64.90, 60.64, 54.34, 53.20, 29.01; ESI-MS: m/z Calculated 489.44, found $[m/z]$ $[\text{M}+\text{H}]^+$ 490.3.

2.1.3.2. 6-amino-1-(2,4-dinitrophenyl)-4-(4-(piperidin-1-yl)phenyl)-1,4-dihydropyrano[2,3-c]pyrazole-5-carbonitrile (7b).

Brownish orange solid, m.p. 298-301 °C.; Anal. Calc. for $\text{C}_{24}\text{H}_{21}\text{N}_7\text{O}_5$: C, 59.13; H, 4.34; N, 20.11; O, 16.41%. Found- C, 59.31; H, 4.08; N, 20.65%.; IR ν_{max} (KBr) cm^{-1} : 3140 ($\text{N}-\text{H}_{\text{str}}$), 2989 ($\text{C}-\text{H}_{\text{Aromatic, str}}$), 1641 ($\text{C}=\text{C}_{\text{str}}$), 2316 ($-\text{CN}$), 1174 ($\text{C}-\text{O}_{\text{str}}$), 1544, 1383 ($\text{N}-\text{O}_{\text{str}}$).; ^1H NMR: (400 MHz, DMSO): δ : 9.454 (s, 1H), 8.821-8.794 (d, J = 10.8 Hz, 1H), 8.554 (s, 2H), 8.046-8.022 (d, J = 9.6 Hz, 1H), 7.590 (s, 1H), 7.069-7.046 (d, J = 9.2 Hz, 2H), 7.000-6.978 (d, J = 8.8 Hz, 2H), 4.153 (s, 1H), 3.321-3.308 (t, J = 5.2 Hz, 4H), 1.494-1.395 (m, 6H).; ^{13}C NMR: (100 MHz, DMSO): δ : 174.59, 153.09, 151.64, 148.05, 143.29, 138.75, 135.83, 130.16, 129.85, 128.07, 124.15, 123.81, 121.01, 119.13, 116.89, 113.00, 112.87, 60.24, 54.06, 53.64, 25.07, 24.91, 23.90; ESI-MS: m/z Calculated 487.47, found $[m/z]$ $[\text{M}+\text{H}]^+$ 488.4.

2.1.4. Synthesis of 6-amino-1-isonicotinoyl-4-phenyl-1, 4-dihydropyrano [2, 3-c] pyrazole-5-carbonitrile derivative (8a):

An equimolar mixture of isonicotinohydrazide (**1a**) (1.0 eq.), ethyl acetoacetate (**2**) (1.0 eq.), malononitrile (**3**) (1.0 eq.) and aldehyde derivatives (**4a**) (1.0 eq.) were taken in 50 ml FBF (Flat Bottomed Flask) in the presence of SnCl_2 (10 mol %) as a catalyst. The

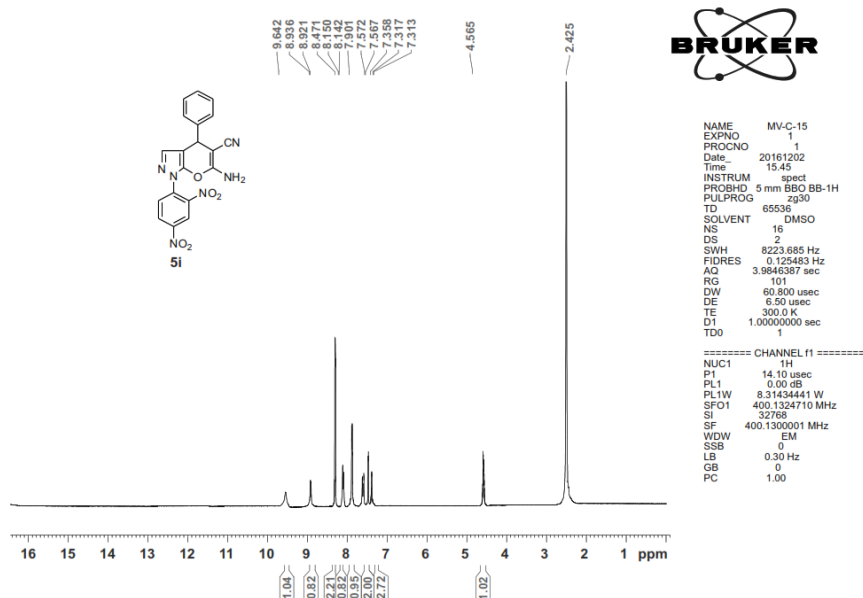
isolation method of the product yield is same as **5a-5u** to obtain compound 6-amino-1-isonicotinoyl-4-phenyl-1, 4-dihydropyrano [2, 3-c] pyrazole-5-carbonitrile **8a**.

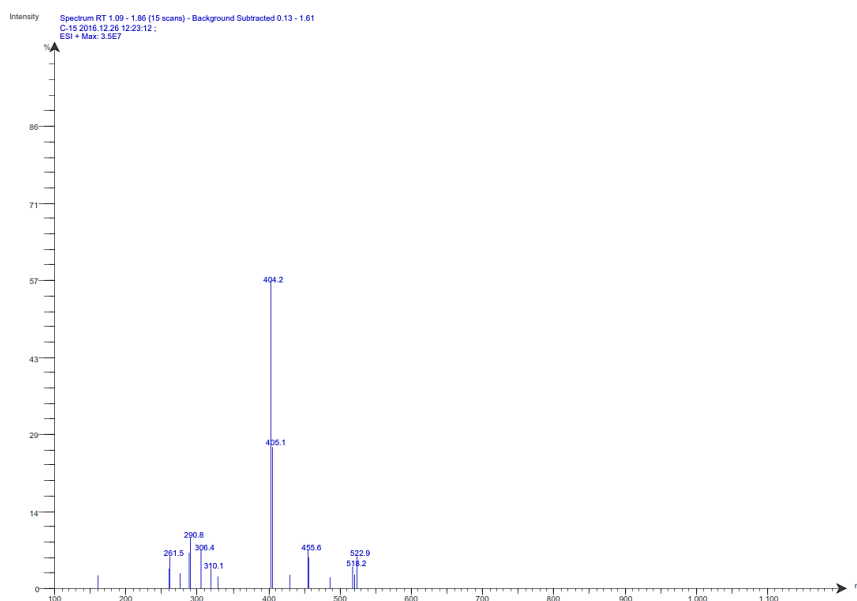
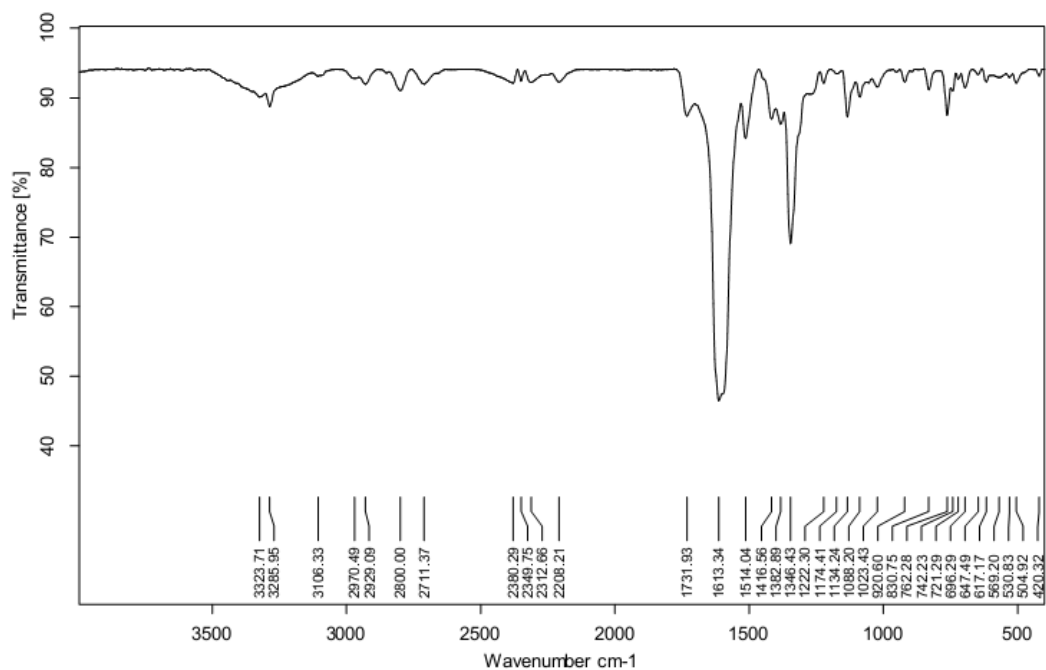
2.1.4.1. 6-amino-1-isonicotinoyl-4-(4-nitrophenyl)-1,4-dihydropyrano[2,3-c]pyrazole-5-carbonitrile (8a).

Light yellow solid, m.p. 268-270 °C.; Anal. Calc. for C₁₉H₁₂N₆O₄: C, 58.76; H, 3.11; N, 21.64; O, 16.48%. Found- C, 58.25; H, 3.07; N, 21.38%.; IR ν_{max} (KBr) cm⁻¹: 3186 (N-H_{str}), 3001 (C-H_{Aromatic, str}), 1685 (C=C_{str}), 2205 (-CN), 1142 (C-O_{str}), 1560 (N-O_{str}).; ¹H NMR: (400 MHz, DMSO): δ ; 8.815-8.797 (d, 2H), 7.957 (s, 2H), 7.650-7.638 (d, J = 4.8 Hz, 2H), 7.479-7.458 (d, J = 8.4 Hz, 2H), 6.534-6.512 (d, J = 8.8 Hz, 2H), 6.492 (s, 1H), 4.526 (s, 1H).; ¹³C NMR: (100 MHz, DMSO): δ ; 174.82, 167.02, 157.34, 152.01, 150.67, 142.25, 141.03, 131.68, 130.09, 129.57, 124.02, 123.83, 123.04, 122.34, 117.86, 117.02, 60.62, 29.18; ESI-MS: m/z Calculated 388.34, found [m/z] [M+H]⁺ 389.2.

2.1.4.2 Spectra of 6-amino-1-(2,4-dinitrophenyl)-4-phenyl-1,4-dihydropyrano[2,3-c]pyrazole-5-carbonitrile (5a).

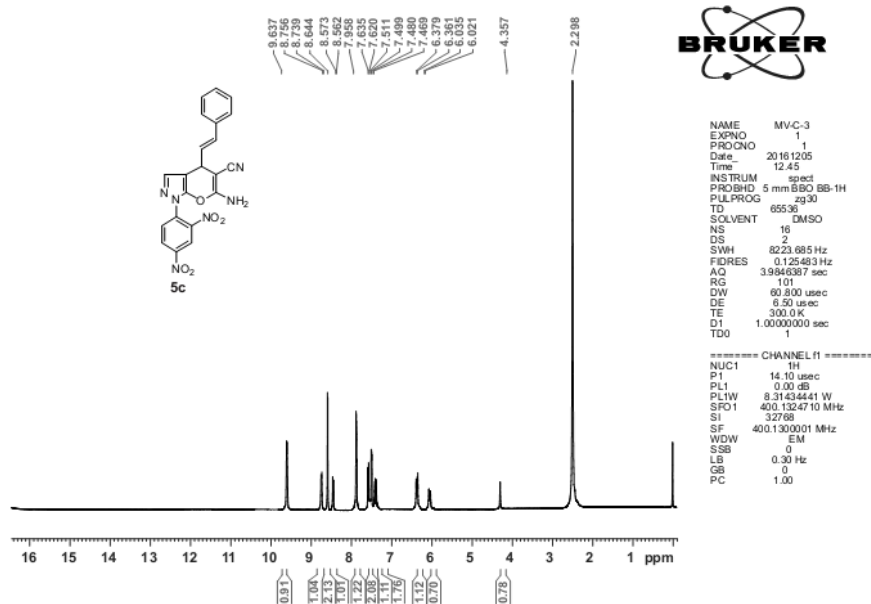
^1H NMR Spectra;



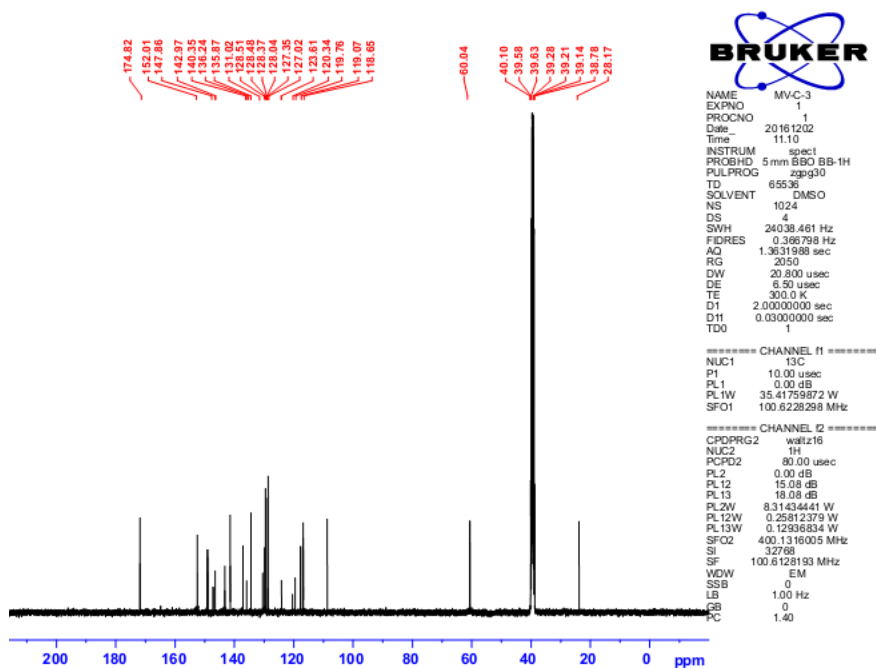
Mass Spectra;**IR Spectra;**

2.1.2.5 Spectra of (E)-6-amino-1-(2,4-dinitrophenyl)-4-styryl-1,4-dihydropyrano[2,3-c]pyrazole-5-carbonitrile (5b).

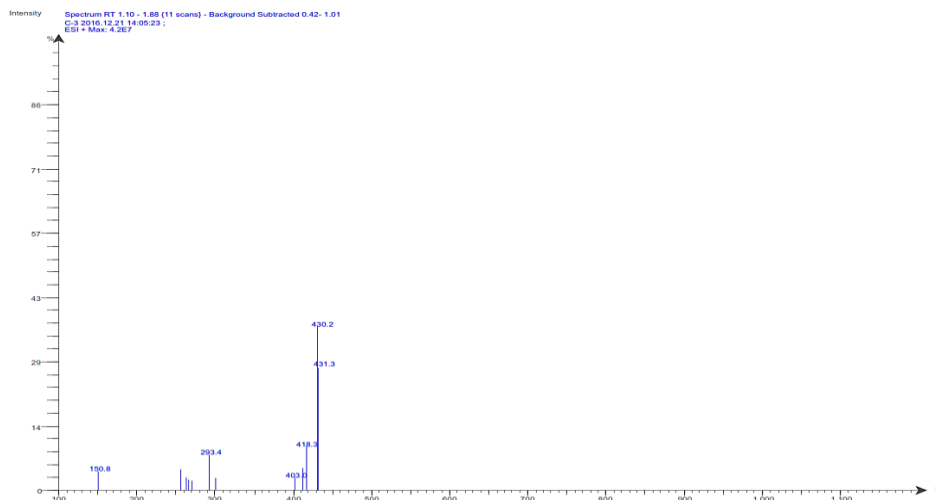
^1H NMR Spectra;



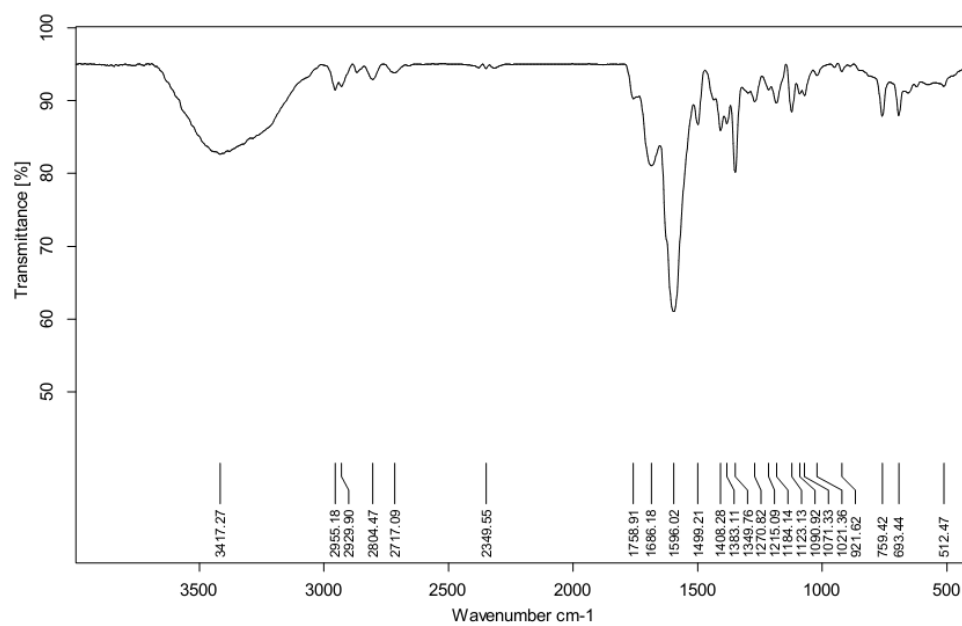
^{13}C NMR Spectra;



Mass Spectra;



IR Spectra;



2.2 Biological assay

2.2.1 *In vitro* anti-bacterial activity

The *in vitro* anti-bacterial activity of synthesized compounds were performed against four different bacterial strains (*E. coli* MTCC 443, *P. aeruginosa* MTCC 1688, *S. aureus* MTCC 96, *S. pyogenus* MTCC 442) and compared with standard drugs according to the method described in **Chapter 3**.

2.2.2 *In vitro* anti-tuberculosis activity and MDR-TB study

The anti-tuberculosis screening of the synthesized compounds was carried out using method described in **Chapter 3**.

2.2.3 *In vitro* anti-malarial and anti-fungal activity

The *in vitro* anti-malarial activity of all the synthesized compounds was carried out in 96 well micro titre plates according to the micro assay protocol described in **Chapter 3**.

2.2.4 Cytotoxicity assay protocol

Human cervical cancer cell line (HeLa) were used for *in vitro* cytotoxicity study of the synthesized compounds **7a**, **8a**, **5a** and **5r**. The cytotoxic activity protocol was used according method used in Desai *et al.* [47].

2.3 Computational Study

2.3.1 ADMET property prediction

A set of ADMET-related properties of the synthesized compounds were predicted by using Qikprop programs (Schrödinger, LLC, New York, NY, 2015) according to method described in **Chapter 2**.

2.3.2 Molecular Docking

The potential binding mode and the binding interaction of the ligand with Enoyl-ACP reductase (oxidoreductase) (PDB; 1QG6, 2NSD, 4TZK, 4TZT) have been investigated by using Maestro, Schrödinger, LLC, New York, NY, 2012. The investigation of docking scores and energies was predicated using method described in **Chapter 2**.

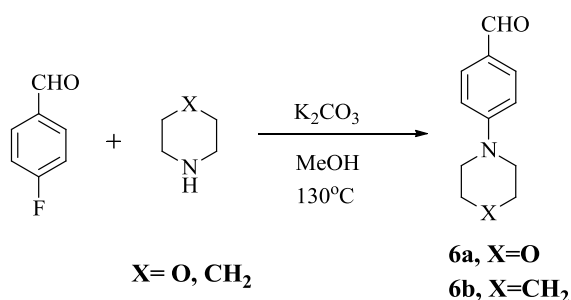
2.3.4 Molecular Dynamics

The natural dynamics on different timescales of docked complex of compound **7b** and protein 5MTQ, thermal average of the molecular properties of complex is predicted by using molecular dynamics (MD) stimulation. The molecular dynamics on 10 ns of the complex was carried out with the help of molecular dynamics (MD) stimulation module, Desmond-GPU in maestro according to the procedure mentioned in **Chapter 3**.

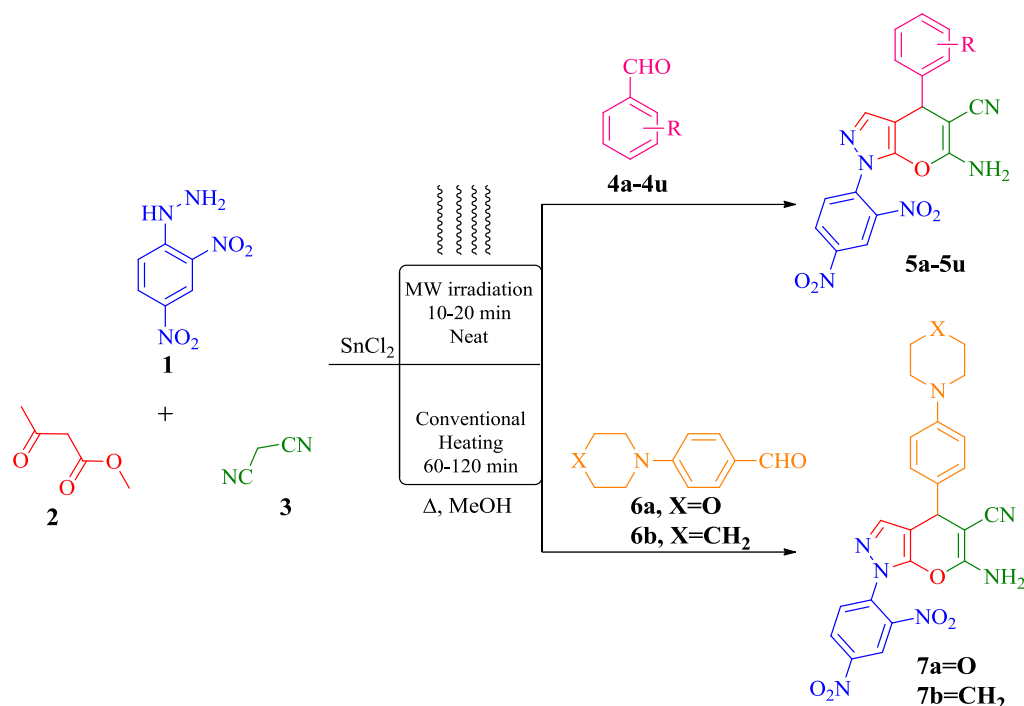
3.0 Results and Discussion

3.1 Chemistry

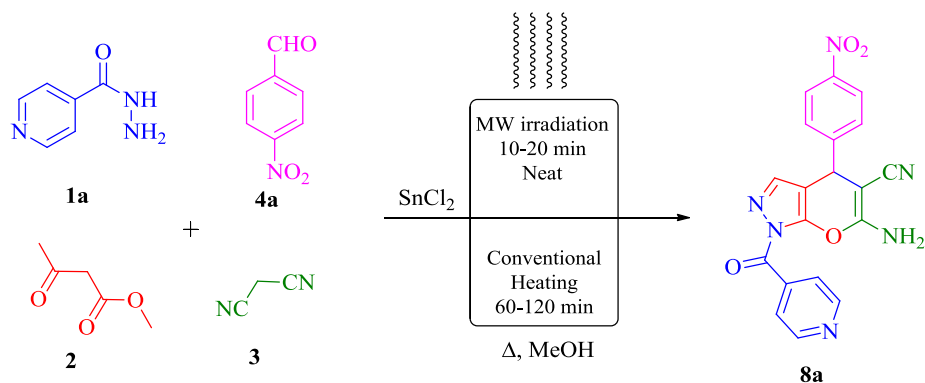
In the present study, it has been synthesized a series of novel compounds based on pyrano[2,3-c]pyrazole (**5a-5u**, **7a-7b** and **8a**) which was illustrated in Scheme 1-3. The synthesis of the series of heterocyclic scaffold performed using MCR methodology following direct addition of the substituted aldehyde derivative (**4a-4u**) with the corresponding 2, 4-dinitrophenyl hydrazine (**1**), ethyl acetoacetate (**2**) and malononitrile (**3**) in the presence of SnCl_2 using Methanol as solvent under microwave irradiation and conventional method (**Scheme 2-3**). Targeted compound 6-amino-1-isonicotinoyl-4-phenyl-1, 4-dihydropyrano [2, 3-c] pyrazole-5-carbonitrile (**8a**) (**Scheme 3**) was synthesised using substituted aldehyde derivative (**4a-4u**), isonicotinohydrazide (**1a**), ethyl acetoacetate (**2**) and malononitrile (**3**) in the same condition as a **5a-5u**. Whereas, to synthesise compound **7a-7b**, a 4- substituted aldehyde derivatives were initially synthesized (**6a-6b**) (**Scheme 1**) via condensation of 4-fluoro aldehyde, piperidine and morpholine in the presence of anhydrous potassium carbonate using Methanol as solvent.



Scheme 1: Synthesis of 4-(piperidin-1-yl) benzaldehyde derivatives (**6a-6b**)



Scheme 2: Synthesis of 6-amino-1-(2,4-dinitrophenyl)-4-phenyl-1,4 dihydropyrano[2,3-c] pyrazole-5-carbonitrile derivatives (**5a-5u**) and (**7a, 7b**)

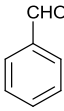
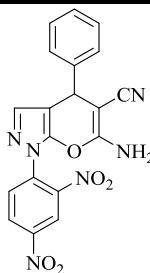
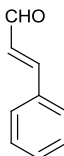
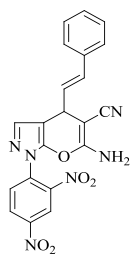
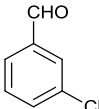
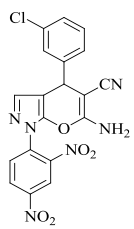
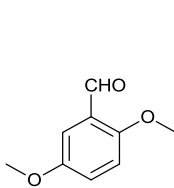
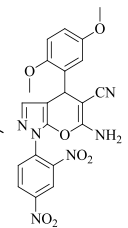
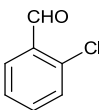
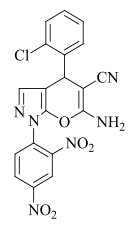


Scheme 3. Synthesis of 6-amino-1-isonicotinoyl-4-phenyl-1,4-dihydropyrano [2,3-c] pyrazole-5-carbonitrile derivative (**8a**)

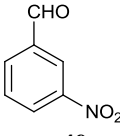
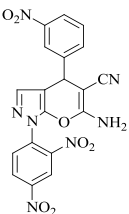
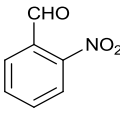
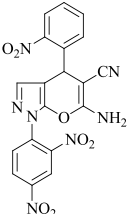
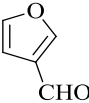
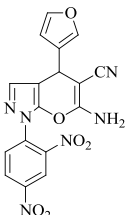
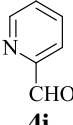
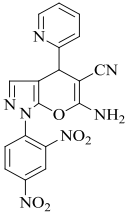
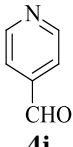
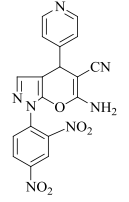
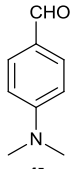
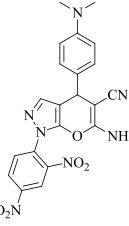
From the current literature survey, we concluded that many researcher have reported desired product formation with lower product yields and longer hours reaction time by using different solvent and catalyst for the synthesis of 1,4-dihydropyrano[2,3-c]pyrazole derivatives [35-45, 52]. Despite this challenge, we have optimized the reaction

conditions using conventional and microwave irradiation to find out the superior method for the synthesis of targeted compound **5a** with higher yield and shorter reaction time. In both the conditions, we first performed a trial reaction with equivalent mole of benzaldehyde, malononitrile and 2,4-dinitrophenyl hydrazine in the presence of SnCl_2 using water, Methanol, ethanol as solvent and without solvent at various temperature (**Table 1**). In the conventional method, Compound **5a** with yield of 67% in 4.2 hrs was obtained when the reaction was performed without catalyst at 80 °C temperature. While, when the reaction was performed in Methanol at 80 °C temperature by using SnCl_2 as a catalyst the yield and time of product **5a** could be improved to 80 % in 1.4 hours. However, the targeted product **5a** was synthesized in 25 min with 88 % of yield in microwave irradiation method, where Methanol was used as a solvent in the presence of SnCl_2 as a catalyst at 180 W temperature. Most of the compounds were synthesized using neat condition in the microwave irradiation method. However, we have also used neat condition while synthesizing compounds via conventional method but the yield of the reaction was quite low as compared to in Methanol. The synthesized compounds are enantiomeric mixture there is no synthetic selectivity. The yield of compound **5a** (80 % by conventional method and 88 % by microwave method) synthesized by our method was significantly higher, than the previously reported protocols [35-45, 52].

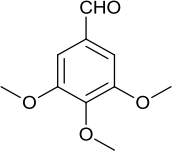
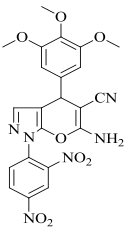
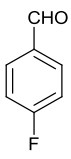
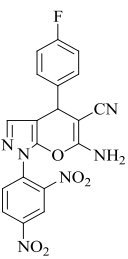
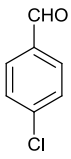
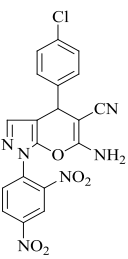
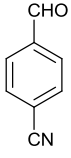
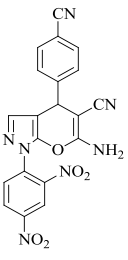
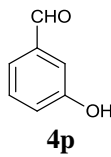
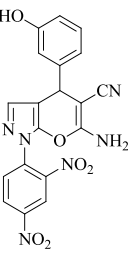
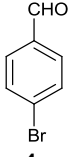
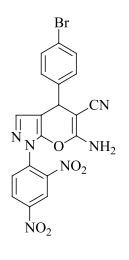
Table 1. Synthesis of 6-amino-1-(2,4-dinitrophenyl)-4-phenyl-1,4 dihydropyrano[2,3-c]pyrazole-5-carbonitrile derivatives (**5a-5u,7a-7b** and **8a**) using SnCl_2 as catalyst by Conventional and microwave irradiation method.

Entry	Code	Aromatic Aldehyde	Product	Conventional Method				Microwave Method			
				Solvent	Temp. °C	Time Min.	Yield %	Solvent	Temp. W	Time Min.	Yield %
1	5a	 4a		MeOH	80	100	80	MeOH/Neat	180	25	88
2	5b	 4b		MeOH	90	90	78	MeOH/Neat	180	20	82
3	5c	 4c		MeOH	80	95	68	Neat	180	15	72
4	5d	 4d		MeOH	80	110	74	Neat	180	15	77
5	5e	 4e		MeOH	80	95	58	Neat	180	15	67

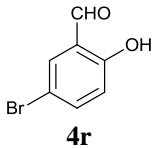
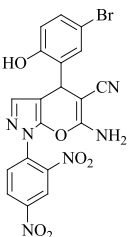
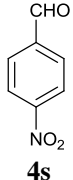
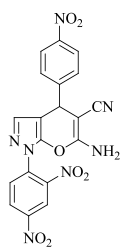
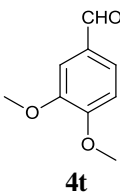
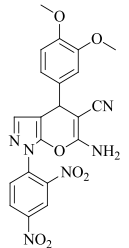
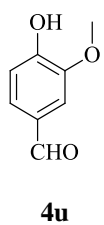
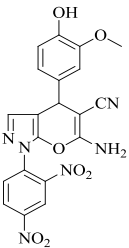
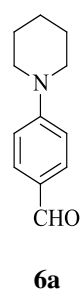
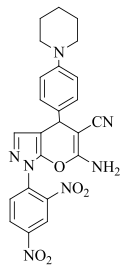
3.0 RESULTS AND DISCUSSION

6	5f			MeOH	80	100	78	Neat	180	15	81
7	5g			MeOH	80	100	69	Neat	180	15	72
8	5h			MeOH	80	90	55	Neat	180	15	64
9	5i			MeOH	80	100	52	Neat	180	15	60
10	5j			MeOH	80	95	54	Neat	180	15	61
11	5k			MeOH	80	120	67	Neat	180	15	71

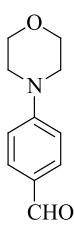
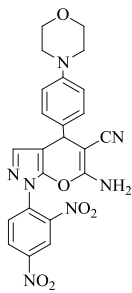
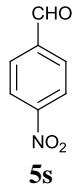
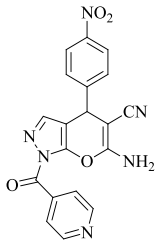
3.0 RESULTS AND DISCUSSION

12	5l	 	MeOH	80	110	73	Neat	180	15	81
13	5m	 	MeOH	80	115	74	Neat	180	15	79
14	5n	 	MeOH	80	100	75	Neat	180	15	78
15	5o	 	MeOH	80	95	63	Neat	180	15	69
16	5p	 	MeOH	80	105	60	Neat	180	15	63
17	5q	 	MeOH	80	100	72	Neat	180	15	76

3.0 RESULTS AND DISCUSSION

18	5r			MeOH	80	100	57	Neat	180	15	62
19	5s			MeOH	80	110	81	Neat	180	15	86
20	5t			MeOH	80	100	71	Neat	180	15	76
21	5u			MeOH	80	105	66	Neat	180	15	69
22	7a			MeOH	80	110	60	Neat	180	18	64

3.0 RESULTS AND DISCUSSION

23	7b			MeOH	80	120	62	MeOH	180	30	65
		6b									
24	8a			MeOH	80	100	67	Neat	180	15	70
		5s									

^a Isolated Yield.

All the synthesized compounds **5a-5u**, **7a-7b**, **8a** were characterized by various spectroscopic methods such as ¹H NMR, ¹³C NMR, IR spectra, Mass analysis and elemental analysis. We have confirmed the synthesised compound **5a** from IR analysis. IR band at 3323 and 3106 cm⁻¹ which confirmed the presence of N-H_{stretch} and aromatic character (C-H_{stretch}) in the moiety respectively. When -CN group showed vibration peak at 2249 cm⁻¹, while C-O_{stretch} showed peak at band at 1023 cm⁻¹ confirm the formation of pyran ring in molecule. From the ¹H NMR data of compound **5a**, the aromatic protons were resonated at 9.642, 8.936-8.921 δ ppm (Nitro containing aromatic ring) and other benzene (Aromatic) ring showed peak at 7.572-7.567, 7.358 and 7.317-7.313 δ ppm. The -NH₂ group resonated at 8.471 δ ppm. The chiral carbon containing proton resonated at 4.656 δ ppm which also supported to synthesised compound **5a**. Also ¹³C-NMR gave full structural conformation of synthesised compound. The peaks at 27.93, 60.18 and 174.91 δ ppm correspond to cyclised chiral carbon, -C-CN containing carbon and -NH₂ containing carbon respectively which gave full confirmation of **5a**. The mass spectra of compound **5a**

showed molecular ion peak at $m/z = 404.2$ (M+H) which support to the structure of compound **5a**.

3.2 Biology

3.2.1 *In vitro* anti-bacterial activity

A series of synthesized compounds were evaluated for their anti-bacterial activity against different bacterial strain such as *E. coli*, MTCC 443, *P. aeruginosa* MTCC 1688, *S. aureus* MTCC 96, *S. pyogenus* MTCC 442 as compared to the standard drug. The activity data were summarized in Table 2. From the bioassay, it can be stated that the compound **8a** which was hybridised molecule of isoniazid with a pyran ring showed significant antibacterial activity against *E. coli* and *P. aeruginosa* at MIC value 12.5 $\mu\text{g/mL}$. Analogue **5a** with high lipophilicity (C log P = 4.1319) exhibited excellent antibacterial activity against *E. coli* and *P. aeruginosa* at MIC value 12.5 $\mu\text{g/mL}$ and 6.25 $\mu\text{g/mL}$ respectively. In addition, Compound **5l** which contained two methoxy groups showed good activity against *E. coli* and *P. aeruginosa* at MIC value 12.5 $\mu\text{g/mL}$ and 25 $\mu\text{g/mL}$ correspondingly. Compound **5n** (C log P = 4.7019) and **7a** (C log P = 3.4449) with higher lipophilicity displayed higher MIC value 12.5 $\mu\text{g/mL}$, 12.5 $\mu\text{g/mL}$, respectively amongst all the active compounds when tested against *S. pyogenus*. Moreover, analogue **5b** and **7a** (MIC value 25 $\mu\text{g/mL}$) shows better inhibitory effect against *S. aureus*. Based on the results, it can be stated that in case on inhibition of the bacterial strain, higher inhibiting efficiency of compounds comes with higher lipophilicity than with lower lipophilicity. Remaining compounds exhibited comparatively superior antibacterial activity against all the tested bacterial strains in comparison to the standard drugs Ampicillin, Chloramphenicol and Ciprofloxacin. The C log P values (P is the partition coefficient) of all the synthesised compounds as well as standard drugs are mentioned in Table 2. Overall, all the results

showed that the MIC value less than that of standard drugs were considered as promising anti-bacterial agent.

Table 2. *In vitro* anti-bacterial, anti-tuberculosis and MDR-TB screening result of synthesized compounds.

Entry	Compound	C log <i>P</i> ^a	Anti-bacterial				Anti-tuberculosis	MDR-TB ^d MIC μg/mL
			Gram-negative ^b		Gram-positive ^c		H ₃₇ RV ^d MIC μg/mL	
			<i>E.c.</i> MIC μg/mL	<i>P.a.</i> MIC μg/mL	<i>S.a.</i> MIC μg/mL	<i>S.p.</i> MIC μg/mL		
1	5a	4.1319	12.5	6.25	100	125	125	250
2	5b	3.4220	100	50	25	125	250	500
3	5c	4.3629	250	250	200	250	250	500
4	5d	2.4919	62.5	25	100	250	500	100
5	5e	4.1539	125	125	250	100	25	100
6	5f	4.2817	100	125	125	62.5	125	250
7	5g	3.1649	125	250	250	100	250	1000
8	5h	4.7019	125	12.5	100	62.5	200	>1000
9	5i	3.9890	200	250	125	100	125	500
10	5j	2.4919	200	250	500	250	100	250
11	5k	3.6520	250	100	250	500	62.5	100
12	5l	3.5969	100	62.5	500	250	100	125
13	5m	3.6469	12.5	25	50	100	250	500
14	5n	4.7019	100	125	250	125	125	250
15	5o	4.7019	125	250	125	250	100	250
16	5p	3.7320	250	125	100	12.5	250	500
17	5q	3.3220	50	100	125	250	500	1000
18	5r	3.1712	100	500	250	200	500	>1000
19	5s	3.7320	250	200	125	100	250	1000
20	5t	4.8519	125	500	100	50	25	100
21	5u	3.2891	100	125	125	250	500	1000
22	7a	3.4449	100	250	25	12.5	25	50
23	7b	4.8269	100	50	250	250	125	250
24	8a	3.1260	6.25	12.5	100	100	50	125
25	Ampicillin	-1.2045	100		250	100	-	-
26	Chloramphenicol	1.2830	50	50	50	50	-	-
27	Ciprofloxacin	-0.7252	25	25	50	50	-	-

38	Isoniazid	-0.6680	-	-	-	-	0.20	-
----	-----------	---------	---	---	---	---	------	---

^a C log P calculated using the ChemBioDraw Ultra, version 12.0, software by Cambridge Soft.

^b *E.c.*: *Escherichia coli* (MTCC-443); *P.a.*: *Pseudomonas aeruginosa* (MTCC-1688).

^c *S.a.*: *Staphylococcus aureus* (MTCC-96), *S.p.*: *Streptococcus pyogenes* (MTCC-442).

^d Minimum inhibitory concentration against H₃₇Rv strain of *M. Tuberculosis* and Multi Drug-Resistance *Tuberculosis* (µg/mL).

3.2.3 *In vitro* anti-tuberculosis activity and MDR-TB study

The promising results obtained from the antibacterial activity encouraged us to go for further biological screening such as *in vitro* anti-tubercular activity. *In vitro* anti-tuberculosis activity of all the newly synthesized compounds was investigated against *Mycobacterium tuberculosis H37Rv* strain by Lowenstein-Jensen method and the corresponding results are shown in Table 2. The result showed that analogue **8a** enhance good activity (25 µg/mL) due to the presence of isoniazid moiety instead of 2, 4-dinitrophenyl hydrazine presented in rest molecules. In addition, compound **7a** and **5r** showed 25 µg/mL of MIC against mycobacterial strain.

Moreover, Compound **5u** showed moderate activity against *H37Rv* strain with MIC value 50 µg/mL. All the remaining compounds were found to display reasonable activity at MIC ranging from 50 to 500 µg/mL. Further, the compounds were screened against MDR-TB (First-line anti-TB drug resistance) in clinical strains. From the data (Table 2) of activity against MDR strain it was observed that only compound **7a** demonstrate moderate activity at MIC value 50 µg/mL. The remaining result of tested compounds against MDR-TB strain were comparatively poor. The lower effectiveness of synthesized compounds against strain not being adapted to laboratory environments and different media, which may affect their apparent susceptibility to certain inhibitors and they exhibit poor effect against strain *in vitro* resulted in the poor activity.

3.2.4 *In vitro* anti-malarial activity and anti-fungal activity

All the synthesized compounds were screened for *In Vitro* antimalarial activity against *Plasmodium falciparum*. The results were compared with the standard drugs Quinine and Chloroquine. Among the series of compounds, analogue **5m**, **5n**, **5s** and **7b** exhibited potent anti-malarial activity and the results are presented in **Table 3**. Moreover, we have observed that compound 5j and 5l showed significant antimalarial activity with IC₅₀ 0.12 and 0.24 µg/mL, respectively which is superior than standard drug quinine. However, remaining compounds exhibited comparatively moderate antimalarial activity against tested malarial strains (*Plasmodium falciparum*) in comparison to the standard drugs Quinine and Chloroquine. The observed result offer new possibilities for further developments about the antimalarial performance of 4*H*-pyran derivatives.

Table 3. *In vitro* anti-malarial, anti-fungal screening result of synthesised compounds.

Entry	Compound	Anti-malarial		Anti-fungal	
		<i>P. falciparum</i> µg/mL	<i>C. albicans</i> MTCC 227 µg/mL	<i>A. niger</i> MTCC 282 µg/mL	<i>A. clavatus</i> MTCC 1323 µg/mL
1	5a	1.34	>1000	250	500
2	5b	1.28	250	1000	1000
3	5c	0.97	250	1000	>1000
4	5d	1.56	500	1000	1000
5	5e	1.49	250	1000	250
6	5f	0.98	1000	1000	500
7	5g	1.03	>1000	500	500
8	5h	0.87	1000	250	500
9	5i	1.35	1000	>1000	1000
10	5j	0.12	250	1000	1000
11	5k	2.03	1000	500	500
12	5l	0.24	250	500	100
13	5m	0.38	200	>1000	500
14	5n	0.36	500	>1000	500
15	5o	0.67	500	250	250
16	5p	0.77	1000	1000	500

17	5q	1.99	250	1000	1000
18	5r	2.03	1000	250	500
19	5s	0.68	250	>1000	>1000
20	5t	1.23	1000	1000	>1000
21	5u	2.32	1000	1000	>1000
22	7a	0.71	500	250	>1000
23	7b	0.36	250	1000	>1000
24	8a	0.28	500	1000	1000
25	Quinine	0.268	-	-	-
26	Chloroquine	0.02	-	-	-
27	Nystatin	-	100	100	100
28	Greseofulvin	-	100	100	100

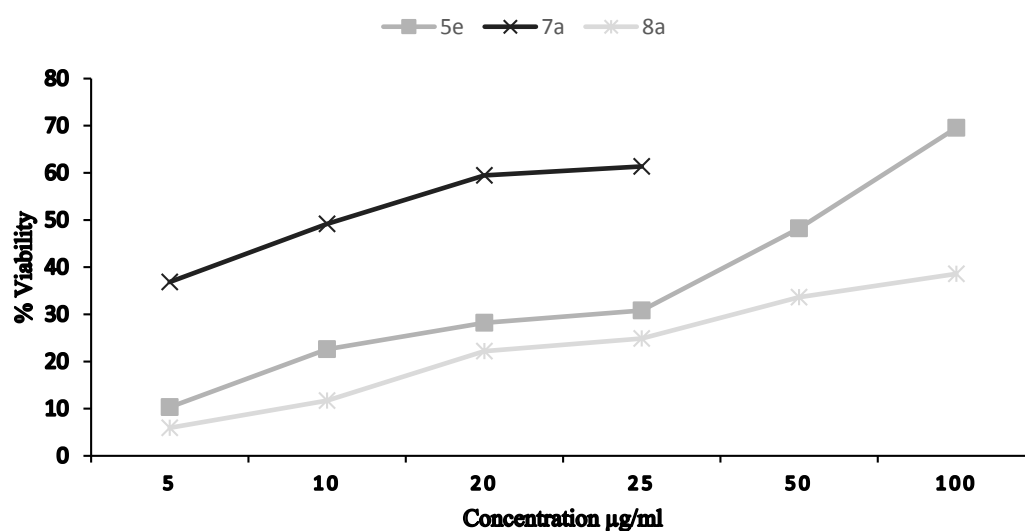
The *in vitro* antifungal activity of all the synthesized were determined against *Candida albicans* MTCC 227, *Aspergillus niger* MTCC 282 and *Aspergillus clavatus* MTCC 1323 by conventional broth micro dilution method. Result of antifungal activity are presented in Table 3. The results indicated that compound 5l was found to be the most promising agent against *A. clavatus* with MIC (100 µg/mL) in comparison with control drug Greseofulvin. Compounds 5a, 5h, 5o, 5r, 7a and 7b displayed comparable anti-fungal activity with the standard drug. However, all other compounds showed less inhibition against the tested microorganisms as compared to the standard drug.

3.2.5 Cytotoxicity assay

In vitro cytotoxic activity of synthesized compounds **5a**, **7a** and **8a** was evaluated against HeLa cell line (human cervical cancer) by the MTT colorimetric assay [47]. The result are summarized in **Table 4**. Percentage cell viability of HeLa cell line at various concentrations for these compounds are shown in **Figure 1**. It was observed that there is no remarkable cytotoxic effect on HeLa cell line, particularly the tested compound **7a**. This activity suggest that these compounds have good proficiency for their future *in vivo* activity for antimicrobial agents.

Table 4. *In vitro* % viability of compound **5e**, **5r**, **7a** and **8a** by MTT assay.

Entry	Compound	Inhibition concentration (µg/mL)	% viability (HeLa Cell-line)
1	5e	5	10.31
		10	22.59
		20	28.21
		25	30.82
		50	48.23
		100	69.53
2	7a	5	36.84
		10	49.16
		20	59.47
		25	61.37
4	8a	5	5.94
		10	11.70
		20	22.19
		25	24.88
		50	33.62
		100	38.60
		200	58.75

**Figure 1.** *In vitro* % viability of compound **5e**, **7a** and **8a** by MTT assay.

3.3 Computational Study

3.3.1 ADMET property prediction

In silico, pharmacokinetic properties leading to drug-likeness of the synthesized compounds were predicted using Qikprop module (Schrodinger, LLC, New York, NY, 2015). The predicted important pharmacokinetic properties of synthesized compounds along with their acceptable limits are showed in Table 5 as compared with the reference compounds. Most of the compounds were found to have good bioavailability except **5s**. One of the important factor to be studied in concern with the absorption of the drug molecule is intestinal absorption, which was ascertained by Caco-2 cell permeability (QPPCaco) prediction. The synthesized compound shows moderate results predicting intestinal absorption in Caco-2 cell permeability. Further, The Qikprop descriptor for blood/brain partition coefficient QPlogBB showed reliable prediction for the synthesized compounds and reference drugs.

Table 5. Predicted ADME parameters for synthesized compounds.

Compound	Percent human oral absorption (>80% – high & <25% – poor)	QPlog BB (-3.0 – 1.5)	QPlog HERG (below - 5)	QPPCaco (<25 poor, >500 great)	QPlog Khsa (-1.5 – 1.5)	PSA (70 – 200 Å)	QPlog S (-6.5 – 5)
5a	46.28	-2.73	-5.86	10.10	0.49	160.71	-6.70
5b	28.40	-3.75	-6.08	2.10	0.31	186.50	-6.36
5c	49.18	-3.22	-6.77	10.12	0.64	160.70	-7.24
5d	41.41	-2.86	-5.94	9.22	0.26	171.58	-5.99
5e	47.13	-3.09	-6.01	9.76	0.61	164.14	-7.19
5f	37.37	-3.21	-5.84	4.15	0.40	181.55	-6.82
5g	40.65	-2.64	-5.35	10.01	0.19	169.62	-5.40
5h	46.92	-2.73	-5.90	9.95	0.54	160.70	-6.86
7a	45.90	-3.01	-5.95	9.83	0.54	173.97	-7.21
7b	50.96	-3.08	-6.03	9.59	0.95	164.32	-8.14
5j	34.90	-3.07	-5.77	5.49	0.16	173.59	-5.76

5k	28.86	-3.68	-5.89	2.00	0.39	203.10	-6.34
5l	46.63	-3.09	-5.85	10.42	0.49	175.74	-6.84
8a	52.87	-2.53	-5.56	13.59	-0.11	158.08	-4.99
5i	44.90	-2.82	-5.98	10.09	0.45	160.71	-6.34
5n	47.76	-2.71	-5.90	10.11	0.56	160.71	-7.07
5o	47.68	-2.74	-5.97	10.07	0.56	160.71	-7.11
5p	24.38	-3.97	-5.90	1.21	0.42	205.60	-6.51
5q	31.24	-3.46	-5.85	3.06	0.28	183.25	-6.06
5r	35.77	-3.42	-5.84	4.58	0.30	187.44	-6.27
5s	24.36	-3.98	-5.91	1.21	0.42	205.61	-6.52
5t	48.21	-2.72	-5.93	10.11	0.59	160.71	-7.18
5m	46.48	-3.14	-5.94	10.10	0.50	173.91	-6.93
5u	47.11	-3.25	-5.83	10.09	0.51	180.14	-7.07
Ciprofloxacin	49.25	-0.61	-3.20	14.27	-0.007	96.22	-3.79
INH	66.83	-0.84	-3.54	275.98	-0.75	81.40	-0.04
Chloramphenicol	65.44	-1.50	-3.25	60.36	-0.81	121.93	-2.00
Ampicillin	20.18	-1.09	-0.28	1.87	-0.94	135.18	-1.51

The predicted results for QPlogkhsa descriptor of Qikprop indicating the predicted values of human serum albumin binding indicated that molecules were found to be in the permissible range (-1.5-1.5). The active molecules were accessed for IC₅₀ value of HERG K⁺ channel blockage prediction, which indicated that the predicted values are in the acceptable range (<-5) as compared to the standard reference entities. The aqueous solubility parameter (QPlog S) of the synthesized compounds were assessed and the compounds were found to be falling out of the acceptable range (-6.5-0.5) signifying incomplete solubility of the synthesized compounds which can be further improved using solubility enhancers.

3.3.2 Molecular docking

Due to lack of enzymatic study, we decided to perform *in silico* computational study of the synthesized compounds which provided more information that could be applied to design new molecules with more potent biological activity. Therefore, Molecular docking

analysis was performed to obtain the detailed molecular interactions and to estimate the binding affinity of the synthesized compounds with Enoyl-ACP reductase (oxidoreductase) with four different proteins (PDB ID: 1QG6, 2B37, 4TZK, 5MTQ). Synthesized pyrano [2,3-c]-pyrazole derivatives and standard ligand Isoniazid was docked into the active site of Enoyl-ACP reductase (oxidoreductase). The docking results of the ligands with Enoyl-ACP reductase (oxidoreductase) with different proteins as per the Glide calculations are given in **Table 6**. The results of docking simulations demonstrated high binding affinity with good interactions for critical residues present in Enoyl-ACP reductase (oxidoreductase). Synthesized compound **7b**, standard compound Isoniazid and Isoniazid with co-factor (NAD^+) showed the catalytic site with binding energies of -10.19, -6.34 and -6.23 kcal/mol, respectively against 5MTQ. The purpose of docking with INH- NAD^+ is to compare the docking result with INH because most of known INH inhibitors bind next to the NAD^+ co-factor. The docking pose of INH without co-factor and with co-factor is presented in **Figure 3**. As per the docking simulations, **7b** was docked into Enoyl-ACP reductase (oxidoreductase) active site with -10.19 kcal/mol of binding energy higher than Isoniazid was seen to be forming conventional hydrogen bond with Gln214 and Arg225, along with carbon hydrogen bond with Pro156 which also show Pi-Cation interaction and Vai203, Met199, Phe149, Leu218, Met155 shows alkyl and Pi-Alkyl interaction with amino acids of Enoyl-ACP reductase (oxidoreductase) in **Figure 2a**. When the docking snapshot of Isoniazid in complex with Enoyl-ACP reductase (oxidoreductase) from *Mycobacterium tuberculosis* was analysed, it was seen that it docked into the active site of Enoyl-ACP reductase (oxidoreductase) with -6.34 kcal/mol of energy and found to be forming direct hydrogen bonds with Gly239; Lys377, and Heme, along with hydrophobic interactions with Ile232; Leu384; Leu230; Leu234; Phe163; Phe226; Val350; Ala264; Ile354; Ala260; Phe291; and Pro241 of enzyme in **Figure 2b**.

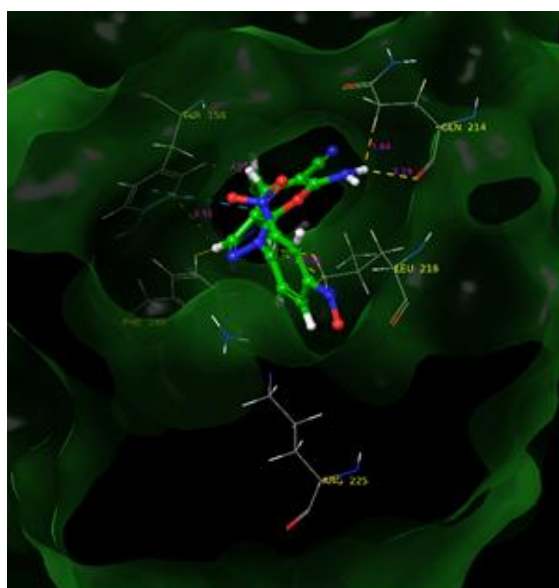
Table 6. Binding energy of Compounds with target protein (kcal/mol)

PDB; 1QG6			PDB; 2B37			PDB; 4TZK			PDB; 5MTQ		
Code	DS*	GE*	Code	DS*	GE*	Code	DS*	GE*	Code	DS*	GE*
5u	-6.533	-55.228	5b	-7.576	-34.142	5c	-7.186	-41.099	7b	-10.190	-54.470
5f	-6.400	-54.231	7a	-7.511	-46.535	7a	-6.979	-48.474	7a	-9.760	-50.300
7a	-6.377	-52.854	7b	-7.493	-40.311	7b	-6.165	-38.703	5c	-8.380	-41.850
5k	-6.046	-52.031	5c	-7.183	-40.033	5l	-5.913	-45.222	5r	-7.000	-45.990
5e	-6.027	-50.009	5n	-7.030	-38.474	5p	-5.631	-46.895	5f	-6.450	-51.450
5o	-5.997	-51.85	5m	-6.949	-39.942	5r	-5.471	-51.598	5m	-6.400	-50.600
5l	-5.962	-50.213	5r	-6.941	-45.771	5m	-5.415	-51.874	5h	-6.300	-44.760
5i	-5.955	-48.033	5e	-6.942	-41.365	5a	-5.400	-38.252	5q	-6.210	-41.450
5s	-5.954	-49.639	5t	-6.867	-40.054	5b	-5.305	-39.658	5p	-6.190	-55.700
5p	-5.954	-51.306	5a	-6.848	-36.639	5q	-5.254	-39.258	5t	-6.160	-48.980
5t	-5.915	-49.045	5o	-6.805	-35.812	5n	-5.210	-46.619	5l	-6.070	-39.190
5b	-5.907	-49.244	5s	-6.239	-46.671	5t	-5.135	-45.243	5a	-6.040	-43.560
5g	-5.847	-46.819	5d	-6.006	-35.774	5o	-5.012	-44.248	5k	-5.940	-49.540
5q	-5.818	-51.270	8a	-5.855	-45.668	5k	-4.899	-40.863	5o	-5.930	-45.390
5d	-5.590	-48.000	5f	-5.842	-48.274	5i	-4.893	-35.894	5g	-5.680	-44.680
8a	-5.447	-51.647	5i	-5.661	-41.220	5u	-4.813	-48.160	5j	-5.610	-42.480
5c	-5.409	-46.538	5g	-5.658	-35.381	5d	-4.771	-34.960	5u	-5.500	-53.670
5a	-4.862	-39.473	5h	-5.327	-40.861	5f	-4.690	-50.455	5e	-5.380	-45.120
5r	-4.189	-48.722	5k	-5.118	-39.871	5s	-4.598	-40.058	5i	-5.360	-34.450
5h	-4.086	-39.169	5q	-5.002	-44.469	8a	-4.504	-49.533	5n	-5.320	-48.800
5n	-4.059	-43.362	5j	-4.982	-43.590	5e	-4.090	-49.154	5d	-5.190	-36.820
5m	-3.811	-51.214	5p	-4.472	-49.983	5h	-4.048	-36.677	5s	-5.170	-32.320
7b	-3.558	-45.738	5l	-4.415	-51.180	5g	-1.899	-45.583	8a	-4.560	-45.340
5j	-5.487	-46.014	5u	-2.974	-42.718	5j	-1.160	-44.153	5b	-10.19	-54.470

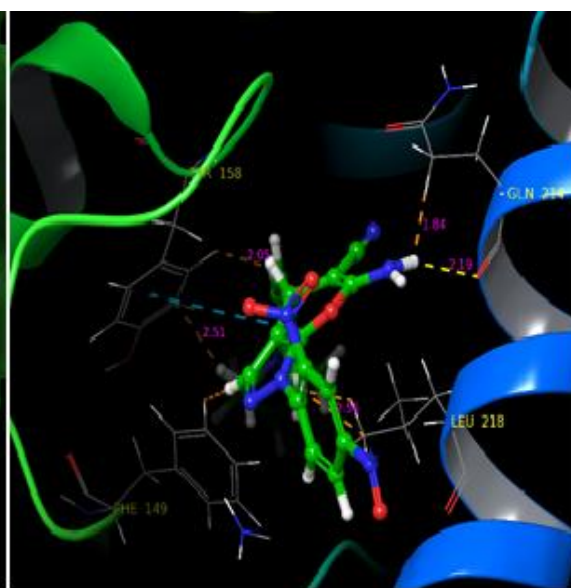
*Where, DS: Docking Score, GE: Glide Energy (Modified Coulomb-Van der Waals energy).; Docking score of INH: -6.34, INH with co-factor: -6.23

Furthermore, compounds 5u and 5f showed good binding affinity towards protein 1QG6 with docking score -6.533 and -6.400, respectively. However, as shown in **Figure 4 (a)** compound **7a** found to generate three hydrogen bond with amino acid residue Gly40, Gly13 and Ala196 with docking score -6.377. In the case of protein 2B37, compound **5b** and **7a** have found to increase their docking score at -7.576 and -7.511, respectively. Here,

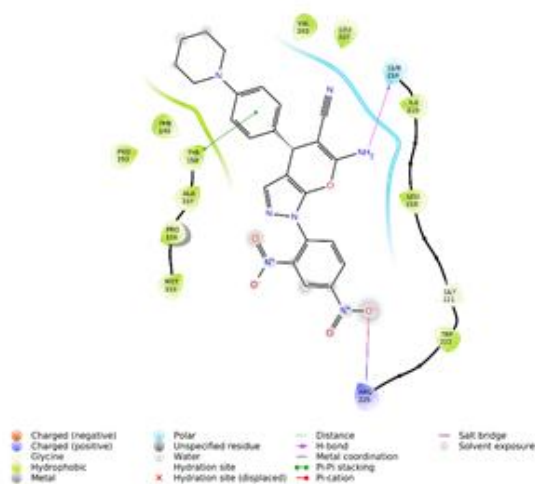
compounds **7a** showed hydrogen bonding interaction with amino acid residue Thr196 and Ile194 (**Figure 4 (b)**). In addition, compounds **5c**, **7a** and **7b** have demonstrated good binding scores and binding energies as compared to standard compounds. The hydrogen bonding interaction between compound **7a** and receptor 4TZK are formed with amino acid residue Phe194 and Thr196 (**Figure 4 (c)**).



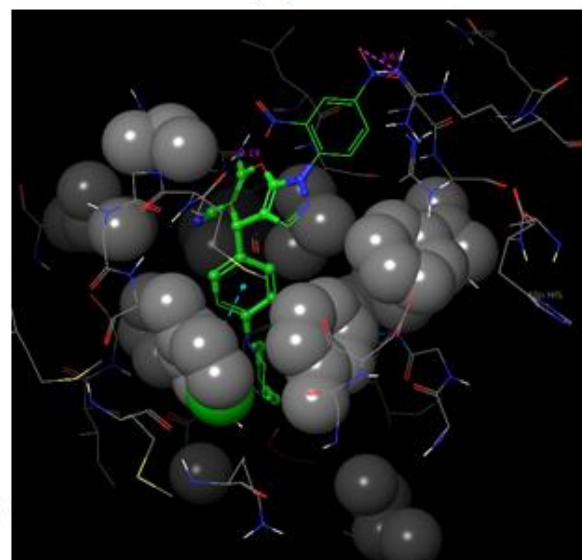
(a)



(b)



(c)



(d)

Figure 2: (a) Interacting amino acids with compound **7b** in 3d (b) 3d diagram of compound **7b** with surface (c) Interacting amino acids with compound **7b** in 2d (d) Hydrophobic interaction of compound **7b** with protein.

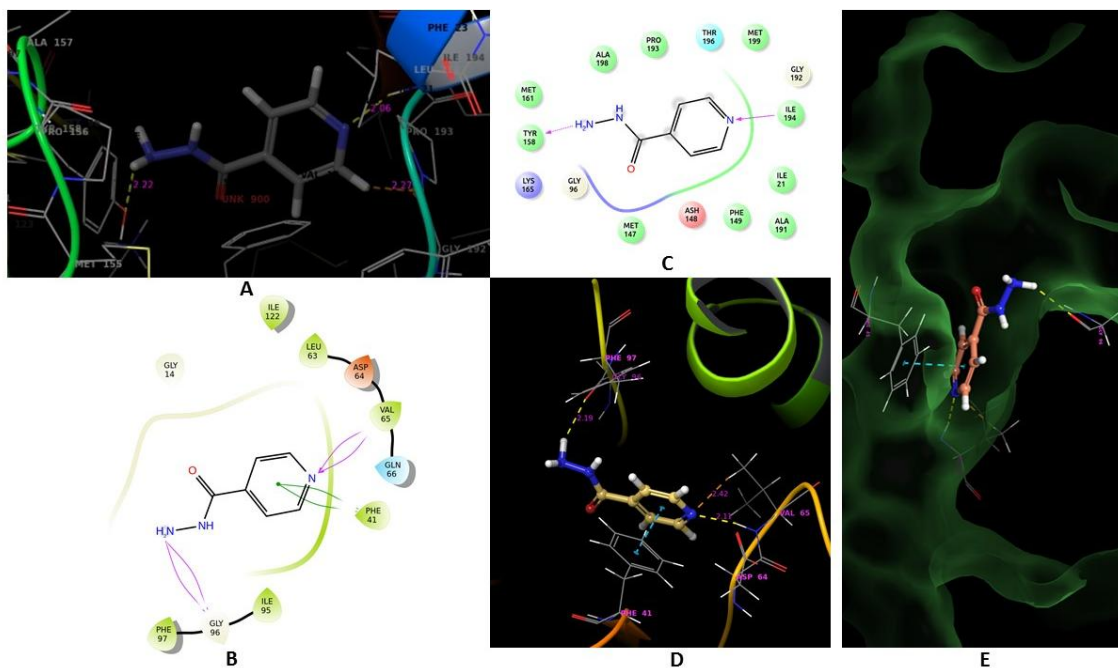


Figure 3: Docked pose of INH without co-factor and INH with co-factor NAD. (a) 3d pose of INH without co-factor, (b) 2d pose of INH without co-factor, (c) 2d pose of INH with co-factor, (d) 3d pose of INH with co-factor ribbon view, (e) 3d pose of INH with co-factor surface view.

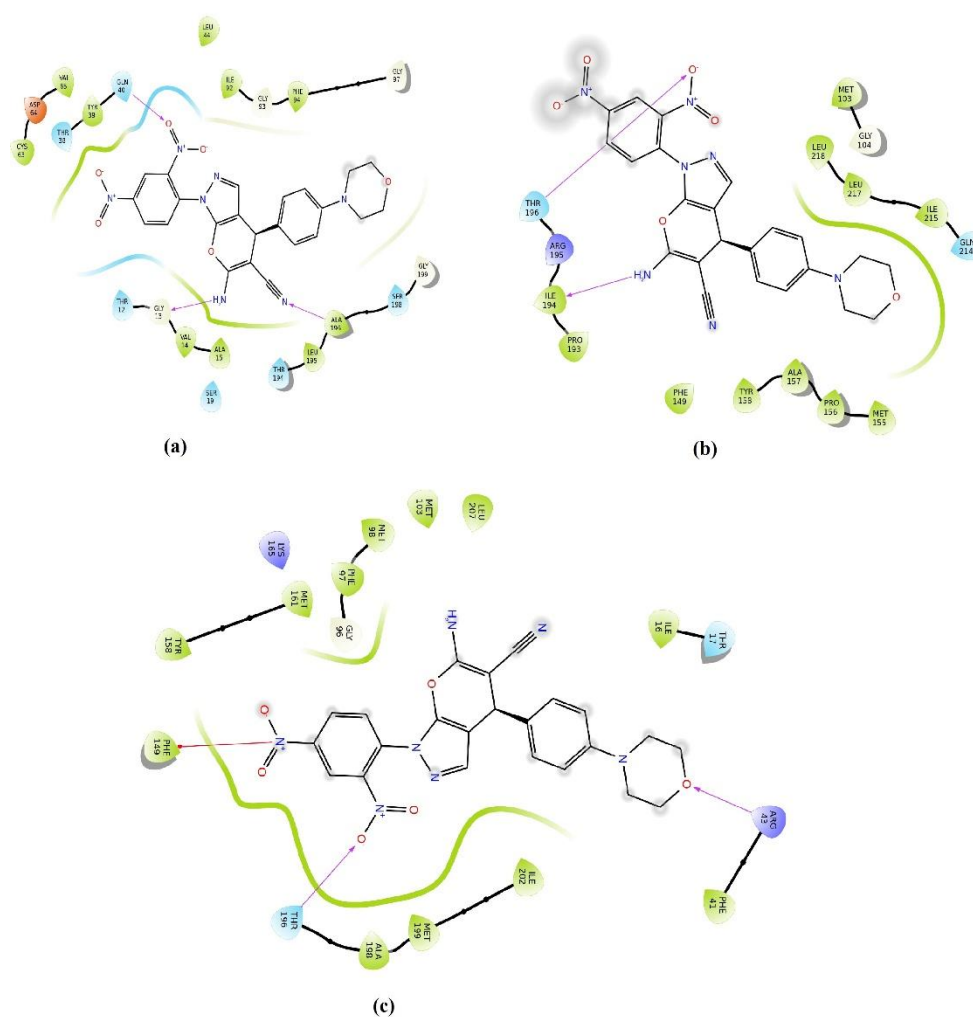


Figure 4: Binding interaction of (a) compound **7a** into the active site of protein 1QG6, (b) Compound **7a** into the active site of protein 2B37, (c) Compound **7a** into the active site of protein 4TZK.

Among 25 compounds analysed, all compounds were successfully docked with a binding energy range of -10.19 to -2.39 kcal/mol. The compound **7b** and **7a** showed the highest binding affinity with lowest binding energy. The compound with highest binding affinity, **7b** was further analysed using molecular dynamic simulation to check the stability of docked complex.

3.3.3 Molecular Dynamics

Molecular Dynamics (MD) simulations were performed to analyse the stability, conformational changes and underlying molecular interactions at atomic level of Enoyl-ACP reductase (oxidoreductase) with compound **7b** at 10 ns. The MD simulations were carried out within the given temperature, pressure and volume defined by simulation quality parameters. The studies were performed in different standard simulation parameters: (i) Root mean square deviation (RMSD), (ii) Root mean square fluctuations (RMSF), (iii) The Ligand Root Mean Square Fluctuation, (iv) Protein-Ligand contacts; (v) total energy, and (vi) Ligand Torsion Profile and properties. The main objective of MD simulation was to understand the dynamics and stability of Enoyl-ACP reductase (oxidoreductase) from *Mycobacterium tuberculosis* protein and its interaction with compound **7b**. The overall statistical data after the analysis of the MD trajectories are explained with **Figure 5**.

RMSF of the Enoyl-ACP reductase (oxidoreductase) protein in complex with **7b** pattern of residue fluctuations were found to be similar from docked structure of protein-ligand shown in Figure 2 and 5 (a). Protein depicted quite stable structure without lacking any major interaction throughout the simulation period. Intra molecular hydrogen bonds were analysed to understand the underlying forces better in relation to protein structure stability. Protein rigidity is represented by increased intra molecular hydrogen bonds. This observation clearly shows that the proposed compound **7b** have the potential to inhibit the protein, with no alterations in Enoyl-ACP reductase (oxidoreductase) rigidity. The overall energy involved for stabilization of Enoyl-ACP reductase (oxidoreductase) state; in complex with **7b** was studied with many other parameters shown in the figures. This data suggests that protein in complex with **7b** has better inhibiting potential as compared to standard drug. A timeline representation of the interactions and contacts shows the total number of specific contacts in which residues interact with the ligand in each trajectory

frame shown in **Figure 5 (d)**. Molecular interactions between protein complex and **7b** during MD simulations shown in Figure 4 (a).

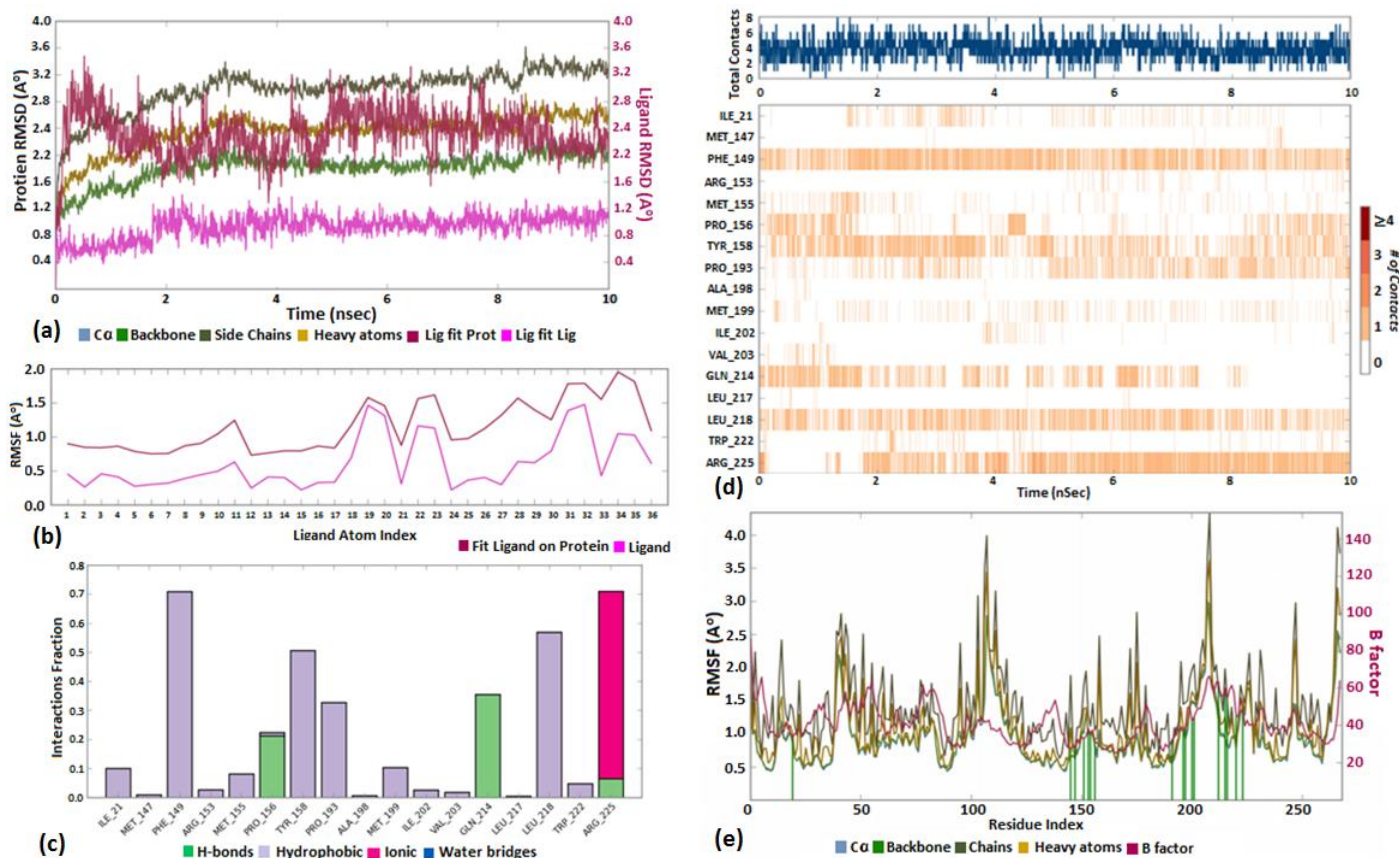


Figure 5. (a) RMSD of protein-ligand (7b) over a period of 10ns, (e) RMSF of protein-ligand (7b) over a period of 10ns, (b) RMSD ligand (7b) over a period of 10ns, (c) Protein (amino acids)-ligand (7b) contact over a period of 10ns, (d) Timeline representation of Protein (amino acids)-ligand (7b) contact over a period of 10ns.

The detailed inter-molecular interactions were studied with simulation interactions diagram using Desmond module of Schrödinger. There were about 0-6 contact found in between protein-compound with 4 hydrogen bonds, with residues Arg225, Arg153, Gln214 and Pro156. Compound also formed pi-pi stacking with PHE149 and various hydrophobic contacts with residues Trp222, Leu218, Ile202, Tyr158, Pro193, Ile21, Met199 and

Met155. On the other hand, residues Arg225 was found to be actively participating in forming water-bridging bonds.

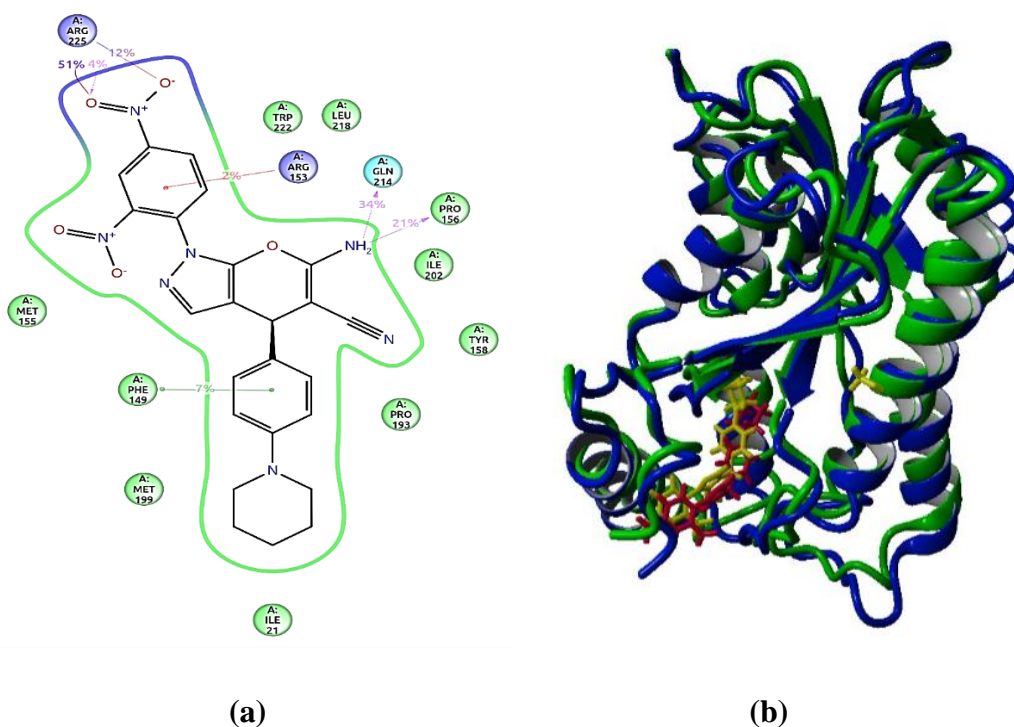


Figure 6. (a) Protein (amino acids)-ligand (7b) interaction over a period of 10ns (b) Superimposition of after 10ns simulation structure on docked structure of protein-ligand.

The torsional degrees of freedom in the ligand given by rotational bonds were studied to understand the dynamics related with it. Each rotatable bond torsion is accompanied by a dial plot and bar plots of the same colour. A total of six rotatable bonds have been observed in **7b**, which present between ligand atoms 27 and 33; 2 and 24; 25 and 30; 9 and 36; 7 and 12 and finally between 15-21. From the dial panels, the above-mentioned rotatable bonds are rotating around, some of them rotated in parts around the clock-wise with gap -130° to -180° / 50° to -60° / 110° to 180° ; 10° to 160° ; 180° to 180° ;

70° to -180° / 70° to -50° / 130° to 180°; -10° to -130° and 40° to -180° / 50° to 180°, respectively in **Figure 7**.

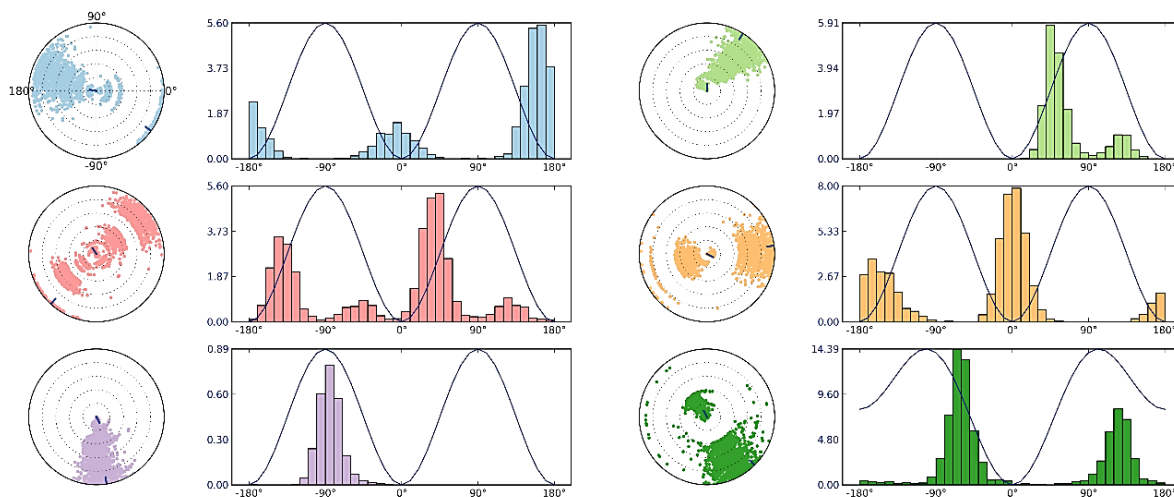


Figure 7. Plot and radial representation of ligand (7b) torsion showing rotatable bonds over a period of 10ns.

Finally, the post docking analysis to check for the similarities between the docked structure and after 10ns simulation structure of *Mycobacterium tuberculosis* Enoyl-ACP reductase (oxidoreductase) with **7b** compound is done via superimposing the structures. The proposed compound's mode of inhibition doesn't show any vast difference after simulation structure specifically, same prominent alignments were observed with the residues are shown in **Figure 6 (b)** indicating protein (blue) with ligand (yellow) structure after molecular dynamic simulation on docked structure protein (green) with ligand (red).

The discoveries of compounds that can inhibit the activation of *Mycobacterium tuberculosis* oxidoreductase protein. This suggest their capability to act as anti-tuberculosis agents. Compound **7b** was found to be strong inhibitors for protein as compared with standard compound Isoniazid. All the compounds discovered here bind the same active binding site of *Mycobacterium tuberculosis* oxidoreductase, by creating hydrogen bonds

and various non-covalent interactions. The computational analysis also supports good binding energy being involved in present compounds being investigated here with the protein combining their complex's thermodynamic stability.

To verify it further, molecular dynamic simulations for 10 ns suggest that the residues of *Mycobacterium tuberculosis* oxidoreductase and ligand interactions, could be useful for its inhibitory activity. The present study gives us vision of the valuable ligand molecule with strong binding affinity towards *Mycobacterium tuberculosis* oxidoreductase protein for plausible anti-tuberculosis activity.

4.0 Conclusion

In the present study, a series of novel hybrid 4*H*-pyran containing pyrazole derivatives were synthesized and characterized by IR, ¹H-NMR, ¹³C NMR and mass spectrometry techniques. We have screened biological activities such as *in vitro* antimicrobial, anti-tuberculosis and cytotoxic MTT assay. From the anti-bacterial activity, it was observed that the compounds **5a**, **5h**, **5m** and **8a** were showed good activity against gram-negative bacterial strain, while other compounds **5b**, **5p** and **7a** gave significant activity against gram-positive bacteria. We have subjected anti-tubercular activity against *mycobacterium tuberculosis* (*H₃₇RV* strain). The compounds **5e**, **5t**, **7a** and **8a** showed potent activity as well as compound **7a** enhanced the moderate activity against MDR-TB. These compounds were further evaluated for their cytotoxic effect in HeLa cell line and was accompanied by relatively low level of cytotoxicity. Compound **7a** were found to be good against biological evolution and cytotoxic assay.

The molecular docking investigation of all the synthesised compounds was carried out in the active site of Enoyl-ACP reductase (oxidoreductase) with using four different protein (PDB ID: 1QG6, 2B37, 4TZK, 5MTQ). Few compounds (**7b**, **7a**, **5c**, **5r**, **5f**, **5m**) displayed good binding affinity in comparison to isoniazid as standard drug and to isoniazid with co-factor against all the targets. From the docking simulations, it can be concluded that these molecules have an excellent affinity for the *Mycobacterium tuberculosis* Enoyl-ACP reductase enzyme making them relevant starting points for structure-based drug design. Furthermore, the MD simulation was carried out to understand the dynamics and stability of Enoyl-ACP reductase (oxidoreductase) protein with its interaction with compound **7b** and based on MD simulation analysis. It can be stated that the docked complex is thermodynamically stable and inhibit the activation of *Mycobacterium tuberculosis* oxidoreductase protein. This suggests their capability to act as strong anti-

tuberculosis agents in comparison to standard drug isoniazid. Additionally, the predicted ADMET properties of the synthesized compounds recognized the drug-likeness of the molecules. Hence, promising in vitro anti-tubercular activity, docking pattern into the active site of Enoyl-ACP reductase (oxidoreductase) and ADMET properties shows that few of these compounds effective lead for further development as potential anti-tubercular agents.

References

1. J.C. Palomino, S.C. Leão, V. Ritacco. Tuberculosis 2007; from basic science to patient care. 1st edition. 2007.
2. WHO. WHO global reports (2017). Geneva:
http://www.who.int/tb/publications/global_report/gtbr2017_main_text.pdf.
3. Banerjee A, Dubnau E, Quemard A, Balasubramanian V, Um KS, Wilson T, Collins D, de Lisle G, Jacobs WR. Science. 1994; 263(5144):227-30.
4. Freundlich JS, Wang F, Vilchèze C, Gulten G, Langley R, Schiehser GA, Jacobus DP, Jacobs Jr WR, Sacchettini JC. ChemMedChem: Chemistry Enabling Drug Discovery. 2009; 4(2):241-8.
5. He X, Alian A, Stroud R. Ortiz de Montellano PR. The Journal of Medicinal Chemistry. 2006; 49:6308-23.
6. Kuo MR, Morbidoni HR, Alland D, Sneddon SF, Gourlie BB, Staveski MM, Leonard M, Gregory JS, Janjigian AD, Yee C, Musser JM. Journal of Biological Chemistry. 2003; 278(23):20851-9.
7. Feng LS, Liu ML, Wang B, Chai Y, Hao XQ, Meng S, Guo HY. European journal of medicinal chemistry. 2010; 45(8):3407-12.
8. Kumar D, Reddy VB, Sharad S, Dube U, Kapur S. European Journal of Medicinal Chemistry. 2009; 44(9):3805-9.
9. Bedair AH, Emam HA, El-Hady NA, Ahmed KA, El-Agrody AM. Il Farmaco. 2001; 56(12):965-73.
10. Khafagy MM, El-Wahab AH, Eid FA, El-Agrody AM. Il Farmaco. 2002; 57(9):715-22.

11. Eid FA, El-Wahab AH, Ali GH, Khafagy MM. *Acta Pharmaceutica-Zagreb*. 2004; 54(1):13-26.
12. Abdelrazek FM, Metz P, Farrag EK. *Archiv der Pharmazie: An International Journal Pharmaceutical and Medicinal Chemistry*. 2004; 337(9):482-5.
13. Paliwal PK, Jetti SR, Jain S. *Medicinal Chemistry Research*. 2013; 22(6):2984-90.
14. Sharma A, Pallavi B, Singh RP. *Heterocycles: an international journal for reviews and communications in heterocyclic chemistry*. 2015; 91(8):1615-27.
15. Morgan LR, Jursic BS, Hooper CL, Neumann DM, Thangaraj K, LeBlanc B. *Bioorganic & medicinal chemistry letters*. 2002; 12(23):3407-11.
16. El-Agrody Am, El-Hakim Mh, El-Latif Ma, Fakery Ah, El-Sayed Es, El-Ghareab Ka. *Acta pharmaceutica*. 2000; 50(2):111-20.
17. Bedair AH, Emam HA, El-Hady NA, Ahmed KA, El-Agrody AM. *Il Farmaco*. 2001; 56(12):965-73.
18. Wu JY, Fong WF, Zhang JX, Leung CH, Kwong HL, Yang MS, Li D, Cheung HY. *European journal of pharmacology*. 2003; 473(1):9-17.
19. Raj T, Bhatia RK, Sharma M, Saxena AK, Ishar MP. *European journal of medicinal chemistry*. 2010; 45(2):790-4.
20. Brown PB. Shaun A. Mason *et al*. *Diabetes, Obesity and Metabolism*, First published: 04 November 2018; 13571.
21. Hanna L. a publication of the San Francisco AIDS Foundation. 1999; 12(2):8.
22. Rueping M, Sugiono E, Merino E. *Chemistry-A European Journal*. 2008; 14(21):6329-32.
23. Sun YS, Peng SW, Cheng JY. *Biomicrofluidics*. 2012; 6(3):034117.
24. Kumar A, Maurya RA, Sharma S, Ahmad P, Singh AB, Bhatia G, Srivastava AK. *Bioorganic & medicinal chemistry letters*. 2009; 19(22):6447-51.

25. Thyagarajan BS. Principles of Medicinal Chemistry, (Foye, William O.; Lemke, Thomas L.; Williams, David A.). Italy, 1991.
26. Safari J, Zarnegar Z, Heydarian M. Journal of Taibah University for Science. 2013; 7(1):17-25.
27. Ping XN, Chen W, Lu XY, Xie JW. RKIVOC. 2016; 6:274-83.
28. Shaabani A, Ghadari R, Sarvary A, Rezayan AH. The Journal of organic chemistry. 2009; 74(11):4372-4.
29. Ellis GP. Chemistry of Heterocyclic Compounds: Chromenes, Chromanones, and Chromones. 1977; 31:1-0.
30. Traven VF, Bochkov AY. Heterocyclic Communications. 2013; 19(4):219-38.
31. Mavandadi F, Pilotti A. Drug discovery today. 2006; 11(3-4):165-74.
32. Ouahrouch A, Ighachane H, Taourirte M, Engels JW, Sedra MH, Lazrek HB. Archiv der Pharmazie. 2014; 347(10):748-55.
33. Brahmachari G, Banerjee B. ACS Sustainable Chemistry & Engineering. 2013; 2(3):411-22.
34. Vekariya RH, Patel KD, Patel HD. The Iranian Journal of Organic Chemistry. 2015; 7:1581-9.
35. Shaterian HR, Azizi K. Research on Chemical Intermediates. 2014; 40(2):661-7.
36. Elinson MN, Dorofeev AS, Miloserdov FM, Nikishin GI. Molecular diversity. 2009; 13(1):47-52.
37. Tayade YA, Padvi SA, Wagh YB, Dalal DS. Tetrahedron Letters. 2015; 56(19):2441-7.
38. Kangani M, Hazeri N, Maghsoodlou MT, Khandan-Barani K, Kheyrollahi M, Nezhadshahrokhhabadi F. Journal of the Iranian Chemical Society. 2015; 12(1):47-50.

39. Kangani M, Hazeri N, Mghsoodlou MT, Habibi-khorasani SM, Salahi S. Research on Chemical Intermediates. 2015; 41(4):2513-9.
40. Dyachenko VD, Chernega AN. Russian journal of general chemistry. 2005; 75(6):952-60.
41. Fallah-Shojaei A, Tabatabaeian K, Shirini F, Hejazi SZ. RSC Advances. 2014; 4(19):9509-16.
42. Baghbanian SM, Rezaei N, Tashakkorian H. Green Chemistry. 2013; 15(12):3446-58.
43. Vekariya RH, Patel KD, Patel HD. Research on Chemical Intermediates. 2016; 42(5):4683-96.
44. Patel RV, Patel PK, Kumari P, Rajani DP, Chikhalia KH. European journal of medicinal chemistry. 2012; 53:41-51.
45. Desai NC, Bhatt N, Somani H, Trivedi A. Acta Pharmaceutica. 2019; 69(2):261-76.
46. Cho AE, Chung JY, Kim M, Park K. The Journal of chemical physics. 2009; 131(13):134108.
47. Shivakumar D, Williams J, Wu Y, Damm W, Shelley J, Sherman W. Journal of chemical theory and computation. 2010; 6(5):1509-19.
48. QikProp, Technical Information (2.1).
49. Schrödinger Release 2015-4: Desmond Molecular Dynamics System, version 4.4, D. E. Shaw Research, New York, NY 2015.
50. Materials Science Suite 2015-4, Schrodinger, LLC, New York, NY 2015.
51. Bhoi MN, Borad MA, Pithawala EA, Patel HD. Arabian Journal of Chemistry. 2016.
52. Mosmann T. Journal of immunological methods. 1983; 65(1-2):55-63.

List of Publication

1. **Vasava MS**, Bhoi MN, Rathwa SK, Shetty SS, Patel RD, Rajani DP, Rajani SD, Patel A, Pandya HA, Patel HD. Novel 1, 4-dihydropyrano [2, 3-c] pyrazole derivatives: Synthesis, characterization, biological evaluation and *in silico* study. Journal of Molecular Structure, Elsevier. 2019; 1181:383-402. (Impact factor: 2.011)
2. **Vasava MS**, Bhoi MN, Rathwa SK, Borad MA, Nair SG, Patel HD. Drug development against tuberculosis: Past, present and future. Indian Journal of Tuberculosis, Elsevier. 2017. Volume 64, Issue 4; 252-275, doi.org/10.1016/j.ijtb.2017.03.002. (Impact factor: 0.32)
3. **Vasava MS**, Nair SG, Patel DB and Patel HD. Development of new drug-regimens against Multidrug-Resistant Tuberculosis. Indian Journal of Tuberculosis, Elsevier. DOI-10.1016/j.ijtb.2018.07.004. (Impact factor: 0.32)
4. **Vasava MS**, Bhoi MN, Rathwa SK, Jethava DJ, Acharya PT, Patel DB and Patel HD. Benzimidazole: A milestone in the field of medicinal chemistry. Mini-Reviews in Medicinal Chemistry (MRMC), Bentham Science Publishers. (Communicated on date 15/10/2018). (Impact factor: 2.903)
5. **Vasava MS**, Bhoi MN, Borad MA, Patel CN, Patel RD, Patel HD. Synthesis, Characterization, Molecular docking and ADME prediction of n'-(7-chloroquinolin-4-yl)-6-methyl-2-oxo-4-phenyl-1,2,3,4-tetrahydro- pyrimidine-5-carbohydrazide derivatives as potent anti-mycobacterial agent. WJPPS, Volume 6, Issue 2 DOI: 10.20959/wjpps20172-8534.
6. Borad MA, Bhoi MN, Rathwa SK, **Vasava MS**, Patel HD, Patel CN, Pandya HA, Pithawala EA, George JJ. Microwave-Assisted ZrSiO₂ Catalysed Synthesis, Characterization and Computational Study of Novel Spiro [Indole-Thiazolidines] Derivatives as Anti-tubercular Agents. Interdisciplinary Sciences: Computational Life Sciences. 2016 Nov 11:1-8. (Impact Factor 0.796)
7. Dhaval B Patel, Rajesh H Vekariya, Kinjal D Patel, Neelam P Prajapati, **Mahesh S Vasava** and Hitesh D Patel. Recent Advances in Synthesis of Quinoline-4-Carboxylic Acid and their Biological Evaluation: A Review Article. Journal of Chemical and Pharmaceutical Research, 2017, 9(2):216-230. (Impact Factor 0.12)

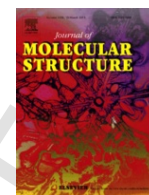
8. Chirag N. Patel, John J. George, Krunal M. Modi, Manoj N. Bhoi, Mayuri A. Borad, Sanjay K. Rathwa, **Mahesh S. Vasava**, Hitesh D. Patel, Moksha B.Narechania & Himanshu A. Pandya. Molecular Recognition Analysis of HumanAcetylcholinesterase Enzyme by Inhibitors:An in Silico Approach. International Science Symposium 2016-17.
9. Manoj N. Bhoi, Mayuri A.Borad, Sanjay K. Rathwa, **Mahesh S. Vasava**, Edwin A. Pithawala, Chirag N. Patel, Rikin D. Patel, Hitesh D. Patel & Himanshu A. Pandya. In-silico ADME prediction and molecular docking study of N-(Benzo [D]thiol-2-yl)-2-(2-6-Chloroquinolin-4-yl)hydrazinyl)acetamide derivatives. 9th national level science symposium. Christ College, Rajkot. 2016
10. Sanjay K. Rathwa, Manoj N. Bhoi, Mayuri A. Borad, **Mahesh S. Vasava**, Edwin A. Pithawala, Chirag N. Patel, Rikin D. Patel, Hitesh D. Patel & Himanshu A. Pandya. Molecular docking and one-pot quick microwave assisted synthesis of 2-amino pyrimidine derivatives as anti-tubercular agents. 9th national level science symposium. Christ College, Rajkot. 2016
11. Dhaval B Patel, Rajesh H Vekariya, Kinjal D Patel, **Mahesh S Vasava**, Smita D. Rajani, Dhanji P. Rajani and Hitesh D Patel. Synthesis, Docking, ADME-Tox Study of 2-(2-(2-Chlorophenyl)quinoline-4-carbonyl)- N -substituted hydrazinecarbothioamide Derivatives and Their Biological Evaluation. Journal of Heterocyclic Chemistry. 2018 Mar;55(3):632-44. **(Impact Factor 1.141)**
12. Sanjay K. Rathwa, **Mahesh S. Vasava**, Manoj N. Bhoi, Mayuri A. Borad and Hitesh D. Patel. Recent advances in the synthesis of C-5 substitution of 3,4-dihydropyrimidin-2-ones analogues: a Review, Synthetic communications, 2018, 48 (9), 963-994. **(Impact Factor 1.377)**
13. IH Khan, NB Patel, VM Patel, **Mahesh Vasava**, Chirag Patel & Hitesh Patel (2018). Synthesis, Pharmacological Evaluation and Docking Studies of Newly Synthesized Fluorine Containing 1,2,4-Triazole Clubbed Benzimidazole. 10.0000/GSC.1000103.
14. Jethava DJ, Acharya PT, **Vasava MS**, Bhoi MN, Bhavsar ZA, Rathwa SK, Rajani DP, Patel HD. Design, synthesis, biological evaluation and computational study of

novel triazolo [4, 3-a] pyrazin analogues. Journal of Molecular Structure. 2019 Feb
5. **(Impact factor: 2.011)**

List of Conferences/Seminars/Workshops:

1. 3rd Nirma institute of pharmacy international conference on “Global challenges in Drug Discovery, Development and Regulatory affairs” 23rd January, 2016, Nirma University Ahmedabad.
2. A Pre-Conference event of 6th International Translation Cancer Research Conference. 3rd February, 2016, Thakorbhai Desai hall, Ahmedabad.
3. XXX Gujarat Science Congress, Challenges for science and technology education during coming decades: Preparing for a Sustainable Gujarat. 6th and 7th, February, 2016, K.S.K.V Kachch University, Bhuj.
4. 9th National level Science Symposium on Recent trends in science and technology. 14th February, 2016. Christ College, Rajkot. **(Poster Presented)**
5. Workshop on “Hands-on training on computational methods in drug discovery”. 23rd and 24th, June, 2016. Department of Chemistry, Gujarat University, Ahmedabad.
6. National conference on “Advances in Chemical, Environments and biological Science” Challenges in 21st century. 10th September, 2016. Department of Chemistry, Government Meera Collage, Udaipur, Rajsthan. **(Poster Presented)**
7. International symposium on computational biology and DNA computing. 26th November, 2016. Dhirubhai Ambani Institute of Information and communication technology, Gandhinagar.
8. National Workshop on Basic ICT Skills, e-Learning and MOOCs for Education. 2nd and 3rd December, 2016. Gujarat University, Ahmedabad.

9. National Seminar on “Innovations in Chemical Sciences for Industries”. 5th August, 2017, Department of Botany, Chemistry and Forensic Science, Gujarat University, Ahmedabad.
10. A workshop on Bioinformatics Leads in Gujarat: (BLG-2017) “Advances in computer Aided Drug Design & Discovery”. 21st and 22nd December, 2017. Department of Botany, Gujarat University, Ahmedabad.
11. A workshop on Molecular Docking, Virtual Screening and Biologicas Discovery. 30th and 31st January, 2018. Department of Chemistry, Gujarat University, Ahmedabad.
12. Seminar on Nuclear magnetic Resonance (NMR) Spectroscopy: Concepts and Applications. 24th and 25th August, 2018. Department of Chemistry, Gujarat University, Ahmedabad.
13. Science Excellence-2018. 20th September, 2018. Department of Botany, Gujarat University, Ahmedabad. **(Poster Presented)**
14. 3rd Schrodinger workshop on. 6th and 7th, March, 2016. Department of Chemistry, Gujarat University, Ahmedabad.



Novel 1,4-dihydropyrano[2,3-c]pyrazole derivatives: Synthesis, characterization, biological evaluation and *in silico* study

Mahesh S. Vasava^a, Manoj N. Bhoi^b, Sanjay K. Rathwa^a, Shilpa S. Shetty^c, Rikin D. Patel^c, Dhanji P. Rajani^d, Smita D. Rajani^d, Alpesh Patel^e, Himanshu A. Pandya^c, Hitesh D. Patel^{a,*}

^a Department of Chemistry, School of Sciences, Gujarat University, Ahmedabad, Gujarat, India

^b Piramal Enterprise Ltd, Plot No.-18, Pharmez, Matoda Village, Ahmedabad, India

^c Department of Botany, Bioinformatics and Climate Change Impacts Management, School of Sciences, Gujarat University, Ahmedabad, Gujarat, India

^d Microcare Laboratory & Tuberculosis Research Centre, Surat, Gujarat, India

^e Genxplore Diagnostic and Research Centre Pvt. Ltd., Ahmedabad, Gujarat, India

ARTICLE INFO

Article history:

Received 8 September 2018

Received in revised form 11 December 2018

Accepted 11 December 2018

Available online xxx

Keywords:

Anti-tuberculosis activity

Anti-bacterial activity

Molecular docking

Molecular dynamics

One-pot synthesis

Pyrano[2,3-c]pyrazole

ABSTRACT

In the present study, a series of novel and biologically potent 6-amino-1-(2,4-dinitrophenyl)-4-phenyl-1,4-dihydropyrano [2,3-c]pyrazole-5-carbonitrile derivatives (**5a-5u**) have been synthesized through multicomponent reaction between various substituted aromatic aldehyde derivative (**4a-4u**), 2, 4-dinitrophenyl hydrazine (**1**), ethyl acetoacetate (**2**) and malononitrile (**3**) in the presence of SnCl₂ as a prompt catalyst using both microwave irradiation method as well as conventional method. The structure of synthesized compounds were confirmed by various spectroscopic methods such as ¹H NMR, ¹³C NMR, IR, Mass analysis and elemental analysis. All the synthesized compounds were subjected in vitro antibacterial, anti-tuberculosis screening and cytotoxicity MTT assay. *In vitro* biological study revealed that the synthesized compound **5a**, **7a** and **8a** are showing good anti-bacterial and anti-tuberculosis activity. The *in silico* study of ADME pharmacokinetic properties were also predicted for synthesized compounds for checking their bioavailability. Furthermore, molecular docking study of synthesized compounds with enoyl-ACP reductase (oxidoreductase) was carry out to find out the binding affinity of compounds. Docking study demonstrated that compound **7b** and **7a** possessed superior binding affinity with target enzyme by strong hydrogen bonding. We have also carried out molecular dynamics simulation to check the stability of docked complex, conformational changes and primary molecular interaction.

© 2018.

1. Introduction

The treatment of infectious diseases that are predominantly endemic into the developing countries, it requires simple medications that can be produced in large quantities at low cost. Tuberculosis (TB) is most dangerous infectious disease which causes maximum fatality by subverting the immune system of the human host due to its long and wide association with humans and is often regarded as a successful pathogen [1]. According to the WHO report 2017, one-third of the world population is potentially infected with TB and millions of new cases occur worldwide every year [2].

There are many drugs available for TB in market, among them, Isoniazid (INH), Rifampicin, Pyrazinamide, and Ethambutol are four milestones in the treatment of TB for more than 50 years. INH is pro-drug which activate by the mycobacterial catalyse peroxidase (KatG), which inhibit the enoyl-ACP reductase of the mycobacterial fatty-II type acid. It involved in the biosynthesis of mycolic acid eventually leading to cell death [3,4]. Studies have confirmed that the front-line anti-TB drugs such as INH and ethionamide is primary targeting

inhA gene [3]. Freundlich et al. revealed that potent triclosan derivatives that inhibit InhA in the nanomolar range with minimum inhibitory concentrations of 5–10 µg/mL [5]. Additionally, several compounds have been reported, such as arylamides derivatives [6], pyrrolidine carboxamide derivatives [7], pyrazole derivatives and indole-5-amides derivatives [8] which targeting inhA enzyme. However, the increasing prevalence of multi-drug-resistant TB (MDR-TB) and extensively drug-resistant TB decrease the effectiveness of these drugs against tuberculosis. Hence, to stop this infection, there is a burning requirement to develop inhibitors targeting InhA directly without prerequisite for activation [9].

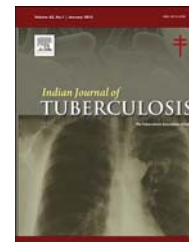
Owing to the vast research on anti-tubercular activity, many synthesized heterocyclic compounds have efficiently displayed anti-tubercular activity. Current literature describing that the 4H-pyrans and pyran-annulated heterocyclic scaffolds have drawn considerable interest in medicinal chemistry from the last several years [10–16]. Fig. 1 represents some of the bioactive pyran-annulated heterocyclic compounds which are good antibacterial agents. Various studies have indicated 4H-pyran derivatives display a potent activity against mycobacterium [17–29] as well as anticancer [20], cytotoxic [21], anti-inflammatory [22], anti-HIV [23,24], antimalarial [25], anti-hyperglycemic, and anti-dyslipidemic [26], anti-neurodegenerative disorders like Alzheimer's, Parkinson disease, Huntington's disease [27],

* Corresponding author.

Email address: drhiteshpatel1@gmail.com (H.D. Patel)

Available online at www.sciencedirect.com

ScienceDirect

journal homepage: <http://www.journals.elsevier.com/indian-journal-of-tuberculosis/>

Review Article

Drug development against tuberculosis: Past, present and future

Mahesh S. Vasava, Manoj N. Bhoi, Sanjay K. Rathwa, Mayuri A. Borad,
Sneha G. Nair, Hitesh D. Patel*

Department of Chemistry, School of Sciences, Gujarat University, Ahmedabad, India

ARTICLE INFO

Article history:

Received 24 October 2016

Accepted 15 March 2017

Available online xxx

Keywords:

Tuberculosis

Drug development

Drug resistance

Antimicrobials

Anti-TB agents

ABSTRACT

Infection of *Mycobacterium tuberculosis* (MTB) was observed as early as 5000 years ago with evidence, which is a primeval enemy of the humanoid race. MTB is the pathogen which is responsible for causing the infectious disease tuberculosis; it remains a major cause of morbidity and mortality in poor low-income countries as well as in developing countries because of non-availability of reliable laboratory facilities. The current treatment for drug-resistant tuberculosis (TB) is lengthy, complex, and connected with severe harmful side effects and poor outcomes. The present cure against tuberculosis has substantial restrictions, in terms of their efficiency, side-effect outline, and complication of handling.

Furthermore, the emergence of multi-drug resistant tuberculosis (MDR-TB) outbreaks during the 1990s and additionally in recent times the vast deadly strains of extensively drug-resistant tuberculosis (XDR-TB) and totally drug resistance tuberculosis (TDR-TB) is hampering efforts to control and manage tuberculosis (TB). As a result, novel methodologies for the treatment of multi-drug-resistant and extensive drug-resistant tuberculosis (TB) are severely desired. A number of new potential anti-tuberculosis drug candidates with novel modes of action have been entered in clinical trials in recent years. These agents are most likely to be effective against resistant strains. The treatment landscape is beginning to shift, with the recent approvals by Food and Drug Administration to the new TB drugs bedaquiline and delamanid. Also, the pipeline of potential new treatments has been fulfilled with several compounds in clinical trials or preclinical development with promising activities against sensitive and resistant MTB bacteria. An additional new chemical entity is also under development. The already existing drugs with their suggested mode of treatment as well as new probable anti-tuberculosis drug moieties which are at present in the pipeline has been summarized in this review.

© 2017 Published by Elsevier B.V. on behalf of Tuberculosis Association of India.

* Corresponding author.

E-mail addresses: maheshvasava@gujaratuniversity.ac.in (M.S. Vasava), drhiteshpatel1@gmail.com, hitesh13chem@rediffmail.co (H.D. Patel).

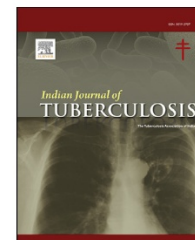
Abbreviations: TB, tuberculosis; MTB, *Mycobacterium tuberculosis*; MDR-TB, multi-drug resistant tuberculosis; XDR-TB, extensively drug resistant tuberculosis; TDR-TB, totally drug resistant tuberculosis; INH, isoniazid; WHO, World Health Organization; RIF, rifampicin; PZA, pyrazinamide; EMB, ethambutol; ETH, ethionamide; CDC, Centers for Disease Control and Prevention; CBC, Complex Blood Count; GI, gastrointestinal; LFT, liver function test; PO, per os; katG, catalase-peroxidase; NADP, nicotinamide adenine dinucleotide phosphate; MRC, Medical Research Council; rRNA, ribosomal RNA; FQs, fluoroquinolones; FDA, Food and Drug Administration; MIC, minimum inhibitory concentration; CYP, cytochrome; GLP, Good Laboratory Practice.

<http://dx.doi.org/10.1016/j.ijtb.2017.03.002>

0019-5707/© 2017 Published by Elsevier B.V. on behalf of Tuberculosis Association of India.

Available online at www.sciencedirect.com

ScienceDirect

journal homepage: <http://www.journals.elsevier.com/indian-journal-of-tuberculosis/>

Review article

Development of new drug-regimens against multidrug-resistant tuberculosis

Mahesh S. Vasava, Sneha G. Nair, Sanjay K. Rathwa, Dhaval B. Patel, Hitesh D. Patel*

Department of Chemistry, School of Sciences, Gujarat University, Ahmedabad, India

ARTICLE INFO

Article history:

Received 10 November 2017

Accepted 3 July 2018

Available online 11 July 2018

Keywords:

Tuberculosis

Drug resistance

Drug development

Mycobacterium tuberculosis

ABSTRACT

Tuberculosis (TB) being the leading infectious killer in the domain wherein globally, almost 20% of all TB strains are resistant to at least 1 major TB drug and there's a growing incidence of multi-drug resistance tuberculosis (MDR-TB). Looking at the current scenario and challenges the existing strategies fall back in terms of treatment of TB. So, to overcome this new, stronger, improved TB drug pipeline and a new standard for the development of novel anti-TB drugs are required in order to make more drug-resistant and efficient drug which also lower the duration period of the treatment of the TB. This review article aims to highlight the recent developments in the anti-tuberculosis agents, those are currently in the clinical development stage.

© 2018 Published by Elsevier B.V. on behalf of Tuberculosis Association of India.

Abbreviations

MTB *Mycobacterium Tuberculosis*TB *Tuberculosis*DRTB *Drug Resistance Tuberculosis*MDRTB *Multi-Drug Resistance Tuberculosis*XDRTB *Extensively-Drug Resistance Tuberculosis*TDRTB *Total-Drug Resistance Tuberculosis*EBA *Early Bactericidal activity*RNA *Ribonucleic acid*rRNA *Ribosomal Ribonucleic acid*HIV *Human immunodeficiency virus*FDA *Food and Drug Administration*INH *Isoniazid*RIF *Rifampicin*Strept *Streptomycin*PZA *Pyrazinamide*EMB *Ethambutol*FQN *Fluoroquinolones*RNTCP *Revised National TB Control Program*

1. Introduction

An infectious bacterial disease Tuberculosis (TB) is caused by bacteria named *Mycobacterium tuberculosis*. These bacteria generally attack the lungs and respiratory system of the human body. The TB illness was thought of reducing. However, due to

the worldwide emergence of the multidrug-resistant *M. tuberculosis* strain it remains an alarming issue with the risk of health.¹ The WHO report of the year 2016 highlights that along with 1 million people who received treatment for rifampicin-resistant TB as well multi-drug resistance tuberculosis (MDR-TB) in 2015 and added to approximately around 4.8 million new cases of MDR-TB is seen. The year 2015 observed a success target

* Corresponding author. Tel.: +91 079 26300969.

E-mail addresses: drhiteshpatel1@gmail.com, hitesh13chem@rediffmail.co (H.D. Patel).

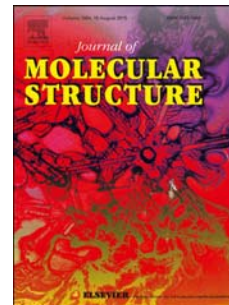
<https://doi.org/10.1016/j.ijtb.2018.07.004>

0019-5707/© 2018 Published by Elsevier B.V. on behalf of Tuberculosis Association of India.

Accepted Manuscript

Design, synthesis, biological evaluation and computational study of novel triazolo [4,3-*a*]pyrazin analogues

Divya J. Jethava, Prachi T. Acharya, Mahesh S. Vasava, Manoj N. Bhoi, Zeel A. Bhavsar, Sanjay K. Rathwa, Dhanji P. Rajani, Hitesh D. Patel



PII: S0022-2860(19)30109-7

DOI: <https://doi.org/10.1016/j.molstruc.2019.01.091>

Reference: MOLSTR 26142

To appear in: *Journal of Molecular Structure*

Received Date: 21 November 2018

Revised Date: 5 January 2019

Accepted Date: 28 January 2019

Please cite this article as: D.J. Jethava, P.T. Acharya, M.S. Vasava, M.N. Bhoi, Z.A. Bhavsar, S.K. Rathwa, D.P. Rajani, H.D. Patel, Design, synthesis, biological evaluation and computational study of novel triazolo [4,3-*a*]pyrazin analogues, *Journal of Molecular Structure* (2019), doi: <https://doi.org/10.1016/j.molstruc.2019.01.091>.

This is a PDF file of an unedited manuscript that has been accepted for publication. As a service to our customers we are providing this early version of the manuscript. The manuscript will undergo copyediting, typesetting, and review of the resulting proof before it is published in its final form. Please note that during the production process errors may be discovered which could affect the content, and all legal disclaimers that apply to the journal pertain.



Recent advances in the synthesis of C-5-substituted analogs of 3,4-dihydropyrimidin-2-ones: A review

Sanjay K. Rathwa, Mahesh S. Vasava, Manoj N. Bhoi, Mayuri A. Borad, and Hitesh D. Patel

Department of Chemistry, School of Sciences, Gujarat University, Ahmedabad, India

ABSTRACT

3,4-Dihydropyrimidin-2-ones act as a versatile scaffold in organic synthesis, which serves as a significant template for the development of various therapeutic agents and shows a wide spectrum of activities. The attractive application of 3,4-dihydropyrimidin-2-ones in organic synthesis is undoubtedly owing to C-5 ester group, which is responsible for the change in its bioactivity. Introduction of various groups like electron-withdrawing and electron-donating groups at positions 1, 2, 3, 5, and 6 greatly increased biological activity. Significant efforts have been undertaken to exploit different synthetic routes to synthesize various derivatives of 3,4-dihydropyrimidin-2-ones. This review article gives a comprehensive account of the synthetic utility of C-5 substitution of 3,4-dihydropyrimidin-2-ones used in the design and synthesis of different types of compounds with greater emphasis on recent literature.

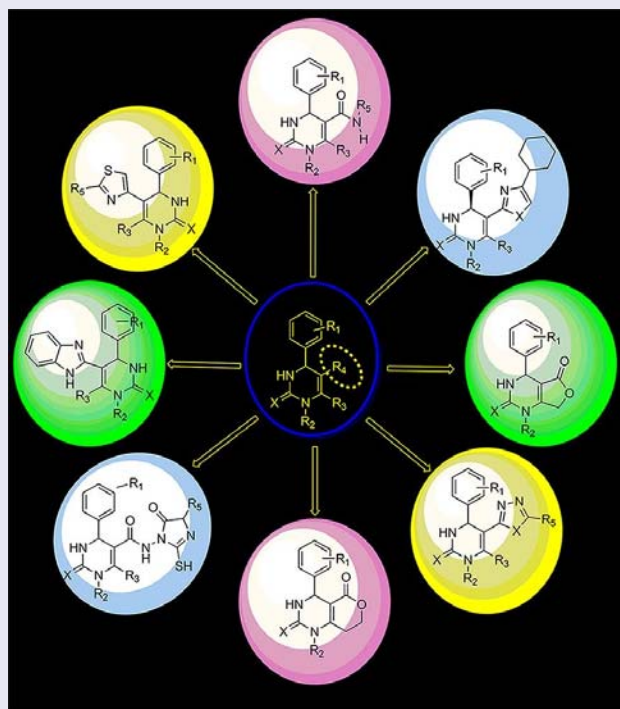
ARTICLE HISTORY

Received 13 November 2017

KEYWORDS

3,4-Dihydropyrimidin-2-ones; Biginelli reaction; dihydropyrimidinone; heterocyclic compounds; multicomponent reaction; organic synthesis

GRAPHICAL ABSTRACT



CONTACT Hitesh D. Patel ✉ drhiteshpatel1@gmail.com ☎ Department of Chemistry, School of Sciences, Gujarat University, Ahmedabad, India.

Color versions of one or more of the figures in the article can be found online at www.tandfonline.com/lsyc.

© 2018 Taylor & Francis

Microwave-Assisted ZrSiO₂ Catalysed Synthesis, Characterization and Computational Study of Novel Spiro [Indole-Thiazolidines] Derivatives as Anti-tubercular Agents

Mayuri A. Borad¹ · Manoj N. Bhoi¹ · Sanjay K. Rathwa¹ · Mahesh S. Vasava¹ ·
Hitesh D. Patel¹ · Chirag N. Patel² · Himanshu A. Pandya² · Edwin. A. Pithawala³ ·
John J. George⁴

Received: 30 May 2016 / Revised: 12 October 2016 / Accepted: 19 October 2016 / Published online: 11 November 2016
© International Association of Scientists in the Interdisciplinary Areas and Springer-Verlag Berlin Heidelberg 2016

Abstract In the current investigation, we prepared a series of novel spiro[indole-thiazolidines] derivatives (**5a–5h**) from 5-substituted isatin derivatives and thioglycolic acid (TGA) with ZrSiO₂ as an efficient catalyst under microwave irradiation. The significant merits of this protocol have some significant merits such as simplicity in operation, simple, efficient workup, good practical yields of product and the employment of recyclable catalyst. All the new synthesized scaffold has been well characterized by various spectroscopic methods and elemental analysis. All the spiro scaffolds were subjected to in vitro anti-mycobacterial activity against the *Mycobacterium tuberculosis* (H₃₇Rv) strain. We have carried out molecular docking study of our synthesized compounds. We also calculated theoretically ADME–Tox parameters for synthesized compounds.

Keywords Green chemistry · Anti-mycobacterial activity · ADMET property · Microwave irradiation · Spiro[indole-thiazolidines] · Spiro compound · ZrSiO₂

1 Introduction

Tuberculosis (TB), an ancient infectious disease caused by microorganism *Mycobacterium tuberculosis* (MTB), signifies the second leading cause in mortality with 1.4 million deaths every year [1]. Generally, tuberculosis causes through not only by the air but also by patient's sneeze, cough or spit [2]. According to World Health Organization (WHO), India has one-third case of tuberculosis and most challenging public health problems in India [3]. On account of the occurrence of multi- and extensively drug-resistant *Mycobacterium tuberculosis*, scientists are always looking for novel and operative anti-TB agents both from natural sources and from chemical syntheses [4]. Therefore, it is alarming need to develop novel, potential drug molecules using sole building blocks, target mode of action and shorten the time of therapy that can be equally effective against MTB, MDR-TB.

In modern organic synthesis, a new environmental benign synthetic process becomes one of the key challenges nowadays for design and implementation in drug discovery [5]. Microwave-assisted synthesis is an area of growing interest, which is not only in industrial laboratories but also in academic field. Microwave (MW) irradiation is one of the key tools in synthetic organic chemistry to synthesize a wide range of molecules in short reaction time with high yields of pure products, less or negligible formation of side products and stereoselectivity [6]. The green synthesis using microwave irradiation is useful for the synthesis of anti-TB agent [7].

Spirocyclic oxindole possesses a highly functionalized synthetic motif that establishes the core structures of many natural products and pharmaceutical scaffolds [8]. Oxindole is one of the good pharmacophores having C-3 position stereogenic centre and important active molecule for

✉ Mayuri A. Borad
mayuri.borad@gmail.com


Hitesh D. Patel
drhiteshpatel1@gmail.com

¹ Department of Chemistry, School of Sciences, Gujarat University, Ahmedabad 380009, Gujarat, India

² Department of Bioinformatics, Applied Botany Centre (ABC), School of Sciences, Gujarat University, Ahmedabad 380009, Gujarat, India

³ Department of Life Sciences, School of Sciences, Gujarat University, Ahmedabad 380009, Gujarat, India

⁴ Department of Bioinformatics, Christ College, Rajkot 360 005, Gujarat, India

Dhaval B. Patel,^a Rajesh H. Vekariya,^a Kinjal D. Patel,^a Mahesh S. Vasava,^a Dhanji P. Rajani,^b Smita D. Rajani,^b and Hitesh D. Patel^{a*} 

^aDepartment of Chemistry, School of Sciences, Gujarat University, Ahmedabad, Gujarat, India

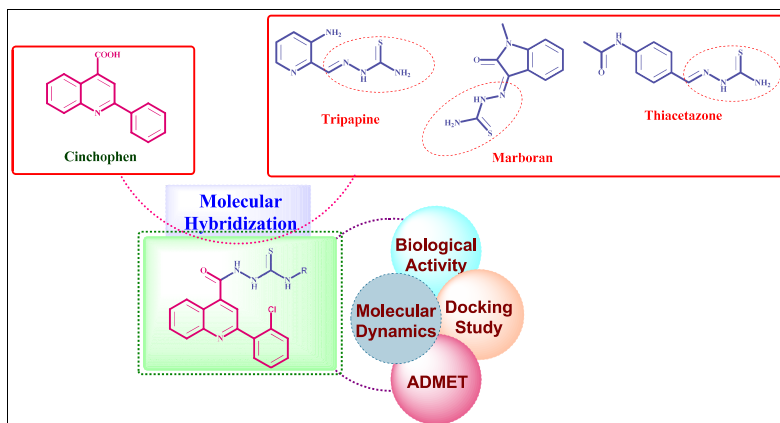
^bMicrocare Laboratory and TRC, Surat, Gujarat, India

*E-mail: drhiteshpatel1@gmail.com

Received July 11, 2017

DOI 10.1002/jhet.3080

Published online 00 Month 2018 in Wiley Online Library (wileyonlinelibrary.com).



A series of 2-(2-(2-chlorophenyl)quinoline-4-carbonyl)-*N*-substituted hydrazinecarbothioamide derivatives were synthesized by facile and efficient conventional method. The structures of the compounds were elucidated with the aid of an elemental analysis, IR, ESI-MS, ¹H-NMR, and ¹³C-NMR spectral data. The synthesized compounds were evaluated for their *in vitro* antibacterial, antifungal, antimalarial, and antituberculosis activity against standard drugs. The bacterial studies were determined against gram-positive and negative bacteria. These compounds were found to a broad spectrum of activity against the screened bacteria, but poor activity was observed against *Pseudomonas aeruginosa* and *Escherichia coli*. Compounds **8d**, **8f**, **8i**, **8l**, and **8n** showed the potent activity against *Staphylococcus aureus*. Compounds **8d**, **8g**, **8k**, **8l**, and **8q** show the potent activity against antimalarial as compared with the standard drugs Chloroquine, Quinine and compounds **8h**, **8n**, and **8o** shows mild activity against *H37Rv* strain. Molecular docking revealed that synthesized derivatives and target proteins were actively involved in a binding pattern and had a significant correlation with biological activity. We have also performed a molecular dynamics and ADME-Tox parameters for the synthesized compounds.

J. Heterocyclic Chem., **00**, 00 (2018).

INTRODUCTION

Despite of many significant progresses in the antimicrobial therapy, infectious diseases caused by bacteria, and fungi remain a major worldwide health problem due to the rapid development of resistance against the existing antibacterial and antifungal drugs. In particular, the emergence of multidrug resistant strains of gram-positive bacterial pathogens such as methicillin-resistant *Staphylococcus aureus* and *Staphylococcus epidermidis* and Vancomycin-resistant *enterococcus* are problem of ever-increasing significance [1,2]. Ciprofloxacin is an antibiotic used to treat number of bacterial infections, while norfloxacin is a synthetic chemotherapeutic antibacterial agent, occasionally used to treat common as well as complicated urinary tract infections

(Fig. 1) [3]. Malaria is an endemic in over 100 countries, affecting especially at tropical areas of Africa, Asia, and Latin America [4]. According to world health organization, every year up to one million people die because of malaria worldwide [5]. Four different types of malaria parasites are *Plasmodium falciparum*, *Plasmodium vivax*, *Plasmodium ovale*, and *Plasmodium malaria* in which *P. falciparum* was mostly lead of infected patients [6]. But among them, untreated travelers are significantly higher [5]. In recent year, many drugs for malarial disease have been developed by pharmaceutical companies (Fig. 2).

Tuberculosis disease is a worldwide caused by drug resistant *Mycobacterium tuberculosis* in human. The antitubercular strategies were based on pyrazinamide, isoniazid, ethambutol, streptomycin, and rifampicin [7]. HIV patients were mostly infected by tuberculosis, so